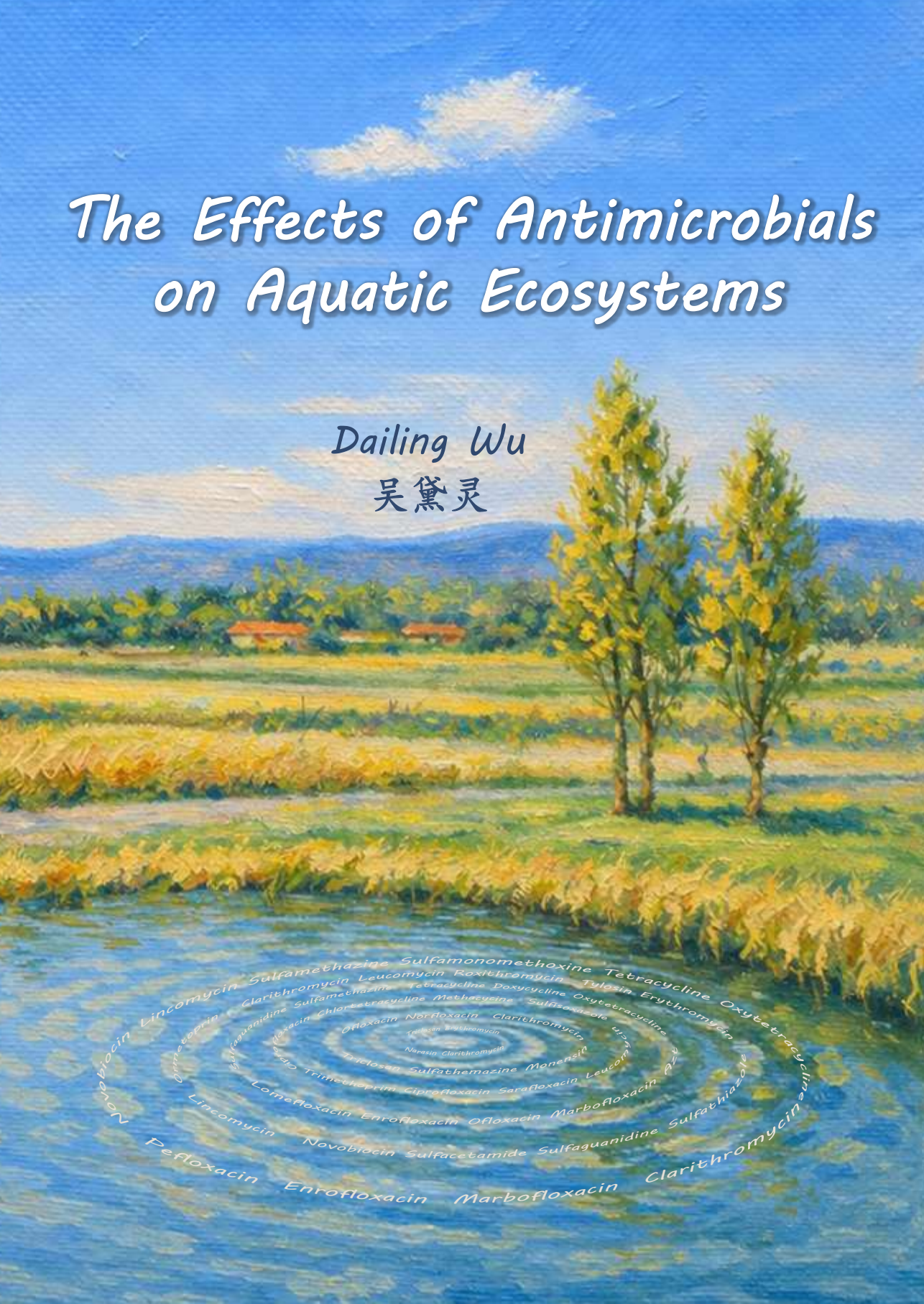
The Effects of Antimicrobials on Aquatic Ecosystems

Dailing Wu
吴黛灵



Propositions

1. Judge a treatment technology by what it changes in ecosystems, not only by what it removes from water.
   (this thesis)

2. Confirmation of hormesis will reshape ecological risk assessment.
   (this thesis)

3. Good questions come from thinking, and reliable answers come from practice.

4. Correction of a mistake after careful consideration leads to greater growth than an unreflective success.

5. Scientific writing takes multiple forms and does not conform to a single fixed template.

6. Pursuing absolute equality is hypocritical.

Propositions belonging to the thesis, entitled

The effects of antimicrobials on aquatic ecosystems

Dailing Wu
Wageningen, May 8, 2026

The Effects of Antimicrobials on Aquatic Ecosystems

Dailing Wu

Thesis committee

Promotor

Prof. Dr Paul J. van den Brink
Professor in Aquatic Ecology and Water Quality Management
Wageningen University & Research

Prof. Dr Hauke Smidt
Professor in Microbiology
Wageningen University & Research

Co-promotors

Prof. Dr Guang-Guo Ying
Dean and Distinguished Professor, School of Environment
South China Normal University, Guangzhou, China

Other members

Prof. Dr Tânia Vasconcelos Fernandes, IHE Delft/Wageningen University & Research
Prof. Dr Mirco Bundschuh, RPTU Kaiserslautern-Landau, Landau, Germany
Dr Annelies Veraart, Radboud University, Nijmegen
Dr Ivo Roessink, Wageningen University & Research

This research was conducted under the auspices of the Graduate School for Socio-Economic and Natural Sciences of the Environment (SENSE)

The Effects of Antimicrobials on Aquatic Ecosystems

Dailing Wu

Thesis

submitted in fulfilment of the requirements for the degree of doctor
at Wageningen University
by the authority of the Rector Magnificus,
Prof. Dr C. Kroeze,
in the presence of the
Thesis Committee appointed by the Academic Board
to be defended in public
on Friday 8 May 2026
at 1p.m. in the Omnia Auditorium.

Dailing Wu
The Effects of Antimicrobials on Aquatic Ecosystems,
218 pages.

PhD thesis, Wageningen University, Wageningen, the Netherlands (2026)
With references, with summary in English

ISBN: 978-94-6534-341-9
DOI: https://doi.org/10.18174/681478

Contents

Chapter 1 7

Introduction

Chapter 2 24

From river to groundwater: Antibiotics pollution, resistance prevalence, and source tracking

Chapter 3 50

Individual and mixture effects of the antibiotics sulfamethazine and tetracycline on freshwater ecosystems

Chapter 4 81

The effects of triclosan on microbial communities in different sources of water and sediments

Chapter 5 102

Trophic transfer and biological effects of azithromycin across a freshwater food chain

Chapter 6 124

The ecological gain of using bioactivated carbon and ozone sewage treatments assessed using freshwater microcosms

Chapter 7 172

General discussion

References 185

Summary 203

Acknowledgements 207

Scientific publications 213

About the author 215

SENSE diploma 216



Lake Como, Italy

Chapter 1

Introduction

Dailing Wu



Water is the driving force of all nature.

— Leonardo da Vinci

1.1 Antimicrobials as emerging contaminants in freshwater environments

Since the discovery of penicillin by Alexander Fleming in 1928, antimicrobial agents have profoundly transformed human society over the past century (Nwakoby et al., 2025). What began as a chance observation on a Petri dish has developed into one of the most influential classes of chemicals in modern history. Antimicrobials triggered a revolution in clinical medicine by turning many formerly lethal bacterial infections into treatable conditions, enabled the safe performance of surgery and organ transplantation, underpinned livestock and aquaculture production, and became embedded in a wide range of household cleaning and personal care products (Laxminarayan et al., 2016; Nwakoby et al., 2025). At present, more than 3,000 pharmaceutical compounds are in use worldwide, a substantial fraction of which exhibits antimicrobial activity, including therapeutic antibiotics used in human and veterinary medicine and a variety of antimicrobial agents used in household, personal care and industrial applications (Aus der Beek et al., 2016; Laxminarayan et al., 2016; OECD, 2019). A spatial modelling study including 204 countries and territories estimated that global antibiotic consumption rates in the human health sector increased by about 46% between 2000 and 2018, reaching roughly 14 defined daily doses (DDD) per 1,000 population per day, or about 40 billion DDDs in 2018 (Browne et al., 2021). Antimicrobial use in food-producing animals has been estimated at around several tens of thousands of tonnes per year, and multiple assessments indicated that a large proportion of global antimicrobial sales, in some cases more than 70%, is used in animal production systems (Acosta et al., 2025; Ardakani et al., 2024; Mulchandani et al., 2023). At the same time, the extensive use of antimicrobials has contributed to a global rise in antimicrobial resistance (AMR), which is now among the leading causes of mortality following infections (Murray et al., 2022). Reflecting this burden, AMR has been framed as a major global health and development threat within a One Health perspective that explicitly links human, animal and environmental health (Murray et al., 2022; WHO, 2023).

Antimicrobial compounds were once regarded primarily as life-saving medicines, but in recent decades they have also come to be recognized as an important group of emerging contaminants in aquatic environments, because their continuous release and biological activity may cause unintended effects beyond their targets (Picinini-Zambelli et al., 2025; Puri et al., 2025). Given their high usage levels and the wide range of application sectors, a considerable fraction of antimicrobials inevitably reaches the environment. A global monitoring synthesis based on more than 1000 publications reported the detection of up to about 600 active pharmaceutical ingredients in environmental samples from 71 countries, including many antibiotics and other compounds with antimicrobial activity (Aus der Beek et al., 2016). This synthesis also identified urban wastewater treatment plant (WWTP) effluents

as one of the main sources of pharmaceuticals entering aquatic systems. A subsequent cross-regional assessment of 1,052 samples from 258 rivers worldwide found that at about one quarter of the sampling sites, at least one active pharmaceutical ingredient exceeded concentrations considered safe for aquatic organisms, with antibiotics and other antimicrobials among the compounds most frequently exceeding these thresholds (Wilkinson et al., 2022). Consistent with this, numerous monitoring studies have shown that antibiotics, antimicrobial agents used in personal care products such as triclosan, and other related compounds are widely detected in WWTP effluents, rivers, lakes, estuaries and sediments, typically at concentrations in the ng/L to µg/L range (Kobayashi et al., 2025; Petrie et al., 2015). Although groundwater has long been regarded as a relatively well protected resource with low contamination risk, recent review studies have documented frequent detection of pharmaceuticals and personal care products, including various antibiotics, in aquifers affected by urban drainage, riverbank filtration or leakage from wastewater systems (Li et al., 2015d; Sanusi et al., 2023; Sui et al., 2015). These findings collectively indicate strong hydrological connectivity between surface water and groundwater, allowing contaminants in one compartment to be transferred to another through recharge and exchange processes. Once antimicrobials enter groundwater and are not effectively controlled, they may persist for many years or even decades because of the long residence times of aquifer systems (Sui et al., 2015). The main usage and exposure pathways of antimicrobials in freshwater systems are summarized in Fig. 1.1.

Once released into freshwater ecosystems, the environmental fate of antimicrobials is governed by their physicochemical properties and by local environmental conditions. Parameters such as pKa, octanol–water partition coefficient, hydrophobicity and organic carbon–water partition coefficient determine their partitioning between the dissolved phase, suspended particles and sediments, and thereby influence their persistence, bioavailability and potential for trophic transfer in aquatic food webs (Al-Khazrajy and Boxall, 2016; Monteiro and Boxall, 2010). Under the combined influence of photolysis, oxidation and microbial transformation, antimicrobials can also be converted into a range of metabolites and transformation products, some of which may retain antimicrobial activity or exhibit different ecotoxicological effects (Chen et al., 2025). In real-world settings, antimicrobials almost never occur as single compounds. Instead, they co-occur with other pharmaceuticals, personal care product ingredients, nutrients and organic matter as complex mixtures (Oluwole et al., 2020). Because different compounds act through different targets and modes of action, mixture exposures can give rise to additive, synergistic or antagonistic effects that are difficult to predict from single-compound toxicity data alone (Backhaus and Faust, 2012; Kidd et al., 2024). Consequently, there is a growing need to understand how antimicrobials are distributed and transported in freshwater systems and how they may affect aquatic community structure and ecosystem functions under realistic mixture

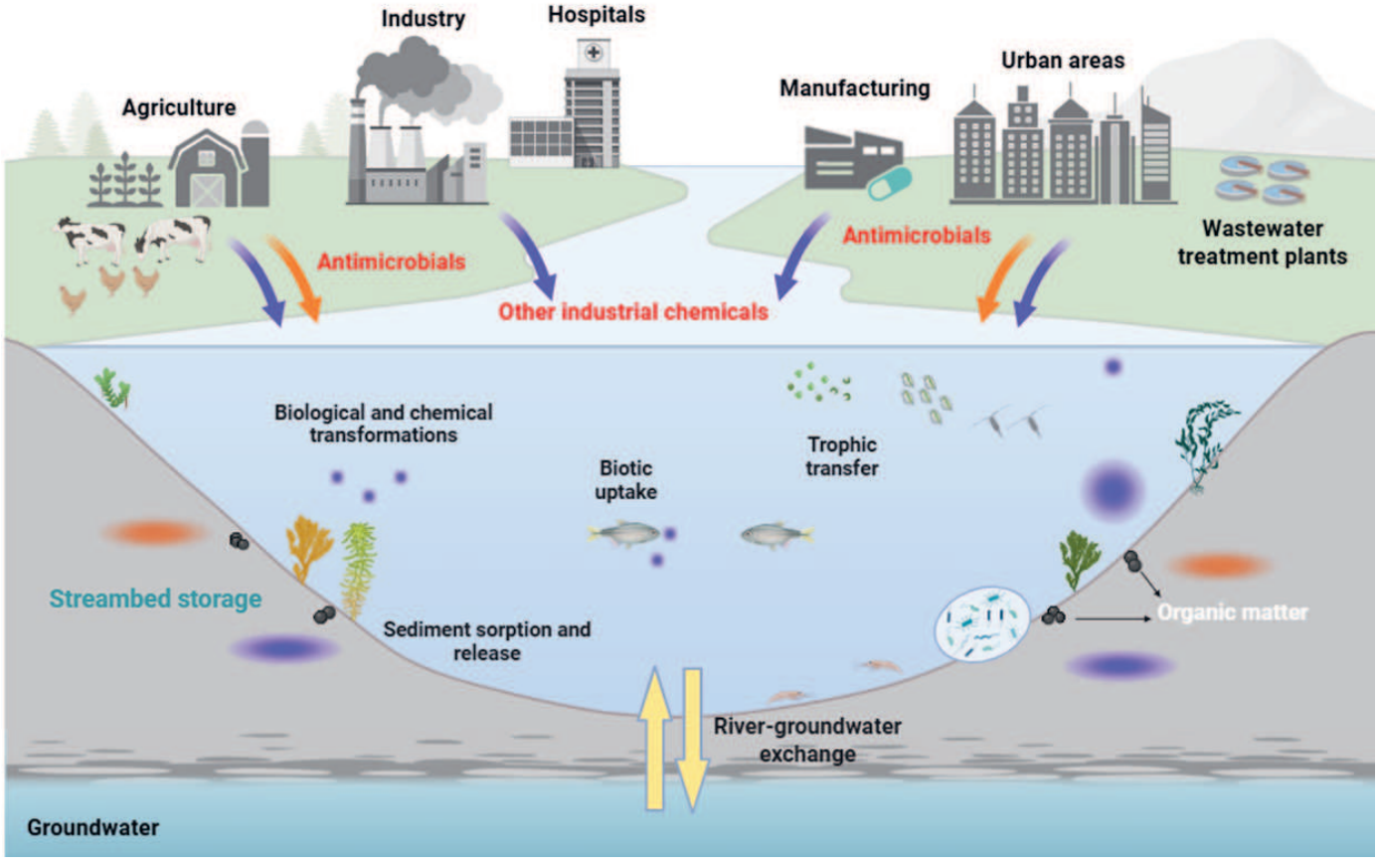


Figure 1.1. Conceptual model of the release pathways, fate and ecological effects of antimicrobials in freshwater environments. Figure created with BioRender.com.

conditions, which has become an important focus in ecotoxicology and environmental risk assessment.

1.2 Effects on microbial communities

Microorganisms are among the most sensitive and ecologically critical targets of antimicrobials in aquatic ecosystems. Broadly defined, antimicrobials - including antibiotics such as sulfonamides, macrolides and tetracyclines, and biocidal agents such as triclosan and triclocarban - are designed to interfere with essential microbial processes, ranging from protein and DNA synthesis to cell-wall formation, membrane integrity and energy metabolism (Fig.1.2a) (Gillings, 2013; Martinez, 2009). Field and laboratory studies show that exposure to antimicrobials typically leads to shifts in microbial community composition, reductions in diversity, and increases of tolerant or degrading taxa, often accompanied by changes in key ecosystem processes (Fig. 1.2b,c) (Caracciolo et al., 2015; Grenni et al., 2018; McClellan and Halden, 2010).

A large body of work has documented that antibiotic exposure can induce bacterial community reassembly in rivers, sediments, WWTP effluents, and freshwater microcosms. River-basin-scale, multi-compartment environmental DNA surveys showed that mixtures of micropollutants, including antibiotics, substantially altered bacterial community composition in river water, sediments, and biofilms, and enriched taxa with pollutant-degrading or antibiotic-resistant traits (e.g., *Nitrospira*) (Inostroza et al., 2025). In urban rivers receiving WWTP effluents, discharges have been shown to reduce the abundance and diversity of benthic bacterial communities and reshape their structure (Drury et al., 2013a). In controlled freshwater microcosms, exposure scenarios within the range reported from field monitoring of multiple antibiotics or pharmaceutical mixtures similarly induced significant changes in the metabolic fingerprints and taxonomic composition of river-water bacterial communities (Pino-Otín et al., 2023), while triclosan was shown to modify microbial community structure and dominant taxa at concentrations close to those detected in the environment (Clarke et al., 2019; Nietch et al., 2013).

These structural shifts are often accompanied by functional perturbations, including effects on nitrogen cycling, carbon processing, and microbial respiration (Fig. 1.2c). Review studies indicate that antibiotics, such as sulfonamides, tetracyclines, fluoroquinolones and related compounds can inhibit key microbial processes such as nitrification, denitrification, and anammox at environmentally relevant concentrations, thereby altering nitrogen transformation rates and nitrous oxide emission patterns in aquatic and soil systems (Pashaei et al., 2022). For example, studies on livestock wastewater treatment systems have shown that wastes containing sulfonamide and tetracycline antibiotics significantly

suppressed microbial metabolic activity in anaerobic lagoons, lowering organic matter removal efficiencies and biogas production rates (Loftin et al., 2005). In stream and wetland systems, inputs of urban wastewater containing antimicrobials and other micropollutants can shift the balance between autotrophic and heterotrophic metabolism and can alter reach-scale primary production and ecosystem respiration (Diamond et al., 2021). In addition, triclosan has been shown to reduce bacterial abundance and diversity in stream mesocosms and freshwater microcosms, weaken leaf-litter decomposition and biofilm respiration, and promote the relative abundance of tolerant or potentially pathogenic taxa (Clarke et al., 2019; Contardo-Jara et al., 2021; Nietch et al., 2013).

The environmental context strongly modulates both the sensitivity of microbial communities to antibiotics and biocides and the magnitude of their responses. Sediments and soils with higher organic matter contents generally exhibit stronger sorption capacities for antimicrobials, which substantially reduces freely dissolved concentrations and often leads to smaller biological effects compared with low-organic or artificial matrices (Al-Khazrajy and Boxall, 2016; Dobor et al., 2012; Yamamoto et al., 2009). Similarly, nutrient-rich waters can partially buffer metabolic stress or promote faster recovery of community structure and function after pollution pulses, as shown in studies combining nutrient and micropollutant gradients (Inostroza et al., 2025). Seasonal variation in hydrology, temperature, and dissolved oxygen further shapes benthic and planktonic habitat conditions and thereby influences how microbial communities respond to contaminant exposure and how such exposure is coupled to ecosystem processes such as metabolism, decomposition, and nutrient cycling (Diamond et al., 2021; Mejia et al., 2019). These environment-dependent responses explain a substantial part of the heterogeneity in effects observed across studies and underscore the importance of comparative assessments across spatial and environmental gradients.

Moreover, interactions between antimicrobials and microbial communities extend beyond overt toxicity. Sub-inhibitory concentrations can select for and enrich antimicrobial resistance genes (ARGs) and reshape their host communities, with long-term ecological and public health implications (Larsson and Flach, 2022; Pruden et al., 2006). In groundwater, where nutrient availability is low and physical disturbance is limited, microbial communities may exhibit lower resilience; even relatively low levels of antibiotics can lead to measurable shifts in community structure or ARG prevalence (Larsson and Flach, 2022). Overall, microbial responses to antimicrobials can be regarded as early indicators of ecological disturbance and provide mechanistic insight into how contaminant pressures propagate to higher levels of biological organization and system-level ecosystem functioning.

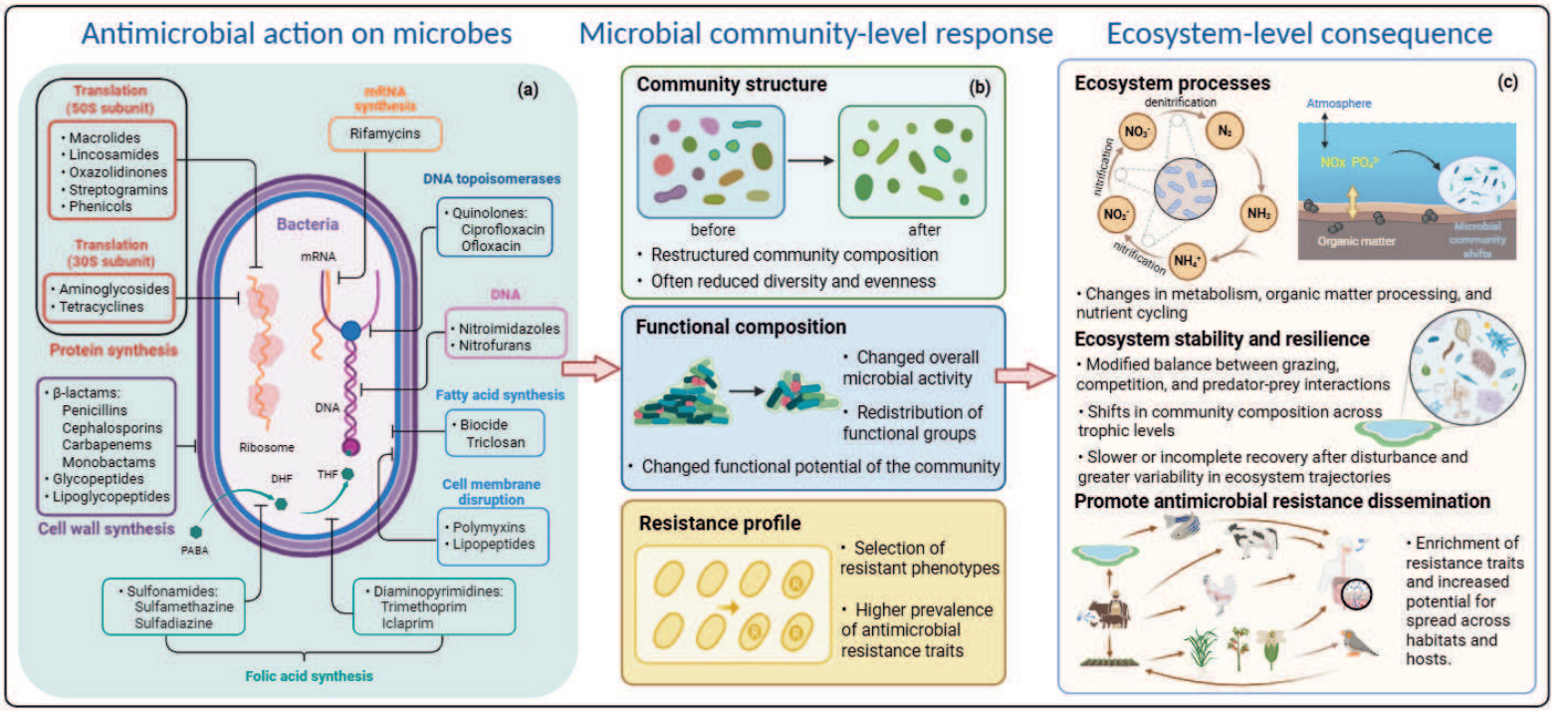


Figure 1.2. Effects of antimicrobials at the level of individual microbes (a), microbial communities (b), and freshwater ecosystems (c). Created with BioRender.com.

1.3 Effects on freshwater ecosystem structure and functions

Beyond microorganisms, the ecological effects of antimicrobials can propagate through food webs, altering community structure and ecosystem functioning at multiple trophic levels in freshwater systems. Reviews and experimental studies focusing on antibiotics and related antimicrobials have shown that environmentally realistic concentrations can induce sublethal responses in algae, benthic biofilms, zooplankton, benthic invertebrates, and fish (Grenni et al., 2018). These responses include changes in growth, physiology, behaviour and species interactions, which in turn can modify community composition and key processes such as primary production, decomposition, and nutrient cycling (Grenni et al., 2018; Gunathilaka et al., 2023; Schuijt et al., 2024a). Such effects are often difficult to detect in single-species toxicity tests but become apparent in multi-species microcosm and mesocosm experiments, where they manifest as shifts in community structure and subtle, yet persistent, deviations in ecosystem processes (Gunathilaka et al., 2023).

At the primary producer level, phytoplankton, benthic algae, and attached biofilms are major entry points for the ecological effects of antimicrobials. Numerous experiments have shown that antimicrobials at concentrations reported from freshwater monitoring studies can alter freshwater algal community composition, dominance patterns and final biomass, even when growth rates are only weakly affected (Kock et al., 2023; Yao et al., 2025). For example, Wilson et al. (2003) observed that triclosan and ciprofloxacin significantly reduced the biovolume of rare algal taxa and thereby changed the structure of experimental algal assemblages. Under near-natural conditions, Quinlan et al. (2011) reported that exposure of stream periphyton to tetracycline at concentrations occurring in natural aquatic environments caused persistent changes in biofilm composition and photosynthetic capacity. As a widely used antimicrobial, triclosan has consistently been shown to exert strong effects on algal and diatom biofilms, reducing biofilm biomass and photosynthetic efficiency and altering cell size, structure and species composition under both chronic and pulsed exposure (Martin et al., 2020; Ricart et al., 2010). Taken together, these studies indicate that antimicrobials can restructure the autotrophic foundation of freshwater food webs, with implications for photosynthetic primary production, nutrient uptake, and resource provisioning for higher trophic levels.

At the consumer level, zooplankton and other invertebrate grazers showed variable but often ecologically relevant responses to antimicrobial exposure. In larger outdoor microcosms, Hillis et al. (2007) found that the veterinary antibiotic monensin altered zooplankton community structure and population abundance over several weeks at microgram-per-litre concentrations. Food-web experiments with azithromycin showed that short-term exposure reduced rotifer fitness and grazing activity, thereby allowing phytoplankton to proliferate,

demonstrating how antibiotics can weaken herbivory and modify lower-trophic community dynamics (Galir et al., 2025). Other studies have reported indirect, behaviour-mediated effects: in a food-selection experiment, the amphipod *Gammarus pulex* preferentially consumed leaf litter not exposed to antibiotics, implying that antimicrobial contamination of detrital resources can alter detritivore feeding and thus leaf-litter processing (Hahn and Schulz, 2007). Nevertheless, recent mesocosm work with sulfamethoxazole suggested that whole-community responses of zooplankton and macroinvertebrates may be weak or taxon-specific at typical environmental concentrations, highlighting substantial context dependence in consumer-level effects (Schuijt et al., 2024a).

At the scale of ecosystem functioning, antimicrobial effects are increasingly being documented in integrated indicators such as metabolism and material fluxes. Stream-channel microcosm studies with sulfonamide antibiotics (sulfamethoxazole and sulfamethazine) have shown that concentrations observed in natural aquatic environments can impair microbial litter decomposition and modify the activity of heterotrophic decomposers, with periphyton sometimes partially compensating for these effects (Paumelle et al., 2021). Complementary experiments in freshwater sediments demonstrated that similar sulfonamide concentrations induced persistent changes in microbial community structure and can either suppress or stimulate heterotrophic activities, thereby altering pathways of carbon processing and biogeochemical cycling (Pesce et al., 2021). Antibiotic exposures have also been linked to changes in nitrification and denitrification: for example, enrofloxacin in freshwater microcosms reduced the abundance of ammonia-oxidizing bacteria and archaea and decreased nitrate production, indicating impairment of nitrification and potential consequences for nitrogen removal (Rico et al., 2014). Yet other studies in streams have found few consistent changes in nitrogen and carbon cycling under antibiotic dosing, underscoring that functional responses can range from clear impairment to negligible or even compensatory shifts (Gray and Bernhardt, 2022). Overall, the available evidence suggests that the impacts of antimicrobials on freshwater community structure and ecosystem functioning arise from the combined effects of direct toxicity to sensitive taxa, indirect changes in species interactions and complex, context-dependent exposure and response scenarios. This reinforces the need for multi-trophic, process-based approaches in ecological risk assessment, rather than relying solely on single-species acute toxicity tests.

1.4 Bioaccumulation, trophic transfer, and higher trophic risks of antimicrobials

When antimicrobials enter aquatic environments, they not only exert toxic effects through instantaneous external exposure, but their accumulation within organisms, transfer along food webs, and residues in higher-trophic organisms also represent critical dimensions of

ecological risk. Unlike classical hydrophobic persistent organic pollutants, many antimicrobials are ionizable organic compounds that occur partly or predominantly in charged forms at environmentally relevant pH, which strongly affects their distribution behaviour in aquatic organisms and their bioaccumulation potential (Armitage et al., 2017; Henneberger and Goss, 2019). Bioaccumulation is commonly quantified using the bioconcentration or bioaccumulation factor (BCF/BAF). Understanding the bioaccumulation potential of contaminants is crucial, because these metrics quantitatively link external environmental concentrations to internal body burdens and are key parameters for assessing long-term exposure, food-web transfer and secondary poisoning risks (e.g. for fish, birds and mammals consuming contaminated prey) (Arnot and Gobas, 2006; Mackay and Fraser, 2000).

However, BCF and BAF values derived from single time-point tissue concentrations in biomonitoring studies essentially provide a "snapshot" of internal exposure under a given scenario, reflecting mainly average enrichment levels and offering limited insight into temporal dynamics driven by growth dilution, metabolism and elimination (Gobas and Lee, 2019; Ratier et al., 2021). In parallel, several studies have shown that measured concentrations of various antimicrobials in fish and invertebrate tissues can span 4–5 orders of magnitude, and that plasma or brain concentrations in a subset of samples may approach a certain fraction of human therapeutic plasma levels (Fick et al., 2010; Miller et al., 2018), indicating a high degree of heterogeneity in internal exposure across tissues and over time. To move beyond such snapshot metrics, a suite of toxicokinetic (TK) and physiologically based kinetic (PBK) models has been developed to link uptake, distribution, metabolisation and elimination processes to time-resolved internal concentrations and derived BCF/BAF values (Saunders and Nichols, 2023). These models integrate empirical bioaccumulation data with mechanistic descriptions of gill and dietary uptake, pH-dependent ionization, sorption to phospholipids and biotransformation, and have increasingly been applied to ionizable pharmaceuticals, including sulfonamide, macrolide and fluoroquinolone antibiotics (Armitage et al., 2017). In doing so, TK and PBK models provide powerful tools to explore how internal exposure trajectories of antimicrobials vary across exposure scenarios, species and life stages, and how these trajectories relate to long-term bioaccumulation and hazard thresholds (Zhu et al., 2023).

In addition, the biomagnification factor (BMF) is commonly used to characterize trophic transfer of contaminants across food webs. Strictly speaking, BMF estimation requires conditions in which waterborne exposure is relatively constant or negligible, contaminated prey is the dominant exposure route, and predator–prey tissue concentrations are near steady state (Gobas et al., 2020; Mackay et al., 2013). Such conditions are difficult to achieve in natural systems, so most current evidence for biomagnification stems from food-

web studies based on environmental monitoring data, where trophic position is inferred from stable isotopes (e.g. $\delta^{15}N$) and trophic magnification factors (TMFs) are derived from regressions of tissue concentrations against trophic levels to distinguish overall "trophic magnification" (TMF > 1) from "trophic dilution" (TMF < 1) (Du et al., 2014; Harriage et al., 2025; Lagesson et al., 2016; Xie et al., 2017). For example, in Lake Taihu, Xie et al. (2017) reported TMFs of 1.11 for the macrolide antibiotic roxithromycin, 0.31 for propranolol and 1.06 for diclofenac, indicating an overall absence of strong trophic magnification for these pharmaceutically active compounds in a freshwater food web. More recently, Sokołowski et al. (2024) reported TMFs between 0.3 and 2.8 for several pharmaceuticals and stimulants, including the fluoroquinolone ciprofloxacin, in a large benthic food web along the European Arctic coast, again demonstrating that some antimicrobials can biomagnify whereas others dilute or remain trophically neutral.

Compared with these TMF-based results, studies that experimentally quantify BMF under controlled waterborne exposure (or negligible water exposure) with contaminated prey as the sole exposure route remain far less common, especially for antimicrobials (Harriage et al., 2025; Lagesson et al., 2016; Miller et al., 2018). Furthermore, even in food webs where no pronounced biomagnification or trophic magnification is observed, it remains poorly quantified whether antimicrobials that are transferred along food chains at relatively low concentrations can, over the full life span of individuals, give rise to ecologically relevant chronic internal exposures and thereby induce sublethal effects on behaviour, growth or energy allocation.

1.5 Mitigation and ecological implications of advanced wastewater treatment technologies

Conventional secondary biological treatment processes (e.g., activated sludge, oxidation ditches) can effectively remove most biodegradable organic matter and nutrients (Metcalf and Eddy, 2014), but their removal of many polar and persistent organic micropollutants, particularly pharmaceuticals, including antimicrobials such as antibiotics and biocides, as well as certain industrial chemicals, is often limited and highly variable (Falås et al., 2016; Matesun et al., 2024; Onesios et al., 2009). Numerous reviews and monitoring studies have shown that, even in well-operated plants, a substantial fraction of pharmaceuticals and other micropollutants exhibit average removal efficiencies below 50% in conventional treatment. Thus, even when current discharge standards are met, effluents from conventional secondary treatment still represent a persistent chemical and ecological pressure, including a chronic source of antimicrobials to downstream ecosystems.

To address the limited removal of micropollutants by conventional secondary treatment, a range of advanced wastewater treatment technologies has been proposed and implemented in recent years. Broadly, the most widely discussed options fall into three main categories: (i) advanced oxidation processes (AOPs), such as ozonation and UV/H_2O_2, which use strong oxidants to rapidly transform a wide spectrum of organic pollutants; (ii) adsorption and bio-adsorption processes, represented by powdered/granular activated carbon (GAC) and biological activated carbon (BAC), which "polish" residual organic contaminants through physical adsorption and biodegradation; and (iii) membrane separation processes such as nanofiltration and reverse osmosis, which physically retain micropollutants and concentrate them into a small-volume waste stream (Margot et al., 2015; Pistocchi et al., 2022). Systematic evaluations indicate that these technologies can, to varying extents, substantially reduce the concentrations of pharmaceuticals, including many antimicrobials, and other organic micropollutants in treated effluents, and are often accompanied by a certain degree of toxicity reduction in bioassays (Margot et al., 2013; Völker et al., 2019). At the same time, they introduce new environmental and ecological considerations, including the formation of large numbers of oxidation transformation products and the risk of inorganic by-products such as bromate in advanced oxidation, the energy and resource demands associated with activated carbon production and regeneration, and the potential environmental burden caused by the handling and disposal of membrane concentrates (Pistocchi et al., 2022; Völker et al., 2019).

Among the available options, ozonation and activated carbon–based processes are widely regarded as mainstream technological routes specifically targeting micropollutant removal, owing to their relatively high removal efficiencies for a broad range of pharmaceuticals and other organic micropollutants. They have been proposed or implemented as a "fourth treatment stage" in several WWTPs in countries such as Switzerland and Germany, and are also used in European-scale assessments to evaluate mitigation potential and costs (Margot et al., 2013; Pistocchi et al., 2022). Ozonation is well suited to rapidly reduce concentrations of highly reactive, high-risk compounds, but it generates complex mixtures of oxidation transformation products and, in bromide-containing waters, can form bromate and other inorganic by-products of concern. Activated carbon, by contrast, achieves relatively stable reductions in dissolved organic carbon and many pharmaceuticals, including antimicrobials through adsorption and biodegradation without producing new oxidative by-products, yet its performance is limited for highly polar, recalcitrant compounds and depends strongly on operating conditions such as carbon age and contact time (Margot et al., 2013; Pistocchi et al., 2022). In practice, the two are often combined in different configurations—for example, using BAC or GAC upstream of ozonation to reduce DOC and ozone demand, or installing BAC/GAC downstream of ozonation as a polishing step to attenuate transformation products and residual organic contaminants (Margot et al., 2013; Pistocchi et al., 2022). Because of

this complementarity in removal spectrum and potential side-effects, the combination of ozonation and activated carbon has become a central focus in current advanced treatment practice and research. This in turn underscores a key question: beyond reductions in target compound concentrations, there is a need for more comprehensive environmental assessments of effluents treated by such technologies, including systematic evaluation of changes in transformation products, dissolved organic matter and nutrient regimes, and the resulting multi-trophic ecological responses (Hamdhani et al., 2020; Kienle et al., 2019).

1.6 Thesis aim and outline

From the preceding sections, it is clear that, although numerous studies have examined the occurrence and ecological effects of antimicrobials in aquatic environments, several critical limitations remain. First, most work has focused on single environmental media or single spatial scales, and there is a lack of systematic studies that simultaneously integrate multiple interconnected "environmental compartments" within the same catchment or hydrological system, such as wastewater effluents, river water, sediments and groundwater. At the same time, for source-control measures such as advanced wastewater treatment, the potential trade-offs between chemical removal efficiency and ecological compatibility have not yet been comprehensively evaluated. Second, in terms of ecological effects, research is still dominated by single-compound and single-species tests. Our understanding of how mixtures occurring in freshwater environments influence microbial communities, higher trophic-level aquatic organisms and ecosystem functions in real or semi-natural freshwater settings remains limited, and it is still unclear how these effects are modulated by environmental context, including nutrient levels, organic matter, sediment type and seasonal variation. Third, at the food-web scale, process-based empirical evidence for the bioaccumulation and trophic transfer of these compounds in freshwater food chains is still scarce.

Against this background, research described in this thesis combines environmental monitoring, indoor and outdoor experimental approaches, and modelling/statistical analyses to investigate antimicrobials from three complementary perspectives: pollution occurrence, ecological responses and mitigation strategies. It is structured around the following four core research questions:

1. **What are the occurrence patterns, exposure levels, and ecological risks of antimicrobials in the freshwater systems investigated, including wastewater effluents, river water, sediments, groundwater, and experimental microcosms?**
2. **How do antimicrobials, alone or in mixtures, affect microbial communities, higher-level aquatic organisms, and ecosystem functions across**

freshwater environments, and how are these effects shaped by environmental context?

3. **To what extent do antimicrobials bioaccumulate and transfer through freshwater food chains, and what are the implications of trophic transfer for ecological risk assessment?**
4. **How can advanced wastewater treatment processes contribute to reducing antimicrobials exposure and mitigating ecological risks in freshwater ecosystems?**

To address these questions, the main content and focal organisms/compartments of each research chapter are summarized as follows, with an overview provided in Figure 1.3.

Chapter 2 uses the highly urbanised Maozhou River in Shenzhen, China, as a case study to investigate pollution patterns along a "river–sediment–groundwater" continuum. The study considers river water, surficial river sediments and groundwater at different depths, with a focus on aqueous antibiotics, ARGs and bacterial community structure. Groundwater *Escherichia coli* is used as an indicator organism for antibiotic resistance and health-related risk. Through combined monitoring and source-tracking analyses, this chapter examines how riverine pollution propagates into groundwater systems and what ecological and health risks may arise.

Chapter 3 employs freshwater microcosms to investigate the effects of two commonly detected antibiotics, sulfamethazine (SMT) and tetracycline (TC), applied individually and in combination, on multi-trophic freshwater ecosystems. The study encompasses phytoplankton (green algae) in the water column, zooplankton communities, microbial communities in water and sediments, as well as leaf-litter decomposition as a key ecosystem process indicator. By comparing response patterns of different trophic levels and functions under single-compound versus mixture exposure, this chapter explores how antibiotic mixtures affect community structure and ecosystem processes under realistic exposure scenarios and under realistic water-quality conditions.

Chapter 4 focuses on triclosan as a model antimicrobial biocide and examines microbial community responses under different combinations of water bodies and sediments. The study targets natural sediments collected from ponds and ditches, OECD artificial sediments incubated in these systems, and the associated overlying water microbial communities. Using sediment microcosm experiments, it compares how triclosan exposure affects bacterial community composition and diversity under contrasting sediment types and water nutrient regimes, thereby assessing how sediment properties and water-column conditions jointly shape the effects of antimicrobials on benthic microbial communities.

Chapter 5 uses a simplified freshwater food chain composed of the green alga *Scenedesmus obliquus* (primary producer), the cladoceran *Daphnia magna* (primary consumer) and the predatory insect larva *Chaoborus obscuripes* (secondary consumer) as a model system to investigate the internal exposure dynamics and trophic transfer of azithromycin (AZT). The study examines AZT concentration dynamics within organisms at different trophic levels, together with their basic growth performance. Through toxicokinetic analysis and trophic-transfer experiments, AZT bioconcentration factors (BCFs) within organisms and its transfer efficiency along the food chain (BMF) are quantified, providing mechanistic insight into the retention and potential ecological risks of antibiotics in freshwater food webs.

Chapter 6 evaluates the balance between chemical removal and ecological responses associated with advanced wastewater treatment technologies centred on BAC filtration and ozonation (O_3). The study examines effluents treated with different BAC–O_3 combinations and their effects in outdoor freshwater microcosms, encompassing micropollutant mixture concentrations (including several antimicrobials) and predicted toxicity, water-quality and nutrient characteristics, as well as multi-trophic biological components such as phytoplankton, zooplankton, macroinvertebrates, and microbial communities in both the water column and sediment. By systematically comparing chemical and ecological outcomes across treatment scenarios, this chapter assesses the trade-offs and optimization potential of advanced treatment technologies as mitigation measures within freshwater ecosystems.

Chapter 7 provides an integrated synthesis of the results from all research chapters, aiming to develop an overarching perspective on the distribution patterns, exposure pathways, and multi-trophic ecological effects of antimicrobials in interconnected freshwater systems. By combining evidence from the river–groundwater continuum, sediment and water-column microcosms, and food-chain–based exposure and bioaccumulation experiments, the chapter identifies key linkages and shared mechanisms across environmental compartments and biological levels. On this basis, it discusses the broader implications for assessing exposure, understanding mixture effects, and designing future studies on potential mitigation measures for freshwater ecosystems.

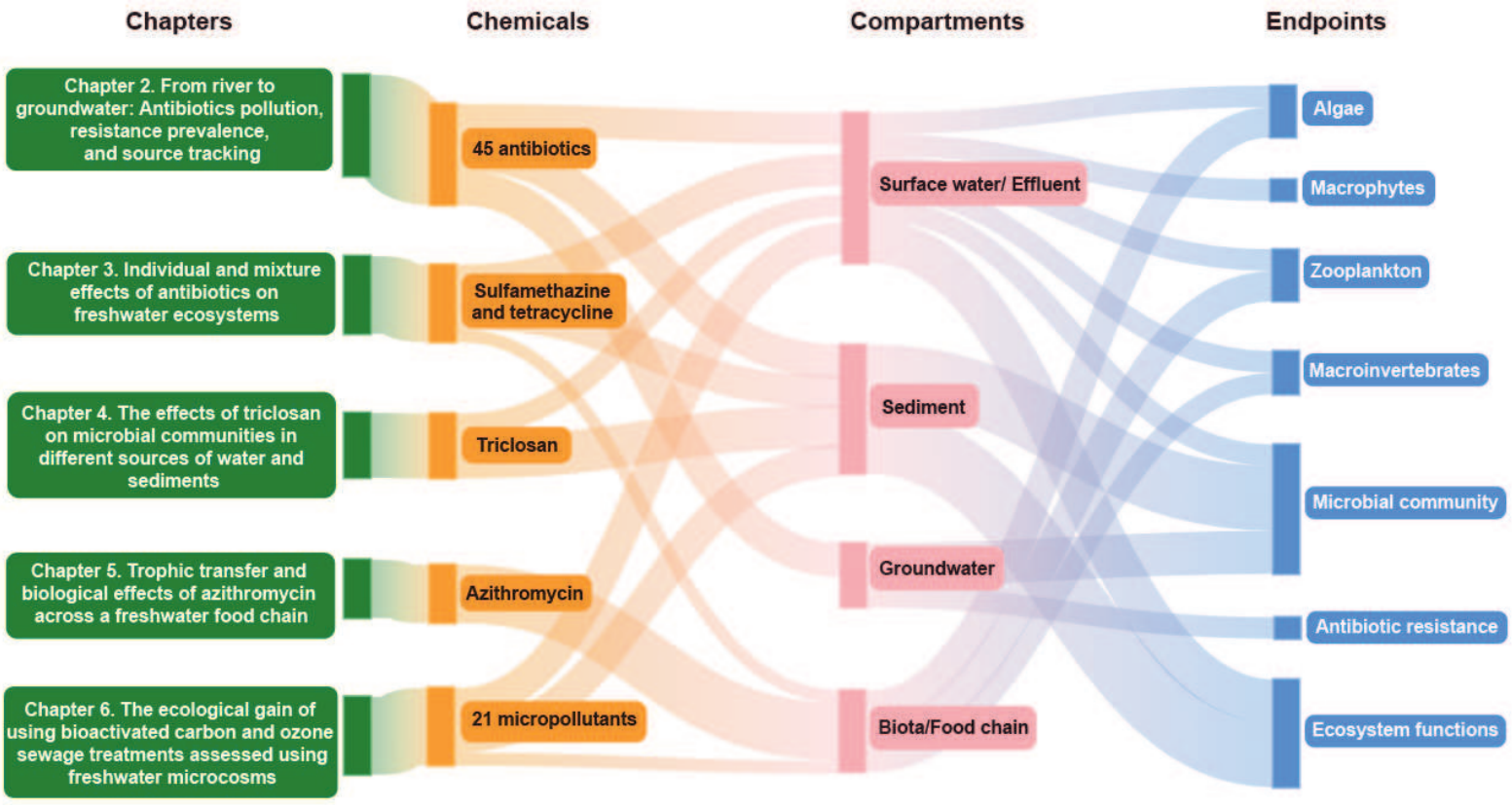


Figure 1.3. Overview of research chapters, focal contaminants, environmental compartments, and ecological endpoints examined in this thesis.



Kinderdijk，the Netherlands

Chapter 2

From river to groundwater: Antibiotics pollution, resistance prevalence, and source tracking

Dailing Wu, Hong Bai, Liang-Ying He, Lu-Xi He, Fang-Zhou Gao, Chong-Xuan Liu, Paul J. Van den Brink, Hauke Smidt, Guang-Guo Ying

This chapter is based on: Wu, D., Bai, H., He, L.Y., He, L.X., Gao, F.Z., Liu, C.X., Van den Brink, P.J., Smidt, H. and Ying, G.G., 2025. From river to groundwater: Antibiotics pollution, resistance prevalence, and source tracking. *Environment International*, 196, p.109305.

Abstract

The extensive use of antibiotics has led to their frequent detection as residues in the environment. However, monitoring of their levels in groundwater and the associated ecological and health risks remains limited, and the impact of river pollution on groundwater is still unclear. This study focused on the highly urbanized Maozhou River and its groundwater. Forty-five antibiotics and microbial community composition were analyzed by high-resolution LC-MS/MS and *16S rRNA* gene sequencing, respectively. These endpoints were measured in sediment, surface- and groundwater sampled during wet and dry seasons, while isolation and resistance profiling of *Escherichia coli* was performed in groundwater. This study aimed to assess the ecological and health risks posed by antibiotics in the Maozhou River and its groundwater, to assess the prevalence and type of antimicrobial resistance in *Escherichia coli*, and to trace the sources of antibiotic resistance genes (ARGs) in groundwater. Multiple antibiotics detected in the river and sediment were predicted to pose high risks to algae growth and bacterial resistance selection. In groundwater, the antibiotics erythromycin and norfloxacin were predicted to pose a medium risk to algae and a low risk towards bacterial resistance. Furthermore, significant positive correlations were observed between several predominant bacterial phyla in the river and groundwater and the detected antibiotics, suggesting a possible effect of local antibiotic residues on bacterial community composition. Antimicrobial susceptibility testing of 76 *Escherichia coli* isolates revealed 74% exhibited resistance to at least one tested antibiotic and 7.9% exhibiting multidrug resistance, which was confirmed by ARG-targeted PCR analysis. SourceTracker analysis of ARGs in groundwater indicated that ARG contamination in shallow groundwater was primarily from river sediments, while contamination in deeper groundwater originated mainly from river water. The results emphasize the need to address river pollution, as it directly impacts groundwater quality, particularly in areas with severe antibiotic contamination.

2.1 Introduction

Antibiotics are extensively used in human and veterinary medicines for therapeutic treatment of infectious diseases, and also in aquaculture and livestock farming as growth promoters (Yang et al., 2024). However, the excessive use of antibiotics has led to their continuous release into the environment (Balzer et al., 2016), along with their metabolic byproducts, resulting in frequent detection in aquatic environments (Liu et al., 2018). Over the past two decades, more than 100 studies in Europe have reported the presence of antibiotics in aquatic environments, with concentrations typically ranging from tens to several hundred ng/L (Carvalho and Santos, 2016). In China, over 100 studies related to surface water have reported the occurrence of 94 antibiotics, most of which have median concentrations below 100 ng/L (Li et al., 2020c). Antibiotic pollution could furthermore lead to a selective pressure on bacteria in these environments and promote the development and dissipation of antibiotic resistance genes (ARGs) (Brüssow, 2024), and negatively impacting non-target species, biodiversity, and ecological functioning (Kar and Roy, 2012; Kovalakova et al., 2020). Antibiotics and ARGs can infiltrate groundwater through various pathways, including rainfall percolation, river recharge, lateral recharge of bedrock fractures, and irrigation return flow (Ying et al., 2011). Once in the groundwater, these contaminants may disrupt microbial communities and accelerate the spread of resistant bacterial strains, posing significant threats to public health and ecosystem stability. However, due to the difficulty of studying groundwater, the extent of antibiotic pollution in groundwater remains poorly understood. As of July 2019, only 12 studies have reported the presence of antibiotics in Chinese groundwater, documenting 45 antibiotics, most of which have median concentrations below 10 ng/L (Li et al., 2020c). Therefore, it is crucial to gain a deeper understanding of antibiotic pollution in groundwater and its potential ecological risks.

Escherichia coli is a member of the commensal microbial community in the intestines of humans and other warm-blooded animals (Hu et al., 2020). It is commonly used as a microbial parameter related to the quality of groundwater and drinking water (Heijnen et al., 2024), and as an indicator for the level of antimicrobial resistance among Gram-negative bacteria (EFSA, 2007). As infections may be transferred from animals to humans through the consumption of food and/or water contaminated with zoonotic pathogens such as *E.coli*, monitoring fecal indicators and pathogens in groundwater is crucial (Economides et al., 2012). Additionally, gut symbiotic antibiotic-resistant bacteria have been reported as significant reservoirs of ARGs, with bacteria acquiring ARGs through horizontal gene transfer from resistant strains (Carlet, 2012; Szmolka and Nagy, 2013). The presence of antibiotic-resistant *E. coli* in groundwater reflects broader trends in intestinal resistance, with multidrug-resistant strains posing a substantial health threat.

In our previous research, we discovered significant ARG contamination in the groundwater of the Maozhou River and speculated that this pollution might originate from surface sources (Wu et al., 2020). To further explore the impact of river pollution on groundwater, we introduced the SourceTracker tool as a continuation of our study. SourceTracker is a Bayesian model-based method used to estimate the proportion of pollutants from various sources in a given environment (Knights et al., 2011). This study represents one of the first applications of SourceTracker in a highly urbanized river-groundwater system, offering a novel approach to quantitatively link surface water pollution with groundwater contamination. Several studies have successfully applied SourceTracker to trace the sources of ARGs, for example in the air of railway station (Bai et al., 2023), deep-sea environments (Henry et al., 2016), and household drinking water (Wang et al., 2023). Additionally, since a large proportion of environmental bacteria cannot be detected using traditional culture methods (Nesme et al., 2014), and the correlation between genotype and phenotype is often unclear, culture-dependent methods are not suitable for tracking ARG contamination (Wang et al., 2023). In contrast, metagenomic sequencing and/or high-throughput quantitative PCR (HT-qPCR) have proven to be more effective tools.

The Maozhou River is one of five major rivers in Shenzhen, China, and is a typical highly urbanized river, heavily polluted by anthropogenic activities. In this study, we estimate the ecological risks of antibiotic pollution in the Maozhou River and the groundwater beneath for different seasons, the association of these antibiotic residues with differences in microbial community distribution, the trends of resistance prevalence in *E.coli* found in the groundwater of this region, and the application of SourceTracker for identifying potential sources of ARGs in groundwater. Our research aims to address the following questions: 1) What are the risks posed by the levels of antibiotics measured in the Maozhou River and its groundwater? 2) What is the pattern of ARG prevalence in *E.coli* found in groundwater? and 3) To what extent does river pollution contribute to ARG contamination in groundwater? The findings of this study aim to contribute to the management of antibiotic pollution in urban rivers and the control and prevention of groundwater contamination.

2.2 Materials and methods

2.2.1 Study area and sample collection

Shenzhen is a megacity located in southern China with a population of more than 17 million. The Maozhou river is one of five major rivers in Shenzhen city with a length of 31 km and 54 branches (Bureau, 2022). As part of the Pearl River Estuary system, it originates from

Yangtai Mountain Forest Park and flows to the Lingdingyang Sea. The river is seriously polluted with urban wastewater containing antibiotics (Bureau, 2022). Furthermore, the groundwater in this region is heavily exploited and consumed for various purposes.

Considering the shallow groundwater table and permeable aquifer in the Pearl River Delta region, the antibiotics in the Maozhou River have the potential to leach into groundwater. To assess this possible source of antibiotics in groundwater, river water samples (R1-R6) and corresponding sediment samples (S1-S6) were collected from the upper reach to lower reach of the Maozhou River (Fig. 2.1). The pollution in the lower reach of the Maozhou River is expected to be higher than in the upper reach due to the higher population density in the lower region. In addition, a water sample was collected from Shiyan Reservoir (SYR) as control of river water. The sediment samples in Shiyan Reservoir and Yangtai Mountain (S-SYR and S-YTM) were collected as control sediments. These control sites were assumed to be pristine.

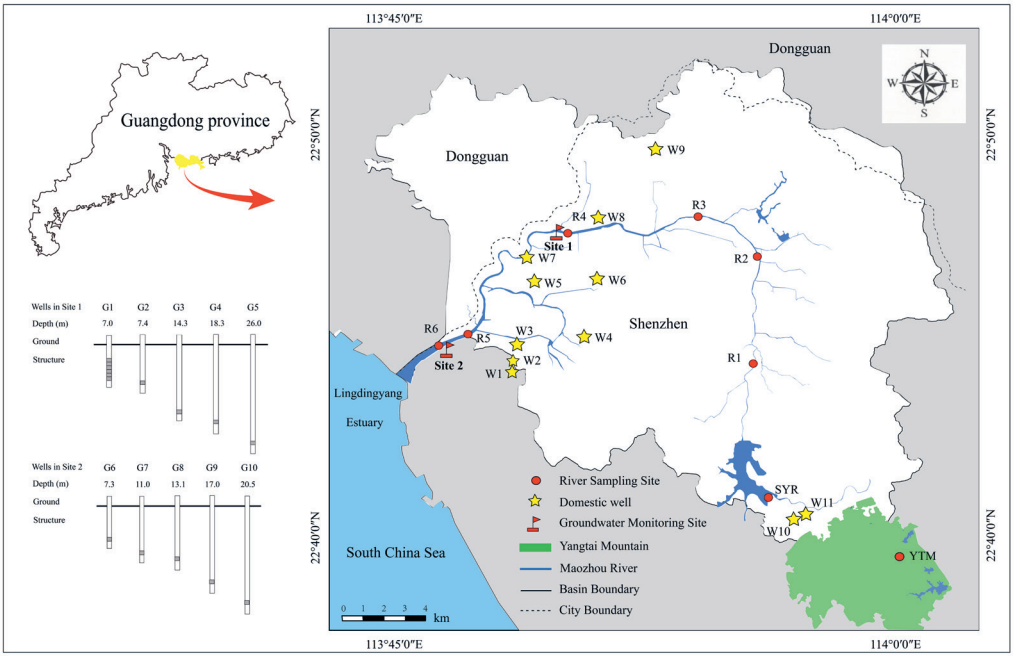


Figure 2.1. The map shows the sampling sites of Maozhou River and groundwater wells. G1-G10 represent groundwater from monitoring sites, with G1-G5 located at Site 1 and G6-G10 located at Site 2; W1-W11 represent groundwater from domestic wells; R1-R6 represent river water monitoring sites, while the corresponding sediment samples collected from these sites are labeled as S1-S6 in the results. SYR and YTM refer to Shiyan Reservoir and Yangtai Mountain, respectively, which are used as reference sites.

Two groundwater monitoring locations along the Maozhou River, referred to as Site 1 and Site 2, were chosen as depicted in Fig. 2.1. Each site was equipped with five pumping wells at varying depths. At Site 1, wells G1 through G5 had depths ranging from 7.0 m to 26 m. At Site 2, located near the Lingdingyang estuary, wells G6 through G10 spanned from 7.3 m to 20.5 m. Additionally, spring water was sampled from a site presumed to be pristine in Yangtai Mountain (YTM).

In our previous study (Wu et al., 2020), a large presence of total coliforms was detected in the groundwater monitoring wells, with even some detections in the YTM spring water, warranting great attention to the antibiotic resistance patterns in this region. Thus, we visited local residences and investigated the use of domestic wells in the Maozhou River basin. In addition to the 10 monitoring wells along the river (Site 1 and 2), we added 11 domestic wells (W1 to W11) from this area into our research on antibiotic resistance in *E.coli* (Fig. 2.1).

Based on the influence of monsoon circulation and water vapor transport, the year in South China is usually divided into wet season (April to September) and dry season (October to March) (Lai et al., 2022). In this study, samples were collected in June and December 2018, which represent the wet season and dry season in Southern China, respectively. The sample collection process, water quality parameters, and the physico-chemical properties of the sediment are provided in supplementary Text S1 and supplementary Tables S1, S2, and S3.

2.2.2 Antibiotic analysis

Extraction procedures and the methods of analytical measurement for antibiotics were adapted from a previous study (Zhou et al., 2012). The detailed extraction procedures for water and sediment samples can be found in Text S2. Agilent 1200 series HPLC coupled with a triple quadrupole mass spectrometer was used to analyze the 45 target antibiotics extracted from water and sediment samples, and Agilent Mass Hunter B 02.01 software was used to conduct qualitative and quantitative analysis of the antibiotics detected in the samples. Instrument parameters, methods such as the injection mode and the detection and quantitation limits of antibiotics (Tables S4 and S5) in various samples were based on our previous paper (Zhou et al., 2012).

2.2.3 Microbial community

Total DNA was extracted from water and sediment samples using the DNeasy® PowerSoil® kit (QIAGEN, Germany) according to the manufacturer's instructions. The concentration and purity of the extracted DNA were measured using a Nanodrop spectrophotometer (Nanodrop

Onec, Termo Scientific, USA). The extracted DNA was stored at -80 °C for *16S rRNA* gene sequencing.

The hypervariable region V3-V4 of the bacterial *16S rRNA* gene was amplified with primer 338F (ACTCCTACGGGAGGCAGCAG) and 806R (GGACTACHVGGGTWTCTAAT). Subsequently, the purified amplicons were sequenced on an Illumina MiSeq PE300 platform (Illumina, San Diego, USA) according to the standard protocols by Majorbio Bio-Pharm Technology Co. Ltd. (Shanghai, China). All of the sequence reads are available at the Sequence Read Archive of the National Center for Biotechnology information (accession number PRJNA1170186). Detailed information can be found in Text S3.

2.2.4 *E. coli* identification and antibiotic resistance determination

The water samples from monitoring and domestic wells were serially 10-fold diluted (1 ~ 103 fold) with physiological saline, and 0.1 mL of the sample was cultured on MacConkey agar (Thermo Scientific™, USA) and incubated at 37 °C for 14 to 16 h. The pink and red colonies were selected and purified, and then inoculated on Eumelam culture medium (Thermo Scientific™, USA) for identification, and the purplish-black colonies with green metallic luster were identified as *E.coli*.

Antimicrobial susceptibility testing was performed using the agar dilution method on Mueller–Hinton agar according to Clinical and Laboratory Standard Institute (CLSI) (Humphries et al., 2021). Seven antibiotics representing six different types of antibiotics were tested on all *E.coli* isolates, including kanamycin (aminoglycoside), gentamicin (aminoglycoside), tetracycline (tetracycline), ampicillin (β-lactams), chloramphenicol (chloramphenicol), ciprofloxacin (quinolone) and meropenem (carbapenem). Multidrug resistance is defined as an organism's resistance to at least one antibiotic in three or more distinct antibacterial categories (Magiorakos et al., 2012). *E.coli* ATCC25922 was taken along for quality control in antimicrobial susceptibility testing. The results were analyzed and interpreted according to CLSI guidelines (Humphries et al., 2021).

The 18 antibiotic resistance gene subtypes conferring resistance to aminoglycosides (*aadA*), tetracyclines (*tetC, tetG, tetH, tetO, tetW and tetB/P*), sulfonamides (*sul1* and *sul2*), β-lactams (*blaTEM*), chloramphenicol (*cfr, feixA, floR* and *cmlA*), quinolones (*qnrD* and *qnrS*), macrolides (*ereA*), polypeptides (*mcr-1*) and three different mobile genetic elements (MGEs) (*intl1, intl2,* and *tn916/1514*) were determined in *E.coli* isolates by PCR. The primers and PCR conditions are shown in Table S6.

2.2.5 Risk assessment

2.2.5.1 Ecological risk assessment of antibiotics

The ecological risks of residual antibiotics in the Maozhou River and its groundwater were assessed by calculating the risk quotient (RQ):

$RQ_{Ecotox} = MEC/PNEC_{Ecotox}$

where MEC represents the maximum measured environmental concentration of a given antibiotic, and $PNEC_{Ecotox}$ represents the predicted no effect concentration to aquatic organisms. The PNECs were obtained from NORMAN ecotoxicology database (https://www.norman-network.com/nds/ecotox/). However, it should be noted that the Norman Ecotoxicology Database reports a lowest PNEC of ofloxacin based on fish toxicity, while the PNEC values for the other antibiotics are derived from primary producers such as algae, identified as the most sensitive taxa. Therefore, we calculated the PNEC value of ofloxacin based on its toxicity to algae (Zhou et al. (2016). RQ_{Ecotox} values above 1 indicate a high ecological risk to aquatic organisms, $0.1 < RQ < 1$ indicates a medium risk, and $RQ < 0.1$ represents a low risk (Li et al., 2015a). The PNEC values for ecotoxicological effects and their assessment factors are provided in Tables S7 and S8.

2.2.5.2 The risk of antibiotic resistance selection

The potential resistance selection risks of the detected antibiotics to bacteria were evaluated by the same formula:

$RQ_{RS} = MEC/PNEC_{RS}$

where the $PNEC_{RS}$ values were obtained from previous studies (Bengtsson-Palme and Larsson, 2016; He et al., 2023). Similar to the classification used for ecological risk evaluation, RQ_{RS} values above 1 indicate a high risk of antibiotic resistance selection, whereas $0.1 < RQ < 1$ and $RQ < 0.1$ represent medium risk and low risk, respectively.

2.2.5.3 Antibiotic resistance in *E. coli*

The multiple antibiotic resistance (MAR) index was employed to assess the degree of multi-antibiotic resistance among *E. coli* isolates. Calculation of the MAR index followed the formula $MAR = A/(N \times B)$, where A represents the total number of antibiotics to which each strain exhibits resistance at a specific sampling site, N represents the number of isolated strains from that site, and B is the total number of tested antibiotics. A MAR index ≤ 0.2 suggests

a low potential risk of antibiotic contamination in the tested environment. Conversely, sites with MAR indices > 0.2 are considered to represent a potentially high-risk source of antibiotic exposure (Bai et al., 2022; Krumperman, 1983).

The multiple antibiotic resistance genes index was used to assess the presence of multiple antibiotic resistance genes in isolates, based on the MAR index. The MARG index was calculated by MARG = A/(N × B), where A represents the total number of ARGs detected in each strain at a given sampling site, N represents the number of isolated strains from that site, and B is the total number of tested ARGs.

2.2.6 Groundwater ARG pollution source tracking

The ARG profile for the Maozhou River and its groundwater was obtained from our previous study (Wu et al., 2020). SourceTracker employs a Bayesian approach to compare ARG profiles in 'sources' with those in 'sinks', estimating the contribution of each source to the sinks (Knights et al., 2011). A total of 190 ARG subtypes were used as potential resistance group sources, with river water and sediment samples serving as the source samples and groundwater as the sink. The computational pipeline followed the procedure outlined by Bai et al. (2023).

2.2.7 Statistical analysis and data visualization

The sampling site map was plotted using Adobe Illustrator 2024, while the bar charts and box plots were generated using Origin 2024. Multivariate analyses (principal component analysis) and Monte Carlo permutation tests to show and evaluate the significance of the correlations between antibiotics detected in Maozhou River and its groundwater and the corresponding microbial communities at the phylum level were performed and visualized using Canoco 5 (ter Braak and Šmilauer, 2012). Statistical tests including One-way ANOVA, Hotelling's T2 test, Two-Proportion Z-test and Kruskal-Wallis H test were conducted using the stats package in R 3.3.1 and the scipy package in Python (v.1.0.0).

2.3 Results

2.3.1 Concentrations of antibiotics in Maozhou River and groundwater

By using LC-MS/MS, we targeted 45 antibiotics for analysis of river water, sediment and groundwater samples taken during the wet season and the dry season in 2018. In river water, 14 and 15 antibiotics were detected with total concentrations ranging from 205 to

421 ng/L and from 194 to 461 ng/L, respectively, in wet and dry season samples (Fig. 2.2a). Erythromycin-H_2O and lincomycin were detected with highest concentrations in both seasons, followed by sulfapyridine and sulfamethoxazole (Fig. 2.2a). Among detected antibiotics, sulfonamides were the most frequently detected antibiotics in river water, followed by macrolides. In the SYR control, 10 and six antibiotics were detected in the wet and dry season, respectively, with concentrations amounting to 39 and 18 ng/L, respectively. The concentration of total antibiotics at the lower reach sampling locations (R4 to R6) was significantly higher than that in the upper reach (R1 to R3) in the wet season (Fig. 2.2a, $P < 0.05$). There were no significant differences in the total antibiotic concentrations or the concentrations of individual antibiotics between the wet and the dry season ($P > 0.05$).

Nineteen antibiotics were detected in the sediment during both seasons (Fig. 2.2b). The total concentration of antibiotics in sediment during the wet and dry season ranged from 100 to 1,497 ng/g and 636 to 3,696 ng/g, respectively. Oxytetracycline and tetracycline were the most abundant antibiotics, followed by ofloxacin and norfloxacin. In sediment, quinolones were the most prevalent antibiotics, followed by tetracyclines. In the wet season, eleven antibiotics were detected at S-SYR and seven at S-YTM, with total concentrations of 54 and 11 ng/g, respectively. During the dry season, the number of detected antibiotics decreased to eight at S-SYR and six at S-YTM, with total concentrations of 23 and 18 ng/g, respectively. Similar to river water, the concentration of total antibiotics in lower reach samples (S4 to S6) was significantly higher than that in upper reach samples (S1 to S3) in the wet season (Fig. 2.2b, $P < 0.05$). No significant difference was observed in the total concentrations of antibiotics between the wet and dry seasons ($P > 0.05$). However, the concentration of ofloxacin in the dry season was significantly higher than that in wet season ($P < 0.05$). Moreover, the total antibiotic concentrations at R1 and S1 during the dry season were significantly higher than during the wet season ($P < 0.05$).

In groundwater, 10 and 11 antibiotics were detected during the wet season and the dry season, with total concentrations ranging from 9 to 38 ng/L and 9 to 177 ng/L, respectively (Fig. 2.2c). Sulfamethazine, norfloxacin, erythromycin-H_2O, lincomycin, clarithromycin, sulfathiazole, sulfadiazine, sulfamonomethoxine, sulfachloryridazine and ofloxacin were detected in both seasons while sulfapyridine was only detected during the dry season. Among the detected antibiotics, sulfamethazine, erythromycin-H_2O and lincomycin were detected from all sites in both seasons. The highest antibiotic concentrations were found in the groundwater from the deepest well of Site 1 (G5) during both seasons. Specifically, the concentrations of sulfamethazine at G5 were significantly higher than those in the other wells ($P < 0.05$). However, the total antibiotic concentrations showed no significant difference between the wet and dry seasons ($P > 0.05$). In the spring water of YTM, serving as the reference point for groundwater, six and four antibiotics were detected in both

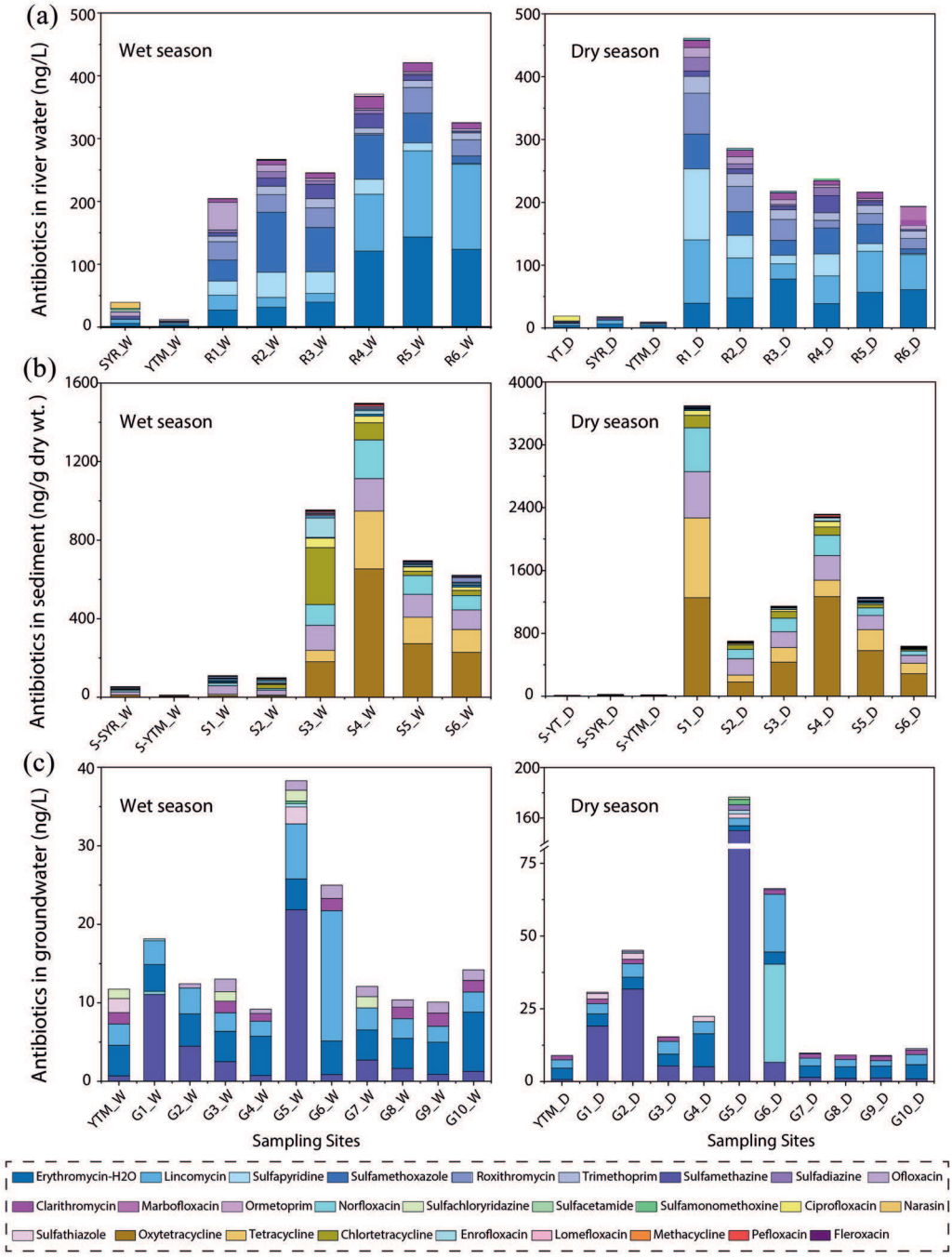


Figure 2.2 Antibiotics detected in Maozhou river water (a), in sediment (b) and in groundwater (c) during wet season (left column) and dry season (right column). Antibiotics with detected concentrations below the quantification limit are not presented in the results. Please note the difference in scale between the different figures.

seasons, with concentrations of 12 and 9 ng/L during wet season and dry season, respectively.

2.3.2 Risk assessment of the antibiotic residues in Maozhou River and groundwater

Based on RQ values, several antibiotics were identified as posing varying levels of ecological and resistance selection risks across different environmental compartments. Erythromycin-H_2O in river water, as well as oxytetracycline, tetracycline, ofloxacin, norfloxacin, chlortetracycline, ciprofloxacin, and enrofloxacin in sediment, posed high toxic risks (RQ > 1) to algae during both seasons (Fig. 2.3a), with ofloxacin in river water showing an additional high risk during the wet season. Medium ecological risks (0.1 < RQ < 1) were observed for roxithromycin in river water and for lincomycin, methacycline, roxithromycin, pefloxacin, and fleroxacin in sediment in both seasons (Fig. 2.3b). In groundwater, erythromycin-H_2O posed medium ecological risks in both seasons, while ofloxacin presented medium risk in the dry season and low risk (0.01 < RQ < 0.1) in the wet season. Lincomycin and clarithromycin consistently exhibited low ecological risks, and sulfamethoxazole was classified as low risk only during the dry season (Fig. 2.3c).

Regarding the resistance selection risks, oxytetracycline, ofloxacin, ciprofloxacin, enrofloxacin, and roxithromycin in sediment consistently posed high risks across both seasons, while tetracycline, chlortetracycline, lincomycin, and sulfamethopyrazine in sediment exhibited medium risks (Fig. 2.3e). In river water, erythromycin-H_2O showed a medium risk level during the wet season and a low risk level in the dry season, whereas trimethoprim, roxithromycin, lincomycin, clarithromycin, and ofloxacin presented low resistance selection risks throughout both seasons (Fig. 2.3d). In groundwater, norfloxacin, erythromycin-H_2O, and lincomycin were associated with low resistance selection risks during the dry season (Fig. 2.3f).

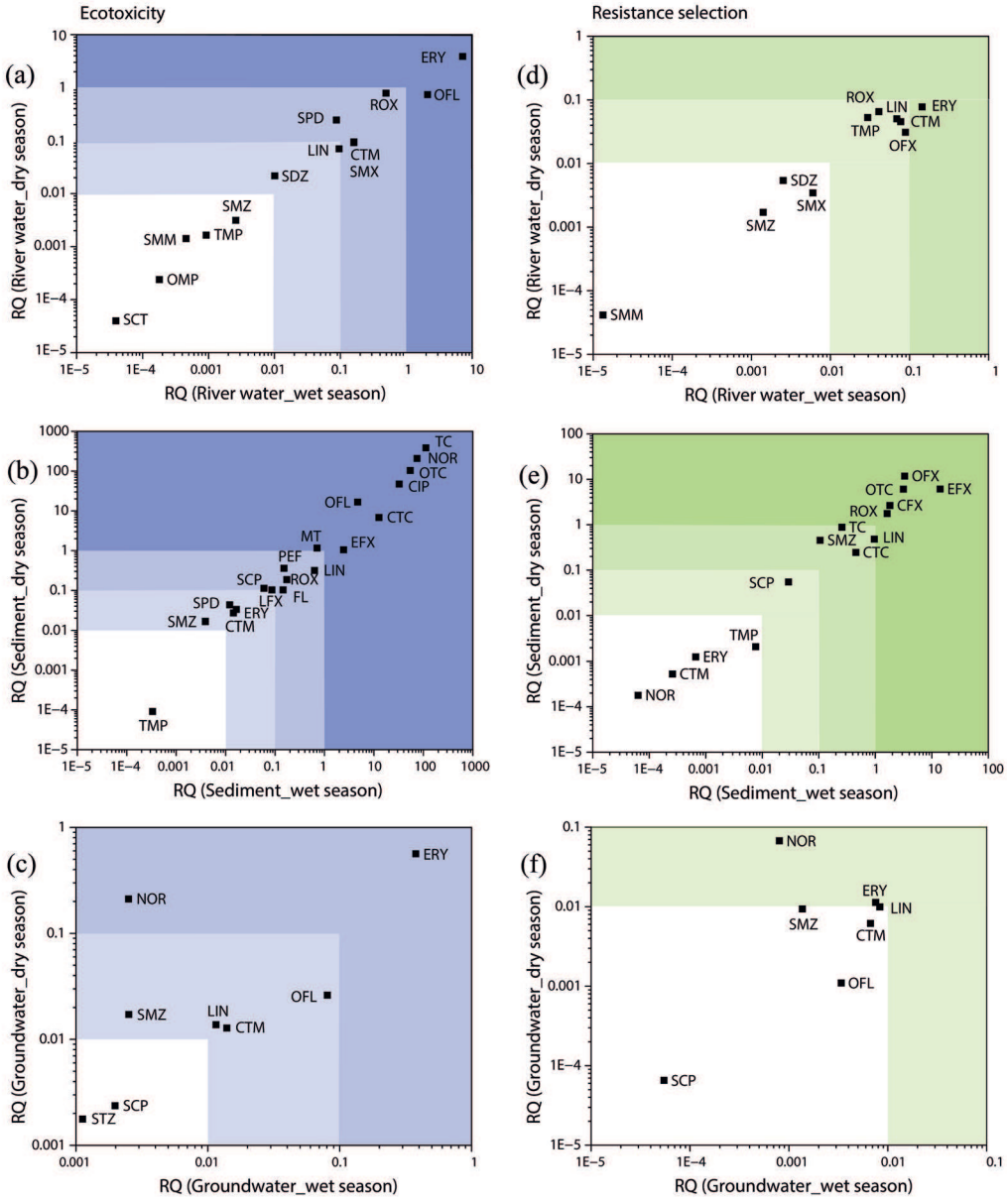


Figure 2.3 Risk assessment of the detected antibiotics from river water (a, d), sediment (b, e) and groundwater (c, f) for green algae (left column) and antibiotic resistance selection (right column) during both seasons. (RQ > 1: High risk; 0.1 < RQ < 1: Medium risk; 0.01 < RQ < 0.1: Low risk; RQ < 0.01: No risk. The explanation for antibiotic abbreviations are provided in Session 2.2.2.)

2.3.3 Microbial communities in Maozhou River and groundwater, and correlations with antibiotics

Microbial community composition was measured based on bacterial *16S rRNA* gene fragments PCR-amplified from the different samples and sequenced using Illumina technology. Overall, approximately 2.3 million high-quality sequence reads were acquired after denoising and filtering, and a total of 2,690 OTUs remained after rarefaction to 12,681 reads, in which 46 bacterial phyla and 838 genera were annotated. The detailed composition of the microbial communities can be found in Fig. S1. Monte Carlo permutation tests revealed significant differences in the microbial community composition among groundwater, river water, and sediments in the Maozhou River ($P < 0.05$), while no significant differences were observed between seasons ($P > 0.05$). Among the 15 most abundant bacterial phyla detected in the data, *Patescibacteria* and *Verrucomicrobiota* were primarily distributed in river water, whereas *Firmicutes* and *Chloroflexi* were mainly present in sediments (Fig. 2.4). Several bacterial phyla, such as *Actinobacteriota*, *Bacteroidota*, *Planctomycetota*, and *Gemmatimonadota*, exhibited high relative abundance in both river water and sediments. *Proteobacteria* showed relatively high relative abundance in both river water and groundwater, particularly dominating in groundwater. Additionally, it is noteworthy that *Campilobacterota* was also highly abundant in groundwater, together with *Proteobacteria* forming the two major bacterial phyla in the Maozhou River groundwater. No significant differences were found in richness and diversity between seasons among each type of samples (Kruskal-Wallis H test, $P > 0.05$) (Table S9). Not surprisingly, the richness and diversity in river water and sediment were significantly higher than those in groundwater during both seasons (Kruskal-Wallis H test, $P_{adjusted} < 0.001$) (Fig. S2).

The PCA results showed that a positive correlation between the relative abundance of *Patescibacteria* and *Verrucomicrobiota* and the concentrations of trimethoprim, sulfamethoxazole, roxithromycin, and clarithromycin. Similarly, *Firmicutes* showed a positive correlation with several antibiotics predominantly detected in sediments, including norfloxacin, ciprofloxacin, and oxytetracycline. Moreover, a positive correlation was observed between methacycline and *Myxococcota* (Fig. 2.4).

When analyzing the data at the genus level as the highest attainable taxonomic resolution (Fig. S3), an intriguing pattern was observed at groundwater Site 2 during the wet season. As the well depth increased, beginning with well G7, the main genera detected in each successive well overlapped with those of the previous one, but the most dominant genus shifted. This pattern indicates that the dominant bacterial genera at groundwater Site 2 varied with depth, showing systematic changes in the composition of microbial communities as depth increased.

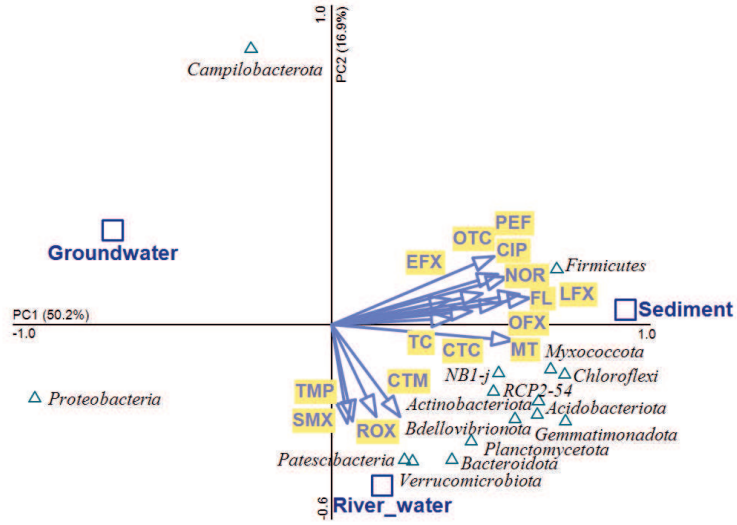


Figure 2.4. Principal Component Analysis (PCA) biplot between antibiotics detected in Maozhou River and its groundwater and the corresponding microbial communities at the phylum level. The 15 most abundant phyla across the entire dataset were shown, and only the antibiotics that significantly explained the model were included (Monte Carlo permutation test, $P < 0.05$).

2.3.4 Antibiotic resistance profiles of groundwater-derived isolates of *E. coli*

From all the groundwater samples, a total of 76 strains of *E. coli* were isolated: nine from monitoring Site 1, 17 from monitoring Site 2, and 50 from domestic wells (Table 2.1). Notably, at least one *E.coli* isolate was obtained from each groundwater sampling well. Two *E.coli* strains were isolated from the spring water of YTM. The results of phenotypic resistance assessment indicated that 56 isolates (74%) exhibited resistance to at least one antibiotic. The most prevalent resistance observed was against ampicillin, with 51 strains (67%) showing resistance, accounting for 91% of all the resistant *E.coli* isolates. The resistance to ampicillin was significantly higher than that to other antibiotics (Two-Proportion Z-test, $P < 0.05$). Remarkably, nine of these strains could survive at the highest tested concentration (128 μg/ml). Tetracycline resistance was the second most prevalent, found in 24 strains (32%), with 10 capable of surviving at the highest tested concentration. Additionally, six *E. coli* strains (7.9%) were identified as multi-drug resistant, showing resistance to three or more antibiotic classes.

Further genetic analysis revealed that 56 strains were found to carry more than one ARG or MGE, with the *blaTEM* (51) being the most frequently detected, which was significantly higher than the other genes (Two-Proportion Z-test, $P < 0.05$), followed by *qnrD* (21), *qnrS*

(13), and *ereA* (13) (Table 2.1). Notably, 12 isolates carried more than three resistance genes, with two strains even carrying more than five. Among the *E. coli* strains isolated from YTM, one showed resistance to ampicillin and tetracycline and carried the *sul1* and *sul2* genes.

Interestingly, among all isolated *E. coli* strains, 13 carried more than one ARG but showed no resistance to any of the tested antibiotics. Moreover, 13 strains did not carry any of the tested genes yet exhibited resistance to ampicillin. Additionally, seven isolates neither carried any of the tested ARGs nor showed resistance to antibiotics, with another *E.coli* isolate obtained from the YTM displaying the same characteristics. Based on these data, the MAR and MARG values from all groundwater sites were at a low-risk level (< 0.2), except for Site 1, where the MAR value was 0.25, indicating a higher risk of antibiotic contamination in *E. coli* at that location (Table 2.1).

Table 2.1. Antibiotic resistance profiles of *E.coli*

		Groundwater (N = 76[a])						Reference site (N = 2)	
		Site 1 (n = 9[b])		Site 2 (n = 17)		Domestic wells (n = 50)		YTM (n = 2)	
	Antibiotic (ug/mL)	Resistant isolates	$Isolates_{maximal\text{-}conc}$[e]	Resistant isolates	$Isolates_{maximal\text{-}conc}$	Resistant isolates	$Isolates_{maximal\text{-}conc}$	Resistant isolates	$Isolates_{maximal\text{-}conc}$
Resistance phenotype[c]	AMP (32, ~128)[d]	55.6%	5	70.6%	12	68%	34	50%	1
	KM (64, ~256)	22.2%	2	5.9%	1	/		/	/
	CL (32, ~128)	44.4%	4	17.6%	3	2%	1	/	/
	GM (16, ~64)	/	/	/	/	2%	1	/	/
	TC (16, ~128)	55.6%	5	17.6%	3	32%	16	50%	1
Resistance genotype[f]	ARGs	*blaTEM, aadA, cfr, ereA, qnrD, qnrS, sul1, sul2, intl 1*		*blaTEM, cfr, ereA, qnrD, qnrS, sul1*		*blaTEM, aadA, cfr,ereA, qnrD, qnrS, sul1, tetC, intl1, intl2*		*sul1, sul2*	
Resistance index	MAR[g]	0.25		0.16		0.15		0.07	
	MARG[h]	0.12		0.04		0.07		0.06	

/: Not detected.
a N: Total number of isolates.
b n: Number of isolates from each site.
c AMP, Ampicillin; KM, Kanamycin; CL, Chloramphenicol; GM, Gentamicin; TC, Tetracycline.
d (CLSI MIC Breakpoints, ~maximal tested concentration, μg/mL).
e Number of isolates with resistance at maximal tested concentration.
f Positive genes.
g MAR: multiple antibiotic resistance index.
h MARG: multiple antibiotic resistance gene index.

2.3.5 Source tracking of ARGs in groundwater

Source tracking of ARGs indicated that at groundwater monitoring Site 1, a significant proportion of ARG pollution in the shallow wells (G1 and G2) originated from sediment (64.8% and 85.8%, respectively), with a smaller proportion coming from river water (30.6% and 11.4%, respectively) (Fig. 2.5). In contrast, for groundwater wells ranging from 14 to 26 m depth, the primary source of ARG pollution shifted to river water (80 ~ 95.2%). In contrast, at groundwater monitoring site 2, the source tracking results were more complex. In the shallowest well (G6), the ARG pollution sources resembled those at Site 1, with the majority of ARGs originating from sediment and a smaller portion from river water. Furthermore, at G8 (13.1 m) and G10 (20.5 m), river water remained the dominant source of ARGs. In contrast, at G7 and G9, the majority of ARGs were attributed to unknown sources (Fig. 2.5).

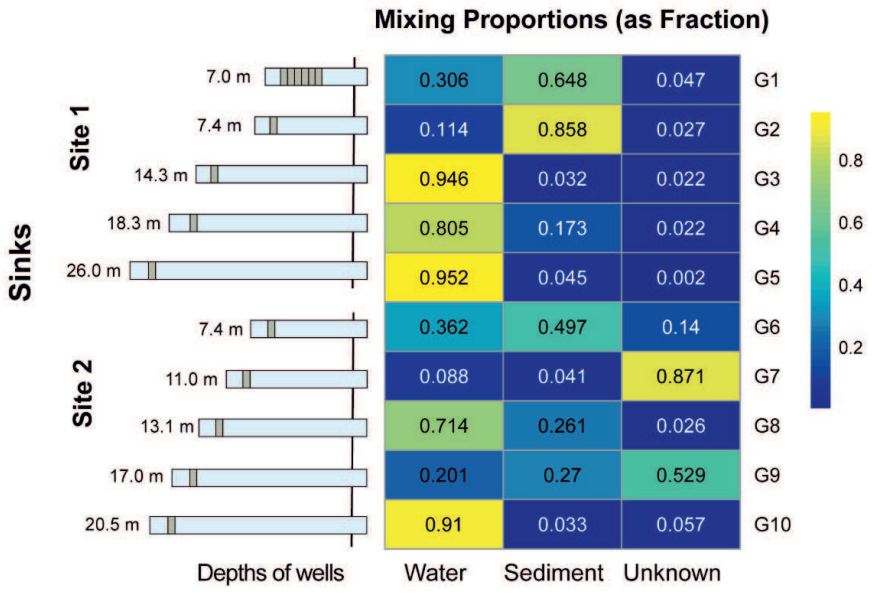


Figure 2.5 Source tracking of antibiotic resistance gene pollution in groundwater using SourceTracker. The numbers in the heatmap represent the proportion of pollutants entering the groundwater from river water, sediment, or unknown sources. The bluer the color, the smaller the proportion, while the yellower the color, the higher the proportion.

2.4 Discussion

2.4.1 Antibiotic pollution in Maozhou River and groundwater

The Maozhou River has drawn significant attention due to its severe pollution with, among other compounds, antibiotics. Compared with two other studies on the same river, the range of concentrations of antibiotics detected in our study was lower than that reported by Qiu et al. (2019) and Zhang et al. (2021), but the average concentration detected was higher than the concentrations found by Qiu et al. (2019) (245 ng/L). This finding underscores the variability in antibiotic concentrations within the same river, influenced by different sampling times and locations. Additionally, high concentrations of ofloxacin and norfloxacin were detected in sediments of the Maozhou River. Although the production and use of these two antibiotics were prohibited in food animals in China starting from September 1, 2015 due to potential safety hazards, and their registration ceased from September 1, 2015 (China, 2015), the continued detection of these antibiotics suggests the persistence of antibiotics or their continued use. Therefore, even after cessation or reduction in use, the environmental accumulation and ecological impact of these compounds warrant attention. Furthermore, many of the antibiotics detected in both the water and sediments of the Maozhou River pose medium to high risks to the growth of algae and the selection of bacterial resistance. This indicates an urgent need to address antibiotic pollution in the Maozhou River.

While the concentrations of antibiotics in the groundwater of the Maozhou River were nearly an order of magnitude lower than in surface water, the types of antibiotics detected in high concentrations were almost the same as those in the river water (Fig. 2.2). This may indirectly indicate the infiltration of river pollution into the groundwater, leading to its contamination (Huang et al., 2018). In this study, we conducted a comparative analysis of the concentrations of antibiotics detected in the groundwater of the Maozhou River with those reported in various other global locations, as detailed in Table S10. This comparison revealed that the concentrations of sulfamethazine, norfloxacin, and clarithromycin in the Maozhou River's groundwater were notably higher than the average levels found in other groundwater sources (Fig. 2.6). This comparison underscores a significant disparity in antibiotic pollution levels, positioning the groundwater of Maozhou River as an area of elevated concern. To this end, our results also indicate that the occurrence of some antibiotics in groundwater pose low risks for the selection of bacterial resistance, which should be a point of concern. In European countries (EMA, 2006), an environmental risk assessment is required for environmental concentrations exceeding 10 ng/L. Regrettably, a unified method for risk assessment of antibiotics in the water environment in China is yet to be established.

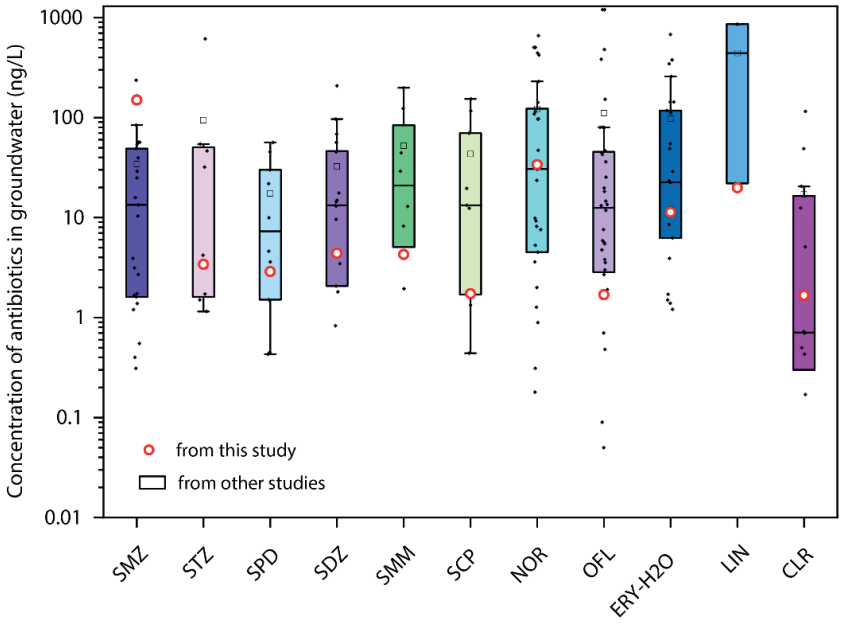


Figure 2.6 Comparison of the detected concentrations of antibiotics from the groundwater samples in this study with other studies all over the world (see Table S10 for details).

Additionally, the relative abundance of certain bacterial phyla, such as *Patescibacteria*, *Verrucomicrobiota*, *Firmicutes*, and *Myxococcota*, showed positive correlations with specific antibiotics, including a.o. trimethoprim, sulfamethoxazole and roxithromycin, suggesting their potential resistance to these compounds. Research has shown that antibiotics can indirectly affect ARGs by influencing microbial community structures (Zhang et al., 2021). The resistance of members of these bacterial phyla to the corresponding antibiotics is noteworthy. While mechanistic explanations for these correlations are meaningful, our current analysis, based on amplicon sequencing, is limited in providing detailed functional insights. Future research should focus on the response of microbial communities to different antibiotics and incorporate more advanced approaches, such as metagenomics, to gain a deeper understanding of the specific effects and underlying mechanisms.

2.4.2 Prevalence of antimicrobial resistance in *E.coli* isolated from groundwater

In our study, 74% of the groundwater-isolated *E. coli* showed resistance to at least one antibiotic, which is similar to the study of Anderson and Sobsey (2006) but much higher than the findings of Economides et al. (2012). Moreover, six out of 76 *E.coli* strains (7.9%) were identified as multidrug-resistant. In comparison, 64% of all isolates from groundwater in an irrigated agricultural region with a large number of intensive dairy farms in California

were multidrug-resistant (Li et al., 2015b). The *E. coli* isolates from the groundwater of Maozhou River showed the most prevalent resistance to ampicillin, followed by tetracycline, which is somewhat similar to a study in Kenya that found all *E.coli* isolates from residential groundwater resistant to ampicillin, tetracycline, cotrimoxazole, streptomycin, and sulfamethoxazole, with 50% showing resistance to gentamicin and chloramphenicol (Wahome et al., 2014). Furthermore, a study in the Mafikeng area of South Africa found that all 63 *E. coli* strains isolated from 19 groundwater samples were multidrug-resistant, with most strains showing high resistance to ampicillin, erythromycin, and vancomycin (Phokela et al., 2011). Hence, the prevalence of antibiotic resistance in *E. coli* in the groundwater of the Maozhou River is not as severe as reported in these aforementioned studies. The low MAR and MARG values obtained in this study indicated that the groundwater of Maozhou River basin was at low potential risk of having been contaminated by antibiotics, and a low risk level of spreading ARGs by *E.coli*. Yet, what is worth noting is that the MAR value at groundwater monitoring Site 1 was 0.25 (> 0.2), indicating a higher risk of antibiotic exposure. However, since only nine strains were isolated from this site, the results may not be highly representative, emphasizing the need for further research on antibiotic resistance in this area.

E. coli is a frequent cause of extraintestinal infections such as urinary tract and bloodstream infections (WHO, 2014), with pathogenic strains often leading to clinical symptoms like diarrhea and sepsis. The isolation of antibiotic-resistant strains from groundwater cannot be overlooked, especially the emergence of multidrug-resistant (MDR) strains. MDR *E.coli* poses a serious threat to public health by limiting treatment options and increasing morbidity and mortality rates associated with infections (Sidjabat and Paterson, 2015). These strains can be transmitted through contaminated water or food, or through contact with humans and other animals (Hu et al., 2020). The incidence and prevalence of infections caused by antimicrobial-resistant pathogenic *E. coli* are rapidly increasing globally (Thaden et al., 2016; WHO, 2014). In addition, *E. coli* is also a member of the commensal intestinal microbiota of humans and other warm-blooded animals. Its genetic flexibility not only ensures successful survival and growth under adverse environmental conditions, but also allows *E. coli* to serve as an efficient recipient and even a disseminator of newly introduced foreign genes through horizontal gene transfer (Szmolka and Nagy, 2013). As a result, MDR *E. coli* holds tremendous potential as a reservoir of antibiotic resistance (Szmolka and Nagy, 2013). Molecular epidemiological studies indicate that the resistance genes carried by MDR *E. coli* can effectively transfer to pathogenic *E. coli* strains or *Salmonella* within animal hosts, and vice versa (Nógrády et al., 2006). This highlights the importance of environmental exposure as a significant risk factor for the spread of fecal resistant *E. coli* and ARGs beyond traditional risks, such as prior antibiotic use (Hu et al., 2020). To mitigate the public health risks posed by MDR *E. coli*, it is crucial to implement actionable strategies such as improving water

treatment processes to reduce the contamination of groundwater by resistant bacteria, promoting the responsible use of antibiotics in agriculture and healthcare to curb the emergence of resistance, and increasing public awareness about the risks associated with environmental sources of antibiotic-resistant bacteria.

Furthermore, in our study, we discovered some *E. coli* strains that could survive at high concentrations of antibiotics without carrying corresponding resistance genes. This could be due to the induction or stress from exposure to other types of antibiotics, antiseptics, or heavy metals, or a combination thereof, leading to co-resistance. When the antibiotic resistance state is activated, multiple resistance mechanisms may be simultaneously triggered (Li et al., 2019). Studies have shown that *E. coli* strains, originally sensitive, not only developed resistance to ampicillin upon induction but also became multidrug-resistant, with their resistance spectrum expanding after induction (Li et al., 2019). Similar findings were observed by Zhang et al. (2016), where chloramphenicol induced a resistant state in sensitive *Shigella* strains, altering their resistance profile. Thus, *Shigella* not only became resistant to chloramphenicol but also to other types of antibiotics. This might partly explain why the presence of resistance genes does not always correlate directly with the local prevalent use of antibiotics. However, it is noteworthy that studies have found the MIC of antibiotics against bacteria increased with time and induced concentrations, indicating that without dosage restrictions, the resistance of bacterial strains could become more and more severe (Li et al., 2019).

2.4.3 The prediction of river contamination to groundwater

We previously detected 190 ARG subtypes in the Maozhou River and its groundwater. In this study, we further analyzed these subtypes using a validated Bayesian machine learning tool, SourceTracker, for source tracking (Knights et al., 2011). The contributions of river water and sediment to the ARG contamination in groundwater were predicted to be 8.8 to 95% and 3.2 to 86%, respectively. Given that river water is a key recharge source for groundwater in alluvial fan areas (Dun et al., 2014), pollutants from the river can potentially infiltrate into groundwater during the recharge process (Lapworth et al., 2009). This connection between river water and groundwater has also been demonstrated in the Yellow River delta, where research indicated that the Yellow River significantly influences groundwater flow in downstream and delta regions 20 to 40 km from the river (Chen et al., 2007). Additionally, a study employing the SWAT and SWAT-LUD models provided a qualitative assessment of the interaction between surface water and groundwater in the Maozhou River basin (Xu and Sun, 2021). The analysis revealed that lateral recharge from surface water to groundwater amounts to approximately 1.0×10^6 m^3 in 2017, along with the transport of NH_3-N (11 tons), TP (1.1 tons), and COD (510 tons). Moreover, floodplain

infiltration further contributes an estimated 6.7×10^6 m^3 of river water to groundwater recharge (Xu and Sun, 2021).

Interestingly, we observed a clear shift in the sources of ARG contamination across different groundwater depths. In shallower groundwater (< 7.4 m), ARG contamination was predicted to be predominantly sourced from sediments, while river water played a minor role. However, as groundwater depth increased (14 to 26 m), river water was predicted to become the primary contributor to ARG contamination. Numerous studies have demonstrated that aquifer microbial populations are closely associated to sediments (Anneser et al., 2010; Griebler et al., 2002). Zhai et al. (2021) conducted laboratorial leaching tests and found that the higher Fe- and Mn- bearing minerals in aquifer sediments, the higher the concentrations of Fe and Mn in groundwater after the release reaches kinetic equilibrium. It is estimated that the Maozhou River contains an approximately 4,000,000 m^3 of polluted sediment (Zhang and Xu, 2019), rich in organic matter and microorganisms, which have accumulated significant amounts of antibiotics and ARGs. Our previous study also showed that the proportion of shared ARGs between groundwater and sediments was as high as 70%. In shallow groundwater, sediments may contribute significantly to the diffusion and infiltration of antibiotic resistant microorganisms into groundwater. However, with increasing depth, changes in sediment permeability and stratigraphy are likely to occur. The Maozhou River, located in the southern central region of the Pearl River Delta, is largely covered by Quaternary sediments (Huang et al., 2018), which consist of interbedded a younger marine sequence (elevation > -20 meters), an older marine sequence (elevation between -15 and -40 meters), and a younger terrestrial sequence. The younger terrestrial sequence, composed of sandy fluvial deposits or clayey silt, form localized intermediate aquifers (Jiao et al., 2010). These structural changes could potentially allow river water to infiltrate deeper aquifers more easily, which might help explain why river water appears to become the primary source of ARGs in deeper groundwater.

Additionally, at monitoring Site 2, samples from G6 and G8 exhibited a significant proportion of ARGs from unknown sources. Notably, the source data used in our analysis were primarily derived from the Maozhou River, and the potential contributions of tributaries, surface runoff within the river basin, or seawater were not fully accounted for. This limitation in source data coverage may have contributed to the classification of some ARGs as "unknown sources" and introduced variabilities in the source-tracking results. However, it is still important to note that seawater intrusion may significantly influence the ARG profiles in the lower reaches of the Maozhou River's groundwater. Studies have shown that coastal environments, influenced by terrestrial inputs, aquaculture activities, and wastewater discharge, are rich in antibiotic resistance genes and are considered important reservoirs of ARGs (He et al., 2022; Zheng et al., 2021). Through processes such as seawater intrusion

into coastal aquifers, mixing of seawater with river water during tidal exchanges, and subsequent infiltration of mixed water into groundwater systems, marine ARGs have the potential to be introduced into the groundwater (Yu et al., 2020). These mechanisms likely facilitate the transfer of ARGs from marine systems to terrestrial systems in the tidal zones of the lower reach of Maozhou River.

Although these phenomena have been observed, the lack of ARG profiles from Lingdingyang Bay limits our ability to determine the actual contribution of marine sources to groundwater ARG contamination. To address this uncertainty, future research should focus on collecting ARG profiles from coastal zones to establish a baseline for marine ARGs, while analyzing water samples from tidal interfaces to identify ARG signatures potentially linked to marine sources. Additionally, employing hydrodynamic models to simulate seawater intrusion under varying tidal conditions could help elucidate the extent of marine influence on groundwater contamination. These efforts are crucial for validating our hypothesis and gaining a comprehensive understanding of the potential impact of marine environments on the distribution of ARGs in coastal groundwater systems.

2.5 Conclusions

The findings revealed that multiple antibiotics present in the river and sediment were predicted to pose high risks to algae growth and the selection of bacterial resistance, with significant correlations observed between certain antibiotics and specific bacterial phyla. In the groundwater, 74% of *E. coli* isolates exhibited resistance to at least one antibiotic, with the presence of multidrug-resistant strains further highlighting the potential public health risks. SourceTracker analysis indicated that ARG contamination in shallow groundwater (< 7.4 m) primarily originated from river sediments, while deeper groundwater contamination was mainly attributed to river water. These results emphasize the need for targeted management strategies to address antibiotic pollution in urban river systems and mitigate the spread of ARGs in groundwater.

Acknowledgements

This study was supported by the National Natural Science Foundation of China (42030703; U22A20604). We acknowledge the China Scholarship Council (CSC) for the support to Dailing Wu (File No. 202006750027).

Supporting information

Supplementary data to this article can be found online at:
https://doi.org/10.1016/j.envint.2025.109305



Rhine River, Wageningen

Chapter 3

Individual and mixture effects of the antibiotics sulfamethazine and tetracycline on freshwater ecosystems

Dailing Wu, Kaisheng Yao, Markus Hermann, Nuo Chen, Anna Huang, Guang-Guo Ying, Hauke Smidt, Paul J. Van den Brink

This chapter is based on: Wu, D., Yao, K., Hermann, M., Chen, N., Huang, A., Ying, G.G., Smidt, H. and Van den Brink, P.J., 2026. Individual and mixture effects of the antibiotics sulfamethazine and tetracycline on freshwater ecosystems. *Journal of Hazardous Materials*, p.141237.

Abstract

Antibiotics frequently co-occur in aquatic environments, yet their combined ecological effects remain insufficiently understood under realistic mixture scenarios. To address this knowledge gap, we established 36 replicated freshwater microcosms and exposed them to two commonly detected antibiotics, sulfamethazine (SMT) and tetracycline (TC), both individually and in combination, at environmentally realistic concentrations over a 28-day period. At the primary producer level, both antibiotics reduced green algal abundance at intermediate and high concentrations alone, whereas their combination exposure did not consistently inhibit growth, suggesting altered ecological effects under mixture exposure. Zooplankton community structure was significantly altered under both individual and mixture treatments, with stimulatory as well as adverse effects observed at different dose levels. Microbial communities responded in a compartment-specific manner. Single-compound exposures significantly shifted community structure in both water column and sediment. In contrast, no significant changes were detected in water-column microbial communities under mixture treatments, suggesting antagonistic interactions between SMT and TC, likely related to their distinct modes of action and compensatory microbial regulation. At the functional level, leaf-litter decomposition was consistently accelerated across multiple treatments, indicating enhanced microbial activity and functional stimulation. Collectively, these findings provide experimental evidence that antibiotic mixtures can exert non-additive effects across trophic levels and ecosystem processes, highlighting the importance of accounting for such interactions in future research and risk assessment frameworks.

3.1 Introduction

Antibiotics have been used ubiquitously as both human and veterinary medicine over recent decades (Carvalho and Santos, 2016; Conde-Cid et al., 2020; Melchiorri et al., 2025). Their extensive use, together with the fact that 30-90% of administered doses can be excreted as biologically active substances (OECD, 2019), as well as the limited removal efficiency of conventional wastewater treatment plants, has resulted in their continuous release into aquatic environments (Michael et al., 2013; Wang et al., 2020). Once present in water bodies, antibiotics exert selective pressure on microbial communities, thereby promoting the emergence and spread of antibiotic-resistant bacteria and resistance genes (Ho et al., 2025; Wang et al., 2025). In addition to resistance development, such selective pressure can also alter microbial community composition and function, with potential consequences for key ecosystem processes such as nutrient cycling and primary productivity. Moreover, increasing evidence indicates that residual antibiotics pose ecological risks to a wide range of non-target aquatic organisms, including algae (Chang et al., 2022), zooplankton (Arreguin-Rebolledo et al., 2024), macrophytes (Ebert et al., 2011), and macroinvertebrates (Schuijt et al., 2024a). These organisms play essential roles in aquatic food webs and biogeochemical cycling, and their disruption can lead to cascading effects that impair overall ecosystem structure and function (Robinson et al., 2005; Schuijt et al., 2024a). Despite these recognized ecological risks, most previous ecotoxicological research has primarily focused on the effects of individual antibiotics (Dalla Bona et al., 2015; Rico et al., 2014; Schuijt et al., 2024a). However, antibiotics typically coexist with other pharmaceuticals and pollutants in aquatic ecosystems, forming complex mixtures that may induce ecological effects distinct from those of single compounds (Kidd et al., 2024). For example, combined exposure to macrolides, sulfonamides, and fluoroquinolones significantly increased toxicity toward sensitive organisms such as algae and cyanobacteria, disrupting critical processes like photosynthesis and redox balance (Chang et al., 2022; González-Pleiter et al., 2013; Guo et al., 2021). Additionally, certain antibiotic combinations have shown antagonistic effects on zooplankton populations even under chronic, low-concentration exposures, suggesting that mixture toxicity is often species-specific and context-dependent (Arreguin-Rebolledo et al., 2024; Danner et al., 2019). Nevertheless, existing studies remain fragmented, with limited integration of representative antibiotics, environmentally realistic concentrations, and endpoints that reflect the structure and function of aquatic ecosystems. Ignoring such complexity could lead to underestimation of ecological risks, highlighting the urgent need for more ecologically relevant investigations (Cedergreen, 2014).

To move beyond the fragmented understanding of antibiotic mixture effects, it is essential to investigate representative compound mixtures that reflect the diversity of environmental behaviours observed among frequently detected antibiotics. Among the most frequently

detected antibiotic classes in aquatic environments, tetracyclines and sulfonamides are of particular interest due to their widespread use in both human and veterinary medicine and markedly different environmental behaviours (Wu et al., 2025). For example, China's 2020 national veterinary antimicrobial use report reported a total use of 32,776 tonnes, with tetracyclines accounting for 30.5% and sulfonamides (including potentiators) accounting for 13.1% (China, 2021). Tetracycline (TC), representing the tetracycline class, has a polycyclic structure with multiple ionizable functional groups, allowing strong interactions with organic matter and divalent cations. This leads to high sediment affinity, with a reported soil-water distribution coefficient (Kd) ranging from 3,102 to 312,447 L/kg (Pikkemaat et al., 2016; Wang and Wang, 2015). In contrast, sulfamethazine (SMT), a typical sulfonamide, is more polar and less sorptive (Kd = 0.7 ~ 70.1 L/kg), resulting in a greater mobility and persistence in the aqueous phase (Pikkemaat et al., 2016). Although the individual behaviours of these compounds are well characterized, whether their differential partitioning leads to distinct or interactive ecological effects remains unclear. Using TC and SMT as model compounds may offer novel insights into how the differential partitioning of antibiotics between water and sediment compartments shapes mixture outcomes in aquatic ecosystems. Their frequent co-occurrence in real-world environments (Wu et al., 2025), combined with their contrasting physicochemical properties, underscores the need to assess potential non-additive effects, as mixture exposures may produce ecological outcomes that differ substantially from those of individual compounds (Hu et al., 2017).

To systematically examine the ecological consequences of antibiotic mixtures, a controlled freshwater microcosm system was established in the laboratory, incorporating key biological components across multiple trophic levels, including phytoplankton, submerged macrophytes, zooplankton, macroinvertebrates, and microbial communities. This experimental system allowed for simultaneous assessment of both structural and functional responses to a range of environmentally relevant concentrations of TC (1.5 - 150 µg/L) and SMT (0.1 - 10 µg/L), applied individually and in combination. By integrating multiple biological endpoints, this study aimed to address the following key questions: (1) Do TC and SMT, alone and in mixture, differentially affect aquatic community structure across multiple trophic levels? (2) At what concentrations do these antibiotics begin to elicit observable ecological effects? (3) How do combined exposures to SMT and TC influence ecosystem functions compared to single-compound exposures? By addressing these questions, this study provides insights into how antibiotics with distinct environmental fates and biochemical mechanisms of action interact to shape ecological outcomes under realistic exposure scenarios.

3.2 Materials and methods

3.2.1 Experimental design

The laboratory microcosm experiment was conducted at the Aquatic Ecology and Water Quality Management Group of Wageningen University & Research, the Netherlands. After a one-month acclimation period, the experiment started on January 18, 2022, and lasted for four weeks until February 14, 2022. Each microcosm consisted of a cylindrical glass tank with a height of 0.38 m and a diameter of 0.25 m. Each tank was filled with 12 L of lake water collected from Lumen Pond (Wageningen Campus, the Netherlands) and filtered through a 30 µm mesh, along with approximately 3 cm of uncontaminated sediment (approximately 1.67 kg wet weight) obtained from the Sinderhoeve experimental station (Renkum, the Netherlands; www.sinderhoeve.org) (Fig. S1). One month prior to the start of the experiment, all microcosms were inoculated with equivalent amounts of phytoplankton, zooplankton communities, and macroinvertebrates. Due to the low natural abundance of phytoplankton in the Lumen pond water during winter, additional cultures of the green alga *Scenedesmus obliquus* were introduced to the microcosms. Zooplankton was collected from an uncontaminated pond located near the Forum building (Wageningen Campus, the Netherlands), while macroinvertebrates were collected from the Sinderhoeve. In each system, 20 individuals of *Asellus aquaticus*, 20 of *Gammarus pulex*, five of *Physella* spp., and five of *Planorbis* spp. (all medium-sized macroinvertebrates) were introduced. Additionally, one shoot of *Elodea nuttallii* (approximately 15 cm in length) and one of *Myriophyllum spicatum* (approximately 10 cm in length) were planted in separate pots, which were then placed in the sediment of each microcosm. To provide a food source for benthic invertebrates, 2 g of dried *Populus* spp. leaves (without branches) were placed in a Petri dish, which was covered with a metal mesh perforated with two holes (approximately 0.5 cm in diameter) to allow macroinvertebrate access, and positioned on the sediment surface. In addition, four 100 mL HDPE bottles (31 mm opening diameter), filled with the same sediment as the tank bottom, were embedded in the sediment of each system to monitor antibiotic sediment concentrations and changes in microbial community. To assess microbially mediated leaf litter decomposition, 144 nylon mesh bags (500 µm mesh size, 14 × 11 cm), each containing 2 g of dried *Populus* spp. leaves, were prepared, and six bags were suspended above the sediment in each microcosm (Fig. S1).

Based on environmental concentrations reported for SMT (Mulla et al., 2023), its experimental concentrations were set at 0.1, 1, and 10 µg/L. Considering that TC concentrations in natural sediment typically range from ng/g to µg/g (Daghrir and Drogui, 2013), and accounting for the water volume and sediment mass in the experiment, TC was added at concentrations of 1.5, 15, and 150 µg/L. These levels were chosen to yield surface

sediment concentrations of approximately 30 to 3,000 ng/g, assuming complete adsorption. For the mixture treatments, the concentrations corresponded directly to those used in the single-compound treatments, resulting in three distinct mixture groups. Each treatment group included three replicates. Due to the addition of 40 µL of methanol during the antibiotic dosing process (equivalent to approximately 0.0033 mL/L), both negative controls (four replicates, without antibiotics or solvent) and solvent controls (five control replicates, with an additional 40 µL of methanol) were included to distinguish potential solvent effects. A total of 36 microcosms were established.

All microcosms were maintained at 20 °C using a flow-through temperature control system and operated under a 12-hour light/dark cycle (Philips HPI-T, 400 W), with light intensity at the water surface maintained at around 140 µW/cm². Continuous aeration was applied throughout the experiment to prevent oxygen depletion, and evaporative water loss was compensated on a weekly basis. Nutrient levels were sustained by weekly additions of NH_4NO_3 and KH_2PO_4 at a molar ratio of 6:1, resulting in final concentrations of 90 µg/L inorganic nitrogen (N) and 15 µg/L phosphate phosphorus ($P\text{-}PO_4$) (Schuijt et al., 2024a). To reduce potential human or system-induced bias, microcosm positions were randomly assigned within the water bath.

3.2.2 Antibiotic application, sampling and analysis in water and sediment

Analytical grades of SMT (CAS No. 57-68-1) and TC (CAS No. 64-75-5) were purchased from Merck (Germany) and prepared as concentrated stock solutions in methanol (analytical grade, Merck, Germany). These stock solutions were then diluted to prepare working solutions, which were dosed into the microcosms to achieve the target exposure concentrations. To monitor antibiotic concentrations in the water phase, depth-integrated water samples were collected by means of long pipette tips from different depths at 1, 4, 12, 24, and 72 h, as well as on Days 7, 14, and 28 after dosing. Sediment samples were collected on Days 7, 14, and 28 by retrieving the pre-installed HDPE bottles filled with the same sediment from the bottom of each microcosm, carefully removing the overlaying water, and storing the sediments at -20 °C until extraction. Detailed information on dosing and chemical analyses is provided in Test S1 of the Supplementary Materials (SI).

3.2.3 Water quality parameters and primary producers

Water quality parameters were measured weekly at 8:30 a.m. using an HQ40d multiparameter meter (Hach, USA). These parameters included electrical conductivity, pH, dissolved oxygen (DO), temperature, and oxygen production, which was calculated as the difference in dissolved oxygen between 8:30 and 19:30 and is referred to as DO_net in the Results section.

Each week, 100 mL of water was collected from each microcosm. Of this, 50 mL was used to analyze total phosphorus (TP) and total nitrogen (TN), while the remaining 50 mL was filtered through a 1.2 µm Whatman glass fiber filter for the determination of orthophosphate, ammonia, and combined nitrite/nitrate. All nutrient analyses were performed using a segmented flow analyzer (Skalar 5100 Autoanalyzer, Breda, Netherlands).

Chlorophyll-a concentrations were measured weekly using a Phyto-PAM fluorometer (Heinz Walz, Effeltrich, Germany), which partitions chlorophyll-a signals into green, blue, and brown algal groups. In this study, we focused on and report only the green algae fraction, as green algae were the dominant phytoplankton group in the experimental system. At the end of the experiment (Day 28), all submerged macrophytes were harvested, and their total length, including both main stems and lateral shoots, was recorded.

3.2.4 Zooplankton and macroinvertebrates sampling

Zooplankton were sampled on Day -1 (prior to treatment), and on Days 7, 14, and 28 of the experiment. For each sampling event, 1 L of depth-integrated water was collected from each microcosm and filtered through a 55 µm mesh. The filtrate was returned to the respective system, while the retained zooplankton were concentrated to 50 - 80 mL, preserved with Lugol's solution and stored at 4 °C until identification.

Zooplankton was identified under an Olympus SZX10 stereomicroscope to the lowest practicable taxonomic level. Both macrozooplankton (i.e., Cladocerea, Copepoda, Ostracoda) and microzooplankton (i.e., Rotifera, Copepoda nauplii) were included. Microzooplankton were identified from a 1 mL subsample. Zooplankton abundance was expressed as individuals per liter.

At the end of the experiment (Day 28), the four introduced species of macroinvertebrate benthic organisms were collected from the water column, plant surfaces, Petri dishes, and sediment in each microcosm, and their abundances were recorded.

3.2.5 Leaf litter decomposition by macroinvertebrates and microbes

Microbial decomposition of organic matter was assessed by measuring the dry weight loss of *Populus* spp. leaf litter in the microcosms. From each microcosm, two bags were retrieved the day before exposure, and two bags were collected on both Days 14 and 28. The remaining leaf material was removed from the bags, oven-dried at 60 °C for 48 h and weighed to determine the percentage of biomass loss based on dry weight.

The same approach was used to estimate leaf consumption by macroinvertebrate benthic organisms. At the end of the experiment (Day 28), the dishes were carefully removed, and all animals were gently separated from the leaves. The remaining leaf material was then oven-dried, in the same way as the microbial decomposition leaf material, and finally weighed to calculate the amount consumed.

3.2.6 Microbial community

Samples for the analysis of microbial community composition were collected from the water column on Days -1, 3, 7, 14, and 28, and from the sediment on Days -1, 7, 14, and 28. DNA extraction, amplification of the V4 region of the *16S rRNA* gene using primers 515F/806R, and sequencing procedures are described in Text S2 of the SI.

Raw *16S rRNA* gene sequence reads were processed using the NG-Tax 2.0 pipeline, including barcode and primer trimming, amplicon sequence variant (ASV) detection, and taxonomic assignment against the SILVA 138 reference database. Only exact barcode–primer matches were retained, and ASVs with a relative abundance below 0.1% per sample were removed as part of the NG-Tax pipeline. The resulting BIOM table and phylogenetic tree were imported into phyloseq (McMurdie and Holmes, 2013) for downstream analyses. Sequences affiliated with mitochondria and chloroplasts were removed prior to statistical analyses. Per-sample sequencing read counts after NG-Tax processing and quality filtering are provided in the Table S1.

3.2.7 Data analysis

The dissipation of antibiotics in the water column was described using a first-order exponential decay model:

$$C_t = A_1 \cdot e^{(-x/t1)} + y_0 \qquad (1)$$

where C_t was the antibiotic concentration at time x_1, A_1 was the amplitude of the decay, t_1 was the decay time constant, and y_0 was the baseline concentration. For both antibiotics, y_0 was fixed at half the LOQ to account for non-zero baseline concentrations. The dissipation rate constant (k) was calculated as $k = 1/t_1$, and the half-life (DT_{50}) was estimated using $DT_{50} = \ln(2)/k$. Parameters were estimated by nonlinear regression.

Water quality parameters, nutrient concentrations, zooplankton community data, and microbial community profiles were analysed using RStudio (R Core Team, 2024). Statistical significance was assessed using the Wilcoxon test. Plant growth indicators, chlorophyll-a concentrations, leaf decomposition rates, and macroinvertebrate abundances were

calculated in Microsoft Excel and visualized using Origin Pro 2025, version 2025a. One-way ANOVA and post hoc comparisons (LSD or Duncan tests) were performed in SPSS, version 28.0.1.1.

No significant differences were observed between the control and solvent control groups across all measured endpoints. Therefore, these groups were pooled and treated as a single control group for subsequent statistical analyses, resulting in a total of nine control replicates.

To reduce the influence of extreme values, abundance data were log-transformed prior to community and population-level analyses: macroinvertebrate data were transformed using ln(2x + 1), and zooplankton data using ln(10x + 1), where x denotes the abundance of a given taxon (see Van den Brink et al. (2000) for rationale). Multivariate analyses were employed to assess treatment-related changes in the macroinvertebrate, zooplankton, and microbial community structure. The Principal Response Curve (PRC) method was employed to evaluate temporal dynamics (Van den Brink and Braak, 1999), with statistical significance tested using 499 Monte Carlo permutations across the entire time series (Van den Brink et al., 1996). Redundancy analysis (RDA) combined with Monte Carlo permutation tests was performed on each sampling day to assess treatment effects at individual time points.

To explore the overall compositional shifts in microbial communities under different antibiotic treatments, principal component analysis (PCA) was performed. The analysis was based on genus-level relative abundance data, which were arcsine-transformed after conversion to percentages. Sample scores were visualized along the first two principal axes to examine treatment-related temporal dynamics. All multivariate analyses were conducted using CANOCO version 5.15 (ter Braak and Šmilauer, 2012).

3.3 Results

3.3.1 Antibiotic concentration

In this study, the half-life of SMT in water was 3.1 to 4.6 days at 1 µg/L, and 5.7 to 6.7 days at 10 µg/L, corresponding to the combined treatment with TC and SMT alone, respectively (Fig. 3.1a, Table S2). For TC, the half-life ranged from 2.5 to 3.1 days at 15 µg/L, while at the highest tested concentration of 150 µg/L, it was notably shorter, ranging from 11 to 20 h (Fig. 3.1b, Table S2). In contrast, half-life values could not be calculated for the lowest concentration treatments of either compound due to measured levels falling below the quantification limits (LOQ_{SMT}: 0.02 µg/L; LOQ_{TC}: 2.0 µg/L). No significant differences in the half-lives of either antibiotic were observed between the single and mixture

treatments. In addition, SMT accumulation in sediments was minimal, with concentrations in the highest treatment group reaching only 2 µg/kg dry weight between Days 8 and 28 (Fig. S2).

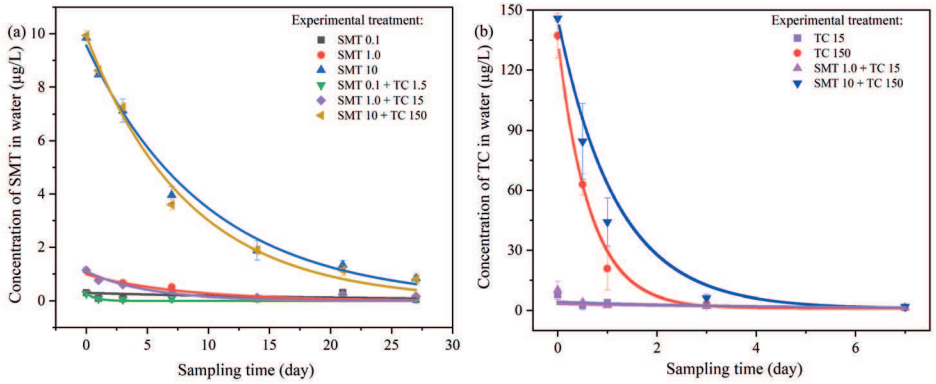


Figure 3.1. Concentration of SMT (a) and TC (b) in the water phase (µg/L) over time across treatments. Treatments with the lowest TC concentrations (TC 1.5 and SMT 0.1 + TC 1.5) are not shown, as their measured concentrations were below the limit of detection (LOD) and could not be reliably fitted.

3.3.2 Water quality, and nutrients

Water temperature, pH, electrical conductivity, and nutrient levels remained stable throughout the experiment and showed no significant differences among treatment groups (Figs. S3.3; S3.4). In contrast, DO levels, which reflect primary productivity, exhibited marked treatment-dependent variation (Fig. S3).

The 1.0 µg/L SMT treatment led to significantly lower evening DO levels and a reduction in net daily DO production on Day 3 ($P < 0.05$). The 1.5 µg/L TC treatment caused a sustained decline in morning DO level from Day 10 onward, whereas the 150 µg/L TC treatment significantly reduced the evening DO level on Day 3. However, none of the TC treatments significantly affected net DO production over the course of the experiment.

The high mixture treatment resulted in an elevated morning DO level on Day 3 ($P < 0.05$). Conversely, the low mixture treatment showed significantly reduced evening DO levels from Day 10 to Day 24. Significant reductions in net DO production were observed on Days 3 and 17 in the low and medium mixture treatments. Notably, in the low mixture treatment, this reduction persisted until Day 28 ($P < 0.05$).

3.3.3 Primary producers

Throughout the experiment, the chlorophyll-a concentrations attributed to the green algae fraction remained relatively stable in the control group, ranging from 15 ± 6.9 to 19 ± 10 µg/L (Fig. 3.2a). In the SMT treatments, a consistent decline was observed from Day 3 for 1 and 10 µg/L treatments, reaching 4.0 ± 2.2 and 2.0 ± 0.6 µg/L, respectively, by Day 27. However, these trends were not statistically significant ($P > 0.05$), likely due to the high variability in the control group. A similar trend was observed in the TC treatments (Fig. 3.2b), where green algae concentrations were markedly lower at 15 µg/L and 150 µg/L treatments than those in the control group, reaching 1.9 ± 0.7 and 2.5 ± 0.7 µg/L, respectively, on Day 27. In contrast, much smaller and non-significant declines were observed at the lowest concentrations (0.1 µg/L SMT treatment and 1.5 µg/L TC treatment).

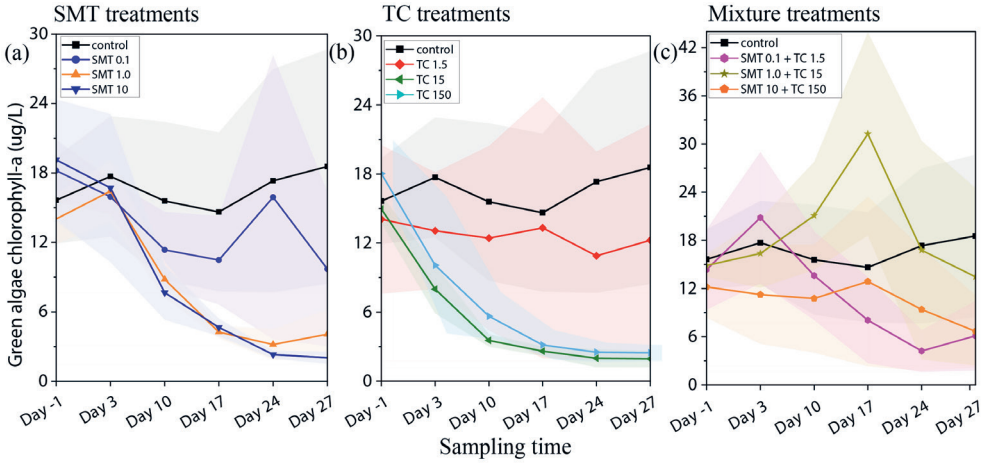


Figure 3.2. Green algae chlorophyll-a concentrations in different treatments over time (µg/L). (a) SMT treatments, (b) TC treatments and (c) Mixture treatments. Shaded areas indicate standard errors. Control groups: N = 9; treatments: N = 3.

Remarkably, in the mixture treatments, green algae concentrations did not show a clear trend as opposed to what was observed in the single compound treatments (Fig. 3.2c). In both the lowest and highest mixture treatments, a slight decline was observed over time, but the changes were not statistically significant. In the medium mixture treatment, the average concentration increased to 31 ± 13 µg/L on Day 17, followed by a decrease in the subsequent week.

Considering macrophyte growth, on Day 28, although some significant differences in the growth of *Myriophyllum* and *Elodea* were observed between certain treatment groups and the control, no overall treatment effect was detected ($P > 0.05$, Fig. S5). These differences

may be attributed to poor plant establishment in some microcosms rather than a true treatment effect.

3.3.4 Zooplankton

A total of 34 zooplankton taxa were identified, comprising 17 micro-zooplankton and 17 macro-zooplankton taxa. PRC analysis revealed that both the individual as well as the mixture treatments induced significant shifts in the zooplankton community composition (Fig. 3.3, $P < 0.05$). In the SMT treatment group, the first two PRC axes explained 69% of the total variation (Fig. 3.3a, PRC1: 47%, $P < 0.01$; PRC2: 22%, $P < 0.01$). For TC-treated communities, 58% of the variation was explained (Fig. 3.3b, PRC1: 31%, $P < 0.05$; PRC2: 27%, $P < 0.05$), while the mixture treatment accounted for 61% (Fig. 3.3c, PRC1: 37%, $P < 0.05$; PRC2: 24%, $P < 0.01$).

Monte Carlo permutation tests indicated a non-monotonic dose-response pattern for the SMT treatments, as evidenced by significant changes in zooplankton community structure at the lowest (0.1 µg/L) and highest (10 µg/L) treatments, but not at the intermediate (1.0 µg/L) treatment (Fig. 3.3a). In the 0.1 µg/L SMT treatment, the zooplankton community structure differed significantly from the control on Days 7, 14, and 28 ($P < 0.05$), with *Lecane gr. luna* showing the highest species weight, suggesting a high response to this concentration (Fig. 3.3a). Community shifts were also observed for the 10 µg/L SMT treatment, although the effect lasted only until Day 14. Interestingly, no significant changes were detected at the 1.0 µg/L SMT treatment for any of the time points, highlighting a U-shaped dose-response (Fig. 3.3a). All TC treatments induced significant changes on Day 7 ($P < 0.05$), with the greatest shift in community structure observed in the 150 µg/L TC treatment (Fig. 3.3b). By Day 14, differences remained significant in the 15 and 150 µg/L TC treatments. Several *Daphnia spp.* received high weights, indicating a lack of sensitivity to TC exposure. In the mixture treatments, community responses appeared delayed compared to single treatments (Fig. 3.3c). By Day 14, significant shifts were observed for all mixture treatments, with the most pronounced changes at the highest dose, followed by the medium dose. *Mytilina ventralis*, *Alona sp.*, and *Trichotria pocillum* contributed most to the observed variation and are indicated to increase in the higher treatments (Fig. 3.3c).

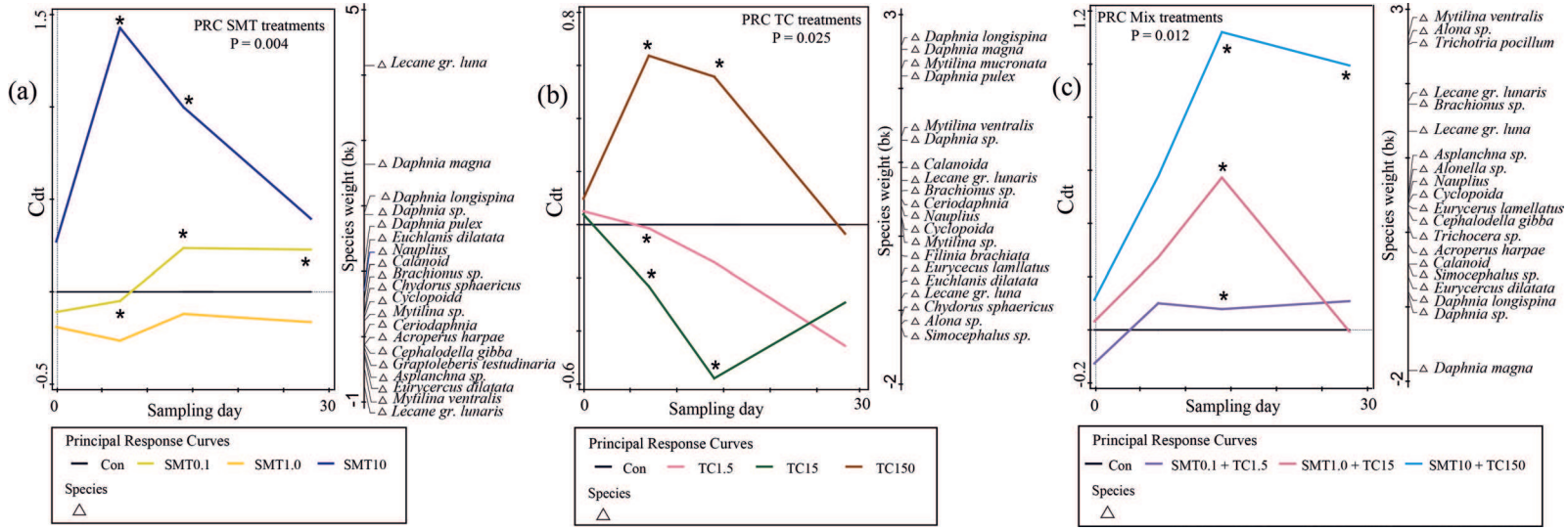


Figure 3.3. PRC analysis showing the temporal changes in zooplankton community structure under different treatments during the experiment. The 20 taxa with the highest species scores (bk values) are shown alongside the PRC curves. (a) SMT treatments, (b) TC treatments and (c) Mixture treatments.

Among all recorded zooplankton taxa, 12 taxa exhibited statistically significant changes in abundance under antibiotic treatments, warranting closer examination as key contributors to the observed community-level dynamics (Fig. 3.4). In the SMT treatments, *Daphnia longispina* and *Lecane gr. luna* showed significantly higher abundance on Day 7 in the 10 µg/L SMT treatment compared to the control ($P < 0.05$). *Mytilina mucronata* declined rapidly within the first week in the control group, whereas in all SMT-treatments, its decline occurred later. Abundances of *Mytilina mucronata* were significantly higher on Day 7 in the treatment groups than in the control ($P < 0.05$). In addition, *Daphnia* sp. exhibited significantly higher abundances in the SMT 10 µg/L treatment ($P < 0.05$) compared to control throughout the first two weeks of the experiment. However, it is important to note that higher abundances of this taxon were already noted prior to exposure (Day -1). This pattern likely reflects an initial difference in starting abundances rather than a treatment-induced effect. Apart from *Daphnia* sp., no other species showed significant differences in abundances between any of the treatments and control.

In the 150 µg/L TC treatment, *Daphnia longispina* and *Mytilina mucronata* showed significantly higher abundances on Day 7, *Daphnia pulex* on both Day 7 and Day 14, and *Daphnia* sp. on Day 14, compared to the control ($P < 0.05$). Although *Lecane gr. luna* abundance was higher across all TC treatments compared to the control on Day 7, statistically significant differences were detected only in the 1.5 and 15 µg/L TC treatments ($P < 0.05$).

The zooplankton individual populations displayed response patterns in the mixture treatments which are distinct from those observed under single treatments. In the high mixture treatment, *Alona* sp., *Alonella* sp., *Lecane gr. lunaris*, and *Mytilina ventralis* exhibited significantly elevated abundances on Day 14 compared to the control ($P < 0.05$). *Brachionus* sp. maintained higher levels than the control across all mixture treatments throughout the experiment ($P < 0.05$), though with differing temporal dynamics. In the low mixture treatment, *Brachionus* sp. abundances peaked on Day 14 before declining to non-significant levels by Day 28. In the medium mixture treatment, abundances remained significantly elevated through Day 28, though lower than the peak observed in the low mixture treatment. In contrast, although abundances in the high mixture treatment steadily increased over time and reached a significantly higher level by Day 28, the rate of increase was slower compared to the lower concentration treatments, indicating a decelerated reproduction trend at higher concentrations. Notably, several *Daphnia* sp. also responded positively in reproduction in the low mixture treatment, while only *Daphnia pulex* showed significantly higher abundance values in the medium mixture treatment compared to the control ($P < 0.05$). *Daphnia* sp. were nearly absent in the high mixture treatment during the first 14 days and only gradually reappeared later in the experiment (Fig. 3.4).

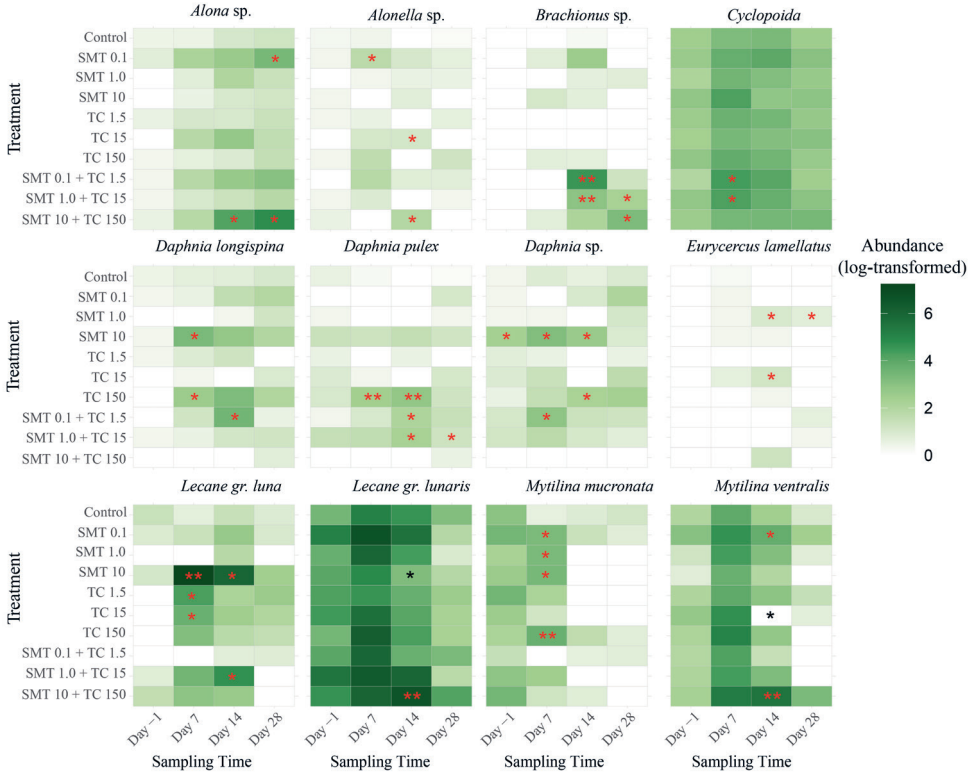


Figure 3.4. Heatmap showing temporal changes in zooplankton abundances (individuals per liter) across different antibiotic treatments. Data were log-transformed using the function ln(2x+1). Darker green indicates higher abundances, while lighter (whiter) shades represent lower abundances. Asterisks (*) denote significant differences compared to the control group, with red indicating significantly higher abundances and black indicating significantly lower abundances. Significance levels: * $P < 0.05$; ** $P < 0.01$.

3.3.5 Macroinvertebrate abundances, food consumption and microbial leaf litter decomposition

Macroinvertebrate abundances were not significantly different in the antibiotic treatments compared to the control (Fig. S6). Similarly, feeding rates did not differ significantly between the treatments and the control (Fig. S7). Within the TC treatments, feeding rates differed between concentrations, with significantly higher values at the highest TC treatment (150 µg/L) compared to the lowest (1.5 µg/L) ($P < 0.05$).

On Day 14 of the experiment, microbial decomposition of *Populus* spp. leaves did not differ significantly between the treatments and the control (Fig. S8). However, on Day 28, leaf decomposition had increased substantially compared to Day 14. Although all antibiotic

treatments showed higher decomposition rates than the control, significant differences were observed only for the 15 µg/L TC treatment, all SMT treatments, and the low and medium mixture treatments ($P < 0.05$).

3.3.6 Microbial community

A total of 46,688,647 high-quality prokaryotic *16S rRNA* gene sequences were obtained, resulting in the annotation of 2,126 ASVs, with a minimum of 15,549 sequences per sample. In total, 505 genera belonging to 29 bacterial phyla were annotated, among which 241 genera were annotated in water samples, and 361 genera in sediment samples. Given that the genus level represents the highest taxonomic resolution confidently attainable with this approach, we performed a PRC analysis at the genus level for both water and sediment microbial communities. SMT and TC, as single treatments, significantly altered the microbial community composition in both environmental matrices ($P < 0.01$) (Fig. 3.5). However, under the mixture treatment, microbial community composition in water was not significantly affected across concentrations, whereas significant changes were observed in the sediment ($P < 0.01$).

In the water samples, PRC axis 1 explained 54% and 41% of the community variation for the SMT and TC treatments, respectively (Fig. 3.5a & c). *Rickettsiella* contributed the most to the observed changes, with its relative abundance being higher in all treatments compared to the control at the beginning of the experiment, declining steadily to a minimum by Day 14, and partially recovering toward the end of the experiment. In the mixture treatments, PRC axis 1 accounted for–33% of the treatment variation that was, however, not significant ($P > 0.05$, Fig. 3.5e). Nevertheless, *Rickettsiella* remained the species with the highest weight in the PRC analysis. Notable changes in *Cyanobium*_PCC-6307 were also observed, following trends in relative abundance like those seen under individual treatments (Fig. 3.5e).

In the sediment, PRC axis 1 explained 46%, 45%, and 45% of the community variation for the SMT, TC, and mixture treatments, respectively ($P < 0.01$, Fig. 3.5b, d & f). In the SMT treatments, *Thermobacillus*, *Pseudonocardiaceae*_unidentified, and *Planifilum* exhibited the highest positive scores in the SMT PRC, indicating a continuous decline in their relative abundances after antibiotic dosing compared to the control, with the most pronounced decrease observed on Day 14 (Fig. 3.5b). Conversely, *Pirellula* and *Nitrospira* showed the highest negative scores, reflecting an increase in their relative abundances compared to the control. In the TC treatments, *Bacillus* and *Bacillales*_unidentified exhibited the highest positive scores (Fig. 3.5d). Their relative abundances remained lower in the 1.5 µg/L treatment than in the control. In the 15 µg/L and 150 µg/L treatments, abundances were

initially higher than in the control during the first 7 days, but then showed a sharp decline and became significantly lower by Day 14. By contrast, *Vicinamibacterales*_unidentified and *Nitrospira* showed opposite trends, with their relative abundances increasing throughout the experiment (Fig. 3.5d). In the mixture treatments, the relative abundances of *Bacillus* and *Nitrososphaeraceae*_unidentified declined by Day 7 and were significantly lower than in the control by Day 14 (Fig. 3.5f). While their relative abundances partially recovered in the low and high mixture treatments thereafter, they continued to decline in the medium mixture treatment. Conversely, *Vicinamibacterales*_unidentified and *Pirellula* exhibited continuous increases in relative abundance compared to the control throughout the treatment period (Fig. 3.5f).

It is noteworthy that the effects of SMT and TC on microbial communities in both water and sediment were not consistently concentration dependent. The response patterns differed between the two matrices (water vs. sediment). In the water column, the 0.1 µg/L and 10 µg/L SMT treatments induced the most rapid and pronounced shifts in community structure compared to the control, whereas the 1 µg/L SMT treatment showed the largest deviation on Day 14 (Fig. 3.5a). For TC, significant effects on the water microbial community were only observed at 15 µg/L TC treatment on Day 3, with no significant changes detected at 1.5 µg/L or 150 µg/L TC treatments at that time (Fig. 3.5c). However, community structure was significantly altered on Day 14 in the 150 µg/L TC treatment when compared to the control.

In the sediment, 15 µg/L and 150 µg/L TC treatments caused significant changes in community structures on Day 14, whereas the 1.5 µg/L TC treatment had no noticeable effect (Fig. 3.5d). In the mixture treatments, the most pronounced changes in sediment microbial communities were also observed on Day 14 across all treatments. The high mixture treatment showed the largest deviation from the control, followed by the low mixture treatment (Fig. 3.5f). Although the medium mixture treatment exhibited a smaller deviation from the control community on Day 14 compared to the other treatment groups, its community shift persisted through Day 28, indicating a longer-lasting effect. In contrast, the low mixture treatment showed a tendency for its community trajectory to shift back towards the control after Day 14 (Fig. 3.5).

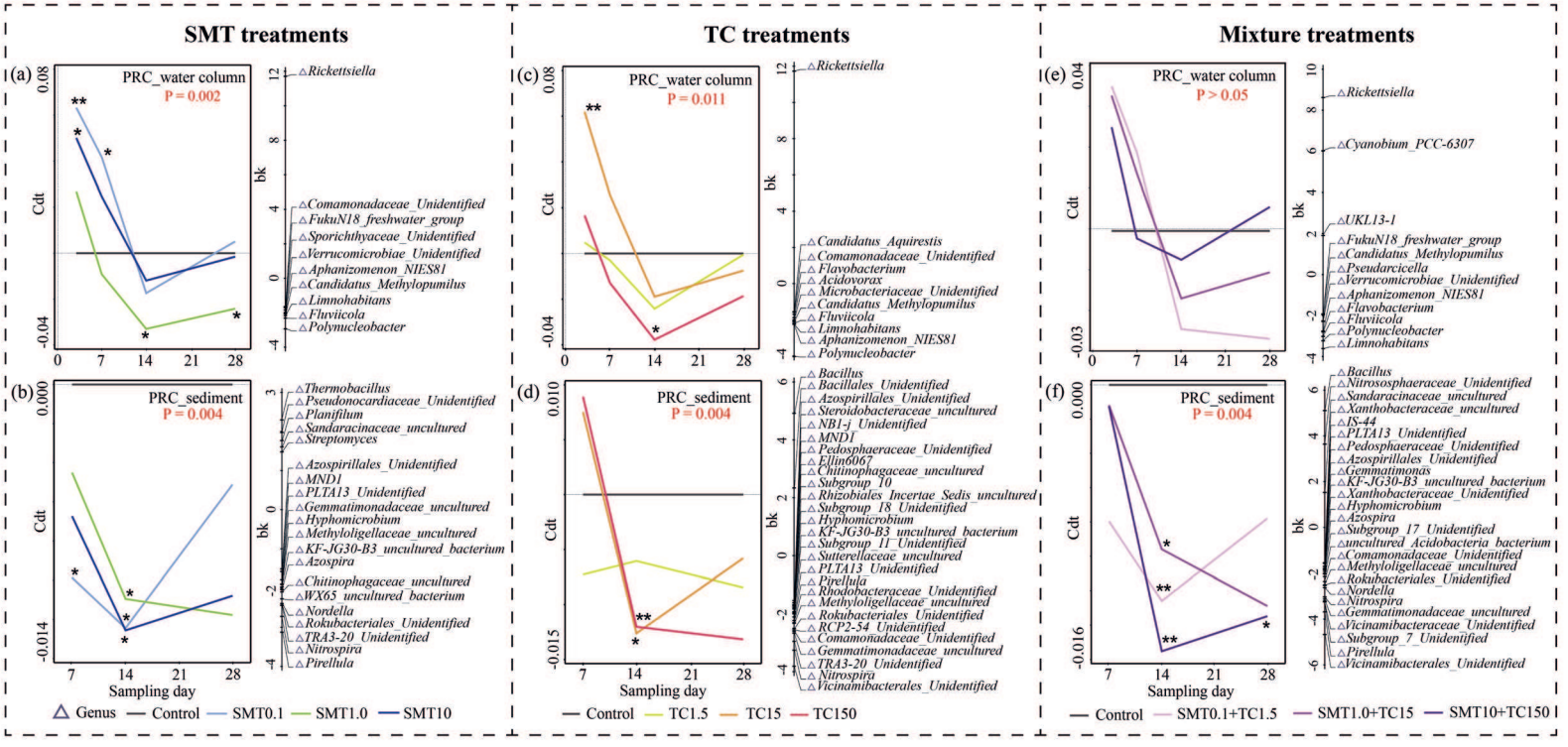


Figure 3.5. PRC illustrating temporal changes in microbial community structure in the water column (Day 3 to Day 28) and sediment (Day 7 to Day 28) under single and mixture antibiotic treatments. Bacterial genera with species weights between -1.5 and 1.5 are not shown. Please note that the scales of the canonical coefficients (Cdt values) differ across subgraphs.

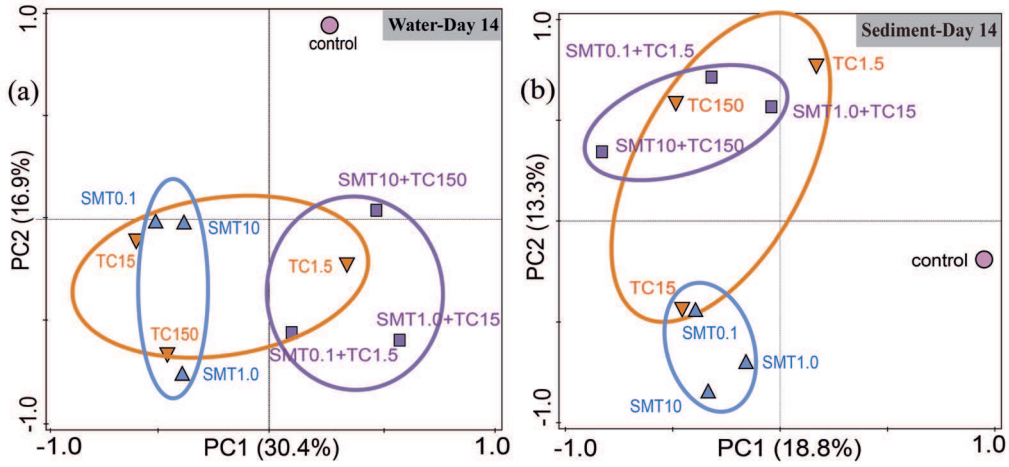


Figure 3.6. PCA based on genus-level relative abundance data showing the distribution of microbial communities under different antibiotic treatments on Day 14 in the (a) water column and in (b) sediment. Upward triangles indicate the centroids of SMT treatments, downward triangles indicate the centroids of TC treatments, squares indicate the centroids of mixture treatments, and circles represent the control group.

PCA analysis showed that in the water column, SMT and TC individually induced distinct changes in microbial community structure by Day 3, although no clear separation was observed between the individual chemicals and the mixture treatment (Fig. S9a). By Day 7, this difference became less pronounced (Fig. S9b). By Day 14, a clear separation had emerged between the SMT treatment group and the mixture treatment group, while the TC treatment group remained largely overlapping with the mixture and SMT treatment groups (Fig. 3.6a; S9c).

In the sediment, on Day 3, a similar pattern of community separation to that observed for the water column was detected on Day 7, with SMT and TC treatments inducing significantly different community shifts (Fig. S9e). However, the mixture treatments did not show clear separation from either the SMT or TC treatments at this time point. By Day 14, a distinct separation was observed between the SMT treatments and the mixture treatments, whereas the TC treatments remained largely overlapping with the mixture treatments, with the TC15 group still showing partial overlap with the SMT treatment group (Fig. 3.6b; S9f).

3.4 Discussion

3.4.1 The fate of sulfamethazine (SMT) and tetracycline (TC)

In this study, the half-life of SMT in the water column ranged from 3.1 to 6.7 days, with slightly longer half-lives observed at higher dosed concentrations (e.g., 5.7–6.7 days at 10 µg/L vs. 3.1–4.6 days at 1 µg/L), suggesting a weak concentration-dependent trend (Fig. 3.1 & Table S2). This aligns with previous reports from natural water systems, where SMT typically showed half-lives around 2-3 days in pond and aquaculture settings (Carstens et al., 2013; Sun et al., 2016). By contrast, much faster degradation was observed in a wastewater effluent (5.03 h at 40,000 µg/L) and in Milli-Q water (9.4 h at pH 7.2) (Conde-Cid et al., 2018; García-Galán et al., 2012). Such variation may be attributed to differences in light availability, antibiotic concentrations and temperature (Batchu et al., 2014; Batista et al., 2014). Photolysis is considered the primary removal mechanism of SMT in surface waters, initiating sulfonamide bond cleavage and removal of the sulfinyl group, leading to desulfonated transformation products (García-Galán et al., 2012; Periša et al., 2013; Yi et al., 2018). The attenuation rate of SMT in sediments is relatively low, primarily due to its weak affinity for sediment particles and associated organic matter, which limits the contribution of adsorption to its dissipation. As an acidic compound, SMT exhibits reduced adsorption capacity in alkaline environments due to electrostatic repulsion between the compound and sediment particles (Gothwal and Shashidhar, 2015). In this study, SMT steadily accumulated in sediments from Day 8 (2 µg/kg) and remained stable through Day 28 (Fig. S2), comparable to the average concentration of 4.7 µg/kg reported in natural rivers (Kim and Carlson, 2007).

For TC, adsorption and photodegradation are the main pathways of dissipation in aquatic environments (Chabilan et al., 2023). A mesocosm study showed that sediment adsorption accounted for 52% of TC dissipation in water, while photodegradation contributed 35% (Chabilan et al., 2023). In the same study, the half-life of TC in water was reported to be 2 days, which aligns well with the range of 11 h to 3.1 days observed in our microcosm experiment. In addition, under neutral to alkaline conditions, TC undergoes hydrolysis, resulting in isomerization and dehydration reactions that produce 4-epitetracycline and anhydrotetracycline, which have also been reported to possess ecotoxicological relevance in aquatic environments (Song et al., 2021; Yuen and Sokoloski, 1977). Although in this study we were not able to measure TC concentrations in sediments due to its strong adsorption to sediment particles and the resulting low extraction efficiency, previous research has shown that once it enters the sediment, it binds strongly to sediment particles through electrostatic attraction, cation bridging, and chelation with multivalent metal ions (Li et al., 2010). This strong binding significantly slows its degradation in soil and sediment environments. For

instance, under dark conditions at 25 °C, the half-life of TC in soil ranges from 20 to 41 days (Li et al., 2010). However, the conditions of the present study (20 °C, 12 h light : 12 h dark) differ slightly from those of the above-mentioned studies, and the reported half-life values of TC in sediments therefore serve as supporting evidence rather than direct confirmation.

3.4.2 Effects of single and combined antibiotic exposure on primary production

Photosynthetic primary producers, among which green algae, form the foundation of aquatic food chains, and their reduction can directly disrupt the balance of aquatic ecosystems (Santos et al., 2010). Although green algae are not direct targets of antibiotics, their chloroplasts originate from endosymbiotic cyanobacteria and possess bacterial characteristics, such as being enclosed by at least two membranes and containing a DNA genome along with transcription and translation systems (McFadden and Roos, 1999). Consequently, some antibiotics exhibit toxicity toward green algae, making chloroplasts potential targets. Chronic toxicity studies have shown that algae are highly sensitive to antibiotics, and exposure to these compounds can significantly inhibit algal growth (Santos et al., 2010).

In this study, we found that SMT inhibited the growth of green algae from Day 3 onward when applied individually at concentrations of 1 and 10 µg/L (Fig. 3.2a). Previous studies have shown that nearly all sulfonamide antibiotics exhibit toxicity towards algae, with EC_{50} values ranging from 1,230 to 32,250 µg/L (Brain et al., 2008; Chen et al., 2020). The variation in toxicity among sulfonamide antibiotics may be related to their molecular structure, particularly the number of $-CH_3$ groups in the side chain (Białk-Bielińska et al., 2011). Generally, a greater number of $-CH_3$ groups corresponds to lower toxicity. SMT contains two $-CH_3$ groups in its side chain, suggesting a relatively high toxicity to algae. However, the concentrations at which the inhibition was observed in our study were much lower than those reported in previous research. This discrepancy may be attributed to differences in the experimental setup, as our system consisted of a mixed algal community rather than a single-species culture. While multi-species communities are generally assumed to be more resistant to disturbance due to functional redundancy, it is possible that particularly potentially sensitive subsets of the community dominated the response. In addition, the experiment was conducted during the winter season, when algal communities may include dormant or cold-adapted species that exhibit increased sensitivity upon reactivation under laboratory conditions.

Similarly, when TC was applied individually at concentrations of 15 and 150 µg/L, a comparable inhibitory effect on algae was observed (Fig. 3.2b). TC has also been reported to exhibit strong toxicity to green algae, with concentrations ranging from 250 to 30,000

μg/L significantly inhibiting the growth of various algal species (Amangelsin et al., 2023). In a seven-day exposure experiment, the EC_{50} of TC for *Microcystis aeruginosa* was found to be 90 μg/L, while that for *Selenastrum capricornutum* was 2,200 μg/L (Halling-Sørensen, 2000). Additionally, González-Pleiter et al. (2013) reported that TC at a low exposure concentration of 32 ± 8 μg/L could cause significant growth inhibition (EC_{10}), which is consistent with the effect concentration observed in the present study.

In the mixed treatments, we observed a more incoherent pattern. In the low mixture treatment, the green algae concentration initially increased slightly, but noticeably decreased after Day 3 (Fig. 3.2c). Importantly, the decrease after Day 3 suggests a toxic effect even in the low mixture treatment, consistent with González-Pleiter et al. (2013), who reported toxicity of TC–erythromycin mixtures at very low concentrations (EC10 = 4.6 ± 2.4 μg/L). This combined effect might result from the antibiotics acting on different physiological targets within the green algae. However, in the medium mixture treatment, the green algae concentration increased during the first 17 days, followed by a gradual decline, while in the high mixture treatment, the algae concentration remained stable until a noticeable decrease after the Day 17. Multiple studies have shown that common environmental pollutants, including antibiotics, heavy metals, and personal care products, can induce a hormesis effect (Jiang et al., 2020; Liu et al., 2017b; Mo et al., 2025). Hormesis refers to a biological phenomenon in which low doses of a chemical stressor trigger an over compensatory response to initial damage, resulting in enhanced growth or reproduction (Stanley et al., 2013). This effect typically follows a biphasic dose-response curve, characterized by stimulation at low concentrations and inhibition at higher levels. For example, Jiang et al. (2020) found that mixed exposure to four antibiotics, including TC and sulfamethoxazole, significantly enhanced the productivity of *Microcystis aeruginosa*. Similarly, Liu et al. (2017b) reported that a mixture of ciprofloxacin and sulfamethoxazole promoted the growth of *Microcystis aeruginosa* and increased its photosynthetic activity. Moreover, Mo et al. (2025) demonstrated that a mixture of three antibiotics, including SMT, could induce a stimulatory effect on *Scenedesmus obliquus*, especially under stressful environmental conditions, leading to excessive production of reactive oxygen species. This increase in reactive oxygen species may trigger oxidative stress, which green algae counteract by enhancing the activity of primary antioxidant enzymes, such as superoxide dismutase and catalase (Hong et al., 2024). These findings highlight that the combined toxicity of antibiotics exhibits significant dependency on the mixing ratio, concentration, and exposure duration (Zhao et al., 2023). Given the complex effects of TC and SMT on algae, it would be valuable for future research to conduct more comprehensive metabolomic analyses to gain a better understanding of the dynamic metabolic responses of green algae under mixed antibiotic stress, including the potential identification of hormetic patterns.

3.4.3 Effects of single and combined antibiotic exposure on aquatic invertebrates

In the SMT and TC treatments, a significant increase in the abundance of several zooplankton species was observed within one to two weeks of exposure (Fig. 3.4). These organisms included multiple *Daphnia* species (*Daphnia pulex*, *Daphnia longispina* and *Daphnia* sp.), as well as rotifers such as *Mytilina mucronata* and *Lecane gr. Luna* (Fig. 3.4). We found some evidence in the literature that this pattern may result from a hormetic response to the antibiotic concentrations used. Similar responses have been observed in *Daphnia* exposed to various environmental contaminants such as pesticides, heavy metals, and explosive compounds, suggesting that such hormetic effects may be relatively common in aquatic organisms. Mechanistically, the hormetic response in *Daphnia* has been linked to shifts in polyunsaturated fatty acid metabolism. In particular, exposure to low concentrations of toxicants has been associated with increased accumulation of short-chain lipid molecules and degradation of long-chain lipids, potentially contributing to the observed stimulatory effects (Stanley et al., 2013). Similar metabolic responses may also be triggered by SMT and TC in our study, potentially underlying the increased abundance observed in several zooplankton taxa.

In the present study, such "hormetic effects" were observed at relatively high concentrations of single-compound treatments in larger-bodied crustaceans such as *Daphnia* (the 10 µg/L SMT treatment and the 150 µg/L TC treatment). In contrast, smaller-bodied rotifers, including *Mytilina mucronata* and *Lecane gr. Luna* exhibited similar responses at much lower concentrations, such as the 0.1 µg/L SMT treatment and the 1.5 µg/L TC treatment. These findings suggest that species- or size-specific sensitivity may influence the threshold concentrations at which hormetic responses are triggered. A comparable pattern of low-dose stimulation has also been observed in response to other environmental toxicants, however, these toxicants belong to a different compound class than our investigated antibiotics. For example, Schunck and Liess (2023) found that exposure to the insecticide esfenvalerate at concentrations of ≤1/30 of its EC_{50} led to significant increases in biomass and abundance of *Daphnia magna* over seven weeks. According to existing literature, the lowest observed effect concentration ($LOEC_{21}$) of SMT for reproduction in *Daphnia magna* is 3,125 µg/L (De Liguoro et al., 2009), while the reproductive EC_{50} of TC is approximately 10,000 µg/L (Kim et al., 2012). In comparison, the concentrations at which the hypothesised hormetic responses were observed in this study were approximately 1/300 (SMT) and 1/67 (TC) of those respective values. This suggests that antibiotics may still cause substantial ecological effects even at concentrations far below traditional toxicity thresholds. Moreover, the hypothesised hormetic responses of these zooplankton species in our experimental system gradually diminished as antibiotic concentrations decreased over time. However, such declining exposure is not representative of natural aquatic environments, where organisms

are often subjected to continuous and long-term exposure to contaminants which are released, for instance, through wastewater treatment plant discharges.

In the mixture treatments, increased abundances of all *Daphnia* species were observed at lower mixture concentrations, which may reflect hormetic-type responses. However, as the concentration increased, these organisms gradually disappeared from the system, possibly indicating that higher mixture levels led to mortality or inhibition of reproduction. Notably, *Alona* sp. and *Brachionus* sp. did not show significant hormetic responses under individual SMT or TC treatments but exhibited increased abundances in the mixture treatments from Day 14 to Day 28 (Fig. 3.4). These results suggest that co-exposure to SMT and TC induced stronger stimulatory effects on *Alona* sp. and *Brachionus* sp. compared to single-compound exposures. Furthermore, the delayed responses observed in these two species suggest that mixture toxicity may vary not only among species, but also over time.

In contrast to the clear responses observed in zooplankton, no significant effects were detected on benthic macroinvertebrates under the single and mixture treatments. This may indicate a higher tolerance of these taxa, or differences in exposure pathways such as limited uptake from the water column. In addition, food consumption differed between TC treatments, with significantly higher consumption observed at the high TC treatments (Fig. S7). Notably, *Gammarus* abundance was higher in the TC 1.5 µg/L treatment, whereas total benthic macroinvertebrate abundance did not differ significantly among the TC treatments, indicating that food consumption was not directly driven by macroinvertebrate abundance. This may be related to changes in the microbial community on leaf surfaces that enhanced litter decomposition, potentially making the leaves more accessible to macroinvertebrates as further discussed in Section 4.4.

Taken together, these observations raise important questions about the adequacy of traditional ecotoxicological assessment approaches that primarily focus on lethal effects or the inhibition of growth and reproduction, thereby overlooking potential ecosystem-level disturbances caused by low-dose exposure. While hormesis offers one possible explanation for the observed population increases, alternative mechanisms, such as changes in grazing pressure on primary producers, cannot be ruled out and deserve further investigation. It is therefore important to consider not only the direct effects of contaminants on individual species, but also how such responses may be mediated through ecological interactions and trophic dynamics. To better assess the environmental risks of pharmaceuticals at low concentrations, future evaluations should incorporate more sensitive endpoints such as LOECs for growth and reproduction, and apply ecological modelling approaches to identify potential hormetic thresholds and nonlinear population-level responses.

3.4.4 Effects of single and combined antibiotic exposure on microbial communities

In this study, we found that SMT significantly affected microbial communities at environmentally relevant concentrations. Even at a dosing concentration as low as 0.1 µg/L, SMT induced changes in the aquatic microbial community structure on Day 3 of exposure. Additionally, significant effects were observed on the sediment microbial community on Day 7 (Fig. 3.5). These results are consistent with previous findings by Yergeau et al. (2010) and Kergoat et al. (2021). Yergeau et al. (2010) reported that exposure to 0.5 µg/L SMT for eight weeks induced transcriptional changes in biofilm microbial communities, while Kergoat et al. (2021) found that SMT at 0.5 and 5 µg/L significantly altered bacterial community structure within stream biofilms over 28 days of exposure. In contrast, TC at 1.5 µg/L did not cause significant changes in microbial community structures in either water or sediment. However, when the concentration increased to 15 and 150 µg/L, the community structure exhibited significant changes. Similarly, Zhang et al. (2013) reported that the microbial diversity in a sequencing batch reactor peaked at a TC concentration of 1 µg/L, but diversity significantly decreased when the concentration increased to 50 and 100 µg/L. These findings suggest that antibiotics, even at sub-inhibitory concentrations, can rapidly alter microbial communities in natural water environments, potentially impacting the ecological processes they support.

Beyond community-level changes, we also examined responses of specific bacterial taxa, including both sensitive and resistant genera in the water column and sediment. *Rickettsiella* was the most significantly responding genus in the water column. Further analysis revealed that this increase was primarily attributed to ASV_32651444. Using the NCBI 16S rRNA BLAST, this ASV was identified as *Rickettsiella massiliensis*-like (98.6% similarity, 100% query coverage). *Rickettsiella massiliensis* was originally isolated from the hard tick *Ixodes ricinus* and is commonly found in various arthropods, including insects and ticks. Typically, *Rickettsiella* spp. are considered intracellular symbionts or pathogens of various arthropods, including insects and crustaceans (Fryer and Lannan, 1994). However, in our study, changes in the abundance of ASV_32651444 did not correlate with changes in *Daphnia* or total zooplankton abundance, suggesting that the observed increase of this ASV cannot be readily explained solely by variation in these taxa, as *Rickettsiella* may be associated with a broader range of hosts than those quantified here.

In sediments, different antibiotic treatments exhibited distinct effects on sensitive taxa. For instance, the SMT treatments decreased the relative abundance of *Thermobacillus*, *Pseudonocardiaceae*_unidentified, and *Planifilum* compared to the control, while the TC treatments significantly reduced the relative abundance of *Bacillus* and *Bacillales*_unidentified. In the mixture treatments, the relative abundance of *Bacillus* and

*Nitrososphaeraceae*_unidentified also showed significant reductions. Notably, *Bacillus* has demonstrated varying antibiotic sensitivity in different environments. For example, *Bacillus cereus* is known to possess multidrug resistance (Cha et al., 2023). However, in our study, the relative abundance of *Bacillus* significantly decreased in the mixture treatments, indicating an increased sensitivity to specific antibiotic combinations. On the other hand, resistant genera exhibited consistent patterns across treatment groups. For instance, the relative abundances of *Vicinamibacterales*_unidentified, *Pirellula*, and *Nitrospira* consistently increased under various treatments compared to the control. This suggests that these genera may exhibit intrinsic tolerance or reduced susceptibility , have readily acquired resistance genes, or exhibit strong ecological adaptability in response to antibiotic pressure. Further studies employing metagenomic analysis could investigate whether these resistant taxa harbour or acquire resistance genes and assess their association with mobile genetic elements. This would help elucidate resistance mechanisms and potential pathways for the spread of resistance genes.

The observed microbial community shifts were further reflected in ecosystem functions, such as leaf litter decomposition. By the Day 28, the decomposition rates in nearly all antibiotic-treated groups were higher than in the control group (Fig. S8). In contrast, no significant differences in leaf litter decomposition were observed among the treatment groups on the Day 14. This finding partially aligns with Paumelle et al. (2021), who found that treatment with 5 µg/L sulfamethoxazole and SMT in a microcosm experiment did not significantly affect leaf decomposition after 16 days of exposure. In our study, significant increases in leaf decomposition were only observed on the Day 28. Although antibiotics did not significantly influence leaf decomposition within 16 days in a study of Paumelle et al. (2021), they did stimulate the activity of specific β-glucosidase enzymes in the leaves. β-glucosidases catalyze the hydrolysis of terminal β-D-glucosidic linkages, breaking down cellobiose and other small oligomers containing β-D-glucosidic bonds into monosaccharides (Deshpande and Eriksson, 1988). Enhanced enzyme activity often indicates an increased rate of cellulose degradation. Additionally, as discussed earlier, the increased relative abundance of *Vicinamibacterales_unidentified* and *Pirellula* in sediments may also contribute to the observed increase in leaf decomposition rate, given that some species within these genera have been identified as potential degraders of cellulose and polysaccharides (Klimek et al., 2024; Yadav et al., 2023). Besides these specific genera, the stimulatory effects of antibiotics on other bacteria might also play a role in promoting the leaf litter decomposition process (Paumelle et al., 2021).

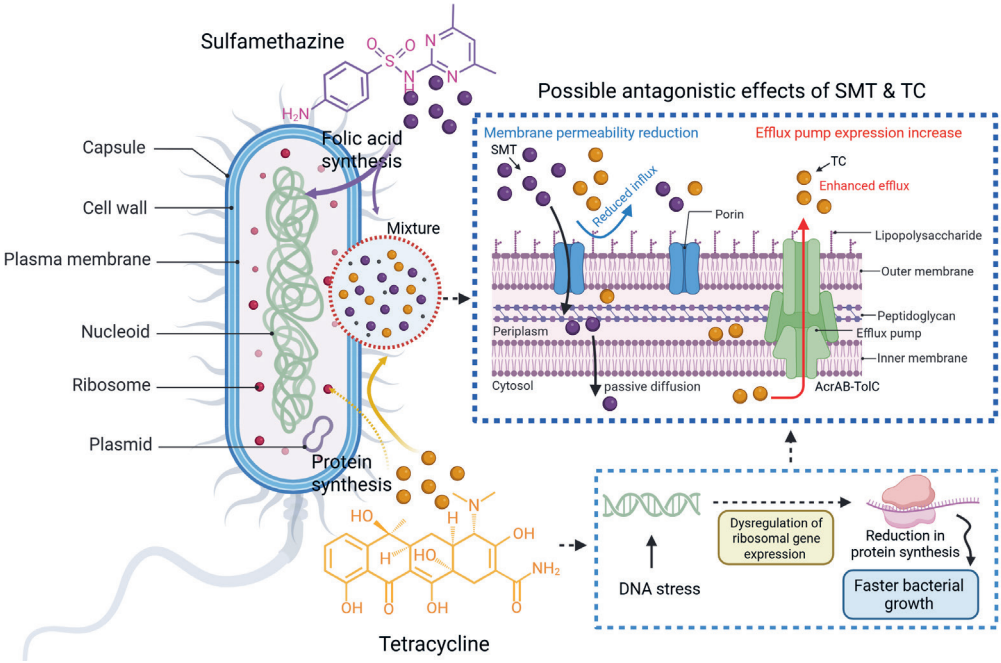


Figure 3.7. Cartoon of possible modes of action for SMT-TC interactions that function antagonistically in bacteria by altering membrane permeability, increasing efflux pump activity, and inducing nonoptimal regulation of cellular processes.

It is noteworthy that, in our study in water column, the combined exposure of SMT and TC, even at varying concentrations, did not significantly impact the microbial community composition. SMT competitively inhibits dihydropteroate synthase, blocking dihydrofolate synthesis and disrupting bacterial DNA synthesis (Mulla et al., 2023), while TC binds to the 30S ribosomal subunit, preventing aminoacyl-tRNA association and thus inhibiting protein synthesis and bacterial growth (Daghrir and Drogui, 2013) (Fig. 3.7). However, studies have shown that combining DNA and protein synthesis inhibitors can unexpectedly accelerate bacterial growth. Bollenbach et al. (2009) proposed the theory of nonoptimal regulation of ribosomal gene expression under DNA stress, stating that when DNA replication is inhibited, cells tend to maintain high levels of protein synthesis, leading to an imbalance in resource allocation and consequently restricting growth (Fig. 3.7). In contrast, suppressing protein synthesis with ribosomal inhibitors can alleviate the metabolic burden, freeing up resources for DNA repair and essential growth processes, thereby promoting bacterial recovery. Therefore, combining DNA and protein synthesis inhibitors may paradoxically enhance bacterial growth by mitigating the misallocation of resources.

Similar phenomena have been observed with other antimicrobial combinations, where antagonistic interactions were more common than synergistic ones, particularly when drugs

targeting different cellular processes were combined (Brochado et al., 2018). In *E. coli* experiments, Brochado et al. (2018) found that 14 out of 16 drug combinations with gentamicin or ciprofloxacin reduced intracellular antibiotic concentrations by either decreasing membrane permeability, thereby inhibiting proton-motive force-driven uptake, or by increasing the expression of the AcrAB-TolC efflux pump (Fig. 3.7). This reduction in intracellular levels weakened the antibacterial effects of combined therapy. Given the frequent occurrence of such antagonistic interactions, similar mechanisms may explain the lack of microbial community effects observed with SMT and TC co-exposure. To further illustrate this hypothesis, we have depicted the potential antagonistic mechanisms associated with SMT and TC co-exposure in Fig. 3.7.

Apart from that, interestingly, PCA results showed that microbial community structures were more similar in the mixture treatments to those in the TC treatments, while clearly separated from those of the SMT treatments. This pattern was consistently observed in both the water column and the sediment and was particularly evident on Day 14 (Fig. 3.6). Although SMT can induce strong community perturbations even at low concentrations, its influence did not dominate the community trajectory under co-exposure. This suggests that the presence of TC likely altered the SMT-induced direction of community development.

Based on the known mechanisms of action of SMT and TC at the bacterial level, we propose that TC may not have exerted higher toxicity in this context, but rather acted as a regulatory factor that actively modified the trajectory of community responses. This role may involve not only buffering the intensity of the disturbance but also reshaping the way microbial ecosystems respond to antibiotic mixtures. As a result, the microbial community structure under co-exposure does not appear to be a simple extension of either single-compound effect, but rather reflects a distinct interaction-specific state. This finding highlights the importance of identifying not only the individual toxicities of compounds in mixture scenarios, but also the regulatory roles they may play in shaping ecological outcomes.

3.5 Conclusions

This study employed a microcosm approach to systematically assess the ecological impacts of SMT and TC at environmentally relevant concentrations, both individually and as a mixture. The results revealed differential sensitivities among biological groups, with nonlinear, hormetic, and interactive responses across trophic levels. Notably, mixture treatments led to community shifts that were not consistent with simple additivity, highlighting the presence of complex biological interactions. In particular, microbial communities in the water column

exhibited clear antagonistic responses under mixture exposure, highlighting the complexity of antibiotic–antibiotic interactions. Furthermore, significant ecological disturbances occurred even at concentrations far below conventional toxicity thresholds. These findings underscore the importance of incorporating ecologically relevant endpoints and explicitly considering chemical interactions in future environmental risk assessment frameworks.

Environmental implication

This study employed a microcosm approach to systematically assess the ecological impacts of sulfamethazine and tetracycline at environmentally relevant concentrations, both individually and as a mixture. The results revealed differential sensitivities among biological groups, with nonlinear, hormetic, and interactive responses across trophic levels. In particular, microbial communities in the water column exhibited clear antagonistic responses under mixture exposure, highlighting the complexity of antibiotic–antibiotic interactions. Furthermore, significant ecological disturbances occurred even at concentrations far below conventional toxicity thresholds. These findings underscore the importance of incorporating ecologically relevant endpoints and explicitlyconsidering chemical interactions in future environmental risk assessment frameworks.

Acknowledgements

This work was supported by the National Natural Science Foundation of China (U22A20604, and 42030703). We acknowledge the China Scholarship Council (CSC) for supporting Dailing Wu (File No. 202006750027). Markus Hermann was supported by the EU Horizon 2020 project ECORISK2050 (No. 813124).

Supporting information

Supplementary data to this article can be found online at:
https://doi.org/10.1016/j.jhazmat.2026.141237





Bergen, Norway

Chapter 4

The effects of triclosan on microbial communities in different sources of water and sediments

Dailing Wu, Paul J. van den Brink, Hauke Smidt, Hong Bai, Guang-Guo Ying, Lara M. Schuijt

This chapter is based on: Wu, D., van den Brink, P.J., Smidt, H., Bai, H., Ying, G.G. and Schuijt, L.M., 2025. The effects of triclosan on microbial communities in different sources of water and sediments. *Ecotoxicology and Environmental Safety*, 303, p.118778.

Abstract

Triclosan is a widely used antimicrobial agent frequently detected in aquatic environments. Although its effects on environmental microorganisms have been extensively studied, findings often remain inconsistent due to variations in experimental setups and sediment characteristics. Comparative studies that assess microbial responses across different sediment types, however, are still scarce. Here, we employed a microcosm approach to assess triclosan-induced changes in microbial communities colonizing natural (pond and ditch) and OECD artificial sediments, aiming to compare microbial responses across sediment types and to identify environmental factors influencing triclosan effects. Natural sediments were collected from uncontaminated waterbodies, while artificial sediments were prepared following OECD guidelines and incubated for one month in pond and ditch sites, while natural sediments remained at their original locations. Following incubation, all sediments were exposed to triclosan (up to 1000 µg/L, resulting in a maximum sediment concentration of almost 1000 ng/g) under controlled laboratory conditions for seven days. Microbial community shifts were assessed using *16S rRNA* gene sequencing. The results showed significant differences in microbial community composition between ditch and pond sediments, as well as within water bodies, between natural and OECD sediments. Following triclosan application, microbial communities in the sediment of the OECD ditch, natural ditch, and natural pond groups exhibited significant differences compared to the control treatment at the highest concentrations (380 ng/g, 643 ng/g, and 661 ng/g, respectively). Several bacterial families known for triclosan degradation or resistance increased in relative abundance. Redundancy analysis indicated that water nutrient concentrations and sediment organic matter content significantly influenced microbial responses to triclosan exposure. Nutrient-rich environments supported greater microbial complexity and resilience, while high organic matter likely reduced triclosan bioavailability through adsorption. Overall, this study underscores the importance of both sediment characteristics and overlying water conditions in modulating microbial sensitivity to emerging contaminants. Our findings highlight the need to account for environmental heterogeneity when designing experiments and conducting ecological risk assessments for chemical pollutants.

4.1 Introduction

Triclosan has broad-spectrum antimicrobial activity against most Gram-negative and Gram-positive bacteria (Jabłońska-Trypuć, 2023). It inhibits bacterial growth by inhibiting fatty acid synthesis through the inhibition of the enzyme enoyl-acyl carrier protein reductase (DeLorenzo et al., 2008). As a result, it is widely used in personal care products, household items, medical devices, and clinical settings (Milanović et al., 2023). However, as awareness of triclosan's endocrine-disrupting potential and its role in promoting microbial resistance has grown, the United States, the European Union, and Canada have gradually banned or restricted its use since 2017 (EU, 2016; Food and Drug Administration, 2017; Gray et al., 2020). Despite these measures, triclosan is still present in many consumer products, as many countries have not yet banned its use. High concentrations of triclosan have frequently been detected in raw wastewater and surface water in countries such as Spain, Thailand, China, India, and South Africa (Milanović et al., 2023). It is speculated that due to incomplete and/or insufficient removal by wastewater treatment plants, triclosan can enter surface water, groundwater, and soil through municipal and industrial effluents (Huang et al., 2014). During the COVID-19 pandemic, the use of triclosan-based disinfectants increased significantly, leading to a notable rise in environmental emissions and raising concerns about increasing pollution (Adhikari et al., 2022).

Due to its high octanol-water partition coefficient (log Kow = 4.76), triclosan can be widely distributed across various environmental media, including water and sediment (Gray et al., 2020), aquatic organisms (Lu et al., 2019), and various human tissues (Bräuner et al., 2022), after being released into the environment through (treated) wastewater discharge (Barrett et al., 2022). In environmental matrices, triclosan has been observed to persist for extended periods, particularly under anoxic conditions (Chalew and Halden, 2009). It has been reported that triclosan has a predicted half-life of 120 days in soil, which extends to 540 days in sediments (Ying et al., 2007). Due to the high capacity for accumulation, sediments are considered an important sink for triclosan (Huang et al., 2015). For instance, triclosan concentrations ranged from 345 to 1,329 ng/g in sediments from the Pearl River system in China (Zhao et al., 2010). In a tributary of the Rhine River, triclosan concentrations in sediments were found to be as high as 450 ng/g (Kronimus et al., 2004).

To date, multiple studies have reported aquatic environmental risks of triclosan (Do et al., 2024; Kumar et al., 2021; Ricart et al., 2010). Triclosan exhibits acute toxicity to various aquatic species at concentrations ranging from micrograms to milligrams per liter (Do et al., 2024; Kumar et al., 2021). Additionally, triclosan has been shown to significantly reduce bacterial abundance in river biofilms at environmentally relevant concentrations (Ricart et al., 2010) and alter benthic microbial communities (Drury et al., 2013b; Peng et al., 2019).

Sediments serve as important reservoirs for carbon and other substances, characterized by high biomass and diversity of the microbial community (Liao et al., 2021). Microorganisms in sediments act as key drivers of biogeochemical cycles, playing critical roles in organic matter decomposition, humus synthesis, material transformation, and energy transfer (Frade et al., 2020). Therefore, it is crucial to understand the effects of pollutants on these microorganisms for the protection of these systems. However, the specific effects of triclosan on sediment microbial communities under different environmental conditions remain inadequately studied, particularly in sediments from different water sources.

It is well known that the physicochemical properties of sediments, such as grain size and organic matter content, impact the fate of chemicals, e.g. their partitioning in pore water and bioavailability (OECD, 2021). Consequently, sediment toxicity tests conducted with different sediments, whether collected from the field or artificially prepared, may yield different results. Toxicity testing using field-collected sediments may reflect site-specific characteristics, but due to the variability in sediment properties, the applicability of these results to other sediment locations may be limited. To improve the consistency of sediment toxicity test results across different tests or laboratories, it is recommended to use standardized, formulated sediments that meet the specific requirements of test organisms for triclosan spiking studies (OECD, 2023). While such OECD sediments provide a controlled and reproducible matrix for toxicity testing, their microbial colonization and response to pollutants may differ from those of natural sediments. Therefore, a comparative assessment is necessary to evaluate the ecological relevance of test results obtained from artificial sediments. We hypothesized that microbial community responses would vary depending on sediment origin and environmental context, with natural sediments possessing higher microbial diversity and potentially exhibiting greater sensitivity to triclosan exposure at lower concentrations compared to OECD artificial sediments. To more fully understand the impact of sediment type and triclosan exposure on benthic microbial community composition, we used small microcosms containing sediments from two different water bodies (a pond and a ditch) or artificially prepared sediment, following OECD guidelines. The microcosms were placed into each of the two water bodies to allow for natural microbial colonization and subsequently exposed to triclosan. This experimental design aimed to investigate the effects of triclosan on microbial communities in sediments and waters of different sources and types in order to 1) evaluate how microbial communities respond to triclosan exposure, 2) assess whether those responses differ between waterbodies and sediment type, and 3) evaluate the suitability of using in situ colonized artificial OECD sediment for assessing of the effects of pollutants on microbial communities. Together, these objectives aim to inform ecological risk assessments by elucidating the influence of environmental heterogeneity on microbial sensitivity to triclosan, and unlike previous studies that focused on single sediment types or specific experimental systems (Drury et al., 2013b; Peng et al., 2019), this study provides

a systematic comparison of microbial community responses to triclosan in both natural and OECD artificial sediments under environmentally relevant conditions. By linking microbial shifts to overlying water and sediment physicochemical properties, our work enhances understanding of how sediment characteristics influence microbial sensitivity to triclosan and improves the ecological relevance of toxicity assessments.

4.2 Materials and methods

4.2.1 Microcosm setup

In this microcosm experiment, we used 84 glass beakers (with a volume of 500 ml) containing a 2 cm sediment layer (approximately 200 g wet-weight of sediment) and a 300 ml water layer. The sediment layer in the microcosms consisted either of natural sediment collected from two water sources or artificial sediment. The artificial sediment was prepared according to OECD guidelines 218 (OECD, 2023) and is referred to as OECD sediment. Natural freshwater sediments were collected from a pond with sandy sediment on the campus of Wageningen University & Research (referred to as Natural Pond sediment, NP; 51°59'15.9"N 5°40'06.1"E), and a ditch with sediment containing a high clay fraction at the experimental field station Sinderhoeve (referred to as Natural Ditch sediment, ND; www.sinderhoeve.org; 51°59'56.2"N 5°45'18.8"E).

The upper 5 cm of the natural sediment from each core was sliced, and large particles such as leaves, rocks, and macrophytes were removed. The collected sediment from each site was thoroughly mixed and then distributed across the respective microcosms. The OECD sediment was composed of 4 to 5% (dry weight, d.w.) peat, 75% (d.w.) quartz sand and 20% (d.w.) kaolinite clay. Deionized water was added to obtain sediment with a water content in the range of 30-50%. To adjust the pH of the final mixture of the sediment to 7.0 ± 0.5, calcium carbonate of chemically pure quality ($CaCO_3$) was added (OECD, 2023).

After the two different natural sediments were added to half the microcosms and artificial sediment to the other half, each microcosm was covered with gauze with a 2 mm mesh to prevent disturbance from macroinvertebrates and other large aquatic animals. We submerged the microcosms with natural sediment in their corresponding waterbody and also added half of the microcosms with OECD sediment to each waterbody, allowing for microorganism colonization for one month. After this period, the microcosms were retrieved from the field sites and consisted of a natural or OECD sediment layer and an unfiltered water layer of pond or ditch water. The combination of two sediment types (OECD sediment

and natural sediment) and two water sources (the pond and ditch) used for the microcosm colonization resulted in 4 sediment*water groups, as shown in Table 4.1.

Table 4.1. Set-up of the microcosms and colonization location and corresponding treatment groups

Type of sediment	Water source	Location for colonization	Treatment groups (sediment*water groups)
OECD sediment	Pond	Pond	OECD*Pond (OP)
OECD sediment	Ditch	Ditch	OECD*Ditch (OD)
Pond sediment	Pond	Pond	Natural*Pond (NP)
Ditch sediment	Ditch	Ditch	Natural*Ditch (ND)

Microcosms were transferred to the laboratory and placed in a water bath maintained at 15 °C. We maintained gentle water movement in the microcosm by some light aeration. To prevent excessive algae growth and avoid photolysis of triclosan in subsequent procedures, average light conditions were maintained at 10 μE/m²/s. Microcosms were acclimatized in the laboratory for a period of seven days before exposure to triclosan.

4.2.2 Triclosan exposure

After the acclimatization period, triclosan ($C_{12}H_7Cl_3O_2$, 99.8 % Purity (HPLC), purchased as Irgasan from Sigma-Aldrich.) was spiked into the water column of the microcosms to achieve concentrations of 0 (controls), 10, 30, 100, 300 and 1000 μg/L. The stock solutions were made by dissolving triclosan in acetone. The volume of acetone in the microcosms was below 0.1 ml/L, and each microcosm received the same amount of acetone. The controls received the same amount of acetone (solvent control) or demineralized water (water control). The dosing solutions were applied using a pipette and gently mixed throughout the water column. Each treatment had two replicates, and the two control treatments (water control and solvent control) had four replicates, resulting in a total of 72 microcosms. The exposure period was set to seven days, aiming to evaluate short-term microbial community responses to triclosan.

4.2.3 Abiotic water properties and sediment sampling

Water quality indicators, including pH, dissolved oxygen (DO), temperature (T) and electrical conductivity (EC), were measured by a HACH multimeter (HQ40d) at the start (Day 0) and the end of the experiment (Day 7). Nutrient concentrations, including total nitrogen (TN), total phosphorus (TP), nitrate & nitrite, orthophosphate and ammonia, were analyzed by a segmented flow analyzer (Skalar 5100 Autoanalyser, Breda, The Netherlands). The

chlorophyll-a concentrations, indicative of algal biomass, were measured across different treatments by using a PHYTO-PAM phytoplankton analyzer (Heinz Walz, Effeltrich, Germany).

Sediment samples for the microbial composition analysis, organic matter content and triclosan concentration were collected before exposure (Day 0) and at the end of the experiment (Day 7). Sediment samples were collected by first gently removing the water layer with a syringe, and then the sediment was stored frozen at -20 °C until further analysis.

4.2.4 Triclosan extraction and analysis

Prior to extraction, 100 µL of 1 mg/L triclosan internal standard ($^{13}C_{12}$-triclosan; Cambridge Isotope Laboratories, Andover, USA) was added to 1.0 g of freeze-dried sediment. The mixture was thoroughly vortexed and stored at 4 °C overnight to allow equilibration. The next day, the spiked sediment samples were extracted three times with methanol using ultrasonication. Each extraction used 10 mL of methanol and was performed for 15 minutes. The three extracts were combined and diluted with Milli-Q water to reduce the methanol concentration to 10%, then acidified with 120 µL of 4 M H_2SO_4 and mixed well.

Oasis HLB cartridges (200 mg, 6 mL) were conditioned with 10 mL methanol followed by 10 mL of Milli-Q water. The diluted extracts were passed through the cartridges at a flow rate of 5-10 mL/min. After filtration, the cartridges were dried under vacuum and analytes were eluted by three successive additions of 4 mL ethyl acetate. The eluates were collected in glass tubes and evaporated using a SpeedVac Vacuum Concentrator (Thermo Fisher Scientific, USA) at 40 °C. The dried residues were reconstituted in 1 mL of methanol, filtered through a 0.45 µm organic phase filter membrane, and stored in a 2 mL amber vial at -20 °C until analysis.

Triclosan was quantified using an Agilent 1200 series ultra-high-performance liquid chromatograph (Agilent, USA) coupled to an Agilent 6460 triple quadrupole mass spectrometer equipped with electrospray ionization operated in both positive and negative ionization modes (UHPLC-ESI-MS-MS). Detailed instrumental parameters and quantification procedures are provided elsewhere (Huang et al., 2022).

4.2.5 Organic matter content and the adsorption capacity of triclosan in sediment

Organic matter content was measured for each treatment group at three time points: prior to in situ colonization (four replicates), after a 30-day colonization period (five replicates), and following 7 days of laboratory exposure (eight replicates). Ten grams of fresh sediment (Mfs) from each sediment sample was added to pre-ignited crucibles (M_c) and put in the drying oven at 105 °C for 16 h. The weight of sediment including the crucible after drying

was recorded (M_d). After that, the crucibles with sediments were put in a furnace at 550 °C for three hours. After cooling in a desiccator, the weight of the sediment and crucible was recorded after ignition (Mi). To control for potential weight changes unrelated to sediment content, blank crucibles were subjected to the same drying and ignition steps. No detectable change in crucible mass was observed across heating steps, confirming the stability of the measurement system. All samples and blanks were weighed using a precision analytical balance (± 0.1 mg). The percentages of water content (W_w) and organic matter (I_i) were calculated by the following formulas:

$$Ww = \frac{(\mathrm{Md} - \mathrm{Mc})}{\mathrm{Mfs}} \times 100 \qquad (1)$$

$$Ii = \frac{(\mathrm{Md} - \mathrm{Mi})}{(\mathrm{Md} - \mathrm{Mc})} \times 100 \qquad (2)$$

where W_w is the water content (% m/m); I_i is the loss-on-ignition on basis of oven-dry sediment (%, m/m); M_d is the mass of crucible with oven-dry sediment (g); M_c is the mass of empty crucible (g); M_{fs} is the weight of fresh sediment (10 g per sample); and M_i is the mass of crucible with ignited sediment (g).

The percentage of adsorbed triclosan to sediment was calculated as follows:

$$TCad = \mathrm{Ct} \times Vw \qquad (3)$$

$$Wds = \frac{\mathrm{Wfs} \times (100 - \mathrm{Ww})}{100} \qquad (4)$$

$$Adsorption\ \% = \frac{Cm \times \mathrm{Wds}}{\mathrm{TCad} \times 1000} \times 100 \qquad (5)$$

here TC_{ad} is the added mass of triclosan in each microcosm (μg); C_t is the nominal concentration of triclosan in each microcosm (μg/L); V_w is the volume of water in each microcosm (L); W_{ds} is the dry weight of sediment in each microcosm (g); C_m is the measured triclosan concentration in sediment (ng/g, dry weight basis).

4.2.6 *16r RNA* gene sequencing and microbial community data analysis

The total DNA was extracted from sediment samples using the DNeasy PowerSoil Kit (QIAGEN, Germany) following the manufacturer's protocol. The V4 region of the *16S rRNA* gene was amplified using barcoded primers 515F and 806R (Walters et al., 2016), as described in Zhang et al. (2022). Each 50 μL PCR reaction contained HF Green buffer, Phusion Hot Start II DNA Polymerase (Thermo Fisher), 500 nM of each primer and dNTPs, 10 ng template DNA, and nuclease-free water. The PCR cycling protocol was: 98 °C for 30

s; 25 cycles of 98 °C for 10 s, 50 °C for 10 s, 72 °C for 10 s; and a final extension at 72 °C for 7 min. Products were checked on 1% agarose gel, amplified in duplicate, pooled, and purified with CleanPCR beads (cleanNA). DNA concentrations were measured with Qubit (Thermo Fisher), and equimolar amplicons, along with positive and negative controls, were sequenced on the HiSeq2000 platform (Eurofins Genomics, Germany).

The obtained raw reads were processed with NG-Tax 2 (Poncheewin et al., 2020), including primer filtering, ASV picking, and taxonomic assignment using the SILVA 138 database (Capella-Gutiérrez et al., 2009). A 0.1% abundance threshold was applied to remove low-frequency ASVs. Output Biological Observation Matrix (BIOM) and tree files were imported into phyloseq, and subsequent analyses were performed using the phyloseq and microbiome R packages. *Mitochondrial*, *chloroplast*, and archaeal sequences were removed prior to analysis. The remaining ASV table was then rarefied to the minimum sample depth of 21,220 reads to ensure comparability across samples.

4.2.7 Statistical analyses

Multivariate analyses (Principal Component Analysis, PCA; Redundancy Analysis, RDA) and Monte Carlo permutation tests were performed to test the significance of the treatment variation and environmental variables on microbial community composition and visualized using Canoco 5 (ter Braak and Šmilauer, 2012). Given the limited number of replicates available to assess the effects of triclosan concentration on the microbial community, the scores from the first principal axis of the PCA were used for statistical analysis with the William's test. The rationale for using the values of the first principal axis was provided by Van den Brink et al. (1996).

The differences in water quality, nutrients and organic matter between different sediment*water groups were statistically compared using control samples (not individually specified in the results section) and analyzed with One-Way ANOVA or Dunnett T3 in IBM SPSS Statistics (v.28.0, Chicago, SPSS Inc.). A forward selection method using RDA and Monte Carlo permutation tests was employed to identify the key environmental factors influencing microbial community composition. Additionally, the difference between water control and solvent control groups was analyzed using a Monte Carlo Permutation test based on RDA. The difference in Shannon diversity between sediment*water groups was tested using the Dunnett T3 test in IBM SPSS due to heterogeneity of variance.

4.3 Results

4.3.1 Water and sediment quality

4.3.1.1 Water quality parameters, nutrients and chlorophyll-a

The water quality parameters (including DO, pH, water temperature and EC) did not exhibit significant differences across the different triclosan concentrations within each sediment*water treatment group ($P > 0.05$) (Fig. S1). However, the EC was notably higher in the pond groups (OP and NP groups) compared to the ditch groups (OD and ND groups) ($P < 0.05$), with values following the order OP > NP > OD > ND ($P < 0.05$). Additionally, the pH in the ND group was significantly lower than that in the other three groups ($P < 0.05$) (Fig. S1).

Notably, the levels of total nitrogen and ammonia in the pond water were significantly higher than those in the ditch water ($P < 0.05$) (Fig. S2). The nitrate and nitrite concentrations were highest in the NP group and lowest in the OD group, with values below the detection limit. The concentrations of orthophosphate in the ND group were the highest, significantly exceeding those of the other three groups ($P < 0.05$) (Fig. S2). In contrast, the ND group exhibited the lowest total phosphorus content ($P < 0.05$). Additionally, a notable trend emerged, with the levels of nitrate & nitrite sharply declining in all groups (except the OD group) when triclosan nominal concentrations exceeded 300 ng/L, approaching zero (Fig. S2).

The application of triclosan had no impact on chlorophyll-a in any of the sediment*water groups ($P > 0.05$, Fig. S3). However, chlorophyll-a concentrations in the ND group were significantly lower than those in the other groups ($P < 0.05$).

4.3.1.2 Organic matter in sediment

The initial OECD artificial sediment had an organic matter content of 3.9% (Table 4.2). However, the pond sediment was primarily sandy, while the ditch sediment was loamy, with organic matter contents of 0.52% and 2.06%, respectively. After one month of field microbial colonization and seven days of laboratory incubation, the organic matter content in the OD and OP group sediments was 3.4% and 3.5%, respectively, which was significantly higher than in the NP and ND groups ($P < 0.05$). At the end of the acclimatization, the ND group had an organic matter content of 2.0%, while the NP group had the lowest at 0.80%. Interestingly, by the end of the experiment, the organic matter content in all sediment groups had increased substantially by 6.0%, 6.0%, 3.4% and 1.2% in the OD, OP, ND and

NP groups, respectively. No significant dose-response relationship was observed between triclosan and organic matter in the sediment*water groups ($P > 0.05$, Fig. S4).

4.3.2 Triclosan in sediments

The triclosan spiking recovery test showed that the extraction recovery rate of triclosan in this study ranged from 102% to 120%. After seven days of exposure, the OP group had the highest triclosan sediment concentrations among the four groups, ranging from 11 to 916 ng/g (Table 2). Based on the amount of triclosan added, the amount adsorbed to the OP group sediment was calculated to range from 36% to 46%. The ND and NP groups followed, with triclosan concentrations ranging from 10 to 643 ng/g and 9 to 661 ng/g, corresponding adsorption of 24% to 37% and 27% to 40%, respectively. The OD group showed the lowest triclosan concentrations in sediments, ranging from 10 to 380 ng/g, with adsorption between 17% and 46% (Table 2).

4.3.3 Microbial community composition in sediments

A total of 15,027,904 reads were obtained by sequencing, with 1,902 ASVs being annotated. After normalization, each sample retained 21,220 reads. 34 bacterial phyla and 183 families were annotated across all samples. 14, 20, 27, and 23 bacterial phyla were annotated in the sediments of the OD, OP, ND, and NP groups, respectively, with phylum *Proteobacteria* being the most abundant in all groups (ranging from 35% to 68%), followed by *Bacteroidetes* (ranging from 10% to 18%) (Fig. 1). In addition, a high relative abundance of *Firmicutes* was found in the OD group, ranging from 23% to 24%. Monte Carlo permutation tests revealed that the microbial community phylum composition of the four sediment*water groups (i.e. OD, ND, OP and NP) significantly differed ($P < 0.05$).

The analysis of the alpha diversity of microbial composition in control groups, as shown in Fig. S5a, revealed significant differences in the Shannon diversity index at ASV level among the four sediment*water groups ($P < 0.001$), with the diversity ranking as follows: ND > NP > OP > OD. The microbial community composition in the water-control and solvent-control differed significantly in the OD group (Fig. S6, Monte Carlo Permutation test, $P < 0.05$). Therefore, the solvent control was used as a reference in all subsequent comparisons for all groups.

Table 4.2. Concentrations of triclosan in the sediment (ng/g dry weight) with its corresponding adsorption (%) in the microcosms measured at the end of the experiment (Day 7) and the organic matter content in different types of sediment of the microcosm experiment.

Nominal concentration (µg/L)		OECD sediment				Natural sediment			
		In pond		In ditch		In pond		In ditch	
		Concentration in sediment (ng/g)	Adsorption[a]	Concentration in sediment (ng/g)	Adsorption	Concentration in sediment (ng/g)	Adsorption	Concentration in sediment (ng/g)	Adsorption
0		< LOQ [b]	-	< LOQ	-	< LOD [c]	-	< LOD	-
10		11.4 ± 2.11	44.5%	10.4 ± 6.35	45.7%	8.86 ± 0.38	39.8%	10.1 ± 2.42	37.2%
30		35.5 ± 2.26	46.1%	17.6 ± 3.38	25.9%	18.5 ± 1.26	27.7%	23.7 ± 1.26	29.2%
100		94.2 ± 4.31	36.7%	46.3 ± 2.72	20.4%	65.5 ± 5.93	29.4%	67.9 ± 3.05	25.1%
300		282 ± 24.7	36.6%	164 ± 13.7	24.2%	240 ± 3.10	36.0%	201 ± 5.48	24.8%
1000		917 ± 47.9	35.8%	380 ± 10.1	16.8%	661 ± 34.2	29.7%	643 ± 15.0	23.8%
Water content (%)		41.5 ± 2.47		33.8 ± 0.54		32.6 ± 2.94		32.6 ± 2.94	
Organic matter (%)	Pre-treated[d]	3.89 ± 0.06				0.52 ± 0.02		2.06 ± 0.14	
	After acclimatization (Day 0)	3.48 ± 0.16		3.35 ± 0.15		0.80 ± 0.13		1.99 ± 0.07	
	End of experiment (Day 7)	6.05 ± 0.35		6.00 ± 0.03		1.24 ± 0.18		3.42 ± 0.14	

a. The percentage of applied triclosan that was adsorbed to the sediment.
b. LOD > 1 ng/g.
c. LOQ > 3 ng/g
d. Sediment introduced in the microcosms after collection (for natural sediments) or preparation (OECD sediment)

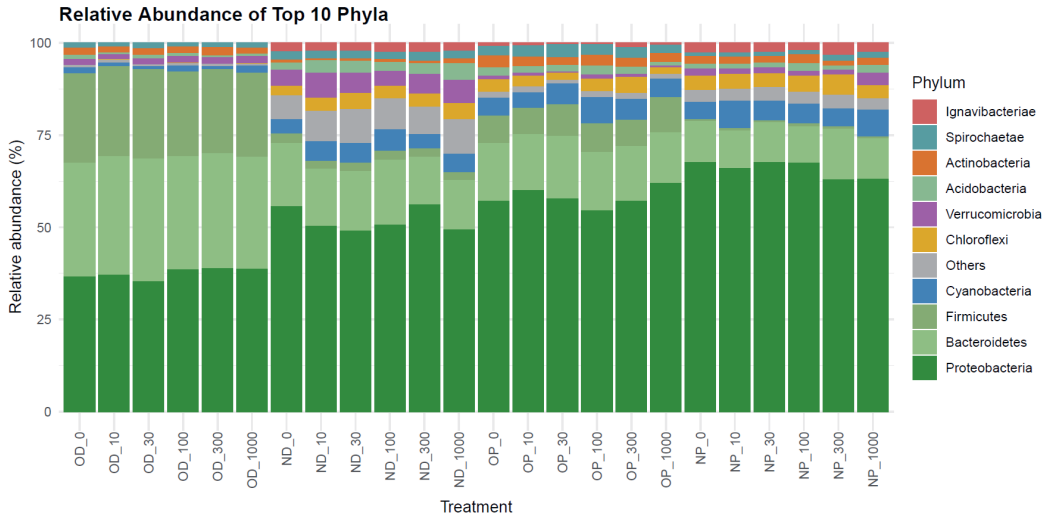


Figure 4.1. Mean relative abundance of the top 10 most abundant microbial phyla in the microcosm under triclosan treatment (0, 10, 30, 100, 300 and 1000) in different sediment*water groups (OD, ND, OP and NP) collected at the end of the experiment (Day 7). The triclosan treatment is based on the water's nominal triclosan (TCS) concentrations (µg/L). Abbreviations of sediment*water groups stand for OECD*Ditch (OD), Natural*Ditch (ND), OECD*Pond (OP) and Natural*Pond (NP). Less abundant phyla were aggregated into "Others".

4.3.4 Effects of triclosan on microbial community

The RDA showed that triclosan application accounted for 38% to 48% of the total variance in community composition across all four sediment*water groups. Additionally, the first two biplot axes together explained 24% to 33% of the variation in the bacterial community composition caused by triclosan (Fig. 4.2). Triclosan significantly affected the bacterial community composition of OD, ND and NP groups at the highest concentration (Williams test, NOEC = 300 µg/L, $P < 0.05$). However, in the OP group, triclosan treatment had no significant impact on the bacterial community composition ($P > 0.05$). In line with this observation, triclosan treatments did not significantly affect the Shannon diversity index as a measure of microbial alpha diversity at the ASV level in any sediment*water groups (Fig. S5b, $P > 0.05$).

Based on the results of RDA, the bacterial families that showed the largest response in the higher triclosan treatments (300 µg/L and 1000 µg/L) in each group are listed in Table S1. Interestingly, among the top 20 bacterial families displayed in the RDA biplot, 10 families appeared at least twice across different sediment*water groups (Table S1). These families included *Sphingomonadaceae*, *Rhodocyclaceae*, *Methylophilaceae*, *Chromatiaceae*,

Methylococcaceae, *Geobacteraceae*, *Desulfobulbaceae* and *Desulfurellaceae* from the phylum *Proteobacteria*, as well as *Chitinophagaceae* and *Sphingobacteriaceae* from the phylum *Bacteroidetes*. To further illustrate the treatment-induced changes, the relative abundance patterns of these key family across treatments are presented in Fig. S7 to S10.

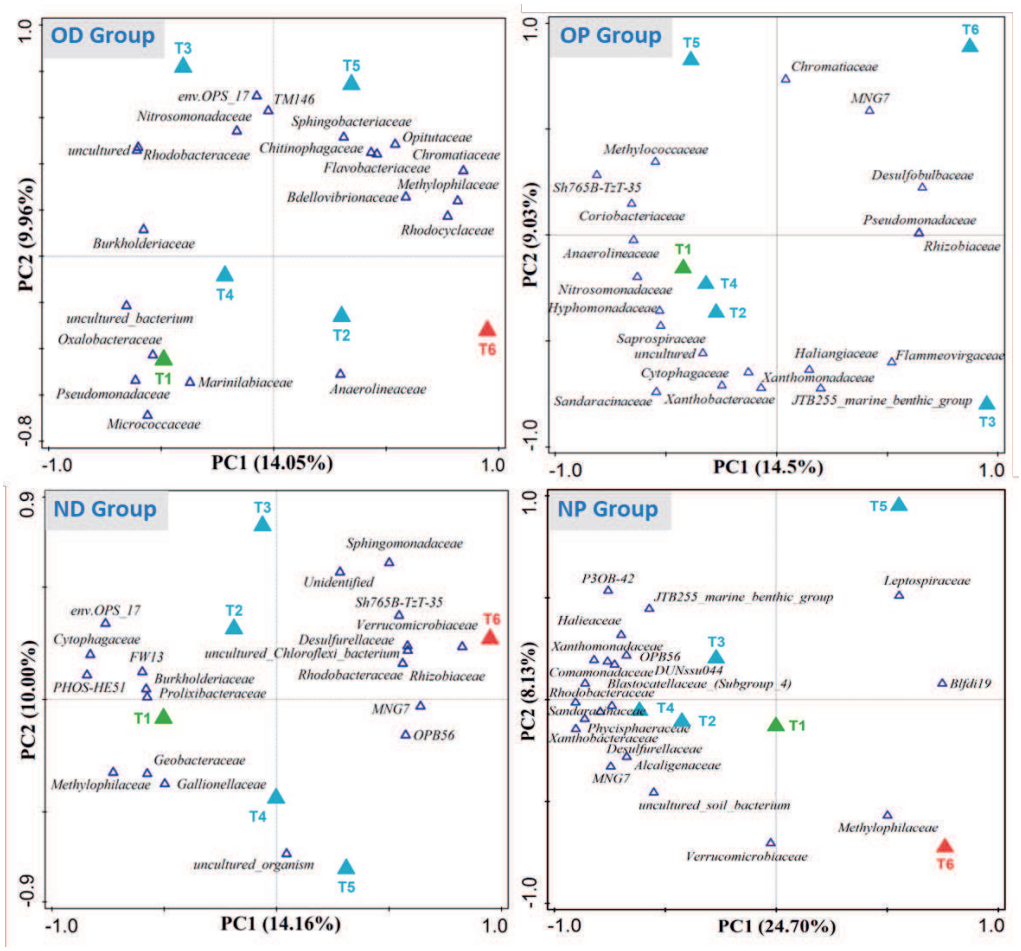


Figure 4.2. RDA biplots showing the effects of triclosan treatments on microbial community composition at the family level for the different sediment*water groups. The first and second RDA axes explained 24.01%, 25.35%, 24.16%, and 32.83% of the variation in bacterial community composition associated with triclosan treatments in the OD, OP, ND, and NP groups, respectively. The biplots show the 20 best-fitting families from the RDA analyses using sediment*water groups as explanatory variables. (In all biplots, T1: Solvent Control; T2: 10 µg/L; T3: 30 µg/L; T4: 100 µg/L; T5: 300 µg/L; T6: 1000 µg/L. The triangles represent the centroids of each treatment group, with those having significant effects shown as red triangles in the figure.). The triclosan treatment is based on the water's nominal triclosan concentrations (µg/L). Abbreviations of sediment*water groups stand for OECD*Ditch (OD), Natural*Ditch (ND), OECD*Pond (OP) and Natural*Pond (NP).

4.3.5 The effects of nutrients and water quality on microbial community

Through forward selection of the environmental variables using Monte Carlo Permutation tests under the RDA option, it was determined that several variables significantly contributed to explaining the observed variation in microbial community composition in the controls of different sediment*water groups. Variables included sediment type, water body location, ammonia, nitrite & nitrate, total phosphorus, orthophosphate, pH and organic matter (Table S2, $P < 0.05$). These variables were included in a PCA showing the difference in community composition between the solvent control treatment of the different sediment*water groups and their correlation with the environmental variables (Fig. 4.3). Compared to the ditch groups, the water of the pond group microcosms was richer in nitrogen nutrients, including ammonia, and nitrate & nitrite levels. The natural sediment groups had higher orthophosphate and nitrate & nitrite concentrations in the water, while the OECD sediment groups had higher total phosphorus and organic matter levels. Furthermore, the pH value in the OP group was higher than in other groups.

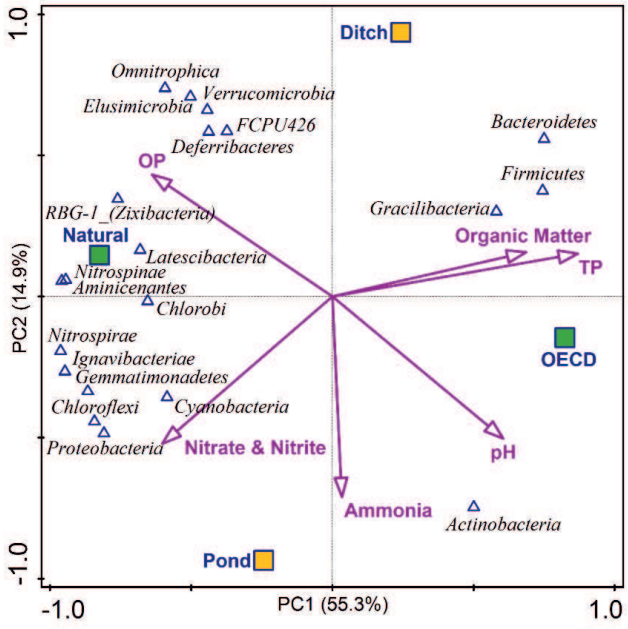


Figure 4.3. PCA biplot shows the correlation between nutrients, water quality parameters, organic matter and sediment*water groups, and the microbial community composition at the phylum level of the solvent control microcosms (20 phyla which fit the model best were presented).

4.4 Discussion

4.4.1 The effects of triclosan on microbial community

Previous studies have reported concentrations of triclosan in freshwater sediments of up to 53,000 ng/g (Chalew and Halden, 2009). In our study, after applying various triclosan concentrations for 7 days, triclosan levels detected in different sediment types ranged from 9 to 917 ng/g dry weight (Table 4.2), representing an environmentally relevant range.

In our study, significant changes in bacterial community composition were observed in the OD, ND, and NP groups at the highest concentrations compared to their respective control groups ($P < 0.05$). Despite these compositional shifts, no significant changes were observed in Shannon diversity. This may indicate that the changes were driven by shifts among dominant taxa without markedly altering overall richness or evenness. Moreover, the limited number of replicates may have reduced the statistical power to detect more subtle alpha diversity changes. Compared with previous studies, this finding represents the lowest effective concentration reported to date that significantly impacts sediment microbial community composition. For example, significant differences in bacterial community composition were found in artificial stream sediments after 14 and 34 days of exposure to triclosan concentrations of 5,700 and 8,100 ng/g dry weight (dw), respectively Drury et al. (2013b) . Similarly, the alpha diversity of microbial communities of biopurification microcosms was significantly lower than that of the control, and the bacterial activity was negatively affected after 50-day of triclosan exposure at a concentration of 20,000 ng/g (Aguilar-Romero et al., 2020). In another study, Peng et al. (2019) found no significant effects on the structure and richness of sediment bacterial communities at 800 ng/g dw after 28 days of exposure. However, at concentrations of 80,000 ng/g dw or higher, significant changes in sediment bacterial community structure and richness were observed. Furthermore, McNamara et al. (2014) reported structural changes in anaerobic bacterial communities following exposure to biosolid triclosan concentrations exceeding 50,000 ng/g. The concentrations of triclosan reported to affect microbial communities in sediments are very different. One of the reasons may be attributed to differences in application methods (Peng et al., 2019). For instance, in our study and that of Drury et al. (2013b), triclosan was introduced into the water phase, allowing it to partition between water and sediment, whereas Peng et al. (2019) directly spiked triclosan into the sediment, potentially leading to stronger sorption and lower bioavailability in porewater. Additionally, microcosm studies such as ours generally involve smaller water volumes and static conditions, which can result in more stable exposure concentrations and higher effective doses experienced by sediment microbes. By contrast, Drury et al. (2013b) used artificial stream systems with larger water volumes and continuous water flow, which could influence the partitioning dynamics and

reduce triclosan exposure levels in sediments. Furthermore, differences in the native microbial community composition and functional redundancy may substantially influence sensitivity to triclosan. At the taxon level, more diverse communities may show effects at lower concentrations because the likelihood of including sensitive taxa is higher. However, at the functional level, higher functional redundancy often enhance community resilience, resulting in higher effect concentrations (Lawrence et al., 2015). Other potential factors that could affect the response to triclosan, as well as to other chemicals, include sediment depth, flow rate of the overlying water and concentrations of dissolved organic carbon and inorganic nutrients (Lawrence et al., 2015).

Additionally, it was found that ten bacterial families belonging to the phyla *Proteobacteria* and *Bacteroidetes* were repeatedly recorded at the higher triclosan treatments across the four sediment*water groups (Fig. 4.2; Table S1). This presence suggests that these bacteria may utilize triclosan as a carbon source or possess protective mechanisms to survive under high concentrations of triclosan. Notably, bacterial families observed in our study, such as *Sphingomonadaceae*, *Rhodobacteraceae*, *Chitinophagaceae*, *Sphingobacteriaceae* and *Methylophilaceae,* have previously been reported to exhibit strong triclosan degradation capability in nitrification and denitrification systems, biopurification systems, and activated sludge enrichment cultivation systems (Aguilar-Romero et al., 2020; Dai et al., 2022; Lolas et al., 2012). In artificial streams, a significant correlation has also been observed between triclosan concentrations and the relative abundance of *Methylobacterium* (Drury et al., 2013b). Additionally, *Geobacter* from the family *Geobacteraceae* has been shown to directly metabolize a wide range of halogenated compounds, including triclosan, through de novo cobalamin synthesis (Chen et al., 2024). Interestingly, members of the *Sphingomonadaceae* family have been shown to exhibit strong genomic plasticity, which allows them to acquire new traits for pollutant degradation. Within this family, *Sphingobium* is an important vector for plasmid-mediated gene transfer in wastewater environments, contributing to the dissemination of antibiotic-resistance genes (Zhang et al., 2011). In contrast, it has also been reported that *Defluviicoccus*, a glycogen-accumulating bacterium from the family *Rhodobacteraceae*, has the potential to become resistant without carrying antibiotic resistance genes, being able to survive in environments with high triclosan concentrations (Li et al., 2020a). Last but not least, the development of bacterial resistance to triclosan appears to be highly sensitive, with a significant correlation observed between triclosan concentration and resistance in sediment at concentrations as low as 1 to 107 ng/g (Drury et al., 2013b). Therefore, at the triclosan concentrations used in this study, these bacteria with triclosan degradation capabilities or tolerance mechanisms may have been selectively increased in relative abundance, allowing them to dominate the microbial community.

In contrast, triclosan degradation by members of the families *Chromatiaceae*, *Desulfobulbaceae*, and *Desulfurellaceae* has not been observed. However, our study still detected these families at high triclosan concentrations, suggesting that they employ alternative survival strategies. Sulfate-reducing bacteria, *Desulfobulbaceae* and *Desulfurellaceae* can produce extracellular polymeric substances (EPS), especially proteins, to protect themselves when stimulated by toxins (Tang et al., 2022b). Apart from that, *Chromatiaceae* are efficient exopolymer producers, and their biostabilisation potential was significant (Hubas et al., 2013). It has been shown that total polysaccharides play a crucial role in promoting cell-to-cell adhesion and the binding of extracellular enzymes, while proteins typically function as protective barriers and structural components (Fulaz et al., 2019; Zhu et al., 2015). The increase in EPS, particularly the protein components, may help bind cells together and protect sulfate-reducing bacterial consortia from the toxicity induced by polyethylene microplastics (Tang et al., 2022b). It can be hypothesized that under the protection of EPS, bacteria from these families can survive in environments with high concentrations of triclosan, as observed in our study. However, as this mechanism remains hypothetical in the context of triclosan exposure, it would be valuable for future studies to directly measure EPS production under such conditions.

4.4.2 Nutrient availability affects the microbial communities and the effects of triclosan

Our results revealed significant differences in bacterial community composition between natural sediments from the pond and ditch and in OECD artificial sediments colonized in these environments. Differences in nutrient concentrations might cause these differences in community composition. Many studies have reported the impact of total nitrogen on bacterial community composition in lake sediments (Zeng et al., 2012; Zhao et al., 2012). Nitrogen concentration may directly or indirectly affect bacterial composition by altering biomass and plankton composition. Meanwhile, microorganisms play a key role in nutrient cycling and energy transport in freshwater lake ecosystems, contributing to crucial processes such as nitrogen fixation, ammonification, nitrification, and denitrification (Klump et al., 2009; Zhao et al., 2019). In this study, higher concentrations of inorganic nitrogen nutrients were detected in the pond water compared to the ditch (Fig. S2), and the relative abundance of *Proteobacteria, Chloroflexi* and *Cyanobacteria* in the pond sediment was strongly associated with nitrate & nitrite levels (Fig. 4.3). Furthermore, bacterial phyla such as *Nitrospinae, Aminicenantes, Chlorobi, Nitrospirae, Ignavibacteria* and *Gemmatimonadetes* showed significant correlations with both nitrate & nitrite and orthophosphate levels in the pond sediments (Fig. 4.3). This can be explained by the fact that nitrate, nitrite and orthophosphate are nutrients that certain bacteria can directly utilize, and many bacteria in these phyla have been functionally identified to facilitate nitrogen and phosphorus cycling in

water-sediment environments (Zhou et al., 2019). For example, strains of *Candidatus Accumulibacter* from the phylum *Proteobacteria* possess denitrification genes such as *narG* and *nirK* (Zeng et al., 2016). *Nitrospira*, a representative of *Nitrospirae*, contributes to nitrite oxidation (Ushiki et al., 2017). Certain taxa within *Chloroflexi* mediate dissimilatory nitrate reduction to ammonium (Bovio-Winkler et al., 2023), and some *Cyanobacteria* carry *nifH* genes involved in nitrogen fixation (Warshan et al., 2016). However, in the nutrient-poor ditch, the relative abundances of *Bacteroidetes* and *Firmicutes* were significantly higher than in the other groups (Fig. 4.1, $P < 0.05$). These bacteria exhibited negative correlations with most detected nutrients (Fig. 4.3), indicating that they have a metabolic advantage in oligotrophic environments. More interestingly, another study found that bacterial network complexity was higher in a hypereutrophic lake compared to an oligotrophic lake (Xie et al., 2024). Numerous studies consistently demonstrated a strong positive correlation between bacterial network complexity and its stability (Montoya et al., 2006; Yuan et al., 2021). This correlation hypothesis suggests that bacterial communities from oligotrophic environments may respond more rapidly to disturbances, thereby making their community structure more susceptible to changes (Dai et al., 2017). This may explain why the microbial communities in the sediments of OD and ND groups were significantly affected by triclosan, while this was not the case in the OP group.

In addition to the water's nutrients, the sediment's organic matter content may also play a crucial role in helping microbial communities resist triclosan stress. Triclosan has strong hydrophobicity and readily binds to dissolved organic matter, humic substances, and sediment particles, influencing its bioavailability and reducing its direct toxicity to microbes (Chalew and Halden, 2009). In the nutrient-rich pond sediment, the organic matter content in the OP group was much higher than in the NP group, and the OP group adsorbed the highest amount of triclosan (916 ng/g) at the highest exposure concentration. The higher organic matter content in the OP sediment may have led to increased sorption of triclosan, thereby reducing the concentration of its freely available form, including in the interstitial water. This reduced availability likely limited the direct exposure of microbial communities to triclosan, which may explain why the NP group showed significant community shifts at the highest concentration, while the OP group was less affected. Furthermore, after oxidation and degradation, humic substances transform into smaller molecular weight carbon sources, which are more easily absorbed and utilized by microorganisms (Kristensen et al., 1995). During anaerobic respiration, certain bacteria can even use humic substances as electron donors or acceptors (Klüpfel et al., 2014), which may further enhance the stability of microbial communities in the OP group sediments and their resistance to external stressors.

4.5 Conclusions

Through *16S rRNA* gene sequencing, it has been revealed that environmental concentrations of triclosan significantly affect the composition of microbial communities in sediments of different types and sources. These effects were primarily influenced by the abundance of inorganic nutrients in the water body, with microbial communities in oligotrophic systems being more sensitive to antimicrobial disturbances than those in eutrophic systems. Furthermore, the study suggests that the organic matter content in sediments may also modulate the impact of triclosan on microbial communities. Sediments with high organic matter content can adsorb more compounds, reducing their bioavailability and consequently mitigating their effects on microbial communities. Therefore, future research should consider nutrient availability to assess better the impact of chemical compounds on microbial communities in environmental matrices. Additionally, while artificial sediments offer an effective approach to minimize experimental biases caused by the complexity of natural sediments, making them suitable for biotoxicity testing, their findings may not fully reflect the comprehensive effects observed in natural environments. For instance, our results showed that natural sediments possessed higher microbial diversity compared to OECD artificial sediments, highlighting a limitation that should be carefully considered in future research. These results suggest that ecological risk assessments for triclosan should account for sediment-specific microbial responses and nutrient conditions to ensure accurate predictions of ecological impacts.

Acknowledgements

This study was supported by the Dutch Research Council (NWO) domain TTW, KWR, STOWA and commercial parties through the EMERCHE project: Effect-directed Monitoring tools to assess Ecological and human health Risks of CHemicals of Emerging concern in the water cycle (File number 15760). We acknowledge the China Scholarship Council (CSC) for supporting Dailing Wu (File No. 202006750027).

Supporting information

Supplementary data to this article can be found online at:
https://doi.org/10.1016/j.ecoenv.2025.118778





Mount Kilimanjaro, Tanzania

Chapter 5

Trophic transfer and biological effects of azithromycin across a freshwater food chain

Dailing Wu, Anna Huang, Guang-Guo Ying, Hauke Smidt, Paul J. Van den Brink

This chapter is based on: Wu, D., Huang, A., Ying, G.-G., Smidt, H. and Van den Brink, P.J. Trophic transfer and biological effects of azithromycin across a freshwater food chain. Paper under review.

Abstract

Antibiotics in the aquatic environment can bioaccumulate in aquatic organisms and transfer to higher trophic levels. While the direct toxic effects of antibiotics on aquatic organisms have been extensively studied, research on their transfer through aquatic food chains and their indirect effects on ecosystems remains limited. This study investigated the transfer and toxicity of the antibiotic azithromycin within a simplified food chain comprising the primary producer *Scenedesmus obliquus*, the primary consumer *Daphnia magna*, and the predator *Chaoborus obscuripes*. Toxicokinetic analyses revealed a high bioconcentration potential of azithromycin in *S. obliquus*, with a bioconcentration factor (BCF) of 1,017 L kg^{-1}, whereas *D. magna* exhibited a lower BCF of 372 L kg^{-1}, indicating interspecific differences in uptake and elimination kinetics. In the trophic transfer experiment, the biomagnification factor from *D. magna* to *C. obscuripes* was lower than 0.032, suggesting negligible biomagnification and a tendency toward trophic dilution. Despite the limited transfer efficiency, *C. obscuripes* exposed to azithromycin-contaminated prey exhibited a significant reduction in growth ($P < 0.05$), implying possible sublethal metabolic or physiological stress. Collectively, these results demonstrate that azithromycin can be efficiently accumulated by primary producers but is unlikely to biomagnify along freshwater food chains, although its indirect effects on higher trophic organisms merit further attention under environmentally relevant conditions.

5.1 Introduction

The widespread use of antibiotics has led to increasing concern about their release into the aquatic environment via multiple pathways, including waste discharges from manufacturing, human and veterinary excretion and agricultural applications (Hanna et al., 2023; Tan and Xi, 2025). Aquatic ecosystems worldwide are now experiencing pervasive antibiotic contamination, with concentrations in surface waters typically ranging from ng L^{-1} to µg L^{-1} (Chen et al., 2025; Hanna et al., 2023). The environmental risks of aquatic antibiotics depend not only on their exposure levels but also on their distinct hazard profiles, such as strong biological activity and the potential to disrupt microbial communities (Zhu et al., 2022). Environmental concentrations of antibiotics are generally unlikely to cause acute toxicity to most aquatic organisms (Crane et al., 2006; Schuijt et al., 2024b). However, chronic exposure to low concentrations of antibiotics has been reported to affect individual behaviour and reduce fertility in the freshwater crustacean *Daphnia magna* (Bownik et al., 2019; Nguyen et al., 2021). Given the widespread use of *Daphnia* as a model in ecotoxicity testing and its ecological representativeness for many freshwater invertebrates, these findings raise concerns that similar sub-lethal effects may also occur in other aquatic invertebrates.

In addition to direct exposure to aqueous antibiotics, aquatic organisms may also receive antibiotics through food consumption. Consequently, antibiotics can bioaccumulate within organisms and be transferred to higher trophic levels, potentially resulting in biomagnification. Field studies have reported biomagnification of certain antibiotics in aquatic food webs (Liu et al., 2017a; Tang et al., 2020; Tang et al., 2022a). However, these studies were based on organisms collected from natural environments where exposure may have occurred simultaneously through water, sediment ingestion and diet. As a result, the reported trophic magnification patterns reflect the combined influence of multiple exposure pathways, and the individual contribution of dietary transfer cannot be determined clearly (Harriage et al., 2025). Therefore, controlled studies that isolate foodborne exposure are needed to clarify how antibiotics are transferred across trophic levels.

To better understand and predict the transfer of antibiotics across food webs, it is necessary to quantify how they accumulate in organisms at the lower part of the food chain, such as primary producers and primary consumers. At these basal trophic levels, continuous contact with the water column means that waterborne exposure can represent a major uptake pathway. Accordingly, the bioconcentration factor (BCF) provides a key metric to characterize antibiotic uptake from water in these organisms (Wang et al., 2022). However, conventional BCF estimates derived from single time-point tissue concentrations provide only a snapshot of internal exposure under a given scenario and therefore offer limited

insight into how internal burdens change through time as uptake and elimination proceed (Ratier et al., 2021). Toxicokinetic (TK) approaches address this limitation by explicitly linking uptake and elimination processes to time-resolved internal concentrations (Miller et al., 2016). Within such TK frameworks, BCFs are derived from first-order kinetic models fitted to internal concentration–time data, providing a process-based measure of bioconcentration potential that constrains the fraction of antibiotic burdens available for subsequent trophic transfer (Miller et al., 2016).

In this study, we developed a simplified aquatic food chain to investigate the bioconcentration, bioaccumulation and biomagnification of an antibiotic and its effects across different trophic levels. The chain comprised the primary producer green algae (*Scenedesmus obliquus*), the primary consumer water flea (*Daphnia magna*), and the secondary consumer phantom midge (*Chaoborus obscuripes*). For *S. obliquus* and *D. magna*, we conducted toxicokinetic experiments to quantify bioconcentration. Organic chemicals are considered potentially bioaccumulative when their $\log K_{ow}$ exceeds 3 (Zenker et al., 2014). Accordingly, we selected azithromycin (AZT), a macrolide antibiotic, as our compound of interest because its hydrophobicity (logKow = 4.01) places it in the range of compounds considered potentially bioaccumulative (Zhu et al., 2023).

5.2 Materials and methods

5.2.1 Organism culture and maintenance

S. obliquus and *D. magna* were obtained from a stable culture maintained in the laboratory of the Aquatic Ecology and Water Quality Management group at Wageningen University & Research. The cultivation of organisms followed the methodology established in our previous research (Zhao et al., 2020) with minor adaptations. *S. obliquus* was cultured in WC medium under continuous illumination and aeration at 20 °C to ensure sufficient biomass growth for subsequent experiments. *D. magna* was maintained in RT medium (Kang et al., 2022) under 16 h light/8 h dark cycles at 20 °C, and was fed *S. obliquus* daily. The predator, *C. obscuripes,* was collected from the Sinderhoeve field station (Renkum, the Netherlands; www.sinderhoeve.org) six days before the experiment and kept in a covered bucket with pond water from the same location. Upon arrival at the lab, *C. obscuripes* were acclimated at 4 °C in pond water from the Sinderhoeve for one day, after which WC medium was gradually introduced over the next three days, reaching 20%, 50%, and 80% of the total volume on consecutive days, respectively. To slow down moulting, *C. obscuripes* were kept

at 4 °C throughout acclimatization. During this period, *C. obscuripes* were fed uncontaminated *D. magna* individuals every 72 h.

5.2.2 Toxicokinetic experiments

5.2.2.1 *S. obliquus*

The experiment consisted of two phases: an uptake phase and an elimination phase, each lasting 24 h. During the uptake phase, *S. obliquus* was exposed to AZT at a concentration of 48 μg L^{-1}, a level previously shown to be non-toxic to this species (Xiong et al., 2019). The initial AZT concentration in the exposure medium was confirmed by analyzing water samples taken at the start of the uptake phase. For the uptake experiment, 70 mL of *S. obliquus* culture (cell density: 10^6 cells mL^{-1}) was dispensed into each of 22 Erlenmeyer flasks (100 mL), and AZT solution (Sigma-Aldrich, Germany; dissolved in WC medium) was added to achieve the target concentration. Samples of *S. obliquus* were collected at 4, 8, and 24 h (three replicates each) and concentrated by centrifugation at 2000 rpm for 5 min. To remove AZT adsorbed on the cell surface, the pellets were washed twice with clean WC medium and centrifuged under the same conditions.

After 24 h of exposure, *S. obliquus* from the remaining Erlenmeyer flasks was collected, washed by centrifugation as described above, and resuspended in 70 mL of clean WC medium to initiate the elimination experiment. During the elimination phase, *S. obliquus* was sampled at 3, 6, and 24 h (three replicates each). The samples were centrifuged and washed twice with clean WC medium to remove residual AZT, following the same procedure as in the uptake phase. All algal pellets from both the uptake and elimination phases were immediately stored at −20 °C for subsequent AZT extraction and analysis.

5.2.2.2 *D. magna*

D. magna individuals were exposed to 48 μg L^{-1} AZT, a concentration well below the reported 24 h EC_{20} of 49,000 μg L^{-1} (Li et al., 2020b). Both uptake and elimination phases lasted 24 h. Approximately 30 individuals (7–9 d old) were placed in each of 18 glass jars containing 300 mL RT medium spiked with 48 μg L^{-1} AZT. During the uptake phase, *D. magna* individuals were sampled at 4, 15, and 24 h (three replicates per time point), gently rinsed twice with Milli-Q water through a fine mesh to remove surface residues, and immediately stored at −20 °C for chemical analysis. A water sample was taken at the start of the uptake phase to verify the exposure concentration.

After 24 h of exposure, the remaining individuals were washed as described above and transferred to nine jars containing clean RT medium to initiate the elimination phase.

Samples were collected at 3, 14, and 24 h (three replicates each), processed identically, and dead individuals were removed before storage.

5.2.3 Food chain experiment

In addition to the toxicokinetic experiments, a model freshwater food chain consisting of *S. obliquus* (algae) – *D. magna* (zooplankton) – *C. obscuripes* (benthic invertebrate) was established to study the accumulation, biomagnification, and potential toxic effects of AZT across three trophic levels. The entire 21-day feeding exposure was conducted in a climate-controlled room (temperature: 20 °C; photoperiod: 16 h light : 8 h dark; light intensity: ~20 µE m^{-2} s^{-1}).

To ensure that AZT concentrations remained within measurable levels during trophic transfer, *S. obliquus* was first exposed to a relatively high AZT concentration (1,000 µg L^{-1}) for 24 h. Specifically, 500 mL of algal suspension (cell density: 10^6 cells mL^{-1}) was added to a 1 L Erlenmeyer flask containing AZT stock solution adjusted to the target concentration. After 24 h of exposure, algal cells were harvested and rinsed with clean medium to remove surface-bound AZT residues (Phase 1 in Fig. 5.1). To characterize AZT levels in both the algae and the medium over the course of the exposure, samples of *S. obliquus* and the surrounding WC medium were collected at 3, 21, and 24 h.

The AZT-exposed algae (hereafter referred to as "algae-AZT") were then used as food for *D. magna* to study the bioaccumulation of AZT through dietary exposure (Phase 2 in Fig. 5.1). The collected algae-AZT were resuspended in 500 mL RT medium to reach a density of 10^5 cells mL^{-1} (OECD, 2011). Approximately 150 neonate *D. magna* (1–2 d old) were introduced into each vessel and exposed to the resuspended algae for 48 h (Kowalewska et al., 2020). A parallel control treatment was performed under identical conditions, using unexposed *S. obliquus* as food at the same density. At the end of exposure, both the control and AZT-fed *D. magna* (hereafter "*Daphnia*-AZT") were collected for the next trophic level exposure. To quantify AZT accumulation in *D. magna* during the 48 h feeding period, individuals were sampled at 24 and 48 h. Dissolved AZT concentrations in the surrounding RT medium were monitored by sampling at 0, 24, and 48 h.

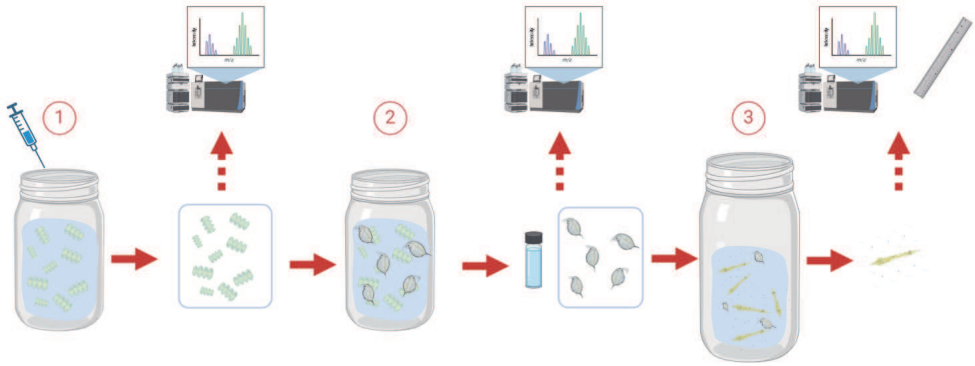


Figure 5.1. Setup of the three-phase food-chain experiment (*S. obliquus–D. magna–C. obscuripes*). Phase I: *S. obliquus* was exposed to AZT and harvested for use as food. Phase II: *D. magna* was fed AZT-exposed *S. obliquus* to quantify dietary uptake and trophic transfer. Phase III: *C. obscuripes* was fed exposed *D. magna* to quantify trophic transfer.

Before being fed with *Daphnia*, all *C. obscuripes* individuals were starved for 24 h at 20 °C to empty their guts. A total of 120 similar-sized larvae were evenly distributed among 24 glass jars containing 1 L of WC medium, with five individuals per jar. Twelve jars were assigned to the AZT-exposed group (fed with *Daphnia*-AZT) and 12 as the control group (fed with clean *Daphnia*). Feeding occurred every 72 h, and the number of *Daphnia* provided was twice the number of surviving *C. obscuripes* in each jar (Phase 3 in Fig. 5.1).

Notably, to maintain consistent food freshness and exposure conditions, each batch of *Daphnia*-AZT used for feeding was newly produced and had undergone 48 h of exposure to algae-AZT, ensuring that *C. obscuripes* always consumed 1–2 day-old *Daphnia*. Similarly, all algae-AZT used in the experiment were freshly prepared after 24 h of AZT exposure. This dynamic feeding design was technically demanding but ensured the accuracy and ecological relevance of AZT transfer along the food chain.

C. obscuripes and *C. obscuripes-AZT* were sampled at the end of the 21-day exposure. All individuals were photographed to determine body length. To ensure sufficient biomass for chemical analyses, larvae from 12 jars per treatment were randomly pooled into three biological replicates.

All biological samples were rinsed with Milli-Q water and stored at −20 °C. Aqueous samples were filtered through 0.45 µm cellulose-acetate syringe filters and stored at −20 °C until further analysis. To compensate for evaporation, the medium volume in each jar was

replenished to 1 L every 72 h. Dead individuals and pupae were removed promptly throughout the experiment.

Prior to the start of the experiment, 60 *C. obscuripes* larvae were randomly selected to measure initial body length for growth comparison. To avoid additional handling stress, these individuals were not included in the exposure experiment.

5.2.4 Measurement of algal cell density and animal body length

The cell density of *S. obliquus* was determined using a CASY cell counter (model TT). For each measurement, an aliquot of algal suspension was diluted 100-fold with CASYton solution. Each sample was measured three times, and the mean value was used for further analysis.

The body length of *D. magna* was measured under a Leica Stereo MZ12 microscope. Images were captured using Micro Capture software (version 2.9.4), and body length was determined from the anterior edge of the eye to the posterior margin of the carapace, excluding the apical spine.

The body length of *C. obscuripes* was measured using a Carson digital microscope. Larvae were first anesthetized by brief immersion in carbonated water. Once immobilized, individuals were placed on a measuring pad, photographed under the microscope, and their body length was determined from the scale markings on the pad.

5.2.5 Extraction and quantification of azithromycin

The extraction of AZT from organism samples followed a protocol adapted from our previous study (Huang et al., 2021). Briefly, organism samples were freeze-dried for 24 h to ensure complete dehydration, and the dry mass of each sample was recorded. The dried material was then transferred into 2 mL centrifuge tubes, and 100 µL of the internal standard erythromycin (100 µg L^{-1} in methanol) was added. The tubes were placed on ice with caps open overnight to allow methanol to evaporate.

After complete evaporation of methanol, 1 mL of acetonitrile was added to each tube for extraction. The samples were agitated three times with beads using an MP FASTPREP-24™ 5G at 4.0 m s^{-1} for 30 s, followed by 15 min of sonication and centrifugation at 10,000 × g for 5 min. The resulting supernatant was transferred to new tubes. This extraction process, including acetonitrile addition, bead-beating, centrifugation, and supernatant collection, was repeated twice, yielding three extractions in total. The combined supernatants were stored at −20 °C for 12 h to allow lipid precipitation. The samples were then centrifuged again at

10,000 × g for 5 min, and the clear supernatant was transferred to 10 mL round-bottom glass tubes. Acetonitrile was removed using a SpeedVac vacuum concentrator (Thermo Fisher Scientific, USA) for approximately 2 h. The dried extracts were reconstituted in 1 mL of analytical-grade methanol, filtered through 0.45 µm cellulose acetate syringe filters, and stored at −20 °C until LC–MS/MS analysis.

Quantification of AZT was performed using an Agilent 1200 Infinity liquid chromatography system coupled with an Ultivo Triple Quad mass spectrometer (Agilent Technologies, USA) equipped with an Agilent Jet Stream electrospray ionization (AJS-ESI) source operating in positive mode. Chromatographic separation was achieved on an Agilent ZORBAX Eclipse Plus C18 column (4.6 × 50 mm, 2.7 µm) maintained at 35 °C. The mobile phase consisted of (A) methanol with 0.1% formic acid and (B) Milli-Q water with 0.1% formic acid, run isocratically at 50:50 (v/v) with a flow rate of 0.5 mL min^{-1}. The injection volume was 10 µL. Nitrogen was used as both the nebulizing and collision gas. The capillary voltage was set at 3500 V, the ion source temperature at 300 °C, the gas flow at 5.0 L min^{-1}, the sheath gas temperature at 250 °C, and the sheath gas flow at 11 L min^{-1}. AZT was detected in multiple reaction monitoring (MRM) mode with two transitions (m/z 749.6 → 591.6 and 749.6 → 158.3). The MRM transitions for the internal standard erythromycin A were m/z 734.4 → 576.4 and 743.4 → 158.2.

Recovery tests were performed prior to sample analysis to evaluate extraction efficiency. Known concentrations of AZT (2, 10, and 30 µg L^{-1}) were spiked into known biomasses of *S. obliquus*, *D. magna*, and *C. obscuripes*. The recoveries ranged from 80–123%, 77–106%, and 88–106% for the three species, respectively, indicating good extraction performance for all species (Table S5.1). The limit of detection (LOD) and limit of quantification (LOQ) of AZT were 0.6 and 2.0 µg L^{-1}, respectively.

5.2.6 Data processing

5.2.6.1 Toxicokinetic experiments

We applied a one-compartment toxicokinetic (TK) model described by the following ordinary differential equation (Miller et al., 2016):

$$\frac{dC_{organism}(t)}{dt} = k_u C_{water} - (k_e + \mu) C_{organism}(t) \quad (1)$$

where $C_{organism}(t)$ (µg kg^{-1} dry weight, dw) represents the internal concentrations of AZT in the organism, C_{water} (µg L^{-1}) is the AZT concentration in water, k_u (L kg^{-1} h^{-1}) is the uptake rate constant, and k_e (h^{-1}) is the elimination rate constant. The term µ (h^{-1}) denotes the growth rate, which applies only to *S. obliquus* to account for growth dilution due to its rapid

cell division (Maes et al., 2014). For *Daphnia*, the growth rate (μ) was assumed to be zero. During the uptake phase, C_{water} was considered constant (equal to the initial exposure concentration), while during the elimination phase, C_{water} was set to zero. In this equation, the term $k_u C_{water}$ represents the uptake of AZT, whereas $k_e C_{organism}(t)$ represents its elimination. During the elimination phase, the uptake term ($k_u C_{water}$) becomes negligible and is therefore omitted, simplifying the equation as follows:

$$C_{organism}(t) = \begin{cases} \frac{k_u C_{water}}{k_e + \mu}\left(1 - e^{-(k_e + \mu)t}\right), & 0 \leq t \leq 24h \\ C_m e^{-(k_e + \mu)(t - 24)}, & t > 24h \end{cases} \quad (2)$$

where C_m (μg kg^{-1} dw) represents the internal AZT concentration at the beginning of the elimination phase (i.e., at 24 h). This value can be calculated from the following expression:

$$C_m = \frac{k_u C_{water}}{k_e + \mu}\left(1 - e^{-(k_e + \mu) \cdot 24}\right) \quad (3)$$

Parameter estimation for k_u and k_e was performed by fitting the model to the measured internal concentrations using nonlinear least squares regression (Cichocki et al., 2017). The mean values of replicates and their associated standard deviations were used for model fitting. Curve fitting was performed in R (version 4.3.1) using the nls() function.

The bioconcentration factor (BCF) (L kg^{-1}) was subsequently derived from the estimated k_u and k_e values. Assuming steady-state conditions, where the internal AZT concentration remains constant ($dC_{organism}(t)/dt = 0$), the relationship between uptake and elimination is expressed as:

$$k_u C_{water} = (k_e + \mu) C_{organism} \quad (4)$$

Hence, the BCF can be calculated as the ratio between the uptake and elimination rate constants:

$$BCF = \frac{k_u}{k_e + \mu} \quad (5)$$

5.2.6.2 Calculation of the biomagnification factor

The biomagnification factor (BMF) for *D. magna* and *C. obscuripes* was calculated using the following equation:

$$BMF = \frac{C_f}{D_f} \quad (6)$$

where C_f (µg kg^{-1} dw) represents the mean internal concentration of AZT in the consumer organism (*D. magna* or *C. obscuripes*), and D_f (µg kg^{-1} dw) represents the mean internal AZT concentration in its dietary source (*S. obliquus* for *D. magna,* and *D. magna* for *C. obscuripes*).

Statistical analysis was conducted in R (version 4.3.1). A Student's t-test was applied when data met the assumptions of normality and homogeneity of variances; otherwise, the non-parametric Mann–Whitney U test was used.

5.3 Results

5.3.1 Toxicokinetics and bioconcentration

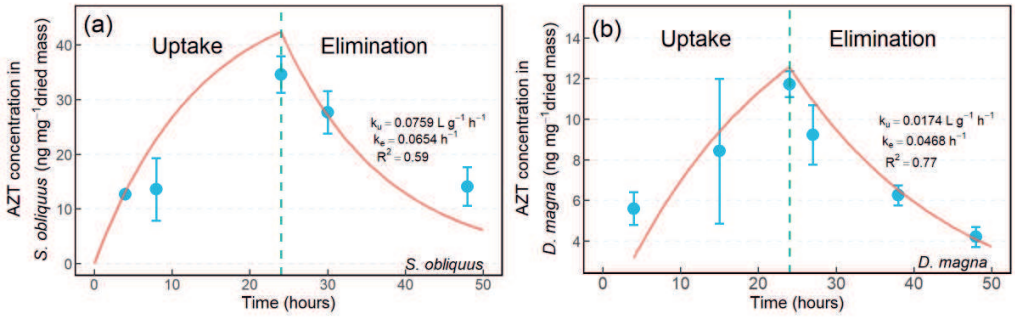


Figure 5.2. Toxicokinetic modelling of (a) *S. obliquus* and (b) *D. magna*. The red line represents the nonlinear least-squares fit of the model, while blue points show the measured internal concentrations (mean ± SE). Please note that y-axis scales differ between figures.

The fitted TK model adequately described the uptake and elimination of AZT in both *S. obliquus* and *D. magna* (Fig. 5.2). Parameter estimates and model performance statistics are summarized in Table 5.1. Overall, *S. obliquus* exhibited higher estimated uptake and elimination rate constants than *D. magna*, which was reflected in a higher BCF estimate (1,017 vs. 372 L kg^{-1}). Growth dilution contributed approximately 12.3% to the total elimination of *S. obliquus*, based on its measured growth rate (0.00917 h^{-1}).

Table 5.1 Parameter estimates obtained by the toxicokinetic modelling for *S. obliquus* and *D. magna*

Organism	k_u (L g^{-1} h^{-1})	SE [a]	p-value [b]	k_e (h^{-1})	SE	p-value	R^2	BCF (L kg^{-1})
S. obliquus	0.0759	0.0029	< 0.001	0.0654	0.014	0.013	0.59	1017
D. magna	0.0174	0.0024	0.0019	0.0468	0.0077	0.0037	0.77	372

a. SE: standard error.
b. P-values evaluate whether parameter estimates differ significantly from zero within each model.

5.3.2 Trophic transfer and biomagnification potential

The internal AZT concentrations in *S. obliquus* at 21–27 h ranged from 110 to 150 mg kg^{-1} (Fig. S5.1a). *S. obliquus* cells containing AZT within this concentration range were subsequently used as food for *D. magna*. After exposure to AZT-contaminated algae for 48 h, the internal AZT concentrations in *D. magna* were 0.139 ± 0.024 ng $individual^{-1}$ at 24 h and 0.137 ± 0.052 ng $individual^{-1}$ at 48 h (Fig. S5.2c). Based on the reported dry mass of 12.7 µg $individual^{-1}$ for juvenile *D. magna* (Simčič and Brancelj, 1997), these values correspond to estimated internal concentrations of 11.0 ± 1.9 mg kg^{-1} at 24 h and 10.8 ± 4.1 mg kg^{-1} at 48 h. Upon transfer of *S. obliquus* to clean RT medium, AZT concentrations in the medium remained below the LOQ throughout the sampling period (Fig. S5.2b).

Accordingly, the BMF (*S. obliquus* → *D. magna*) was estimated to be 0.07–0.10, indicating no biomagnification (i.e., BMF < 1). For *C. obscuripes*, all measured internal AZT concentrations were below the LOQ, preventing a direct calculation of the BMF (*D. magna* → *C. obscuripes*). However, based on the LOQ and sample dry weight, the internal AZT concentration in *C. obscuripes* was estimated to be < 0.35 mg kg^{-1}, yielding an upper-bound BMF (*D. magna* → *C. obscuripes*) of < 0.032.

5.3.3 Toxicity to *C. obscuripes*

During the experiment, the total mortality rate of *C. obscuripes* was 8.4% in the control group and 3.8% in the exposed group, which was fed with *D. magna* previously exposed to AZT-contaminated *S. obliquus*. The total pupation rates were 10.8% and 11.7%, respectively (Fig. S5.3). No significant differences were found between the control and exposed groups in either mortality or pupation rates ($p > 0.05$).

Based on 60 *C. obscuripes* individuals measured at the start of the experiment, the average initial body length was 10.34 mm (SD = 0.82, median = 10.20 mm). After 21 days of feeding

exposure, the average final body length was 10.5 ± 0.8 mm (median = 10.3 mm) in the exposed group and 10.8 ± 0.9 mm (median = 11.0 mm) in the control group, with the exposed group being significantly smaller ($P < 0.05$; Fig. 5.3). Compared with the initial measurements, *C. obscuripes* in the control group showed significant growth ($P = 0.013$), whereas no significant change was observed in the exposed group ($P > 0.05$).

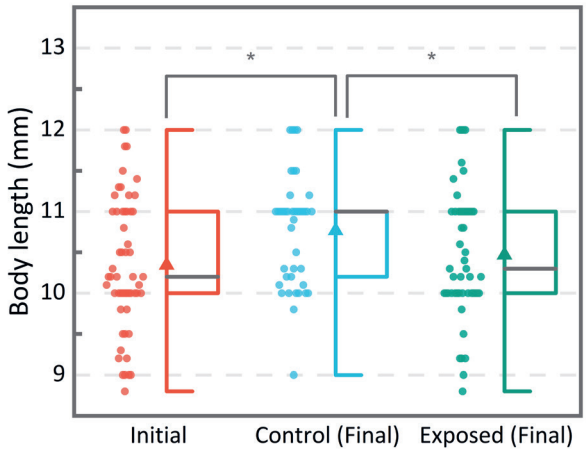


Figure 5.3. Body length of *C. obscuripes* at the beginning (left) and after 21 days of the food-chain experiment in the control (middle) and exposed groups (right). Boxes represent the interquartile range (25th–75th percentiles), whiskers indicate 1.5 times the interquartile range, solid grey lines inside the boxes show the medians, and filled triangles denote mean values. An asterisk (*) indicates a significant difference at the 0.05 level.

5.4 Discussion

5.4.1 Bioconcentration behaviour of AZT

The toxicokinetic modelling showed that the BCF of AZT in *S. obliquus* reached 1,017 L kg^{-1}, exceeding the commonly used threshold of 1,000 L kg^{-1} for significant bioaccumulation (Zhu et al., 2023). This indicates that this alga has a strong ability to retain and concentrate AZT under continuous exposure conditions, consistent with previous modelling predictions (Zheng et al., 2025). Antibiotic uptake by algal cells mainly occurs through passive diffusion, facilitated diffusion, and, in some cases, energy-dependent transport (Long et al., 2024; Xiong et al., 2018; Xiong et al., 2021). In passive diffusion, small and moderately hydrophobic molecules such as AZT can readily permeate the cell membrane from high- to low-concentration regions due to the lipophilic nature of the membrane (Xiong et al., 2021). Therefore, if AZT persists in aquatic environments, phytoplankton could act as an important

sink for this antibiotic and serve as an initial entry point for its transfer to higher trophic levels.

The antibiotic AZT has a logKow of 4.01 (Zhu et al., 2023), which is relatively high compared with most other antibiotics (Table S5.2) and suggests a potential for partitioning into algal lipids. Hydrophobicity is indeed a primary determinant of bioconcentration, as hydrophobic organic chemicals tend to move from water into cellular lipid compartments (Schüürmann et al., 2007). Several organic compounds with similar logKow values, such as 17α-ethinylestradiol, pentachlorobenzene, and 4-tert-octylphenol, exhibit strong bioconcentration in algae (Achar et al., 2020; Maes et al., 2014; Sijm et al., 1998). However, logKow alone is an imperfect predictor of actual BCF. The relationship between logKow and log BCF is not strictly linear (Wang et al., 2014), and compounds with comparable hydrophobicity often show highly variable BCFs. This variability arises because bioconcentration is also influenced by factors such as molecular size, ionization, bioavailability, and interactions with dissolved organic matter (Wen et al., 2012). Therefore, hydrophobicity provides only a preliminary expectation of accumulation potential, and quantitative estimation requires explicit modelling of uptake and elimination kinetics, as performed in this study.

Compared with *S. obliquus*, *D. magna* exhibited a lower BCF (372 L kg^{-1}), suggesting a reduced but still appreciable capacity to accumulate AZT. This contrast in bioconcentration may be attributed to variations in growth rate, lipid content, metabolic enzyme activity, feeding rate, and assimilation efficiency (Li et al., 2018; Zhang and Wang, 2007). Generally, higher growth rates, higher metabolic activity, and more efficient enzymatic degradation are associated with lower bioaccumulation of contaminants.

5.4.2 Trophic transfer and biomagnification potential of AZT

The food-chain experiment demonstrated that AZT can be transferred from the primary producer *S. obliquus* to the primary consumer *D. magna* through dietary exposure. The estimated BMF (*S. obliquus* → *D. magna*) ranged between 0.07 and 0.10. At a higher trophic level, the internal AZT concentrations detected in the secondary consumer *C. obscuripes* were extremely low (< 0.35 ng mg^{-1}), and the estimated BMF (*D. magna* → *C. obscuripes*) was below 0.032. These findings indicate that dietary transfer of AZT along the studied trophic pathway was limited, without any significant biomagnification (BMF < 1).

Studies on the biomagnification of antibiotics in aquatic organisms remain limited, yet existing evidence generally suggests a low potential for trophic magnification. However, differences among antibiotic classes are evident. Kim et al. (2014) reported a dietary BMF

of 0.19 ± 0.04 for tetracycline in *D. magna*, showing no magnification. Zheng et al. (2025) modelled the trophic transfer of multiple antibiotics across different food chains (*Chlorella sorokiniana* → *D. magna* and *D. magna* → *Danio rerio*) and found that sulfonamides were more prone to bioaccumulation and biomagnification, whereas predictions for *β*-lactams and tetracyclines showed little to no magnification. Similarly, field studies based on trophic magnification factors (TMFs), which quantify changes in contaminant concentrations across entire food webs rather than within a single predator–prey pair as in BMFs, have revealed comparable patterns. Wu et al. (2021) observed TMFs below 1.0 for erythromycin-H_2O, enrofloxacin, and ciprofloxacin in a marine food web of the Beibu Gulf. In the Laizhou Bay food web, Liu et al. (2017a) reported elevated TMFs (1.2–3.9) for sulfonamides, whereas fluoroquinolones and macrolides exhibited TMFs < 1.0, suggesting trophic dilution. Further evidence indicated that with increasing trophic level, enhanced metabolic and excretory capacities in higher consumers facilitate the biotransformation or elimination of these compounds, thereby reducing the likelihood of biomagnification (Goutte et al., 2020; Zheng et al., 2025).

As a macrolide antibiotic, AZT is weakly basic and amphiphilic (pKa ≈ 8.5; log Kow = 4.01). Under neutral aquatic conditions, it is partially ionized, which limits passive diffusion across biological membranes and reduces uptake efficiency in aquatic organisms. In addition, AZT can be rapidly eliminated from invertebrate tissues through biotransformation and excretion (Zhu et al., 2020), resulting in low tissue retention even under dietary exposure. Nevertheless, algae with high BCFs may serve as transient "antibiotic reservoirs" in aquatic systems. The accumulated compounds can be released back into the water through exudation, grazing, or cell lysis, thereby influencing the persistence, cycling, and bioavailability of antibiotics within aquatic ecosystems.

5.4.3 Ecotoxicological implications for higher trophic levels

Although AZT did not exhibit significant biomagnification along the studied food chain, a measurable biological response was observed in the secondary consumer *C. obscuripes*. Growth inhibition occurred in the exposed group, whereas mortality and pupation rates remained unaffected. This pattern suggests that dietary exposure to AZT did not cause acute toxicity but may have subtly interfered with energy allocation or metabolic processes. Such findings indicate that even at low tissue concentrations, AZT can exert sublethal effects on higher trophic-level organisms by influencing their growth performance and energy utilization.

The growth inhibition induced by AZT may be associated with indirect disturbances of physiological metabolism. Previous studies have shown that antibiotic exposure can alter

the composition and function of gut microbiota in aquatic invertebrates and suppress the activities of key digestive enzymes (Gorokhova et al., 2015; Li et al., 2023; Yan et al., 2019). Such disruptions are typically characterized by reduced microbial diversity, depletion of symbiotic taxa involved in nutrient processing (e.g., taxa from the phyla *Bacteroidota* and *Bacillota*), and increased proliferation of resistant or opportunistic bacteria, all of which contribute to impaired digestive efficiency and nutrient absorption (Motiei et al., 2020). In addition, the expression of metabolic enzymes such as amylase, protease, and Na^+/K^+-ATPase may be altered under dysbiosis and physiological stress, redirecting energy from growth and tissue synthesis toward maintenance and detoxification processes (Lyu et al., 2022; Thakur et al., 2016; Yan et al., 2019). Meanwhile, prey organisms such as *D. magna* exposed to AZT may exhibit reduced nutritional quality or altered energy content, thereby lowering their energetic value for predators (Akbar et al., 2020; Gorokhova et al., 2015). Collectively, these effects can reduce the efficiency of nutrient assimilation and metabolic conversion, providing a plausible explanation for the growth inhibition observed in *C. obscuripes* despite its low internal AZT residues.

From an ecological perspective, even modest growth inhibition may have broader implications for population fitness and trophic energy dynamics. Reduced somatic growth can delay development, lower predation efficiency, and diminish reproductive output in aquatic insects, ultimately affecting food availability for higher consumers such as fish, amphibians and insectivorous birds. Therefore, even in the absence of measurable biomagnification, antibiotics like AZT can induce sublethal physiological effects that cascade through aquatic and terrestrial ecosystems by altering growth and energy transfer processes.

5.4.4 Limitations and future perspectives

This study systematically investigated the toxicokinetic behaviour and trophic transfer of AZT in a simplified freshwater food chain. However, several limitations should be acknowledged when interpreting the results.

First, the experiment was conducted in a three-trophic-level system (*S. obliquus*–*D. magna*–*C. obscuripes*), which simplifies the structural and functional complexity of natural freshwater ecosystems. In natural environments, multiple predator–prey interactions, detrital loops, and microbial reprocessing pathways coexist. Future studies could include higher trophic levels (e.g., fish or amphibians) or consider benthic–pelagic linkages to better represent the ecological behaviour and transformation of antibiotics.

Second, the accuracy of trophic transfer estimation was limited by analytical sensitivity and the small biomass of organisms. In this study, the internal AZT concentration in *C.*

obscuripes was below the LOQ, while the low dry weight of *D. magna* hindered the accurate determination of the internal concentrations. Consequently, the calculated BMFs should be regarded as conservative estimates. Future work could improve quantification by increasing sample biomass, enhancing extraction efficiency, and/or applying more sensitive analytical techniques.

In addition, the trophic transfer experiment required a dynamic feeding setup to provide AZT-exposed food to higher trophic organisms continuously. This represented a major logistical challenge, as it was necessary to obtain more than 240 *D. magna* neonates every 48 h to be exposed to AZT-contaminated *S. obliquus* and subsequently serve as prey for *C. obscuripes*. Due to the difficulty of maintaining such large-scale synchronized cultures, it was not feasible to supply *C. obscuripes* with freshly exposed prey every day. Instead, feeding was performed once every 72 h, with two *D. magna* individuals provided per larva each time. This constraint may have masked subtle treatment-related differences. Future studies should improve experimental design by optimizing the synchronization and feeding regimes of prey organisms to ensure stable food availability for higher trophic consumers.

Finally, although *C. obscuripes* showed growth inhibition despite its low internal AZT residues, the underlying physiological and microbiome-associated mechanisms remain unclear. Integrating toxicokinetic data with molecular and microbiome analyses could help elucidate how antibiotics interfere with host metabolism and energy allocation and assess their potential long-term or transgenerational effects.

5.5 Conclusions

This study provides an integrated assessment of AZT bioaccumulation, trophic transfer, and biological effects in a simplified freshwater food chain. Toxicokinetic modelling indicated efficient uptake of AZT by the primary producer *S. obliquus*, whereas the primary consumer *D. magna* showed lower accumulation, reflecting species-specific differences in uptake and elimination dynamics. Dietary exposure further demonstrated that AZT can be transferred through the food chain without biomagnification. In the trophic transfer experiment, *C. obscuripes* exhibited growth inhibition after feeding on AZT-contaminated prey, suggesting indirect physiological disturbances possibly related to altered energy metabolism or gut microbiota.

Overall, these findings indicate that while AZT can enter aquatic food webs via dietary pathways, it is more likely to undergo trophic dilution than biomagnification. Its sublethal effects at higher trophic levels warrant further investigation, particularly regarding long-

term metabolic and ecological consequences under environmentally relevant exposure conditions.

Acknowledgements

We acknowledge the China Scholarship Council (CSC) for supporting Dailing Wu (File No. 202006750027).

Supplementary information

Table S5.1. Recovery test results for the organisms (concentration shown in µg L-1)

Organism	Low spiked concentration		Medium spiked concentration			High spiked concentration		
	Spiked conc.	Measured conc.	Spiked conc.	Measured conc. ± SD	Recovery (%) ± SD	Spiked conc.	Measured conc. ± SD	Recovery (%) ± SD
S. obliquus	2	ND	10	8.04 ± 0.25	80.4 ± 2.5	30	37.09 ± 0.03	123.6 ± 0.09
D. magna	2	ND	10	7.66 ± 0.50	76.6 ± 5.0	30	31.77 ± 1.54	105.9 ± 5.1
C. obscuripes	1	ND	10	8.76 ± 1.15	87.6 ± 11.5	20	21.27 ± 2.02	106.4 ± 10.1

*ND: not detected; NA: not available

Table S5.2. Physicochemical properties (logKow and pKa) of different antibiotics

	Antibiotic	CAS	Molecular formula	logKow	pKa
Quinolones	Enoxacin	74011-58-8	C15H17FN4O3	-0.2	7.04, 8.19
	Ciprofloxacin	85721-33-1	C17H18FN3O3	0.28	6.43, 8.7
	Norfloxacin	70458-96-7	C16H18FN3O3	0.46	6.34, 8.75
	Ofloxacin	82419-36-1	C18H20FN3O4	−0.39	7.26, 7.81
	Enrofloxacin	93106-60-6	C19H22FN3O3	0.7	7.59, 8.7
	Balofloxacin	127294-70-6	C20H24FN3O4	0.99	NA
	Fleroxacin	79660-72-3	C17H18F3N3O3	0.24	5.5, 8.2
	Lomefloxacin	98079-51-7	C17H19F2N3O3	−0.3	5.7
	Moxifloxacin	151096-09-2	C21H24FN3O4	0.95	6.3, 9.3
	Sparfloxacin	110871-86-8	C19H22F2N4O3	2.5	NA
	Pipemidic Acid	51940-44-4	C14H17N5O3	−2.15	NA
Sulfonamides	Sulfapyridine	144-83-2	C11H11N3O2S	0.35	2.59, 8.43
	Sulfamethoxazole	723-46-6	C10H11N3O3S	0.89	1.6, 5.7
	Trimethoprim	738-70-5	C14H18N4O3	0.91	7.12,
	Sulfamethazine	57-68-1	C12H14N4O2S	0.89	2.65, 7.65
	Sulfathiazole	72-14-0	C9H9N3O2S2	0.05	2.2, 7.24
	Sulfamonomethoxine	1220-83-3	C11H12N4O3S	0.7	NA
	Sulfacetamide	144-80-9	C8H10N2O3S	−0.96	NA
	Sulfadiazine	68-35-9	C10H10N4O2S	−0.09	6.36
	Sulfamethiazole	144-82-1	C9H10N4O2S2	NA	NA
	Sulfamethoxypyridazine	80-35-3	C11H12N4O3S	0.32	NA
	Sulfameter	651-06-9	C11H12N4O3S	0.41	NA
Macrolides	Erythromycin	114-07-8	C37H67NO13	3.06	8.8

	Roxithromycin	80214-83-1	C41H76N2O15	1.7	9.27
	Clarithromycin	81103-11-9	C38H69NO13	3.16	8.99
	Azithromycin	83905-01-5	C38H72N2O12	4.02	8.74
Tetracyclines	Chlortetracycline	57-62-5	C22H23ClN2O8	−0.62	7.44
	Oxytetracycline	79-57-2	C22H24N2O9	−0.9	3.27, 9.5
	Tetracycline	60-54-8	C22H24N2O8	−1.37	3.3, 7.68
	Doxycycline	564-25-0	C22H24N2O8	0.63	3.09
	Florfenicol	73231-34-2	C12H14Cl2FNO4S	−0.12	NA
Amphenicols	Chloramphenicol	56-75-7	C11H12Cl2N2O5	1.14	NA
	Thiamphenicol	15318-45-3	C12H15Cl2NO5S	−0.27	NA
	Penicillin G	61-33-6	C16H18N2O4S	1.83	2.74
Beta-lactam	Amoxicillin	26787-78-0	C16H19N3O5S	−1.99	2.64, 7.39
	Cefalexin	15686-71-2	C16H17N3O4S	0.65	2.5, 7.1
	Cefradine	38821-53-3	C16H19N3O4S	−1.5	2.6, 7.6
	Cefotaxime	63527-52-6	C16H17N5O7S2	−0.5	NA
	Furazolidone	67-45-8	C8H7N3O5	−0.04	NA
Others	Nitrofurantoin	67-20-9	C8H6N4O5	−0.47	7.2
	Lincomycin	154-21-2	C18H34N2O6S	0.2	7.6
	Salinomycin	53003-10-4	C42H70O11	5.11	4.5, 6.5

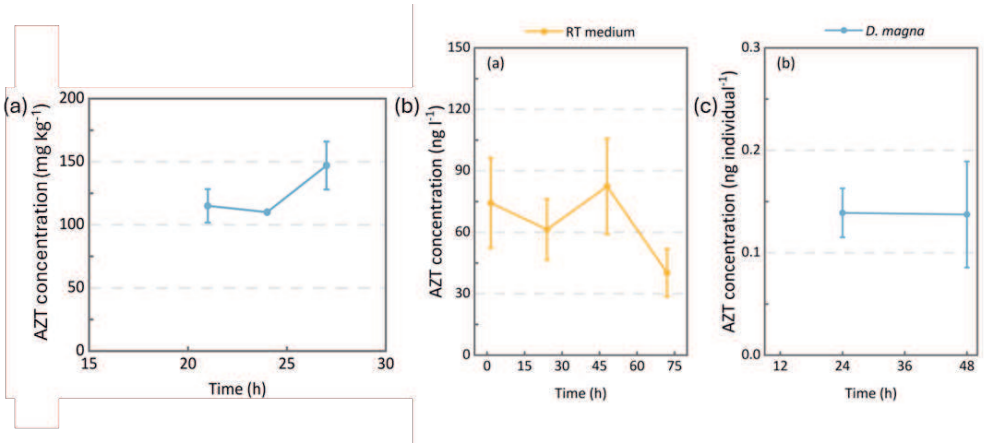


Figure S5.1. (a) Internal AZT concentration in *S. obliquus* over time in the food chain experiment. *S. obliquus* was exposed to 1.0 mg L-1 AZT; (b) AZT concentration in RT medium over time; and (c) internal AZT concentrations in *D. magna* over time. *D. magna* was fed with *S. obliquus* that was pre-exposed to 1.0 mg L-1 AZT for 24 h. Error bars represent standard deviations.



Wetlands, Wageningen

Chapter 6

The ecological gain of using bioactivated carbon and ozone sewage treatments assessed using freshwater microcosms

Dailing Wu, Koen van Gijn, Lara Schuijt, Myrthe van Venetië, Guang-Guo Ying, Hauke Smidt, Paul J. van den Brink

This chapter is based on: Wu, D., van Gijn, K., Schuijt, L., van Venetië, M., Ying, G.-G., Smidt, H. and Van den Brink, P.J. 2026. The ecological gain of using bioactivated carbon and ozone sewage treatments assessed using freshwater microcosms. *Water Research*, https://doi.org/10.1016/ j.watres.2026.125811.

Abstract

Advanced wastewater treatment technologies such as bioactivated carbon (BAC) filtration and ozonation are increasingly implemented to remove micropollutants from effluents. Yet their ecological impacts remain insufficiently understood. In this study, we evaluated the chemical and ecological effects of six wastewater treatment scenarios in outdoor freshwater microcosms over 42 days, including BAC alone, two ozone doses (0.2 and 0.4 g O_3/g TOC), their combinations, and an untreated control. HPLC–MS/MS analysis confirmed the high persistence of micropollutants in untreated effluents, which showed the highest predicted mixture toxicity throughout the exposure. Treatments combining BAC with ozone resulted in the lowest residual micropollutant concentrations, which continued to decline over time. Ecological responses differed across trophic levels. Algal biomass was reduced in ozone-treated effluents, reflecting combined effects of altered nutrient supply, resource availability and residual chemical stress, whereas zooplankton and macroinvertebrate communities remained structurally robust. Microbial communities in the water column showed pronounced treatment-dependent restructuring, and functional prediction indicated reduced representation of taxa involved in pollutant degradation and nitrogen cycling under high ozone conditions. Structural equation modeling supported these patterns by showing that early changes at the base of the food web were linked to shifts in micropollutant levels and nutrient availability, while pathways to higher trophic levels remained weak and did not propagate beyond microbes and primary producers. Overall, combining BAC with moderate ozonation offered the most favourable balance between micropollutant removal and ecological compatibility, whereas high ozone intensity introduced discernible functional impact to microbial communities. These findings highlight the importance of jointly considering chemical removal performance and ecological responses when selecting advanced wastewater treatment strategies.

6.1 Introduction

Micropollutants (MPs), including pharmaceuticals, personal care products, pesticides, and industrial chemicals, are increasingly detected in freshwater systems worldwide due to intensified agriculture, industrialization, urbanization and other human activities (Yang et al., 2017). Even at low concentrations, these biologically active compounds can cause endocrine disruption and behavioral changes in aquatic organisms as exposure is chronic (Hernando et al., 2006; Schwarz et al., 2021). Wastewater treatment plants (WWTPs) are a major source of MPs because conventional secondary treatment processes are not specifically designed to remove them (Aemig et al., 2021; de Wilt et al., 2018). Consequently, residual MPs are discharged into receiving waters, posing potential long-term risks to the structure and functioning of aquatic ecosystems (Sanganyado et al., 2021; Versteegen et al., 2025).

Ozonation is widely applied as an advanced treatment to enhance MP removal (Luo et al., 2014). It works through both direct oxidation and hydroxyl radical (·OH) formation, enabling degradation of a broad spectrum of organic contaminants (Von Gunten, 2003). However, its implementation remains limited by high energy costs and the presence of dissolved organic matter (DOM), which competes for ozone and reduces treatment efficiency (Van Gijn et al., 2021b). Lowering DOM concentrations before ozonation is thus considered an effective strategy to reduce ozone demand and improve overall performance (Nilsson et al., 2017; Van Gijn et al., 2021b). Bioactivated carbon (BAC) has emerged as a promising approach for DOM removal due to its combined adsorption and biodegradation capabilities (Van Gijn et al., 2021a). Studies have shown that BAC filtration can substantially reduce the background organic matter in WWTP effluents, thereby lowering ozone demand and improving MP removal performance (de Wilt et al., 2018; Van Gijn et al., 2021a). The combination of BAC filtration and ozonation, referred to as the BO_3 process, has been recognized for its synergistic potential in advanced wastewater treatment. Nevertheless, the ozonation process has also been shown to generate a wide range of ozonation transformation products (OTPs) and ozonation byproducts (OBPs), some of which may exhibit toxicity equal to or even higher than that of the parent compounds (Gulde et al., 2021; Illés et al., 2014; Magdeburg et al., 2014). To date, the ecological effects of long-term exposure to BO_3 treated effluents in freshwater ecosystems remain largely understudied, particularly with regard to community-level and functional responses across multiple taxa (Völker et al., 2019).

To address this gap, the present study assessed the ecological impacts of BO_3 treated effluents using outdoor freshwater microcosms. Microcosms provide a higher-tier, ecologically relevant methodology to evaluate direct and indirect effects on multiple

biological groups, including algae, zooplankton, macroinvertebrates, and microbial communities (Hermann et al., 2024; Van den Brink et al., 2005), and better reflect long-term interactions than standard toxicity tests (Schuijt et al., 2021). This study employed eight treatments: six based on secondary effluent with additional chemical spiking, including one spiked control without further treatment, BAC filtration alone, ozonation at two dosage levels, and their combinations. In addition, two treatments using unspiked secondary effluent were included as references for comparison with the spiked conditions. This experimental design enabled a systematic comparison of the individual and combined effects of BAC and ozonation pretreatments, the role of ozone dose, and the ecological trade-offs across trophic groups, ultimately allowing evaluation of which treatment configuration best balances MP removal efficiency and ecological compatibility.

6.2 Materials and methods

6.2.1 Experimental design

The effluent exposure experiment was conducted from May to July 2021 at the Sinderhoeve experimental station of Wageningen University & Research in the Netherlands (www.sinderhoeve.org). A total of 80 outdoor freshwater microcosms were established, each containing 58 L of water consisting of 29 L of freshwater and 29 L of differently treated effluents to simulate typical wastewater dilution scenarios. Each microcosm received a tray with 3 L of clean sediment to provide benthic habitat, and zooplankton, macroinvertebrates, green algae, and submerged macrophytes were introduced from nearby clean water bodies to establish a complete community. The microcosms were embedded 0.5 m into the soil to buffer temperature fluctuations and were kept open at the top to allow natural colonization. All treatments were replicated ten times and randomly assigned to microcosms. Prior to effluent exposure, the systems underwent a one-month acclimation period. Treated or untreated effluents were added on Day 0, and destructive sampling was conducted on Days 14 and 42, with five replicates collected per treatment at each time point. Further methodological details are provided in Supplementary Information (SI) Text S6.1.

6.2.2 Effluents and chemicals

The secondary effluent used in this study was collected from a wastewater treatment plant in Bennekom, the Netherlands (51°59'51.2"N, 5°39'31.5"E). A mixture of 21 representative micropollutants, including pharmaceuticals, pesticides, their metabolites, and lifestyle chemicals, was added to the effluent (details in Table S6.1). The effluent then underwent BAC filtration, ozonation at two dose levels (0.2 or 0.4 g O_3/g TOC), or combined BAC-

ozonation treatment (Table 6.1). In addition to the spiked effluents, two unspiked effluents were included: one without further treatment and one treated with BAC followed by 0.4 g O_3/g TOC. All spiked and unspiked effluents were processed at the Environmental Technology laboratory at Wageningen University & Research following the BO_3 procedure described by Van Gijn et al. (2023). Operational details are provided in SI Text S6.2.

Table 6.1. Overview of the treatment groups and included treatment processes.

Treatment	Spiking	Bioactivated carbon treatment	Ozone dose (g ozone/g TOC)
NC0	Yes	No	0
BC0	Yes	Yes	0
BC0.2	Yes	Yes	0.2
BC0.4	Yes	Yes	0.4
NC0.2	Yes	No	0.2
NC0.4	Yes	No	0.4
UnNC0	No	No	0
UnBC0.4	No	Yes	0.4

6.2.3 Community assembly and sampling

6.2.3.1 Zooplankton community

Zooplankton was collected from a pond at the Sinderhoeve using a 55 µm mesh net, mixed thoroughly, and evenly distributed into 80 microcosms two weeks prior to effluent dosing.

On days 14 and 42, zooplankton samples were taken to assess species abundance. A 5 L depth-integrated water sample was collected from each microcosm using a transparent acrylic tube. Samples were filtered through a 55 µm mesh net, and the retained zooplankton was preserved in 50 or 100 mL polyethylene bottles with acetate-buffered Lugol's solution and stored at 4 °C in the dark. Zooplankton individuals were then identified and counted under an Olympus stereo microscope SZX10.

6.2.3.2 Macroinvertebrates

Two weeks before exposure, macroinvertebrates were collected from ponds at the Sinderhoeve site. Each microcosm was stocked with 10 individuals of *Gammarus pulex*, 10 *Cloeon dipterum*, 10 *Chironomus* sp., 10 *Sphaerium* sp., 6 *Asellus aquaticus*, and 6 *Lymnaea stagnalis*, all medium-sized and in active condition.

Macroinvertebrates were sampled on Days 14 and 42 by sacrificing five replicates at each date. Organisms were retrieved by rinsing and sieving the sediment tray, followed by a thorough inspection of the water column and container surfaces using a 0.5 mm net. All specimens were preserved in 70% ethanol for identification and counting.

6.2.3.3 Macrophytes

After introducing the macroinvertebrates, *Myriophyllum spicatum* was collected from ponds at the Sinderhoeve. The plants were thoroughly washed to remove attached fauna and trimmed into 15 cm apical segments. Two shoots were carefully inserted into the sediment of each microcosm.

Macrophytes were sampled on days 14 and 42. The plants were gently removed, wrapped in pre-weighed aluminum foil, and stored at -20 °C. Because destructive sampling caused fragmentation, biomass was quantified by wet and dry weight rather than length. Samples were dried at 70 °C for 72 h and weighed, and final biomass was calculated by subtracting foil weight.

6.2.3.4 Microbial community

Two 200 mL HDPE containers half-filled with sediment were embedded at the bottom of each microcosm for later sediment microbial analysis. Microbial samples from the water column and sediments were collected on Days 14 and 42, subjected to DNA extraction (PowerSoil DNA Isolation Kit, QIAGEN), and analyzed by *16S rRNA* gene amplicon sequencing targeting the V4 region (primers 515F/806R) on the Illumina HiSeq2000 platform (Novogene, UK). Detailed procedures for sampling, DNA extraction, PCR amplification, and sequencing are provided in SI Text S6.3.

Sequence processing was performed using NG-Tax 2 (Poncheewin et al., 2020), including quality filtering, ASV detection, and taxonomic assignment against SILVA 138. ASVs with relative abundance below 0.1% were removed at a per sample basis. The processed BIOM files were imported into phyloseq for community analysis (McMurdie and Holmes, 2013). All

sequence reads are available at the Sequence Read Archive of the National Center for Biotechnology information (accession number PRJNA1377162).

6.2.4 Chemical analysis and toxicity assessment

Water samples were collected on Days 0, 14, and 42. From each depth-integrated sample, 1.9 mL was transferred into a 2 mL Eppendorf tube pre-filled with 100 µL of acetonitrile (Merck, Germany) and stored at -20 °C until analysis. Micropollutants were quantified by ultra-performance liquid chromatography coupled with tandem mass spectrometry (UPLC-MS/MS). The limit of quantification (LOQ) for all compounds was 50 ng/L, and further details of the analytical procedure are provided in Van Gijn et al. (2021b).

Risk quotients (RQ) were calculated as the ratio between the measured environmental concentration of each micropollutant and its predicted no-effect concentration (PNEC), with PNEC values compiled from the NORMAN Ecotoxicity Database. Risk levels were classified as follows: High risk (RQ ≥ 1), Medium risk (0.1 ≤ RQ < 1), Low risk (0.01 ≤ RQ < 0.1), and No risk (RQ < 0.01). The multi-substance Potentially Affected Fraction (msPAF) was calculated by using NOEC-based SSDs (https://www.sleutelfactortoxiciteit.nl/key-factor-toxicity-introduction), providing an estimate of the chronic toxic pressure of micropollutant mixtures on aquatic communities and the fraction of species potentially affected (Posthuma and de Zwart, 2012).

6.2.5 Water quality and nutrient analysis

Water temperature, pH, dissolved oxygen (DO), electrical conductivity and chlorophyll-a (chl-a) were measured weekly in the morning using portable field instruments (HQ40d multiprobe with CDC401 electrode, HACH; AlgaeTorch, BBE Moldaenke).

On each sampling day, 50 mL of water samples were collected and stored at -20 °C for nutrient analysis. Total phosphorus (TP), nitrate & nitrite, orthophosphate and ammonia were quantified using a segmented flow analyzer (Skalar 5100 Autoanalyser, The Netherlands).

6.2.6 Data analysis

To assess differences among treatments at each sampling time point, one-way ANOVA was performed followed by Duncan's multiple range test ($p \leq 0.05$). Prior to community and population-level analyses, abundance data were log-transformed to reduce the influence of

extreme values and improve normality. Macroinvertebrate and zooplankton abundances were transformed using ln(2x + 1) and ln(10x + 1), respectively, where x represents the abundance of a given taxon (Van den Brink et al., 2000).

Multivariate analyses were employed to evaluate treatment effects on community structure. Principal Response Curves (PRC) were used to assess temporal dynamics (Van den Brink and Braak, 1999), and significance was tested using Monte Carlo permutation tests across the full time series (Van den Brink et al., 1996). Treatment differences at individual sampling dates were further examined using redundancy analysis (RDA) with Monte Carlo permutation tests comparing each treatment to the control on Days 14 and 42. All multivariate analyses were performed in CANOCO 5.15 (ter Braak and Šmilauer, 2012).

Microbial functional potential was inferred using QIIME2 (v2020.11) for OTU table generation followed by annotation with FAPROTAX (v1.2.5) (Sansupa et al., 2021). FAPROTAX assigns ecological functions to bacterial taxa based on curated literature linking taxonomy to metabolic capabilities. Predicted functions were processed and visualized in RStudio.

Structural equation models (SEMs) were constructed to evaluate direct and indirect effects of BO_3 treatments across chemical and biological variables (Fan et al., 2016). Models included hypothesised pathways among treatment factors, chemical conditions and trophic groups. Microbial community composition, zooplankton and macroinvertebrate assemblages were represented by the first principal component (PC1) from PCA. All variables were z-standardised. Separate Day 14 and Day 42 models were fitted using lavaan (ML estimation with robust SEs) and evaluated using χ^2, CFI, RMSEA and SRMR.

6.3 Results

6.3.1 Micropollutant concentrations and predicted impacts

At Day 0, the total combined concentration of target MPs in NC0 reached 64,400 ng/L, while the BO_3 pretreatments removed 49-89% of MPs prior to microcosm exposure, with BC0.4 achieving the highest removal (Table S6.2). In NC0, concentrations decreased to 3,070 ng/L by Day 14 and remained near this level through Day 42 (2,930 ng/L) (Fig. 6.1a). BO_3-treated effluents consistently showed lower MP levels, with BC0.4 exhibiting the lowest concentrations throughout the experiment (Fig. 6.1a). However, several MPs including carbamazepine, mecoprop, BAM, 2,4-D, benzotriazole and caffeine remained detectable after BO_3 treatment, with 20–30% of their initial concentrations still present on Day 14 (Table S6.3).

RQ analysis indicated that, despite substantial removal, BO_3-treated effluents still contained 9 compounds with high risk (RQ ≥ 1) at Day 0 (Table S6.4). After 14–42 days of microcosm exposure, most compounds declined to low or negligible risk levels, however, 4(5)-methylbenzotriazole, 2,4-D and caffeine consistently remained at medium to high risk (RQ ≥ 0.1). msPAF results mirrored these patterns (Fig. 6.1b). NC0 exhibited the highest potential ecological impact at Day 0 (27%), declining to < 4% by Day 42, while all BO_3-treated groups maintained significantly lower msPAF values, particularly BC0.2 and BC0.4 ($P < 0.05$, Fig. 6.1b).

The unspiked effluent UnNC0 contained 43,600 ng/L of MPs at Day 0, dominated by sotalol (~29,900 ng/L) (Table S6.5). UnBC0.4 achieved 98% removal before exposure, followed by continued declines during the experiment. A significant decrease in msPAF relative to UnNC0 was observed only in UnBC0.4 at Day 42 ($P < 0.001$).

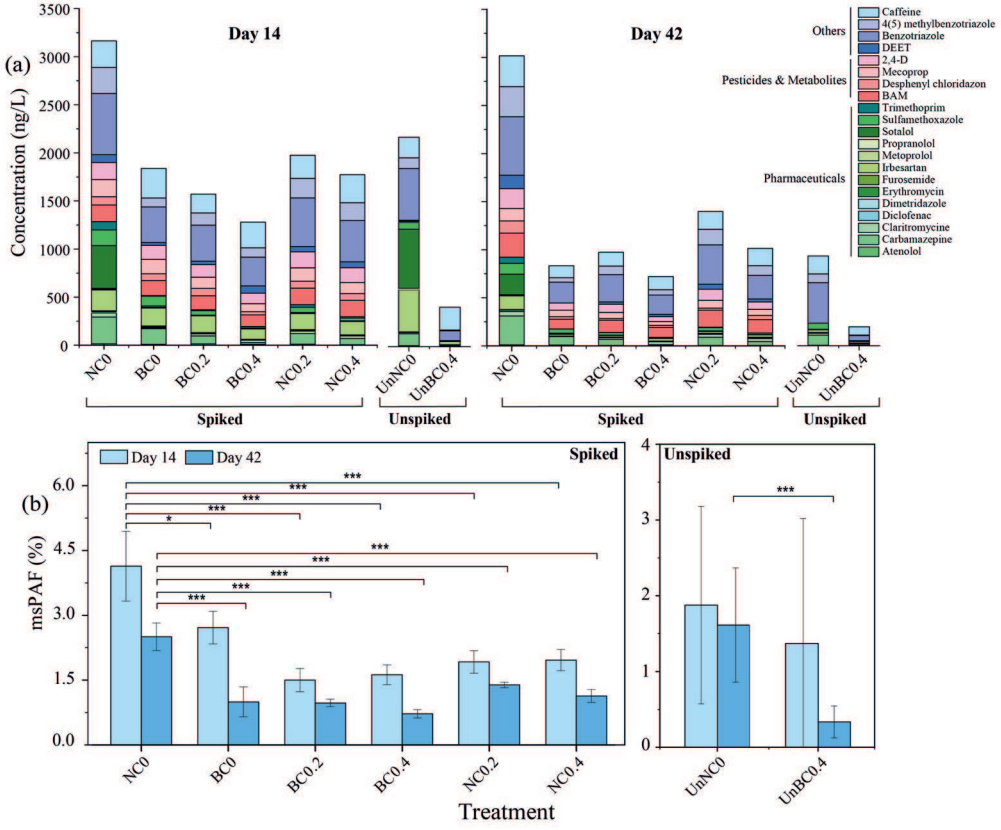


Figure 6.1. (a) Chemical concentrations measured in each treatment; (b) calculated chronic msPAF percentages based on chemical concentrations.

6.3.2 Water quality parameters and nutrients

Water temperature remained between 18 and 23 °C throughout the experiment, and DO levels were consistently around 10 mg/L with a transient increase on Day 7 (Fig. S6.1a,b). EC was initially higher in the spiked treatments than in NC0 but decreased across all groups after D14 (Fig. S6.1c). pH values were similar among treatments (8.0-10.0) (Fig. S6.1d).

On Day 14, nitrate & nitrite concentrations were significantly lower in BC0.4 and NC0.4 than in the other spiked treatments, whereas orthophosphate was significantly higher in NC0.4 (Fig. S6.2a–c). By Day 42, BC0.4 exhibited significantly higher concentrations of ammonia, nitrate & nitrite, and orthophosphate compared with the other spiked groups (Fig. S6.2a–c).

Nutrient levels were largely similar between NC0 and UnNC0 over time. TP was significantly higher in NC0 on Day 14 ($P < 0.05$), and by Day 42, ammonia concentrations were significantly lower in both unspiked groups than in the spiked groups ($P < 0.05$) (Fig. S6.2a,d).

6.3.3 Response of primary producers

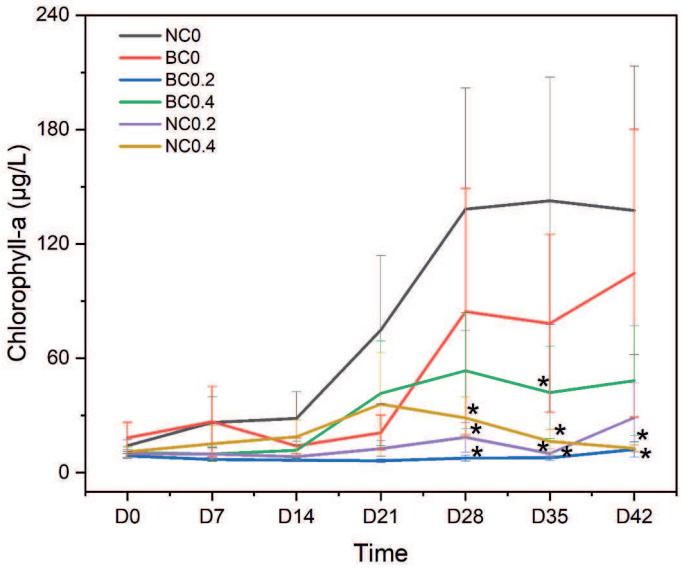


Figure 6.2. Chlorophyll-a concentrations across treatment groups. * indicates significant differences compared to the control group (NC0) at the same time point ($P < 0.05$).

Chlorophyll-a concentrations were comparable among all spiked treatments at Day 0 (8.8–18 µg/L) (Fig. 6.2). From Day 14 onwards, chlorophyll-a increased sharply in NC0, peaking

at 143 µg/L on Day 35 and remaining significantly higher than in all ozone-treated treatments ($P < 0.05$). No significant differences were detected between NC0 and BC0 over the course of the experiment. In the unspiked treatments, chlorophyll-a concentrations did not differ significantly between UnNC0 and UnBC0.4 at any sampling time (Fig. S6.4).

For the submerged macrophyte *Myriophyllum spicatum*, dry biomass on Day 14 ranged from 0.45 to 0.91 g across treatments (Fig. S6.5). NC0 showed the lowest biomass, while BC0.4 was the highest and significantly higher than NC0 ($P < 0.05$). By Day 42, biomass increased in all treatments without significant differences among them.

6.3.4 Zooplankton community and population dynamics

A total of 32 zooplankton taxa were identified, including nine macro- and 23 micro-zooplankton taxa (Tables S6.5, S6.6). In the spiked treatments, PRC analysis showed no significant divergence in zooplankton community structure from NC0 over time ($P > 0.05$, Fig. S6.6). The unspiked treatments also did not differ significantly from each other (Fig. S6.7). Similarly, total abundance, species richness, and Shannon diversity showed no significant differences relative to NC0 (Fig. S6.8). However, RDA with Monte-Carlo permutation testing indicated a significant community shift among spiked treatments relative to NC0 on Day 42 ($P < 0.01$, Fig. S6.10). Therefore, species-level patterns were examined to identify, which taxa contributed to these compositional differences.

At the species level, several zooplankton taxa in the spiked treatments differed significantly from NC0 ($P < 0.05$, Fig. 6.3). For instance, the rotifer *Keratella quadrata* was significantly more abundant in NC0.2 on Day 14. *Cyclopoida* copepods were significantly less abundant in BC0.2 but became significantly more abundant by Day 42, while nauplii were also significantly more abundant in BC0 and NC0.4. Among cladocerans, *Chydorus sphaericus*, *Daphnia pulex*, and *Daphnia longispina* exhibited significantly higher abundances in BC0, BC0.2, and NC0.4 than in NC0, and *Simocephalus* sp. was significantly more abundant in BC0.2 and NC0.4 ($P < 0.05$).

In the unspiked treatments, four taxa displayed significant treatment-related differences in abundance in UnBC0.4 compared to UnNC0 ($P < 0.05$, Fig. S6.11). *D. longispina*, *K. quadrata*, and nauplii were more abundant in UnBC0.4 on Day 14, whereas *C. sphaericus* was more abundant on Day 42. However, total abundance and richness did not differ significantly between UnNC0 and UnBC0.4 nor between spiked and unspiked counterparts (Fig. S6.8).

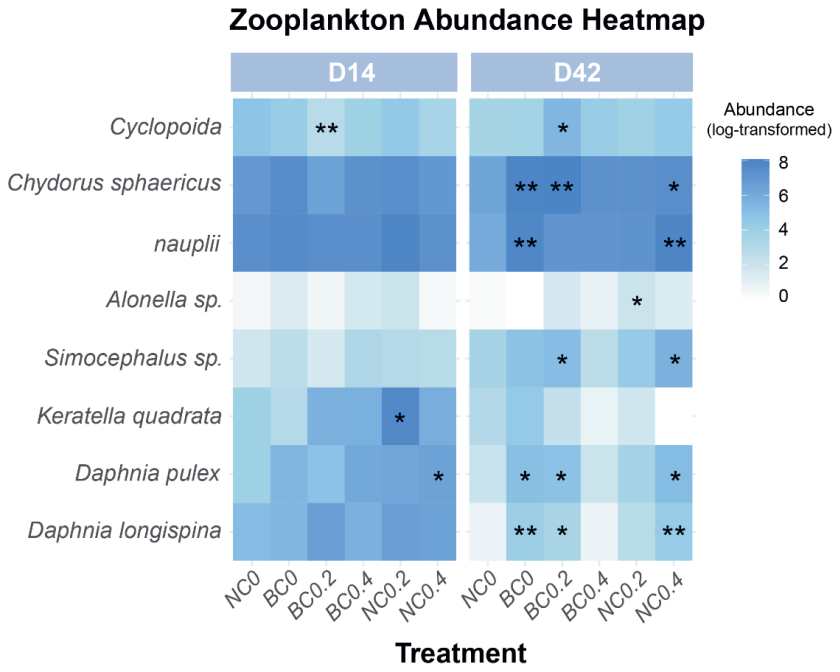


Figure 6.3. Heatmap showing the abundance of zooplankton species (data were ln(10x+1)-transformed). Asterisks (*) denote significant differences in abundance compared to the NC0 group at the corresponding time point ($P < 0.05$); double asterisks (**) indicate highly significant differences ($P < 0.01$).

6.3.5 Macroinvertebrate community and population dynamics

In total, 37 taxa of benthic macroinvertebrates were identified across all experimental groups. PRC analysis indicated that, over time, there was no significant treatment effect on benthic macroinvertebrate community composition (Fig. S6.12), and no significant differences were detected between UnNC0 and UnBC0.4 (Fig. S6.13). However, NC0 exhibited significantly higher species richness and Shannon diversity than those in BC0 and NC0.2 on Day 42 (Fig. S6.14, $P < 0.05$).

At the population level, notably, *Chironomus* abundance was higher in NC0 than in all other spiked treatments on Day 14 ($P < 0.05$, Fig. S6.15). *Chironomus* abundance in NC0 subsequently declined by Day 42. In the unspiked treatments, no significant differences in *Chironomus* abundance were observed between UnNC0 and UnBC0.4 on either sampling date (Fig. S6.15).

6.3.6 Microbial community compositional and functional profiles

6.3.6.1 Water and sediment community dynamics

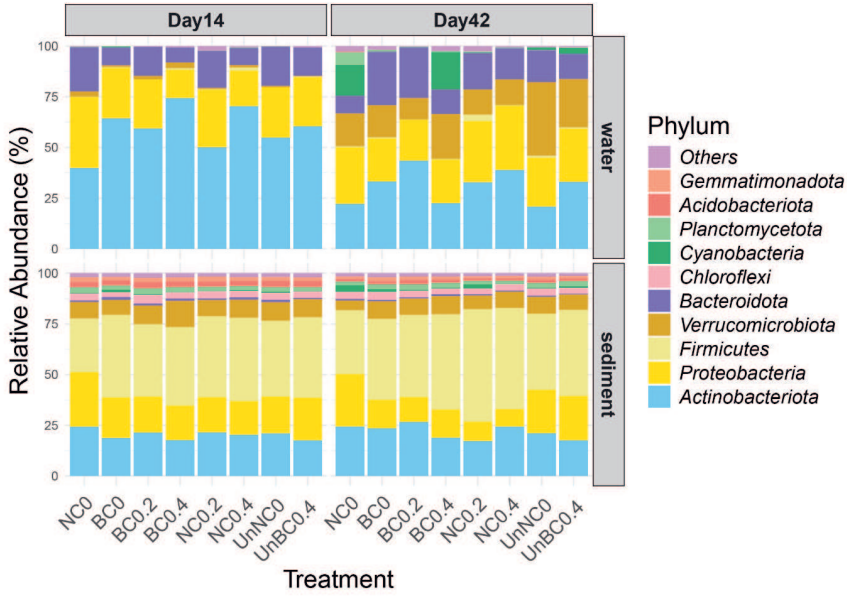


Figure 6.4. Composition of microbial communities in water column and sediment at the phylum level on Days 14 and 42. Taxa beyond the top 10 most abundant phyla were grouped as "Others".

A total of 2,512 ASVs were annotated from 57,222,414 high-quality sequences, representing 34 bacterial phyla and 554 genera across water and sediment samples. Microbial communities exhibited a pronounced temporal shift at the phylum level, characterized by a decline in relative abundance of *Actinobacteriota* and a marked increase in *Verrucomicrobiota* from Day 14 to Day 42 (Fig. 6.4). PRC analysis revealed significant temporal and treatment-related shifts at the genus level ($P < 0.05$), with the first and second PRC axes explaining 35% and 19% of the variation, respectively (Fig. S6.17).

To resolve treatment-specific differences indicated by PRC, Monte Carlo permutation tests based on RDA further showed that on Day 14, microbial community composition in NC0.4 and BC0.4 differed significantly from NC0 ($P < 0.05$; Fig. S6.17). By Day 42, BC0.4 converged toward NC0 and was no longer significantly different, whereas NC0.4 still showed a significant deviation ($P < 0.05$). In contrast, the other treatments exhibited significant differences from NC0 only on Day 42 ($P < 0.05$). In the unspiked treatments, UnBC0.4

showed a significant deviation from UnNC0 on Day 14 ($P < 0.01$) that disappeared by Day 42 (Fig. S6.18).

Across treatments, a growing number of genera showed significant differences in relative abundance from NC0 over time, with nine affected on Day 14 and 15 genera on Day 42 (Figs. 6.5a,b). Notably, the *hgcI_clade* showed significantly higher relative abundance in all treatments except NC0.2 on Day 14 ($P < 0.05$; Fig. 6.5a).

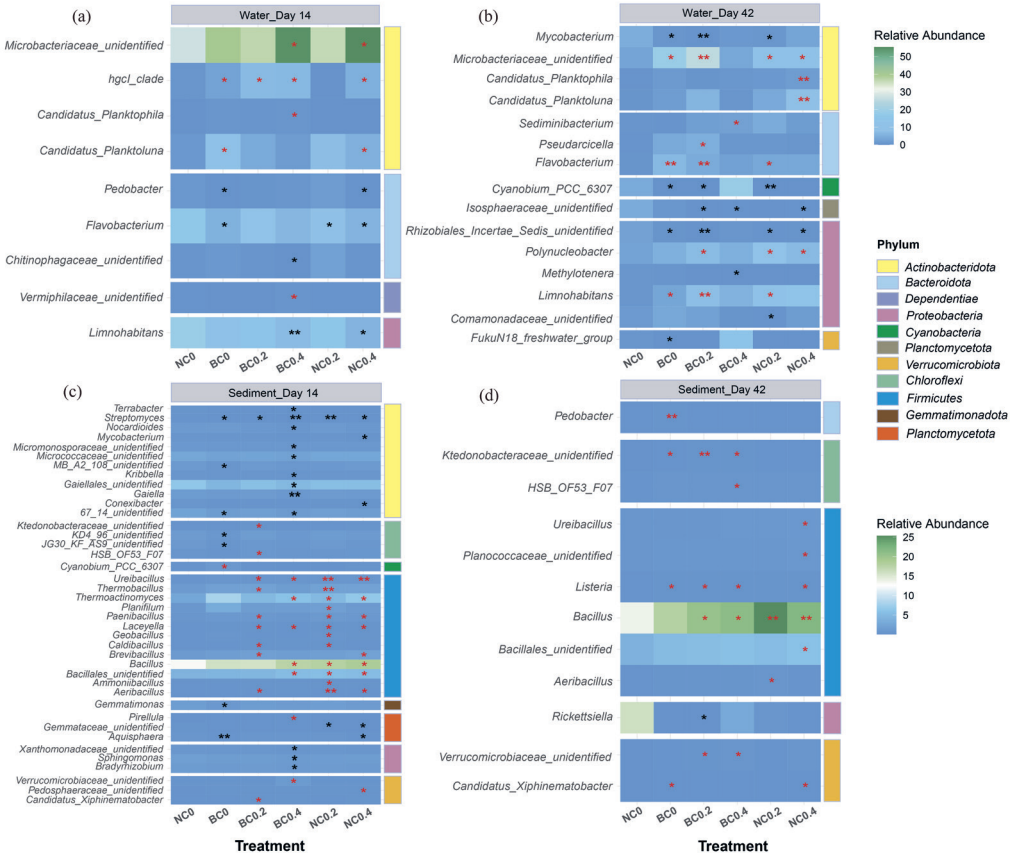


Figure 5. Heatmap of genus-level relative abundance across all treatment groups in the water column and sediment on Days 14 and 42. Red asterisks indicate genera with significantly higher relative abundance compared to the NC0 group, while black asterisks indicate significantly lower relative abundance. * denotes $P < 0.05$; ** denotes $P < 0.01$.

Sediment communities, in contrast to those in the water column, were more resistant to the treatment at the community level. *Firmicutes* and *Actinobacteriota* dominated across treatments (Fig. 6.4). No significant community-level treatment effects were detected by PRC (Figs. S6.19, S6.20), although genus-level analyses identified 40 taxa differing from

NC0 on Day 14, decreasing to 12 taxa by Day 42 (Figs. 6.5c,d). Most genera enriched on Day 14 belonged to *Firmicutes* and *Verrucomicrobiota*, whereas those depleted were primarily affiliated with *Actinobacteriota* and *Proteobacteria*.

6.3.6.2 Functional prediction and ecologically relevant taxa

To further assess the ecological implications of these structural differences, we used FAPROTAX to predict potential functions of the bacterial communities. In total, 44 functional categories were identified, among which 35 were related to environmental processes. Functional inference focused on ASVs belonging to genera that showed significant treatment-related differences in relative abundance (Fig. 6.5), which were extracted from both matrices and matched with their predicted functions (Table S6.7).

In the water column, only a small subset of genera showed assignable functional changes, with two and four genera affected on Days 14 and 42, respectively, primarily involving taxa linked to carbon and nitrogen cycling (Table S6.8). *Cyanobium_PCC_6307*, linked to carbon fixation and nitrogen cycling, showed significantly lower relative abundance in BC0, BC0.2, and NC0.2 on Day 42 compared with NC0, while *Methylotenera*, associated with methane metabolism and volatile organic compound degradation, was lower in BC0.4 ($P < 0.05$; Fig. 6.5a,b).

Functional responses were initially broader in the sediment than in the water column (Table S6.8). Taxa associated with organic matter degradation, such as *Streptomyces*, showed significantly lower relative abundance in all BO_3 treatments compared with NC0 on Day 14 ($P < 0.05$; Fig. 6.5c). BC0.4 induced the largest treatment effects, with manganese-oxidizing *Bacillus* ASVs significantly enriched relative to NC0 ($P < 0.05$; Fig. S6.21). Moreover, several genera predicted to be involved in carbon cycling and xenobiotic degradation (e.g., *Sphingomonas*, *Nocardioides*, and *Bradyrhizobium*) were significantly reduced exclusively in BC0.4 ($P < 0.05$; Fig. 6.5c,d).

6.3.7 Integrated ecological pathways driving system responses to BO3-treated effluents

The SEM based on the data of Day 14 showed that BO_3-treated effluents significantly reduced micropollutant concentrations, with both BAC and O_3 contributing to this effect (Fig. 6.6). O_3-treated effluents further reduced nitrate & nitrite and total phosphorus. These changes influenced primary production: BAC-treatment and phosphorus had a positive direct effect on chlorophyll-a, nitrate & nitrite a negative. In addition, O_3-treatment was associated with the water microbial community, though this pathway was marginally non-significant ($P = 0.06$). Nitrate & nitrite also exhibited a marginal association with the microbial community

(P = 0.051). Sediment microbial community metrics were not retained in the final model, as they explained little additional variance and showed no significant links to other components in the hypothesised network. Total phosphorus significantly influenced macroinvertebrate composition, while all direct or indirect pathways to zooplankton remained non-significant.

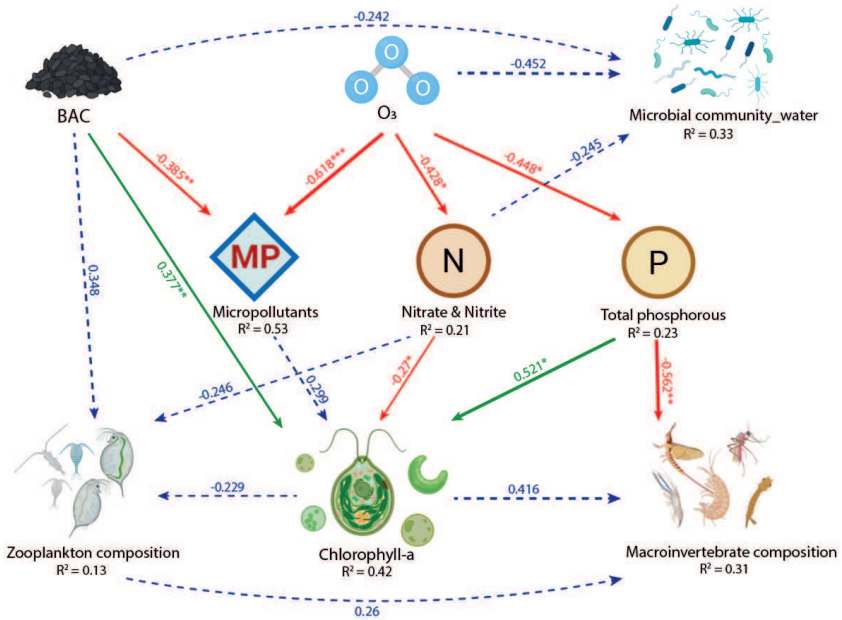


Figure 6.6. Structural equation model (SEM) illustrating the integrated ecological pathways associated with effluent treatments on Day 14. Red solid lines represent significant negative paths, green solid lines represent significant positive paths, and dashed lines indicate non-significant paths. Numbers on the arrows indicate standardized path coefficients (β). R^2 values indicate the proportion of variance explained for each response variable. The model showed a good overall fit (χ^2 = 11.56, df = 13, p = 0.56).

By Day 42, the network became simpler and the number of significant pathways decreased (Fig. S6.22). BAC-treated effluents still had a strong negative effect on micropollutant concentrations, whereas O_3-treated effluents no longer showed direct effects on micropollutants, nutrients, or biotic endpoints. Instead, total phosphorus emerged as the dominant predictor of chlorophyll-a, which was significantly associated with the microbial community in the water column. Pathways to zooplankton and macroinvertebrate composition remained weak and statistically non-significant, indicating limited propagation of cascading effects to higher trophic levels.

6.4 Discussion

6.4.1 Removal efficiency and residual risks of micropollutants

The removal efficiency of MPs by the BO_3 process increased markedly with ozone dose. High-dose ozonation alone (NC0.4) removed 79% of target compounds prior to microcosm exposure, whereas low-dose ozonation (NC0.2) removed 49% (Fig. 6.1a; Table S6.3). This pattern is consistent with ozone reaction mechanisms: molecules containing electron-rich aromatic rings (e.g., erythromycin, propranolol), unsaturated or heteroaromatic structures (e.g., irbesartan, carbamazepine), or amine functionalities (e.g., sulfamethoxazole, sotalol) generally undergo electrophilic addition and oxidative ring cleavage more readily and therefore degrade faster under ozonation (Lim et al., 2022). Incorporating BAC pretreatment increased removal to 65% at 0.2 g O_3 g^{-1} TOC by reducing matrix interferences and improving subsequent ozonation (Van Gijn et al., 2023). When applied at 0.4 g O_3 g^{-1} TOC, the BO_3 process achieved the highest overall MP removal (89%), confirming the benefit of sorptive pre-cleaning prior to high-dose ozonation.

Despite these substantial reductions, several MPs remained present. Compounds such as BAM, 2,4-D, and desphenyl-chloridazon contain strong electron-withdrawing groups, including chloro and carboxyl substituents, which lower electron density on the aromatic ring and could reduce its susceptibility to electrophilic ozonation (Von Gunten, 2003; Zhong et al., 2017). Benzotriazole and 4(5)-methylbenzotriazole also showed persistence because their stable poly-nitrogen heterocycles have inherently low ozone reactivity, as reflected in low second-order rate constants (Benitez et al., 2015; Müller et al., 2012). DEET similarly has a low direct ozonation rate constant (~0.1 $L \cdot mol^{-1} \cdot s^{-1}$) (Benitez et al., 2013). Hydrophilic compounds such as caffeine and benzotriazole also exhibit weak adsorption onto activated carbon due to their low logKow and competition with dissolved organic matter, making them less efficiently removed through BAC or combined BO_3 treatment (Nam et al., 2014; Wang et al., 2021).

Because BO_3 treatment did not fully eliminate all MPs, residual concentrations of several compounds, including 2,4-D, 4(5)-methylbenzotriazole, and caffeine, produced medium- to high-risk quotients based on PNEC values compiled in the Norman Ecotoxicity Database (Table S4). Moreover, the disappearance of parent compounds does not necessarily mean that ecological risks are completely removed. Ozonation can generate hydroxylated products, N-oxides, and aromatic ring-cleavage intermediates, and the toxicity of some transformation products may be comparable to or higher than that of their parents (Hübner et al., 2015; Zilberman et al., 2023). Low-molecular-weight oxidation products such as formaldehyde may also form during ozonation of wastewater effluent and have been shown to exert toxicity

to *Daphnia* sp. (Park et al., 2016). Despite these concerns, studies indicate that ozonation followed by biological filtration or activated carbon substantially reduces the overall mixture toxicity of treated effluents (Völker et al., 2019).

6.4.2 Algal responses under BO_3 treatments

The observed patterns in chlorophyll-a dynamics in the different spiked treatments suggest that neither MPs alone nor BAC alone strongly suppressed algal biomass, and that algal growth was most likely constrained by ozone-related effects (Fig. 6.2). Because ozone addition had ceased before Day 14, the sustained suppression of chlorophyll-a in the ozone-treated groups is more likely attributable to indirect processes than to immediate oxidative damage. Ozonation transforms effluent organic matter into smaller, highly oxidized and low-energy molecules, which reduces the availability of carbon or nutrients that support algal production (Camel and Bermond, 1998). Previous studies have shown that oxidation of certain MPs (e.g., carbamazepine, diclofenac and irbesartan) can generate transformation products exhibiting enhanced toxicity to algae, which may maintain chemical stress during the exposure period and further hinder algal recovery (Kråkström et al., 2020; Lonappan et al., 2016; Medici et al., 2024).

Furthermore, nutrient differences may also have contributed to these patterns. NC0 maintained relatively high TP concentrations throughout the experiment ($P < 0.05$, Fig. S6.2d), which is favorable for sustained algal accumulation (Schindler et al., 2016). By contrast, effluents pretreated with BAC and/or ozone may have reduced the pool of bioavailable phosphorus or altered its speciation, thereby lowering resource availability for algae at the onset of the exposure. In addition, we showed that BO_3 treatments markedly altered the water-column microbial community composition, and functional predictions indicated reduced relative abundances of several taxa associated with nutrient cycling and organic matter degradation in the ozone-treated groups (Fig. 6.5; Fig. S6.17; Table S6.8). The structural equation model further showed that, in the later phase of the experiment (Day 42), chlorophyll-a was positively related to TP and significantly related to microbial community composition (Fig. S6.22). On this basis, we infer that, in the early exposure phase (Day 14), algal suppression more likely reflected a combination of residual toxicity from MPs and their transformation products together with reduced availability of key resources (particularly phosphorus). In the later phase (Day 42), when concentrations had declined, algal dynamics were more likely governed by nutrient limitation and potential resource competition with microbial communities. This interpretation is consistent with the results for the unspiked treatments, where UnNC0 and UnBC0.4 exhibited similar chlorophyll-a and nutrient levels (Fig. S6.2; Fig. S6.4), suggesting that under low pollution loads, algal dynamics are primarily controlled by nutrient conditions rather than by

differences in residual MPs and their transformation products arising from the treatment processes.

6.4.3 Effects on zooplankton and macroinvertebrates

Multivariate analysis revealed that the zooplankton community composition in NC0 and BC0 changed relatively little between Day 14 and Day 42, whereas all ozone-related treatments exhibited pronounced shifts (Fig. S6.9). By Day 42, several taxa (e.g., *Daphnia* spp., *Chydorus sphaericus*) showed strong declines in NC0 and BC0.4, while decreases were smaller or absent in the other ozone-related treatments (Fig. 6.3). Previous studies have shown that prolonged but low-level exposure to pharmaceuticals or other micropollutants can progressively impair zooplankton growth or reproduction (Flaherty and Dodson, 2005; Pavlaki et al., 2014), consistent with the late-stage declines observed in NC0.

For BC0.4, the high-dose combination of BAC and ozonation exhibited the strongest oxidative effects and, therefore, while reducing parent compounds, was also most likely to generate the highest levels of oxidative transformation products, some of which are known to exert chronic toxicity on aquatic organisms (Hollender et al., 2009). This chronic stress may explain the declining trends observed on Day 42. In contrast, BC0.2 may represent a more balanced state, reducing parent MPs while limiting the accumulation of harmful byproducts, resulting in small shifts in community structure rather than marked declines. Given that this study did not directly quantify specific transformation products, these mechanistic interpretations should be viewed as hypotheses rather than evidence.

The slightly higher macroinvertebrate diversity in NC0 may reflect greater benthic food availability due to higher algal-derived food resources (Wellard Kelly et al., 2013), while the decline of *Chironomus* in NC0 likely reflects the natural emergence of adults during the exposure period rather than a treatment effect.

6.4.4 Microbial community responses and functional implications

Water-column microbial communities showed different recovery trajectories in NC0.4 and BC0.4 (Fig. S6.16, S6.17), which may be because BAC pretreatment lowered DOC and labile organic substrates before ozonation, thereby changing resource conditions for microbes and promoting faster recovery in the later exposure phase. At the genus level, the number of genera with relative abundances significantly different from NC0 increased from Day 14 to Day 42 (Fig. 6.5), indicating that BO_3-induced perturbations to water-column bacterial communities persisted and accumulated through time rather than being short-term and reversible (Ruprecht et al., 2021). This pattern aligns with the slower recovery observed under resource-limited conditions. Previous studies showed that low-DOC systems often

exhibit lower microbial resilience (Fang et al., 2022). In this study, the combined BO_3 treatments likely decreased DOC availability and thereby weakened the carbon-source base needed for community reassembly. In addition, all ozone-related treatments showed suppressed algal biomass (Fig. 6.2), indicating a lack of continuous autochthonous DOC input throughout the exposure period. Reduced DOC availability together with lower primary productivity likely constrained microbial recovery in the water column and contributed to the gradual accumulation of structural deviations over time. Supporting this interpretation, the relative abundance of *hgcI_clade* was significantly higher in all treatments except NC0.2 on Day 14 (Fig. 6.5a). This clade is common in oligotrophic waters and typically shows a negative association with total nitrogen, serving as an indicator of nutrient status (Newton et al., 2011; Ruprecht et al., 2021). In our study, NC0 showed the highest TN concentration, corresponding well with the lower relative abundance of *hgcI_clade*.

In contrast, the sediment microbial communities exhibited weaker structural responses, reflecting higher stability and buffering capacity. Although PRC analyses did not detect significant community-level deviations, genus-level analyses identified 40 genera differing from NC0 on Day 14, decreasing to 12 by Day 42. This pattern suggests that sediment communities responded primarily during the early phase of exposure and recovered over time.

Functional predictions indicated no large-scale functional changes; however, several genera predicted to be associated with key biogeochemical functions displayed treatment-specific responses (Table S6.8). *Methylotenera* decreased significantly in BC0.4, a pattern consistent with its sensitivity to strong oxidation during the ozonation pretreatment during processes such as methane oxidation and denitrification (Nguyen et al., 2020; Ren et al., 2019), and aligned with previous reports of high-oxidation treatments suppressing denitrifying bacteria (Asif et al., 2021). Moreover, several genera predicted to be associated with carbon cycling or pollutant degradation, including *Sphingomonas*, *Nocardioides*, and *Bradyrhizobium*, also showed reduced relative abundance in BC0.4, suggesting that high-intensity ozonation may transiently weaken certain functional capacities of both water-column and benthic microbial communities (Asaf et al., 2020; Ma et al., 2023; Meena et al., 2018).

Overall, ozonation intensity affected how microbial community composition changed and recovered over time and influenced the sensitivity of taxa associated with key biogeochemical functions to disturbance. High-intensity ozonation (particularly in the BO_3 configuration) achieved greater pollutant removal but also induced more pronounced structural perturbations and reductions in functional potential. In contrast, moderate ozone treatments appeared to strike a more favorable balance between pollutant removal and the preservation of microbial structural and functional integrity. These findings highlight the

importance of considering the ecological implications of treatment intensity when evaluating advanced wastewater treatment processes.

6.4.5 Integrative interpretation based on SEM

SEMs provide an integrated perspective on how treatment-related changes influenced different trophic levels. On Day 14, BO_3 treatments were associated with lower micropollutant and nutrient concentrations (Fig. 6.6), and these chemical shifts largely explained early algal responses, which, as discussed in Section 4.2, were shaped by a combination of nutrient supply, resource availability and residual chemical stress. At the microbial level, ozone, nitrate and nitrite showed weak associations with the water-column microbial community, consistent with the compositional shifts observed in Section 4.4. Importantly, these chemical and microbial changes did not propagate to zooplankton, and only total phosphorus showed a detectable influence on macroinvertebrate composition, reflecting the overall robustness of consumer communities. By Day 42, the interaction network had become markedly simpler (Fig. S6.22). Nutrient conditions played a predominant role in shaping primary production, while pathways to zooplankton and macroinvertebrates remained weak and statistically non-significant, indicating limited propagation of treatment effects to higher trophic levels.

Overall, the SEM results show that BO_3 primarily affected the base of the food web through chemically mediated influences on microbes and algae during the early exposure phase, whereas later dynamics were governed mainly by nutrient status. Higher trophic levels exhibited substantial resilience, and the ecological gains of BO_3 appear to derive mainly from improvements in water quality and resource conditions rather than from cascading effects within the food web.

It is important to note that our microcosm experiment simulated a single pulse of treated effluent, whereas real WWTP discharges are continuous. Under continuous loading, the system may not transition into the nutrient-dominated stable state observed here, and early-stage chemical perturbations may be sustained for longer periods.

6.5 Conclusions

This study shows that combining bioactivated carbon with ozonation markedly improved effluent chemical quality, while ecological impacts in freshwater microcosms remained largely confined to microbial and primary-producer levels; higher trophic groups were comparatively resilient. Overall, the advanced treatment achieved a balanced outcome

between pollutant reduction and ecological disturbance, with moderate treatment intensity offering greater potential to enhance water quality while maintaining ecological safety. Where necessary, a simple post-treatment step, such as additional bioactivated carbon filtration or a short biological filtration, may further mitigate risks associated with transformation products.

Acknowledgements

The authors would like to thank Marie-Claire Boerwinkel for her assistance with zooplankton identification, and Xuelin Zhu from Nanjing Agricultural University for her contributions to the microbial functional prediction analysis. Lara Schuijt was supported by the Dutch Research Council (NWO) domain TTW, KWR, STOWA through the EMERCHE project: Effect-directed Monitoring tools to assess Ecological and human health Risks of CHemicals of Emerging concern in the water cycle (File number 15760). We acknowledge the China Scholarship Council (CSC) for supporting Dailing Wu (File No. 202006750027).This work was supported by National Natural Science Foundation of China (U22A20604).

Supplementary information

Text S6.1. Microcosm Set-up

Wastewater subjected to different treatments was added to constructed microcosms. Each microcosm consisted of a polyethylene cylindrical container with a height of 67 cm and a diameter of 45 cm. A total of 58 L of water was added to each microcosm, of which 29 L was freshwater from the supply basin of the experimental station, and the other 29 L was untreated effluent or effluent treated by different BO_3 processes. This setup was chosen to simulate the dilution effect of wastewater effluent entering natural freshwater bodies. Additionally, 3 L of clean sediment was placed in a tray in each microcosm to provide a habitat for benthic organisms and to create a complete ecosystem. Subsequently, zooplankton and macroinvertebrate species, as well as green algae and submerged macrophytes, were added from clean freshwater bodies on site. Two grams of dried *Populus* leaves were added as food for benthic organisms.

To maintain system stability and reduce sensitivity to daily temperature fluctuations, all microcosms were buried 0.5 m into the soil. Each treatment group had 10 replicates, resulting in a total of 80 microcosms. To avoid systematic bias, the microcosms were randomly assigned to different treatment groups. The microcosms were kept open at the top without any net covering. A drainage outlet was installed at the top side of each microcosm to release excess water during heavy rainfall. When water levels dropped due to evaporation, water was manually replenished to ensure that water level fluctuations did not exceed 20% of the original volume. Notably, the introduced natural soil contained native microbial communities and possibly insect eggs, which could hatch naturally during the experiment. The open systems also allowed for the natural colonization or emergence of insects and other organisms.

The experiment lasted for six weeks. Before exposure to different effluent treatments, each constructed microcosm contained 29 L of freshwater and underwent a one-month acclimatization period. On Day 0, treated or untreated effluents were introduced into the microcosms. Samples were collected destructively on Days 14 and 42, with five replicate samples taken from each treatment group at each time point.

Text S6.2. Micropollutant Spiking Protocol and BO_3 Reactor Configuration

The effluent was spiked with a mixture of 21 target compounds at a target concentration of approximately 1 µg/L (Van Gijn et al., 2023). The solvent used to prepare the micropollutant stock solution (acetonitrile) was evaporated before addition to avoid introducing solvent into the effluent. The 21 compounds included the pharmaceuticals atenolol, carbamazepine,

clarithromycin, diclofenac, dimetridazole, erythromycin, furosemide, irbesartan, metoprolol, propranolol, sotalol, sulfamethoxazole, and trimethoprim; the pesticides and their metabolites 1,6-dichlorobenzamide (BAM), desphenyl chloridazon, mecoprop, and 2,4-dichlorophenoxyacetic acid (2,4-D); and other compounds including diethyltoluamide (DEET), benzotriazole, 4(5)-methylbenzotriazole, and caffeine. The CAS numbers of these compounds are listed in Table S1. Treatments were performed in differently configured BO_3 reactors as described by Van Gijn et al. (2023). Briefly, the effluent first passed through a biological reactor containing activated carbon, followed by ozone treatment in a bubble column at a flow rate of approximately 4 L/h, corresponding to an empty bed contact time in the activated carbon filter of approximately 15 min. Prior to treatment, the effluent was aerated with pure oxygen to ensure sufficient oxygen availability during the biological process.

Text S6.3. Microbial Community Analysis

Microbial samples from the water column were collected on Days 14 and 42. For each microcosm, 1 L of depth-integrated water was collected from different layers using sterilized opaque plastic bottles. Samples were immediately transported to the laboratory, filtered through 0.22 µm cellulose filter membranes (Millipore, Merck, USA) on the same day, and the filter membranes with the retained material were stored at -20 °C for further analysis. Sediment samples were taken from the pre-installed HDPE containers. Overlying water was gently removed, and the sediment was stored at -20 °C until analysis.

The collected water samples and freeze-dried sediment samples were processed for DNA extraction using the PowerSoil DNA Isolation Kit (QIAGEN, Germany) at the Laboratory of Microbiology, Wageningen University & Research. DNA concentrations were then determined using Qubit (Thermo Fisher Scientific, USA).

Barcoded amplicons targeting the V4 region of the prokaryotic *16S rRNA* gene were generated using primers 515F (5'-GTGCCAGC[AC]GCCGCGGTAA-3') and 806R (5'-GGACTAC[ACT][ACG]GGGT[AT]TCTAAT-3'), both tagged at the 5' end with sample-specific barcodes (Walters et al., 2016). PCR was performed in 50 µL reactions containing 5× HF Green buffer, Phusion Hot Start II polymerase (Thermo Fisher Scientific), 500 nM of each primer, 500 nM dNTPs (Promega), 10 ng DNA template, and nuclease-free water. Cycling conditions were: 98 °C for 30 s; 25 cycles of 98 °C for 10 s, 50 °C for 10 s, 72 °C for 10 s; and a final extension at 72 °C for 7 min. The PCR products (2 µL) were analyzed using the FlashGel® System (Lonza, Switserland). Each sample was amplified in triplicate and the triplicates were then pooled and purified using CleanPCR (cleanNA, Netherlands) according to the manufacturer's instructions. DNA concentration was quantified with Qubit (Thermo

Fisher Scientific, USA). Equimolar amounts of all purified amplicons, including positive (Mock community) and negative (nuclease-free water) controls, were pooled and sequenced on a HiSeq2000 platform (Novogene, UK).

Table S6.1. List of the 21 target compounds spiked into the effluent with their CAS numbers and predicted no effect concentrations (PNECs) found in the NORMAN database.

Category	Compound	CAS-number	PNEC (ng/L)
Pharmaceuticals	Atenolol	29122-68-7	150000
	Carbamazepine	298-46-4	2000
	Clarithromycine	81103-11-9	120
	Diclofenac	15307-86-5	40
	Dimetridazole	551-92-8	29500
	Erythromycin	114-07-8	300
	Furosemide	54-31-9	31300
	Irbesartan	138402-11-6	700000
	Mecoprop	7085-19-0	900
	Metoprolol	37350-58-6	8600
	Propranolol	525-66-6	160
	Sotalol	3930-20-9	6520
	Sulfamethoxazole	723-46-6	600
	Trimethoprim	738-70-5	1200
Pesticides and their metabolites	BAM	2008-58-4	78000
	Desphenyl chloridazon	6339-19-1	250000
	2,4-D	94-75-7	600
Other compounds	4(5) methylbenzotriazole	136-85-6	150
	DEET	134-62-3	88000
	Benzotriazole	95-14-7	7770
	Caffeine	58-08-2	1200

Table S6.2. Concentration of the micropollutants and their removal rates (%) in each treatment on Day 0.

Compound	Day 0										
	NC0	BC0		BC0.2		BC0.4		NC0.2		NC0.4	
	Conc.	Conc.	Removal (%) [a]	Conc.	Removal (%)	Conc.	Removal (%)	Conc.	Removal (%)	Conc.	Removal (%)
Atenolol	1358	236	83	695	49	346	75	1020	25	626	54
Carbamazepine	1372	485	65	491	64	LOQ[b]	> 95	604	56	239	83
Clarithromycine	1549	143	91	363	77	70	95	674	56	182	88
Diclofenac	1411	209	85	360	75	LOQ	> 95	430	70	203	86
Dimetridazole	805	290	64	543	33	304	62	642	20	359	55
Erythromycin	1381	203	85	290	79	LOQ	> 95	622	55	178	87
Furosemide	1892	319	83	241	87	LOQ	> 95	259	86	83	> 95
Irbesartan	5573	1761	68	3372	39	1388	75	4601	17	1547	72
Mecoprop	974	485	50	651	33	373	62	746	23	415	57
Metoprolol	2823	421	85	1391	51	726	74	1736	39	1113	61
Propranolol	1132	LOQ	> 95	177	84	LOQ	> 95	433	62	157	86
Sotalol	32612	3523	89	7460	77	518	> 95	13115	60	3802	88
Sulfamethoxazole	872	398	54	329	62	53	94	328	62	132	85
Trimethoprim	858	72	92	180	79	LOQ	> 95	297	65	107	87
BAM	759	391	49	570	25	409	46	648	15	451	41
Desphenyl chloridazon	1030	626	39	794	23	402	61	792	23	576	44
2,4-D	1030	398	61	678	34	334	68	763	26	460	55
4(5) methylbenzotriazole	1619	289	82	819	49	418	74	1198	26	645	60
DEET	883	247	72	558	37	237	73	587	34	381	57
Benzotriazole	3447	1136	67	2218	36	1261	63	2647	23	1529	56
Caffeine	1053	259	75	513	51	280	73	514	51	456	57
In total	64433	11893	82	22693	65	7119	89	32656	49	13642	79

a. Removal (%) = [1 − Conc(Treatment)/Conc(NC0)] × 100; Conc(NC0) is the Day-0 untreated control. In the Removal (%) columns, greener shading indicates higher removal and orange/brown shading indicates lower removal.
b. LOQ: Detection limits of quantification, 50 ng/L.

Table S6.3. Concentration of the micropollutants (ng/L) and their dissipation rates (%) in each treatment on Day 14 and Day 42.

Compound	Day 14												Day 42											
	NC0		BC0		BC0.2		BC0.4		NC0.2		NC0.4		NC0		BC0		BC0.2		BC0.4		NC0.2		NC0.4	
	Con.	%[a]	Con.	%	Con.	%	Con.	%	Con.	%	Con.	%	Con.	%	Con.	%	Con.	%	Con.	%	Con.	%	Con.	%
Atenolol	LOQ[b]	> 95	LOQ	> 95	LOQ	> 95	LOQ	> 95	LOQ	> 95	LOQ	> 95	LOQ	> 95	LOQ	> 95	LOQ	> 95	LOQ	> 95	LOQ	> 95	LOQ	> 95
Carbamazepine	278	80	161	88	83	94	LOQ	> 95	110	92	58	> 95	301	78	88	94	64	95	LOQ	> 95	86	94	LOQ	> 95
Clarithromycine	LOQ	> 95	LOQ	> 95	LOQ	> 95	LOQ	> 95	LOQ	> 95	LOQ	> 95	LOQ	> 95	LOQ	> 95	LOQ	> 95	LOQ	> 95	LOQ	> 95	LOQ	> 95
Diclofenac	LOQ	> 95	LOQ	> 95	LOQ	> 95	LOQ	> 95	LOQ	> 95	LOQ	> 95	LOQ	> 95	LOQ	> 95	LOQ	> 95	LOQ	> 95	LOQ	> 95	LOQ	> 95
Dimetridazole	LOQ	> 95	LOQ	> 95	LOQ	> 95	LOQ	> 95	LOQ	> 95	LOQ	> 95	LOQ	> 95	LOQ	> 95	LOQ	> 95	LOQ	> 95	LOQ	> 95	LOQ	> 95
Erythromycin	LOQ	> 95	LOQ	> 95	LOQ	> 95	LOQ	> 95	LOQ	> 95	LOQ	> 95	LOQ	> 95	LOQ	> 95	LOQ	> 95	LOQ	> 95	LOQ	> 95	LOQ	> 95
Furosemide	LOQ	> 95	LOQ	> 95	LOQ	> 95	LOQ	> 95	LOQ	> 95	LOQ	> 95	LOQ	> 95	LOQ	> 95	LOQ	> 95	LOQ	> 95	LOQ	> 95	LOQ	> 95
Irbesartan	218	> 95	186	> 95	175	> 95	110	> 95	168	> 95	129	> 95	143	> 95	LOQ	> 95	LOQ	> 95	LOQ	> 95	LOQ	> 95	LOQ	> 95
Mecoprop	177	82	150	85	117	88	84	91	139	86	111	89	129	87	69	93	66	93	LOQ	> 95	81	92	62	94
Metoprolol	LOQ	> 95	LOQ	> 95	LOQ	> 95	LOQ	> 95	LOQ	> 95	LOQ	> 95	LOQ	> 95	LOQ	> 95	LOQ	> 95	LOQ	> 95	LOQ	> 95	LOQ	> 95
Propranolol	LOQ	> 95	LOQ	> 95	LOQ	> 95	LOQ	> 95	LOQ	> 95	LOQ	> 95	LOQ	> 95	LOQ	> 95	LOQ	> 95	LOQ	> 95	LOQ	> 95	LOQ	> 95
Sotalol	444	> 95	LOQ	> 95	LOQ	> 95	LOQ	> 95	LOQ	> 95	LOQ	> 95	213	> 95	LOQ	> 95	LOQ	> 95	LOQ	> 95	LOQ	> 95	LOQ	> 95
Sulfamethoxazole	163	81	101	88	LOQ	> 95	LOQ	> 95	54	94	LOQ	> 95	113	87	LOQ	> 95	LOQ	> 95	LOQ	> 95	LOQ	> 95	LOQ	> 95
Trimethoprim	87	90	LOQ	> 95	LOQ	> 95	LOQ	> 95	LOQ	> 95	LOQ	> 95	64	92	LOQ	> 95	LOQ	> 95	LOQ	> 95	LOQ	> 95	LOQ	> 95
BAM	172	77	155	80	145	81	119	84	171	77	173	77	250	67	101	87	126	83	102	87	176	77	139	82
Desphenyl chloridazon	86	92	71	93	76	93	LOQ	> 95	73	93	61	94	127	88	LOQ	> 95	LOQ	> 95	LOQ	> 95	LOQ	> 95	LOQ	> 95
2,4-D	179	83	146	86	131	87	109	89	166	84	152	85	206	80	75	93	85	92	52	95	115	89	78	92
4(5) methylbenzotriazole	271	83	92	94	126	92	96	> 95	203	87	184	89	312	81	LOQ	> 95	89	95	53	> 95	162	90	101	94
DEET	81	91	LOQ	> 95	LOQ	> 95	75	91	55	94	57	94	140	84	LOQ	> 95	LOQ	> 95	LOQ	> 95	53	94	LOQ	> 95
Benzotriazole	637	82	369	89	375	89	299	91	506	85	424	88	608	82	216	94	286	92	201	94	408	88	245	93
Caffeine	276	74	308	71	195	81	267	75	240	77	290	72	321	70	125	88	143	86	138	87	185	82	180	83
In total	3069	95	1740	97	1424	98	1160	98	1885	97	1638	97	2927	95	674	99	858	99	547	99	1265	98	806	99

a. Removal/Dissipation (%) = [1 − Conc(Treatment)/Conc(NC0)] × 100; Conc(Treatment) is the concentration on Day 14 or Day 42, and Conc(NC0) is the Day 0 untreated control. Colour shading in the (%) columns reflects magnitude (greener = higher).
b. LOQ: 50 ng/L.

Table S6.4. Risk quotients (RQ) of micropollutant concentrations in the water phase of microcosms across sampling times.

Compound	Day 0						Day 14						Day 42					
	NC0	BC0	BC0.2	BC0.4	NC0.2	NC0.4	NC0	BC0	BC0.2	BC0.4	NC0.2	NC0.4	NC0	BC0	BC0.2	BC0.4	NC0.2	NC0.4
Atenolol	0.01				0.01													
Carbamazepine	0.69	0.24	0.25		0.30	0.12	0.14	0.08	0.04		0.06		0.15	0.04	0.03		0.04	
Claritromycine	12.91*	1.19	3.03	0.58	5.62	1.52												
Diclofenac	35.28	5.22	8.99		10.75	5.08												
Dimetridazole	0.03	0.01	0.02	0.01	0.02	0.01												
Erythromycin	4.60	0.68	0.97		2.07	0.59												
Furosemide	0.06	0.01	0.01		0.01													
Irbesartan	0.01				0.01													
Mecoprop	1.08	0.54	0.72	0.41	0.83	0.46	0.20	0.17	0.13	0.09	0.15	0.12	0.14	0.08	0.07		0.09	
Metoprolol	0.33	0.05	0.16	0.08	0.20	0.13												
Propranolol	7.08		1.11		2.71	0.98												
Sotalol	5.00	0.54	1.14	0.08	2.01	0.58	0.07						0.03					
Sulfamethoxazole	1.45	0.66	0.55	0.09	0.55	0.22	0.27	0.17			0.09		0.19					
Trimethoprim	0.72																	
BAM	0.01	0.01	0.01	0.01	0.01	0.01												
Desphenyl chloridazon																		
2,4-D	1.72	0.66	1.13	0.56	1.27	0.77	0.30	0.24	0.22	0.18	0.28	0.25	0.34	0.12	0.14	0.09	0.19	0.09
4(5) methylbenzotriazole	10.79	1.93	5.46	2.79	7.99	4.3	1.81	0.62	0.84	0.64	1.35	1.22	2.08		0.59	0.35	1.08	0.35
DEET	0.01		0.01		0.01													
Benzotriazole	0.44	0.15	0.29	0.16	0.34	0.2	0.08	0.05	0.05	0.04	0.07	0.05	0.08	0.03	0.04	0.03	0.05	0.03
Caffeine	0.88	0.22	0.43	0.23	0.43	0.38	0.23	0.26	0.16	0.22	0.20	0.24	0.27	0.10	0.12	0.12	0.15	0.12

* High risk: RQ $\geqslant$ 1; Medium risk: 0.1 $\leqslant$ RQ < 1; Low risk: 0.01 $\leqslant$ RQ < 0.1; No risk: RQ < 0.01. Colour shading indicates RQ magnitude, with darker shading representing higher RQ.

Table S6.5. Concentration of the micropollutants and their removal rates (%) in unspiked treatment groups.

Compound	Day 0			Day 14				Day 42			
	UnNC0	UnBC0.4		UnNC0		UnBC0.4		UnNC0		UnBC0.4	
	Conc.	Conc.	Removal	Conc.	Dissipation	Conc.	Dissipation	Conc.	Dissipation	Conc.	Dissipation
Atenolol	209	LOQ	> 95	LOQ	> 95	LOQ	> 95	LOQ	> 95	LOQ	> 95
Carbamazepine	659	LOQ	> 95	124	81	LOQ	> 95	106	84	LOQ	> 95
Clarithromycine	383	LOQ	> 95	LOQ	> 95	LOQ	> 95	LOQ	> 95	LOQ	> 95
Diclofenac	725	LOQ	> 95	LOQ	> 95	LOQ	> 95	LOQ	> 95	LOQ	> 95
Dimetridazole	LOQ	LOQ	> 95	LOQ	> 95	LOQ	> 95	LOQ	> 95	LOQ	> 95
Erythromycin	201	LOQ	> 95	LOQ	> 95	LOQ	> 95	LOQ	> 95	LOQ	> 95
Furosemide	1025	LOQ	> 95	LOQ	> 95	LOQ	> 95	LOQ	> 95	LOQ	> 95
Irbesartan	4435	437	90	432	90	LOQ	> 95	LOQ	> 95	LOQ	> 95
Mecoprop	61	LOQ	> 95	LOQ	> 95	LOQ	> 95	LOQ	> 95	LOQ	> 95
Metoprolol	2027	LOQ	> 95	LOQ	> 95	LOQ	> 95	LOQ	> 95	LOQ	> 95
Propranolol	201	LOQ	> 95	LOQ	> 95	LOQ	> 95	LOQ	> 95	LOQ	> 95
Sotalol	29895	51	> 95	622	> 95	LOQ	> 95	LOQ	> 95	LOQ	> 95
Sulfamethoxazole	169	LOQ	> 95	66	61	LOQ	> 95	64	62	LOQ	> 95
Trimethoprim	143	LOQ	> 95	LOQ	> 95	LOQ	> 95	LOQ	> 95	LOQ	> 95
BAM	LOQ	LOQ	> 95	LOQ	> 95	LOQ	> 95	LOQ	> 95	LOQ	> 95
Desphenyl chloridazon	LOQ	LOQ	> 95	LOQ	> 95	LOQ	> 95	LOQ	> 95	LOQ	> 95
2,4-D	39	LOQ	> 95	LOQ	> 95	LOQ	> 95	LOQ	> 95	LOQ	> 95
4(5) methylbenzotriazole	527	LOQ	> 95	112	79	LOQ	> 95	91	83	LOQ	> 95
DEET	134	66	51	LOQ	> 95	LOQ	> 95	LOQ	> 95	LOQ	> 95
Benzotriazole	2426	335	86	541	78	102	> 95	420	83	56	> 95
Caffeine	299	LOQ	> 95	216	28	240	20	187	37	86	71
In total	43557	890	98	2114	95	341	99	869	98	142	99

* In the Removal/Dissipation (%) columns, greener shading indicates higher removal and orange/brown shading indicates lower removal.

Table S6.6. Abundances of macrozooplankton across different treatments and sampling times.

Species	Sampling Day	NC0	BC0	BC0.2	BC0.4	NC0.2	NC0.4	UnNC0	UnBC0.4
Alonella sp.	Day 14	0.2 ± 0.4	1.0 ± 2.0	0.3 ± 0.7	1.1 ± 1.4	1.2 ± 1.4	0.1 ± 0.3	0.8 ± 1.3	0.5 ± 1.0
	Day 42	0.1 ± 0.2	0.0 ± 0.0	1.0 ± 1.5	0.6 ± 1.1	2.0 ± 2.9	0.5 ± 0.5	0.1 ± 0.2	1.6 ± 2.1
Calanoida	Day 14	0.1 ± 0.3	0.0 ± 0.1	0.2 ± 0.2	0.0 ± 0.1	0.1 ± 0.2	0.0 ± 0.1	0.0 ± 0.1	0.2 ± 0.2
	Day 42	0.0 ± 0.0	0.1 ± 0.1	0.0 ± 0.0	0.0 ± 0.1	0.0 ± 0.0	0.0 ± 0.0	0.0 ± 0.1	0.0 ± 0.0
Chydorus sphaericus	Day 14	124.9 ± 69.7	206.1 ± 121.3	87.2 ± 79.7	178.4 ± 98.0	214.4 ± 156.5	129.2 ± 84.0	180.0 ± 101.9	121.2 ± 56.6
	Day 42	93.9 ± 74.9	324.8 ± 158.5	405.6 ± 311.7	211.2 ± 112.7	176.6 ± 101.7	201.8 ± 110.2	145.9 ± 73.6	246.1 ± 197.3
Cyclopoida	Day 14	12.9 ± 7.4	18.0 ± 29.9	1.9 ± 1.2	8.7 ± 10.5	11.8 ± 10.6	4.7 ± 3.8	8.4 ± 7.1	8.1 ± 4.1
	Day 42	5.7 ± 5.6	7.8 ± 9.6	34.4 ± 34.2	9.4 ± 6.5	7.6 ± 6.6	15.1 ± 19.6	8.4 ± 11.9	26.5 ± 33.1
Daphnia pulex	Day 14	15.8 ± 16.3	47.1 ± 40.0	48.8 ± 48.8	84.4 ± 72.1	57.0 ± 37.7	95.5 ± 71.3	49.9 ± 40.9	66.0 ± 44.7
	Day 42	1.6 ± 2.2	51.6 ± 67.1	23.0 ± 22.6	1.4 ± 1.8	33.1 ± 62.8	27.1 ± 24.1	27.0 ± 34.6	16.5 ± 27.9
Daphnia magna	Day 14	0.1 ± 0.3	0.0 ± 0.0	0.0 ± 0.0	0.1 ± 0.3	0.0 ± 0.0	0.3 ± 0.6	0.0 ± 0.0	0.0 ± 0.0
	Day 42	0.0 ± 0.0	0.0 ± 0.0	0.0 ± 0.0	0.0 ± 0.0	0.0 ± 0.0	0.0 ± 0.0	0.0 ± 0.0	0.0 ± 0.0
Daphnia longispina	Day 14	61.1 ± 72.6	40.2 ± 36.6	78.5 ± 21.2	32.3 ± 18.2	98.8 ± 88.7	92.2 ± 56.5	18.9 ± 14.9	46.2 ± 26.4
	Day 42	0.3 ± 0.4	16.0 ± 19.2	10.6 ± 9.6	0.3 ± 0.4	6.5 ± 10.3	14.4 ± 13.8	4.5 ± 9.0	7.4 ± 15.2
Ostracoda	Day 14	0.6 ± 1.0	0.4 ± 0.4	0.2 ± 0.3	1.2 ± 1.9	0.2 ± 0.3	0.6 ± 1.0	0.0 ± 0.0	0.5 ± 0.7
	Day 42	4.7 ± 9.7	2.0 ± 3.2	3.0 ± 3.0	1.6 ± 1.9	5.5 ± 6.8	2.4 ± 5.3	2.4 ± 2.5	0.7 ± 0.8
Simocephalus sp.	Day 14	3.0 ± 5.1	5.9 ± 6.4	1.9 ± 2.8	11.4 ± 19.9	5.7 ± 7.4	3.2 ± 2.7	11.8 ± 14.1	18.0 ± 10.6
	Day 42	4.7 ± 2.5	26.8 ± 34.2	19.1 ± 9.8	8.4 ± 12.5	20.0 ± 31.2	39.5 ± 39.8	20.6 ± 19.3	11.9 ± 16.9

Table S6.7. Abundances of microzooplankton across different treatments and sampling times.

Treatment	Sampling Day	NC0	BC0	BC0.2	BC0.4	NC0.2	NC0.4	UnNC0	UnBC0.4
Anureopsis fissa	Day 14	0.0 ± 0.0	13.0 ± 23.1	0.0 ± 0.0	0.0 ± 0.0	0.0 ± 0.0	1.8 ± 4.1	2.1 ± 4.7	0.0 ± 0.0
	Day 42	329.4 ± 736.7	10.8 ± 11.2	6.9 ± 10.9	189.8 ± 415.3	0.0 ± 0.0	7.5 ± 16.7	47.8 ± 101.3	82.3 ± 102.8
Ascomorpha sp.	Day 14	15.1 ± 24.0	45.9 ± 93.6	1.2 ± 2.8	1.9 ± 4.3	1.8 ± 3.9	1.8 ± 3.9	5.9 ± 9.3	6.2 ± 13.9
	Day 42	14.6 ± 19.5	14.4 ± 12.4	5.2 ± 7.5	1.4 ± 3.1	1.7 ± 3.7	0.0 ± 0.0	14.9 ± 13.9	0.0 ± 0.0
Asplanchna sp.	Day 14	0.0 ± 0.0	0.0 ± 0.0	0.0 ± 0.0	1.4 ± 3.0	0.0 ± 0.0	0.0 ± 0.0	0.0 ± 0.0	0.0 ± 0.0
	Day 42	0.0 ± 0.0	0.0 ± 0.0	0.0 ± 0.0	0.0 ± 0.0	0.0 ± 0.0	0.0 ± 0.0	0.0 ± 0.0	0.0 ± 0.0
Brachionus angularis	Day 14	0.0 ± 0.0	29.2 ± 60.4	0.0 ± 0.0	1.9 ± 4.1	0.0 ± 0.0	0.0 ± 0.0	0.0 ± 0.0	0.0 ± 0.0
	Day 42	81.7 ± 182.6	0.0 ± 0.0	0.0 ± 0.0	0.0 ± 0.0	0.0 ± 0.0	0.0 ± 0.0	0.0 ± 0.0	0.0 ± 0.0
Cephalodella sp.	Day 14	2.3 ± 5.1	7.7 ± 13.2	10.0 ± 19.0	7.8 ± 10.7	1.8 ± 3.9	7.2 ± 11.8	8.7 ± 14.3	2.1 ± 4.6
	Day 42	2.6 ± 3.6	0.0 ± 0.0	0.0 ± 0.0	0.0 ± 0.0	1.7 ± 3.7	1.9 ± 4.3	2.1 ± 4.7	4.4 ± 9.7
Colurella spec.	Day 14	5.2 ± 11.7	35.0 ± 33.3	5.8 ± 13.0	4.6 ± 6.5	0.0 ± 0.0	2.7 ± 6.1	4.5 ± 6.4	9.3 ± 12.7
	Day 42	6.9 ± 8.7	0.0 ± 0.0	0.0 ± 0.0	4.8 ± 6.7	0.0 ± 0.0	3.7 ± 8.4	0.0 ± 0.0	0.0 ± 0.0
Euchlanis dilatata	Day 14	3.5 ± 7.8	11.0 ± 15.2	2.9 ± 6.5	4.4 ± 6.3	5.3 ± 11.8	8.5 ± 14.7	0.0 ± 0.0	2.9 ± 6.6
	Day 42	0.0 ± 0.0	0.0 ± 0.0	25.9 ± 50.7	41.4 ± 92.6	0.0 ± 0.0	10.0 ± 18.9	0.0 ± 0.0	0.0 ± 0.0
Hexarthra sp.	Day 14	0.0 ± 0.0	0.0 ± 0.0	0.0 ± 0.0	0.0 ± 0.0	1.3 ± 2.9	0.0 ± 0.0	0.0 ± 0.0	0.0 ± 0.0
	Day 42	0.0 ± 0.0	0.0 ± 0.0	0.0 ± 0.0	0.0 ± 0.0	2.8 ± 6.3	0.0 ± 0.0	0.0 ± 0.0	0.0 ± 0.0
Keratella cochlearis	Day 14	0.0 ± 0.0	3.0 ± 6.8	0.0 ± 0.0	0.0 ± 0.0	0.0 ± 0.0	0.0 ± 0.0	0.0 ± 0.0	0.0 ± 0.0
	Day 42	0.0 ± 0.0	0.0 ± 0.0	0.0 ± 0.0	0.0 ± 0.0	0.0 ± 0.0	0.0 ± 0.0	0.0 ± 0.0	0.0 ± 0.0
Keratella quadrata	Day 14	85.4 ± 150.8	650.5 ± 1450	40.6 ± 36.0	52.7 ± 57.0	392.9 ± 347.3	58.9 ± 72.8	6.4 ± 9.0	34.8 ± 53.0
	Day 42	12.7 ± 16.7	45.4 ± 78.0	21.2 ± 40.9	1.4 ± 3.1	3.6 ± 4.9	0.0 ± 0.0	29.4 ± 42.9	12.9 ± 23.2
Lecane gr. luna	Day 14	0.0 ± 0.0	7.6 ± 17.0	4.4 ± 9.8	8.7 ± 9.2	1.5 ± 3.4	4.5 ± 6.4	6.0 ± 8.2	6.2 ± 13.9
	Day 42	0.0 ± 0.0	0.0 ± 0.0	0.0 ± 0.0	1.4 ± 3.1	0.0 ± 0.0	6.8 ± 15.2	0.0 ± 0.0	0.0 ± 0.0
	Day 14	25.9 ± 40.1	19.4 ± 25.3	10.2 ± 8.1	8.6 ± 19.1	4.5 ± 4.1	4.8 ± 4.5	10.4 ± 9.8	6.8 ± 6.8

Lecane gr. lunaris	Day 42	35.2 ± 35.2	25.6 ± 27.3	1.3 ± 3.0	3.5 ± 4.9	5.8 ± 12.9	11.1 ± 15.5	8.8 ± 8.9	139.5 ± 311.8
Lepadella patella	Day 14	17.7 ± 19.3	76.7 ± 91.0	17.3 ± 27.5	21.4 ± 10.3	10.2 ± 14.5	6.8 ± 15.2	16.4 ± 11.7	14.5 ± 16.0
	Day 42	6.7 ± 11.6	13.2 ± 13.8	10.0 ± 17.4	51.5 ± 77.3	5.5 ± 8.5	3.7 ± 8.4	5.9 ± 8.6	161.2 ± 360.6
Mytilina mucronata	Day 14	0.0 ± 0.0	0.0 ± 0.0	1.5 ± 3.3	0.0 ± 0.0	0.0 ± 0.0	0.0 ± 0.0	0.0 ± 0.0	0.0 ± 0.0
	Day 42	1.3 ± 2.8	0.0 ± 0.0	0.0 ± 0.0	0.0 ± 0.0	0.0 ± 0.0	3.7 ± 8.4	0.0 ± 0.0	0.0 ± 0.0
Mytilina ventralis	Day 14	0.0 ± 0.0	1.5 ± 3.4	3.9 ± 5.7	0.0 ± 0.0	0.0 ± 0.0	0.0 ± 0.0	1.6 ± 3.7	0.0 ± 0.0
	Day 42	0.0 ± 0.0	0.0 ± 0.0	0.0 ± 0.0	0.0 ± 0.0	0.0 ± 0.0	0.0 ± 0.0	0.0 ± 0.0	0.0 ± 0.0
Polyarthra remata	Day 14	5.0 ± 7.7	91.5 ± 200.1	2.1 ± 4.8	6.4 ± 14.4	9.6 ± 14.7	0.0 ± 0.0	0.0 ± 0.0	0.0 ± 0.0
	Day 42	25.9 ± 57.8	1.9 ± 4.2	0.0 ± 0.0	0.0 ± 0.0	8.5 ± 12.6	0.0 ± 0.0	86.3 ± 160.2	3.2 ± 4.4
Rhinoglena sp.	Day 14	0.0 ± 0.0	0.0 ± 0.0	0.0 ± 0.0	0.0 ± 0.0	0.0 ± 0.0	0.0 ± 0.0	0.0 ± 0.0	1.5 ± 3.3
	Day 42	0.0 ± 0.0	0.0 ± 0.0	0.0 ± 0.0	0.0 ± 0.0	0.0 ± 0.0	0.0 ± 0.0	0.0 ± 0.0	0.0 ± 0.0
Synchaeta sp	Day 14	0.0 ± 0.0	20.6 ± 39.9	1.7 ± 3.8	0.0 ± 0.0	0.0 ± 0.0	0.0 ± 0.0	0.0 ± 0.0	0.0 ± 0.0
	Day 42	0.0 ± 0.0	0.0 ± 0.0	0.0 ± 0.0	8.3 ± 18.5	0.0 ± 0.0	0.0 ± 0.0	0.0 ± 0.0	0.0 ± 0.0
Tichocerca gr. similis	Day 14	8.4 ± 12.1	10.3 ± 14.5	0.0 ± 0.0	3.9 ± 8.6	1.8 ± 3.9	1.7 ± 3.8	3.2 ± 4.4	0.0 ± 0.0
	Day 42	14.1 ± 20.3	49.0 ± 103.0	10.0 ± 13.6	11.1 ± 11.9	3.8 ± 8.6	24.1 ± 20.8	22.2 ± 27.2	11.1 ± 12.5
Trichocerca gr. porcellus	Day 14	5.4 ± 7.9	10.9 ± 14.5	3.4 ± 7.6	1.4 ± 3.0	1.8 ± 3.9	0.0 ± 0.0	1.6 ± 3.7	5.2 ± 4.9
	Day 42	71.5 ± 156.4	172.0 ± 322.6	17.7 ± 20.4	5.1 ± 8.2	7.4 ± 12.5	0.0 ± 0.0	58.1 ± 97.8	4.9 ± 7.0
Trichocerca longiseta	Day 14	0.0 ± 0.0	0.0 ± 0.0	1.2 ± 2.8	0.0 ± 0.0	0.0 ± 0.0	0.0 ± 0.0	0.0 ± 0.0	0.0 ± 0.0
	Day 42	0.0 ± 0.0	0.0 ± 0.0	0.0 ± 0.0	0.0 ± 0.0	8.5 ± 19.0	0.0 ± 0.0	0.0 ± 0.0	0.0 ± 0.0
Trichotria pocillum	Day 14	2.3 ± 5.1	6.2 ± 10.0	1.5 ± 3.3	4.4 ± 6.3	0.0 ± 0.0	1.4 ± 3.0	0.0 ± 0.0	0.0 ± 0.0
	Day 42	0.0 ± 0.0	0.0 ± 0.0	0.0 ± 0.0	0.0 ± 0.0	0.0 ± 0.0	0.0 ± 0.0	0.0 ± 0.0	2.2 ± 4.9
Nauplii	Day 14	239.3 ± 181.8	323.8 ± 289.0	218.7 ± 161.2	185.6 ± 94.3	331.6 ± 173.8	229.8 ± 217.7	165.9 ± 101.9	296.8 ± 159.4
	Day 42	61.1 ± 51.6	471.3 ± 500.1	188.1 ± 155.2	122.8 ± 34.8	154.9 ± 57.1	454.6 ± 350.2	292.4 ± 160.2	313.6 ± 187.6

Table S6.8. Functions of bacterial taxa as predicted using FAPROTAX

Phylum	Genus	Functional ASV number	Water		Sediment		Function1	Function2	Function3
			Day 14	Day 42	Day 14	Day 42			
Actinobacteriota	*Terrabacter*	1 (1)[a]			Detected		aerobic_ chemoheterotrop	chemo-heterotrophy	
Actinobacteriota	*Mycobacterium*	13 (13)		Detected	Detected		aerobic_ chemoheterotrop	chemo-heterotrophy	
Actinobacteriota	*Nocardioides*	8 (8)			Detected		aerobic_ chemoheterotrop	chemo-heterotrophy	aromatic_comp ound_degradati
Actinobacteriota	*Streptomyces*	11 (11)			Detected		aerobic_ chemoheterotrop	chemo-heterotrophy	
Bacteroidota	*Flavobacterium*	62 (63)	Detected	Detected			aerobic_ chemoheterotrop	chemo-heterotrophy	
Bacteroidota	*Pedobacter*	23 (23)	Detected			Detected	aerobic_ chemoheterotrop	chemo-heterotrophy	
Cyanobacteria	*Cyanobium*_PCC-6307	33 (34)		Detected	Detected		oxygenic_ photoautotrophy	photosynthetic_ cyanobacteria	
Firmicutes	*Bacillus*	2 (66)			Detected		manganese_ oxidation		
Firmicutes	*Geobacillus*	5 (5)			Detected		aerobic_ chemoheterotrop	chemo-heterotrophy	
Firmicutes	*Listeria*	1 (1)				Detected	Chemo-heterotrophy		
Firmicutes	*Paenibacillus*	13 (13)			Detected		aerobic_ chemoheterotrop	chemo-heterotrophy	
Firmicutes	*Thermobacillus*	8 (8)			Detected		xylanolysis	chemo-heterotrophy	
Proteobacteria	*Bradyrhizobium*	1 (1)			Detected		aerobic_ chemoheterotrop	chemo-heterotrophy	nitrogen_fixatio n
Proteobacteria	*Methylotenera*	6 (6)		Detected			methanol_ oxidation	chemo-heterotrophy	methylotrophy
Proteobacteria	*Sphingomonas*	15 (15)			Detected	Detected	aerobic_ chemoheterotrop	chemo-heterotrophy	
Verrucomicrobiota	*Verrucomicrobiaceae*_unidentified	34 (34)			Detected		aerobic_ chemoheterotrop	chemo-heterotrophy	

* Values are shown as n (N), where N is the total number of ASVs detected for the genus in this study, and n is the number of those ASVs assigned to the listed function(s) by FAPROTAX.

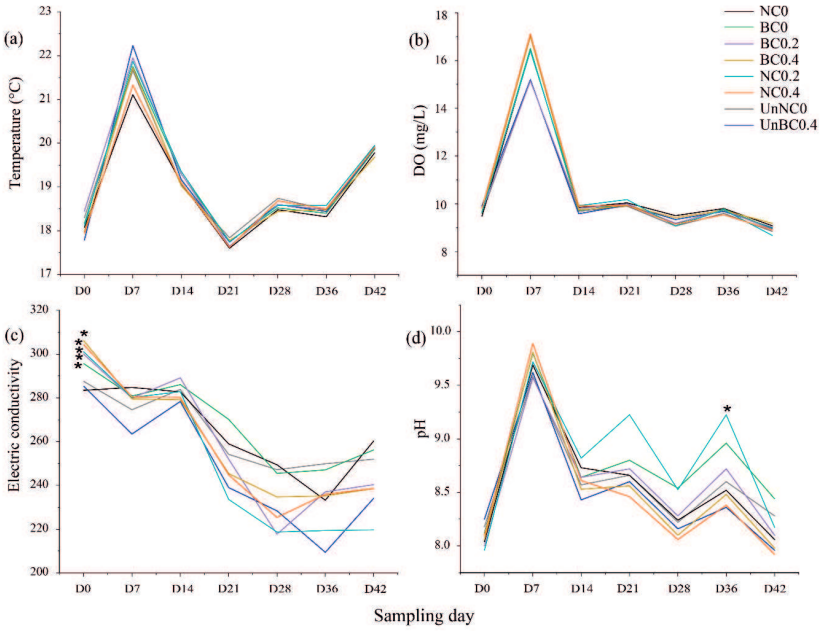


Figure S6.1. Concentrations of weekly measured water parameters: (a) temperature (°C), (b) dissolved oxygen (DO, mg/L), (c) electrical conductivity (EC, μS/cm), and (d) pH. An asterisk (*) indicates a significant difference between a treatment group and the control ($p \leqslant 0.05$).

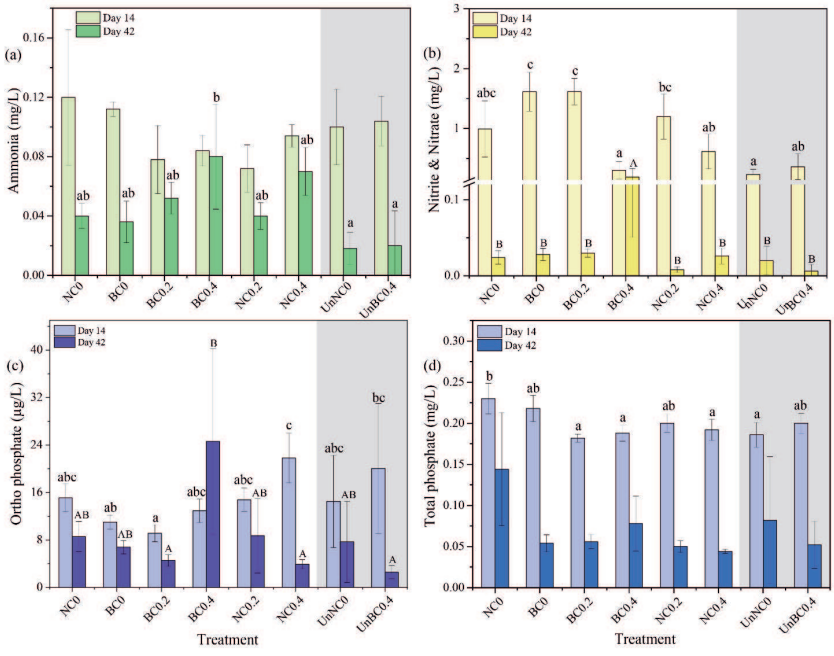


Figure S6.2. Nutrient concentrations in each treatment measured on Days 14 and 42: (a) ammonia (mg/L), (b) nitrite and nitrate (mg/L), (c) orthophosphate (μg/L), and (d) total phosphorus (mg/L). Different letters (a, b, c) denote significant differences among treatments according to Duncan's multiple range test ($p \leqslant 0.05$). The grey shaded area represents the unspiked groups.

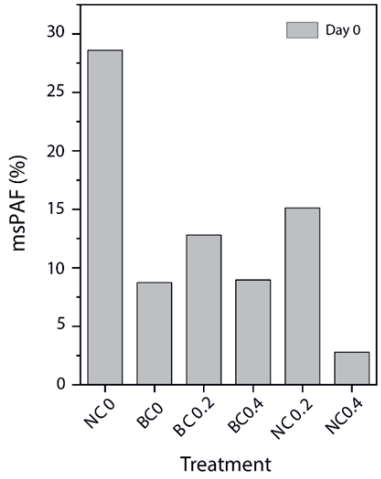


Figure S6.3. msPAF value of all treatments on Day 0.

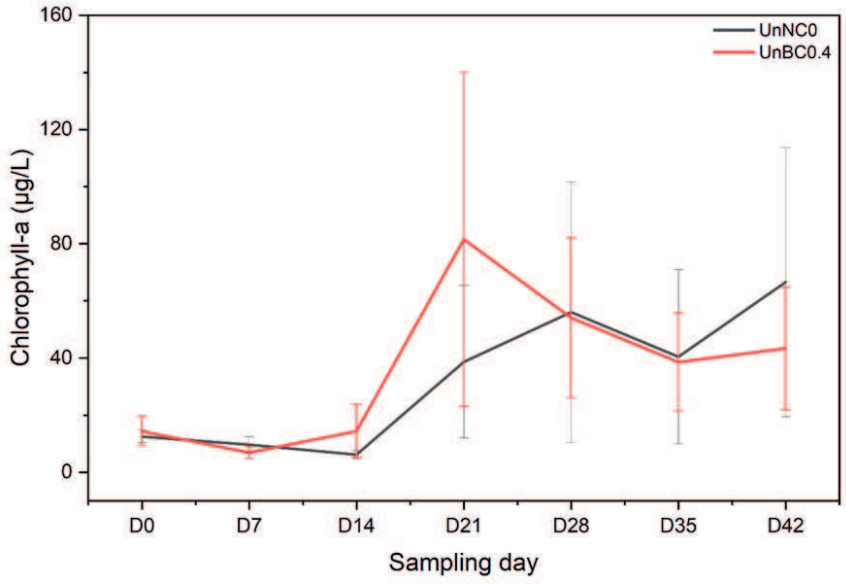


Figure S6.4. Chlorophyll-a concentrations in UnNC0 and UnBC0.4. No significant differences were detected between the two groups at any sampling time.

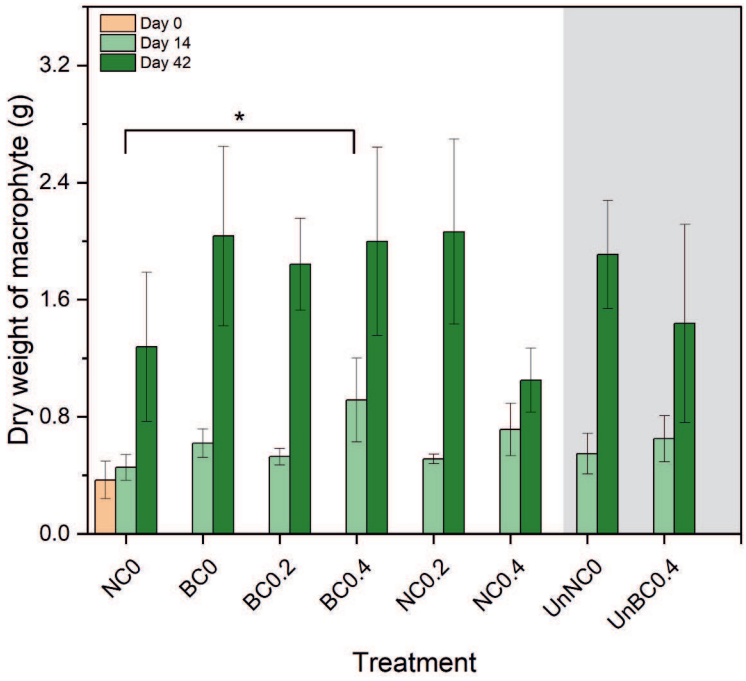


Figure S6.5. Dry biomass (g) of macrophytes in each treatment group. Asterisks (*) indicate significant differences compared to the control group (NC0) ($P < 0.05$). The grey shaded area represents the unspiked groups.

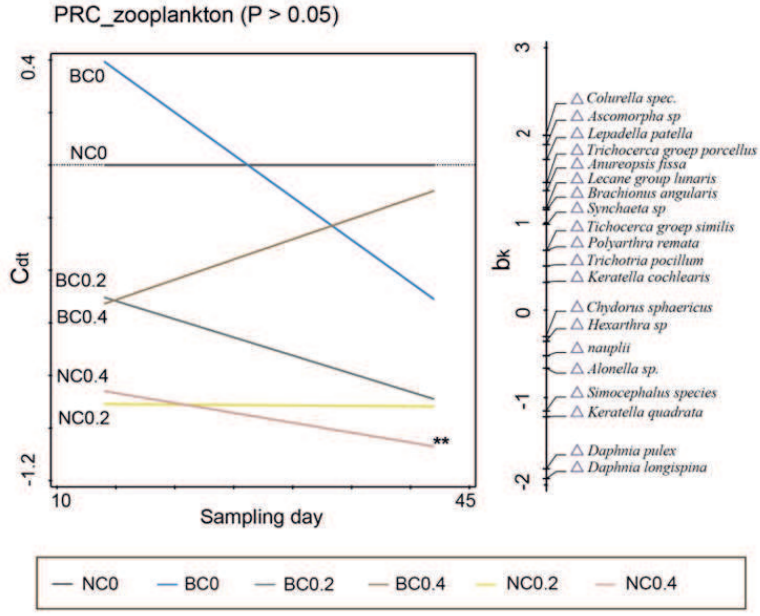


Figure S6.6. Principal Response Curve (PRC) showing temporal changes in zooplankton community structure relative to the control group (NC0). Asterisks (**) indicate significant differences from the control at the corresponding time point ($P < 0.01$). bk values represent species weights, and the top 20 taxa with the highest weights are displayed.

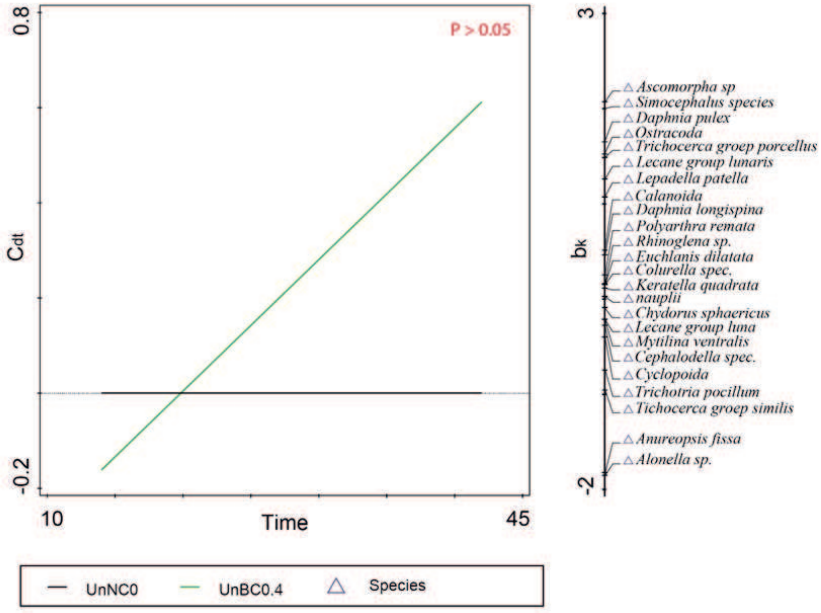


Figure S6.7. PRC showing temporal changes in zooplankton community structure between the unspiked groups. No significant differences were observed between UnNC0 and UnBC0.4, either in overall community structure or at individual time points.

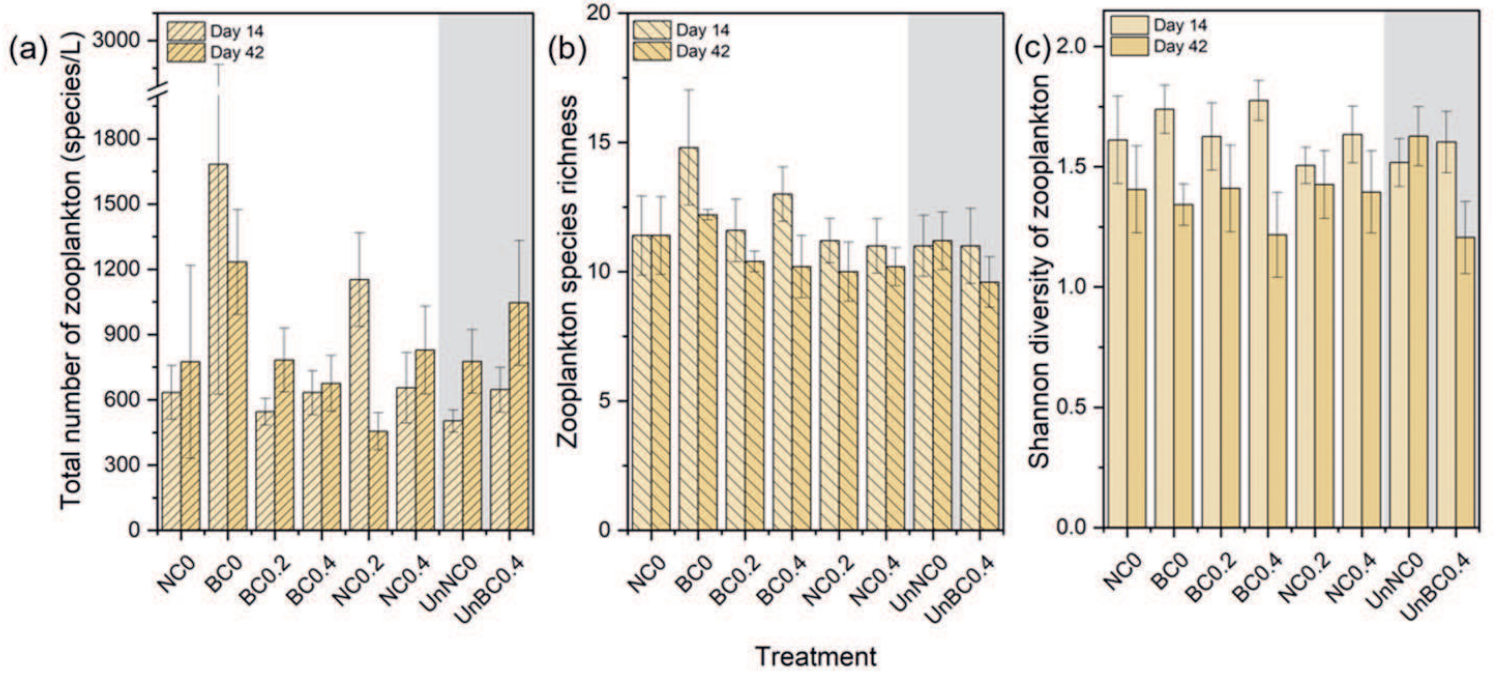


Figure S6.8. Bar plots showing zooplankton abundance and diversity indices: (a) total abundance (individuals/L), (b) species richness, and (c) Shannon diversity index. No significant differences were observed among the treatment groups. The grey shaded area represents the unspiked groups.

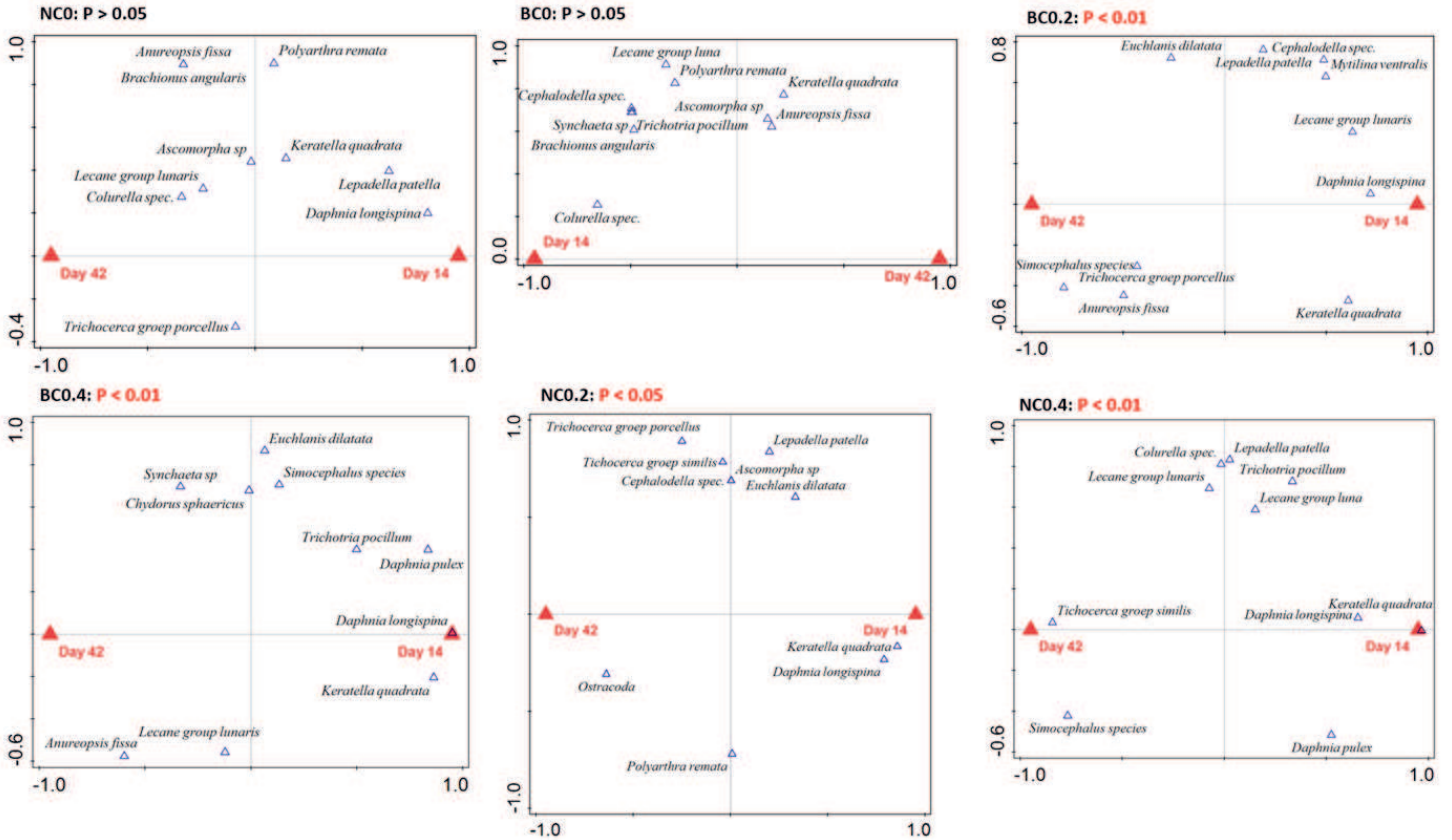


Figure S6.9. RDA plots showing the differences in zooplankton community composition between Day 14 and Day 42. For each treatment, only the 10 most abundant taxa are displayed. P < 0.05 indicates a significant difference in community structure between the two sampling days. Red triangles represent the centroids of replicate samples for each treatment group.

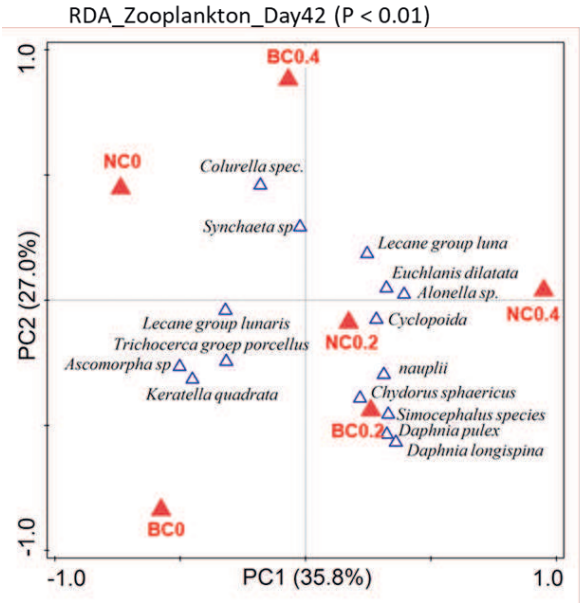


Figure S6.10. The RDA plot shows significant differences in zooplankton community composition among treatments on Day 42 (P < 0.01). Red triangles represent the centroids of replicate samples for each treatment group. Percentages at the axis titles indicate the percentage of variation in the species data explained.

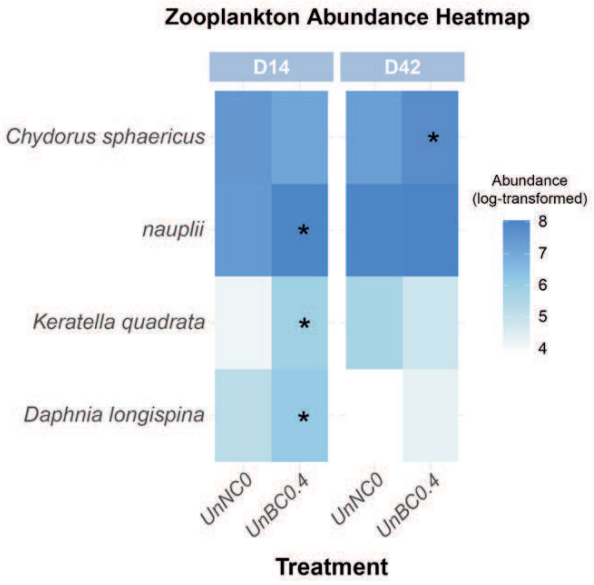


Figure S6.11. Heatmap showing the abundance of zooplankton species (data were ln(10x+1)-transformed) in the unspiked groups. Asterisks (*) denote significant differences in abundance compared to the UnNC0 group at the corresponding time point (P < 0.05).

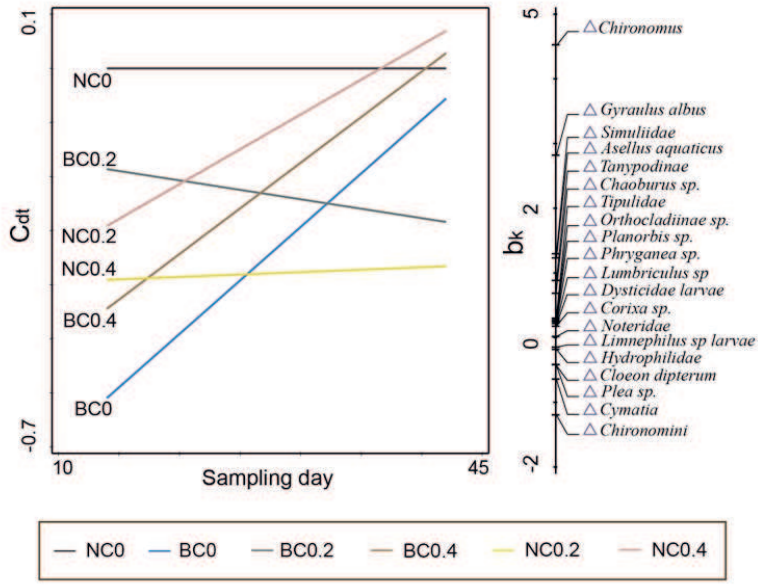


Figure S6.12. PRC showing temporal changes in macroinvertebrate community structures between spiked treatment groups and the control (NC0). No significant differences were observed. bk values represent the species weights of individual benthic macroinvertebrates.

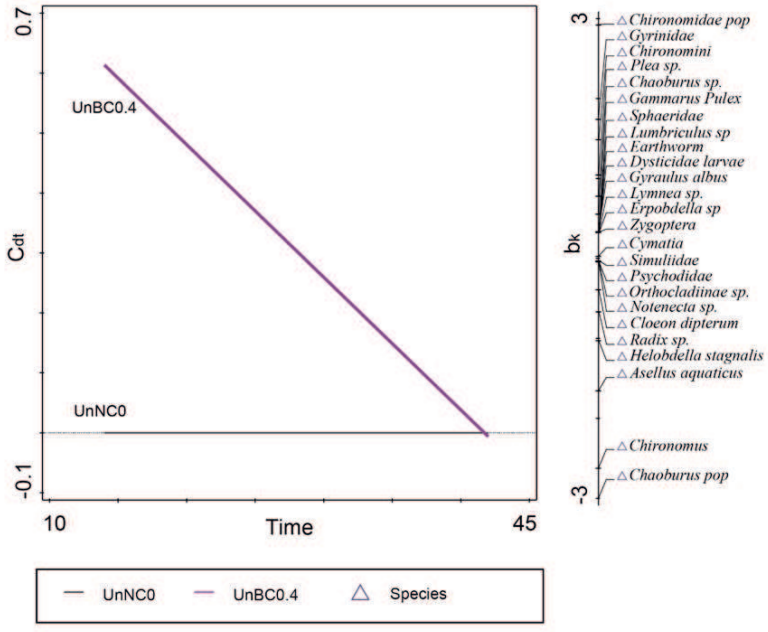


Figure S6.13. PRC showing temporal changes in macroinvertebrate community structures between UnNc0 and UnBC0.4. No significant differences were observed ($P > 0.05$). bk values represent the species weights of individual benthic macroinvertebrates.

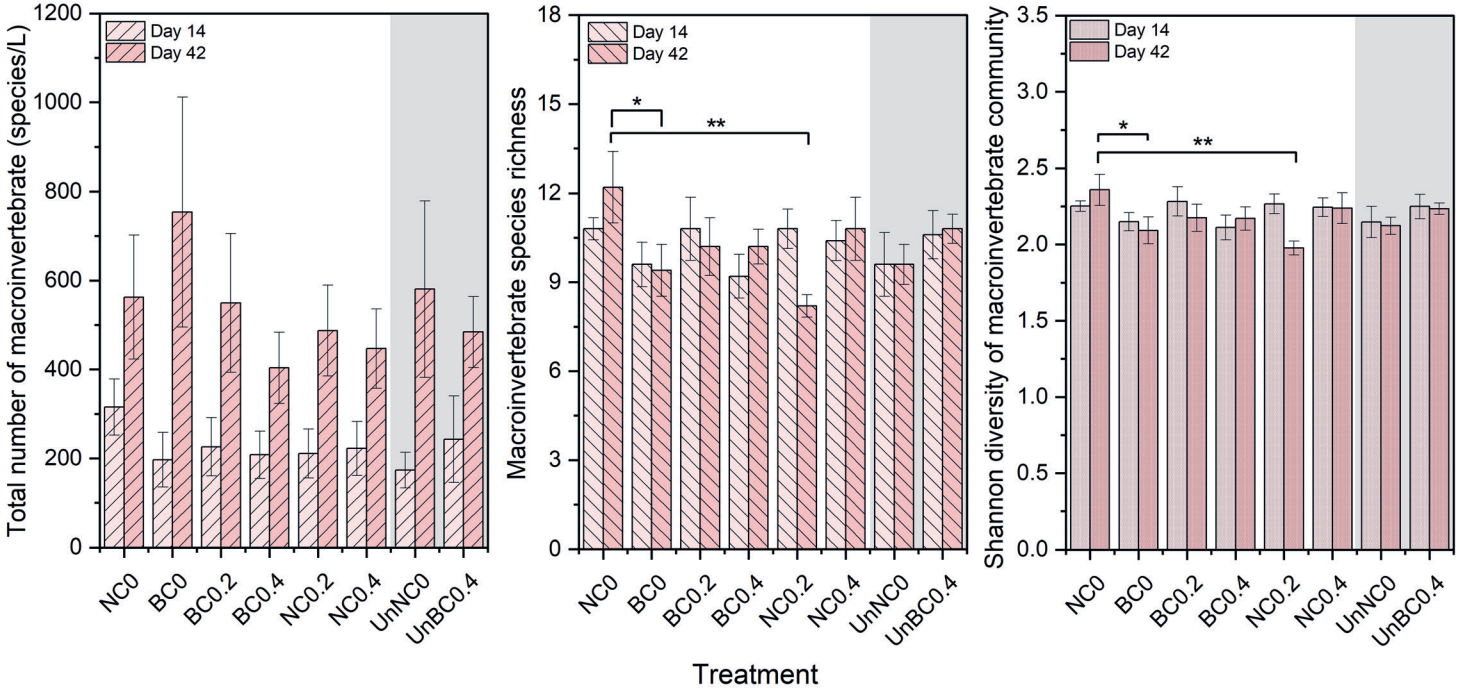


Figure S6.14. Abundance and diversity metrics of benthic macroinvertebrates across treatment groups: (a) total abundance (individuals/L), with no significant differences among groups; (b) species richness, where * indicates $P < 0.05$ and ** indicates $P < 0.01$; (c) Shannon diversity index, where * indicates $P < 0.05$ and ** indicates $P < 0.01$. The grey shaded area represents the unspiked groups.

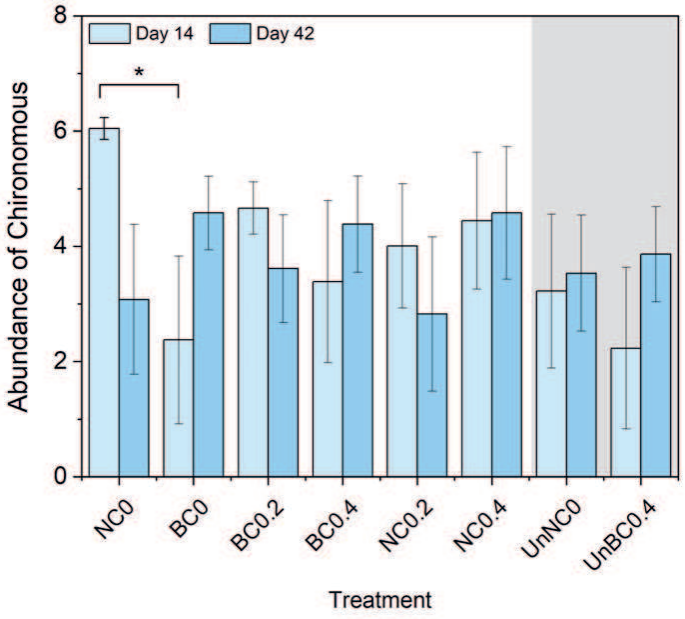


Figure S6.15. Abundance of Chironomus across treatment groups (data was ln(2x+1)-transformed). * indicates a significant difference compared to the control group ($P < 0.05$). The grey shaded area represents the unspiked groups.

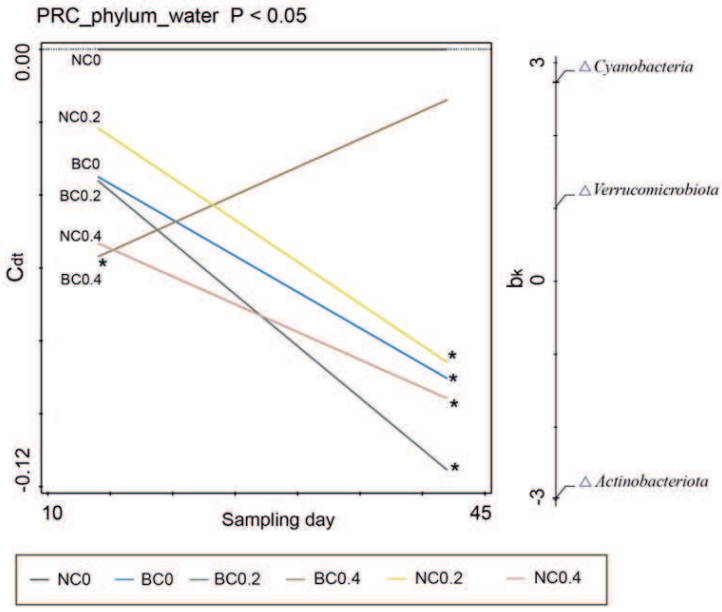


Figure S6.16. PRC showing significant temporal changes ($P < 0.05$) in microbial community structure at the phylum level in the water column of treatment groups compared to the control (NC0). Asterisks (*) indicate significant differences from the control at each time point. bk values represent the species weights of individual taxa; values within the range of -1 to 1 are not shown.

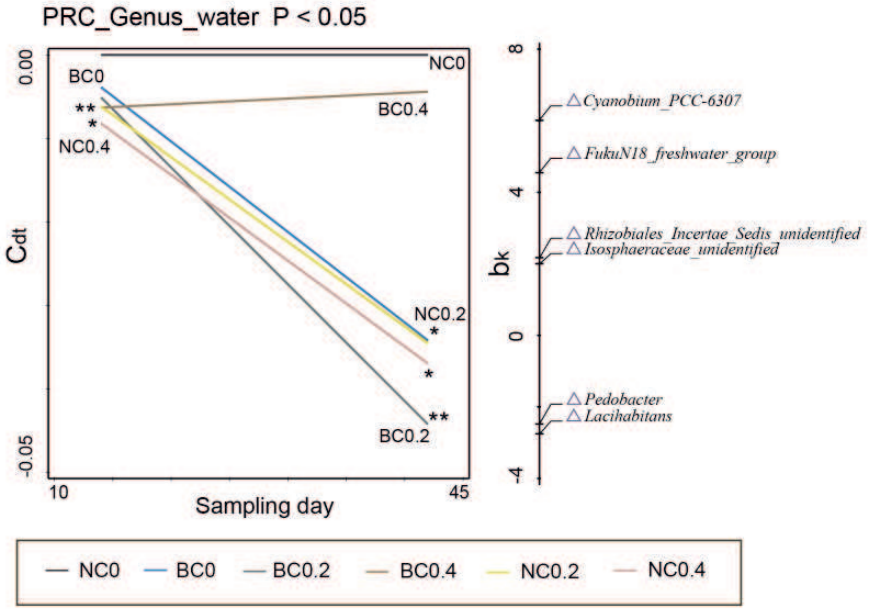


Figure S6.17. PRC showing significant temporal changes (P < 0.05) in microbial community structure at the genus level in the water column of treatment groups compared to the control (NC0). Asterisks (*) indicate significant differences from the control at each time point. bk values represent the species weights of individual genera; values within the range of -1 to 1 are not shown.

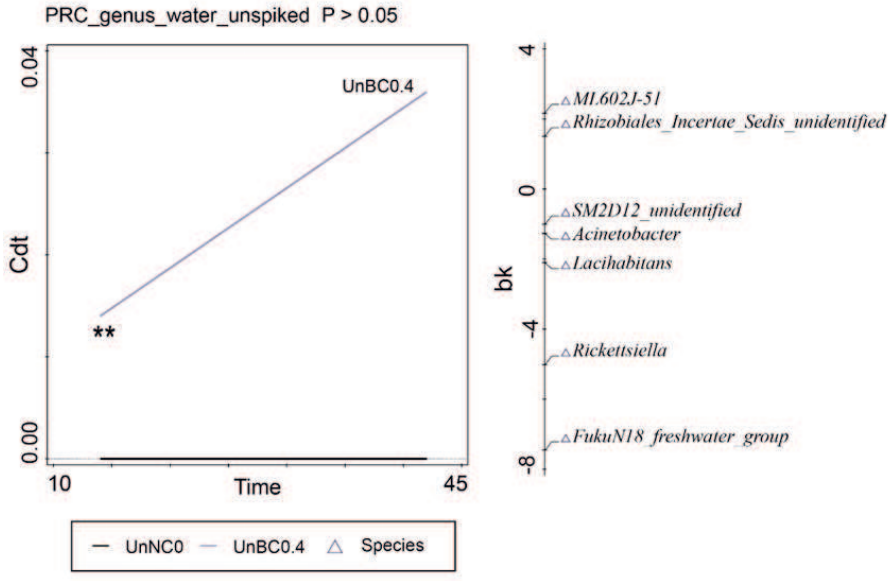


Figure S18. PRC showing temporal changes in microbial community structure at the genus level in the water column of the unspiked groups (UnNC0 and UnBC0.4). Asterisks (*) indicate significant differences from the control at the time point. bk values represent the species weights of individual genera; values within the range of -1 to 1 are not shown.

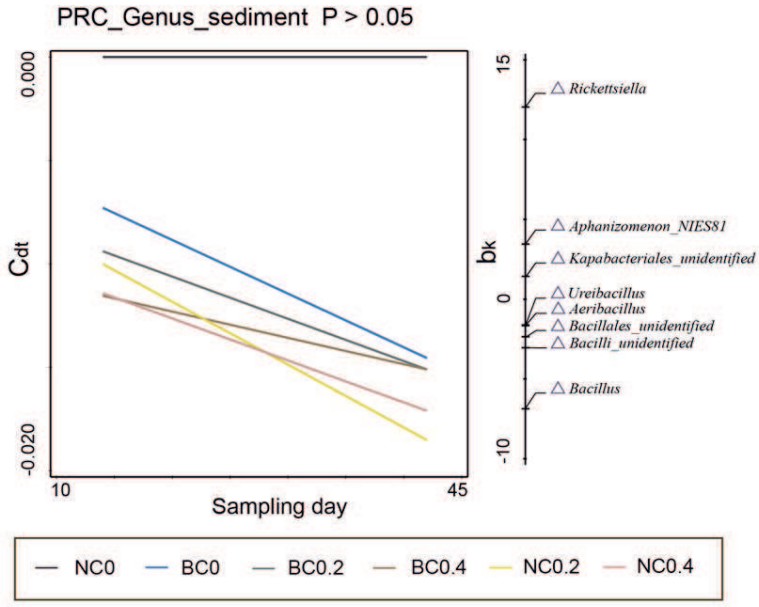


Figure S6.19. PRC showing temporal changes in microbial community structure at the genus level in sediment samples of treatment groups compared to the control (NC0). No significant shifts were observed. bk values represent the species weights of individual taxa; values within the range of -1 to 1 are not shown.

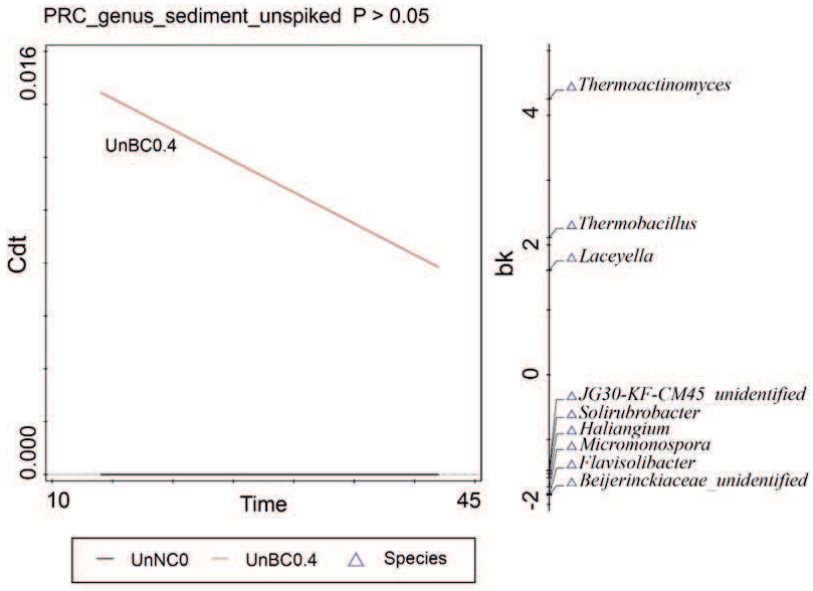


Figure S20. PRC showing temporal changes in microbial community structure at the genus level in the sediment of the unspiked groups (UnNC0 and UnBC0.4). There were no significant differences between two groups at any time point (P > 0.05). bk values represent the species weights of individual genera; values within the range of -1 to 1 are not shown.

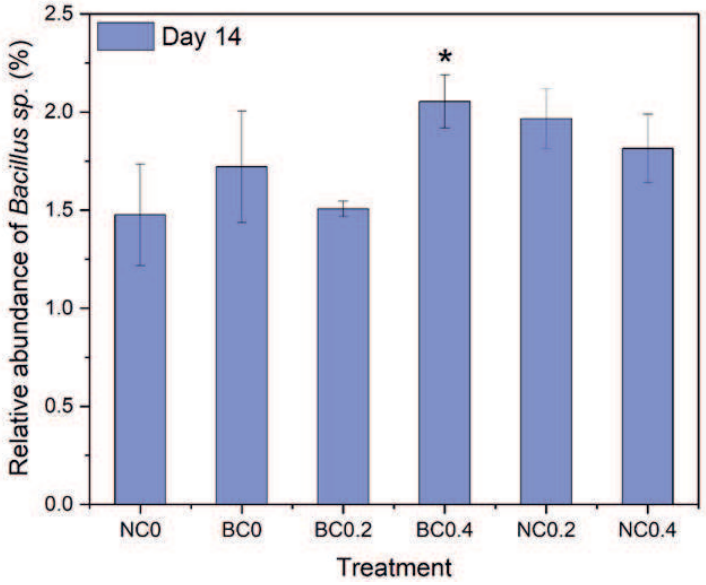


Figure S6.21. Relative abundance of Bacillus sp. predicted to have manganese-degradation potential across treatment groups. FAPROTAX was used for functional prediction. Asterisks (*) indicate significant differences compared to the control group (NC0) ($P < 0.05$).

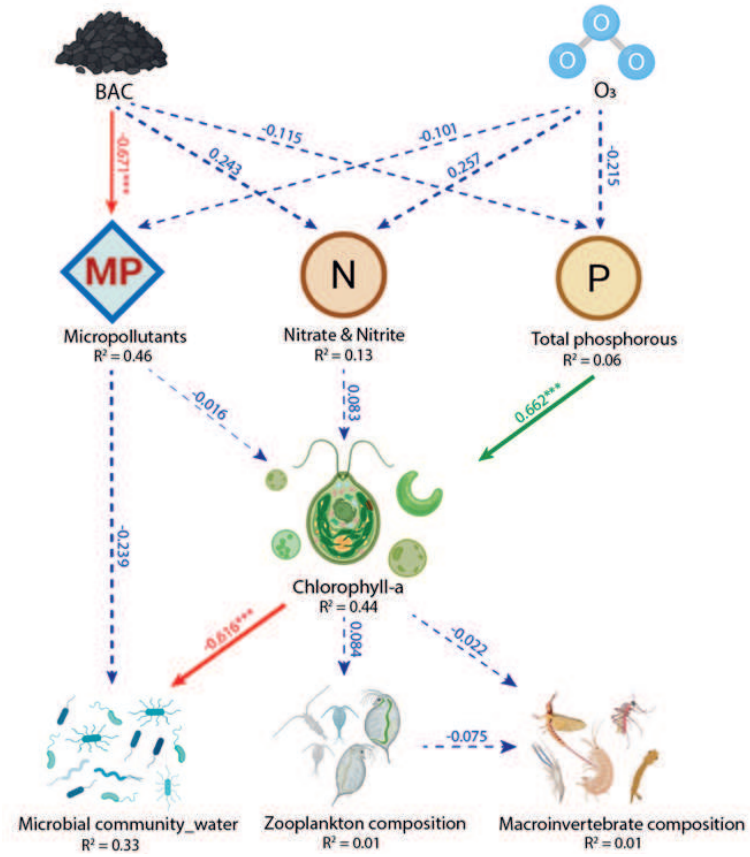


Figure S6.22. Structural equation model (SEM) illustrating the integrated ecological pathways associated with effluent treatments on Day 42. Red solid lines represent significant negative paths, green solid lines represent significant positive paths, anSd dashed lines indicate non-significant paths. Numbers on the arrows indicate standardized path coefficients (β). Sediment microbial community metrics were not included because they explained little additional variance in the network. R^2 values indicate the proportion of variance explained for each response variable. The model showed an acceptable overall fit ($\chi^2 = 24.82$, df = 20, p = 0.21).

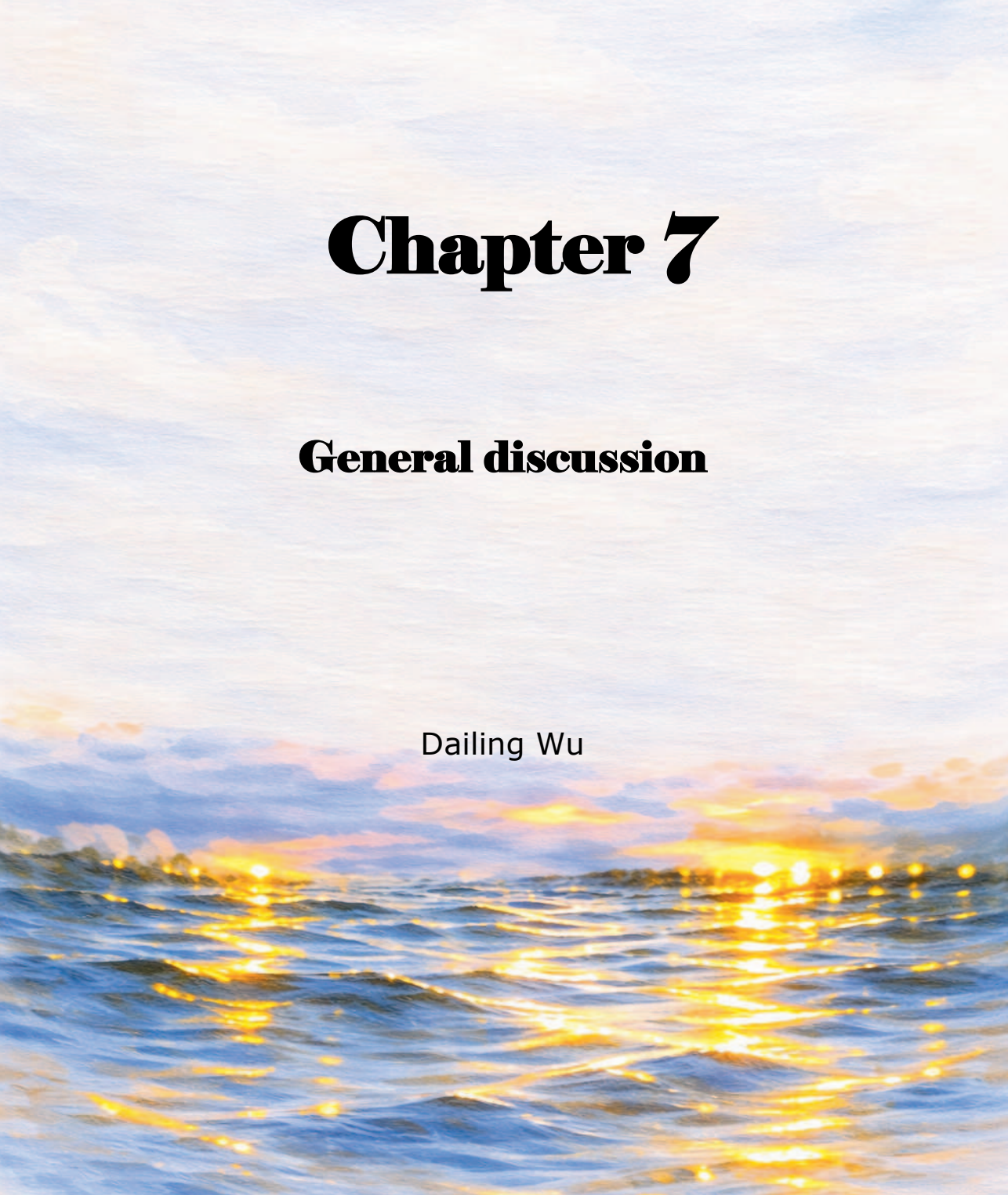


Campus, Wageningen

Chapter 7

General discussion

Dailing Wu



Heaven is under our feet as well as over our heads.

— Henry David Thorea

7.1 Overview

Antimicrobials are extensively used in human and veterinary medicines and in consumer products, and they are continuously introduced into freshwater environments through wastewater-related pathways. Consequently, antimicrobials are typically present at low concentrations but as complex mixtures, giving rise to chronic exposure scenarios rather than isolated contamination events. Beyond potential direct toxicity, such exposure can exert sustained pressure on microbial community composition, alter food-web interactions, and modify key ecosystem processes. Because freshwater systems are simultaneously influenced by effluent inputs, catchment-specific background conditions, and hydrological variability, neither the exposure patterns nor the ecological consequences of antimicrobials can be adequately characterized by studies focusing on a single environmental compartment or a single biological endpoint.

This thesis combined field monitoring and a series of controlled experiments to address antimicrobial impacts across scales, from environmental occurrence and associated risks to community- and food-web-level responses. Field monitoring first characterized occurrence patterns across river water, sediments, and groundwater, evaluated risks to aquatic ecosystems and the potential for antimicrobial-resistance selection, and applied source-tracking analyses to estimate river-to-groundwater contributions to antibiotic resistance in groundwater (**Chapter 2**). Controlled indoor microcosm experiments then evaluated how single-compound and mixture exposures affect the structure of aquatic communities and functional processes, and to what extent these responses depend on the environmental context (**Chapters 3** and **4**). A simplified freshwater food-chain experiment further quantified internal exposure patterns across trophic levels and evaluated the potential for trophic transfer (**Chapter 5**). Finally, outdoor freshwater microcosms were used to assess the effects of advanced wastewater treatment scenarios on the chemical concentrations of pollutants and their ecological consequences. This has been done by jointly examining micropollutant removal, predicted mixture toxicity, and ecological responses across multiple trophic levels. For the latter, structural equation modelling was applied to disentangle the direct effects of the treatments on ecological responses from indirect pathways mediated by treatment-driven changes in chemical stressors, resources, and nutrients (**Chapter 6**).

Together, these complementary lines of evidence allowed me to address four research questions in an integrated manner, spanning occurrence and exposure (RQ1), ecological responses and context dependence (RQ2), internal exposure and trophic transfer within food chains (RQ3), and the extent to which engineering interventions deliver ecological benefits (RQ4) (**Chapter 1**). Collectively, these questions link exposure characterization, mechanistic understanding, food-web processes, and management evaluation within a

single conceptual framework (Fig. 7.1). Building on the chapter-specific results, in this general discussion, I provide a cross-chapter synthesis that highlights patterns that may be less apparent within individual chapters and discuss their implications for exposure assessment, ecological interpretation, and risk assessment and management.

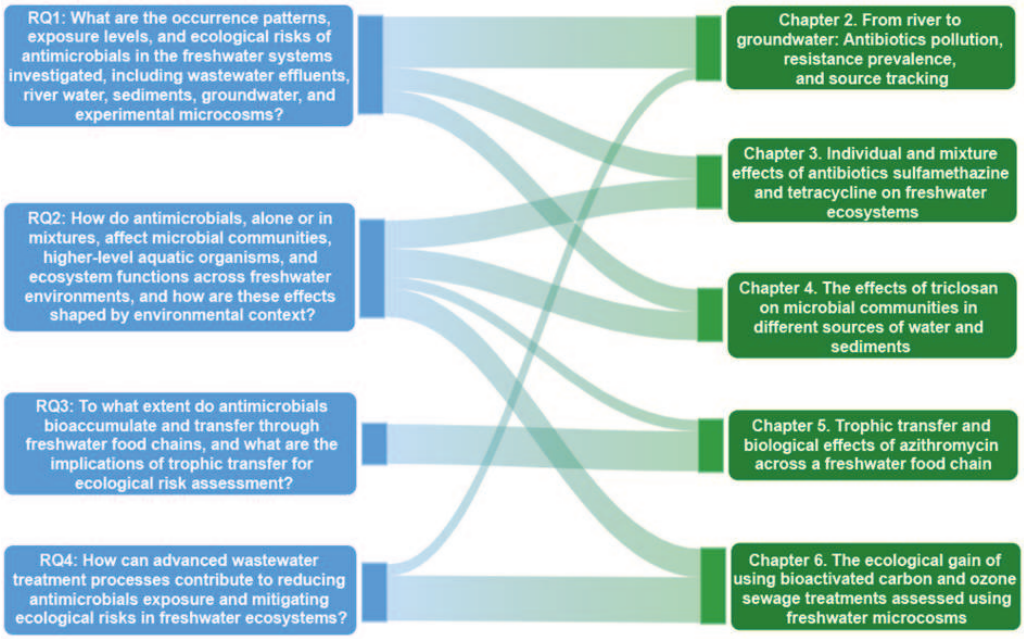


Figure 7.1 Schematic overview linking the four research questions (RQ1–RQ4) to the corresponding thesis chapters.

7.2 From occurrence to exposure pathways: redistribution of antimicrobials across freshwater compartments (RQ1)

In **Chapter 2**, monitoring across river water, river sediments, and groundwater revealed systematic differences in detection profiles and exposure levels. Together, these patterns point to redistribution across freshwater compartments and a clear exposure gradient. River water provides a clear signal of ongoing antimicrobial presence, whereas river sediments act as a retention and enrichment compartment, with many compounds showing a stronger accumulation than in the water column. Groundwater, by contrast, displayed an antimicrobial profile broadly similar to river water but at substantially lower levels, consistent with attenuation during transport and filtration across environmental interfaces. These compartment differences can be explained by compound-specific solid–liquid partitioning

behaviour, whereby variation in distribution coefficients (K_d) shapes whether antimicrobials preferentially remain in the water column or are transferred to and accumulated in the sediment phase (Al-Khazrajy and Boxall, 2016; Zhou and Broodbank, 2014). Microcosm experiments further supported this interpretation by showing that different antimicrobials can have distinct residence times and redistribution dynamics under identical microcosm conditions (**Chapters 3** and **4**). Therefore, characterising occurrence by considering the water column or sediments in isolation may overlook exchange across the water–sediment interface and the role of sediments as a sink; interpreting the interface as a connected system better aligns with the monitoring and experimental evidence presented in this thesis.

This redistribution has important implications for exposure assessment because it can alter the exposure pathways effective for ecological endpoints and the duration of the biologically relevant exposure. When sediments act as an important sink for antimicrobials, a decline in water-phase concentrations does not necessarily imply a synchronous loss of antimicrobial burden from the system. Solid-phase accumulation and potential remobilization can extend the period over which compounds remain present (**Chapters 2–4**). Against this background, inferring risk solely from water-phase concentrations at a single time point is often not robust for protecting aquatic ecosystems. Traditional risk quotient (RQ) approaches based on instantaneous environmental concentrations are also more prone to representation bias when exposure is coupled across compartments and varies over time. This limitation has been highlighted in discussions of pharmaceutical environmental risk assessment frameworks (EMA, 2024). More specifically, calculating RQs directly from total sediment concentrations may overlook bioavailability constraints and thereby overestimate sediment-associated risks, whereas reporting only single-compound RQs may underestimate the pressure associated with long-term mixture exposure across compartments and over time. A more general way forward is to incorporate dose metrics that better reflect bioavailable exposure in sediment risk characterization, such as freely dissolved concentrations or chemical activity. In this context, equilibrium-partitioning concepts and passive sampling may help to estimate freely dissolved concentrations under site-specific physicochemical conditions, supporting bioavailability-informed sediment risk characterization (Mayer et al., 2014). In parallel, mixture-risk assessment and mixture-toxicity frameworks emphasize that ecological responses to mixtures cannot be readily extrapolated from effects observed from single-compounds (**Chapter 3**) (Backhaus and Faust, 2012; Heys et al., 2016). Given that natural freshwater systems are often exposed to numerous co-occurring compounds, such interactions and their ecological implications warrant explicit consideration.

The consequences of redistribution are not confined to river systems but may also extend to groundwater through cross-compartment transport processes. In groundwater, the predicted chemical risks of antimicrobials for resistance selection were generally low,

whereas resistance-related indicators remained pronounced (**Chapter 2**), indicating that resistance-selection risk in groundwater cannot be inferred solely from current water-phase concentrations. Sediments may act as long-term reservoirs that sustain antimicrobial presence and associated selection pressure over extended time scales, and resuspension and remobilization may provide pathways for resistance determinants to propagate across connected compartments (Calero-Cáceres et al., 2017; Heß et al., 2018). Source tracking analyses further showed that resistance determinants in shallow groundwater were more closely associated with river sediments, whereas those in deeper groundwater were more closely linked to river water. This pattern suggests that groundwater resistance backgrounds may partly reflect cross-compartment inputs and propagation rather than being driven exclusively by in situ selection within the groundwater environment. Consequently, understanding ecological risks of antimicrobials in groundwater requires joint consideration of chemical redistribution and the migration of resistance-related elements across environmental compartments in order to understand the apparent paradox of low chemical exposure levels coinciding with pronounced resistance signals.

7.3 Context-dependent antimicrobial effects: multitrophic and functional responses under single and mixture exposures (RQ2)

7.3.1 Effects of single and mixture exposures: non-additive and endpoint-specific responses

In **Chapter 3**, the indoor microcosm experiments showed that mixture effects cannot be reliably inferred from single-compound responses, and that co-exposure often alters the direction and/or magnitude of responses compared with single-compound exposure, in an endpoint- and compartment-specific manner. At the primary producer level, sulfamethazine (SMT) and tetracycline (TC) alone reduced green algal abundance at intermediate to high concentrations, whereas co-exposure did not produce inhibition of comparable magnitude or a consistent direction, indicating non-additive mixture effects. Zooplankton community structure shifted in both the single-compound and the mixture treatments, with taxa showing both stimulatory and adverse responses, suggesting modulation by chemical interactions and food-web feedbacks. Single-compound exposure induced pronounced changes in the microbial community structure in both the water column and the sediment, whereas under co-exposure the water-column community structure did not show significant shifts. This pattern is compatible with antagonistic interactions reported for antimicrobials targeting distinct cellular processes (Brochado et al., 2018). Together, these patterns suggest that, under realistic exposure scenarios, the different antimicrobials in a mixture

may alter the direction and magnitude of effects across trophic levels and compartments, highlighting the limitations of extrapolating community- and process-level outcomes from single-compound evidence.

7.3.2 Endpoint-dependent detection of antimicrobials effects across trophic levels

Across the tested exposure levels and the monitored periods examined in this thesis, antimicrobial-related responses varied markedly among endpoints. Responses were detected more consistently in microbial communities and primary producers, which are directly coupled to the water–sediment matrix and form the base of material cycling and energy flow. In contrast, treatment effects on higher-trophic community-structure metrics (zooplankton and macroinvertebrates) were not consistently detected across experimental systems and time points (**Chapters 3** and **6**). It is worth noting that weak or non-significant higher-trophic structural responses do not necessarily indicate an absence of effects at higher trophic levels and should be interpreted cautiously, as such effects can be indirect or delayed.

At the exposure levels evaluated in **Chapters 3** and **6**, effects on higher consumers are more likely to appear first in individual-level physiology and fitness, whereas pronounced turnover in community composition typically merges only after effects accumulate over time. Individual responses can vary due to differences in life stage, condition, and exposure history. Community-level change typically accumulates through sustained differences in growth, reproduction, and survival, and can be buffered by compensatory dynamics, so early individual-level responses may take time to translate into detectable higher-level outcomes (Ankley et al., 2010). In this thesis, predator growth inhibition under prey-mediated chronic dietary exposure in the simplified food-chain experiment (**Chapter 5**) showed that fitness-related endpoints can respond detectably in the absence of acute mortality. In the outdoor microcosms (**Chapter 6**), zooplankton abundance responded significantly to treatment, while community composition showed no significant shift. Overall, these results suggested that higher-trophic responses were not always consistent across experimental systems, and that their detectability is influenced, at least in part, by endpoint choice and endpoint coverage. At the same time, this thesis primarily assessed higher-trophic responses using community-level metrics and did not include individual-level sublethal endpoints. Such mechanistic measurements are not always required to demonstrate ecosystem-level effects but can help interpret ecosystem-level responses and explain differences among systems when needed. Where relevant, measurements of microbiome structure and function may provide additional context for interpretation.

7.3.3 Response characteristics of ecosystem functional endpoints: functional endpoints are more sensitive than structural endpoints under the conditions studied

Compared with community-structure endpoints, the functional endpoints used in this thesis showed clearer and more consistent treatment effects across systems and helped to identify changes in key ecosystem processes. In the indoor microcosms (**Chapter 3**), even when differences in water-column or sediment microbial community structure were not statistically significant, leaf-litter decomposition rates changed in the same direction across multiple antimicrobial treatments. This indicates that the absence of significant changes in community structure does not necessarily mean that ecosystem processes are unchanged. Over the days-to-weeks' time scales of these experiments, decomposition can shift through changes in the activity of the decomposer community (primarily bacteria and fungi) and in functional expression (e.g., extracellular enzyme activity), which may not be captured consistently by 16S rRNA gene sequencing-based community composition or coarse diversity metrics (Paumelle et al., 2021; Pesce et al., 2021).

In the outdoor microcosm experiment (**Chapter 6**), we observed a similar contrast between compositional and functional endpoints. Sediment microbial community composition showed no significant treatment effects, but FAPROTAX-inferred functional groups did. Under the high-dose ozone treatment, the relative abundance of taxa associated with pollutant degradation and nitrogen cycling decreased. A parsimonious interpretation is that treatment-related functional changes in metabolic potential and nutrient cycling can occur without immediate, detectable effects on community composition as captured by structural endpoints. Therefore, at the system scale, the response to antimicrobial exposure may be primarily functional rather than structural, expressed as shifts in functional-group profiles and changes in predicted process capacity.

7.3.4 Environmental modulation of effect expression: from nutrients and substrate to treatment-induced resource reconfiguration

Across the experimental systems covered in this thesis, the detectability and expression pathways of antimicrobial effects show pronounced context dependence. Nutrient and organic carbon conditions shape baseline microbial community composition and complexity, which in turn influence whether treatment-related structural changes can be detected statistically. In the triclosan microcosm experiment (**Chapter 4**), the different sediment–water combinations differed significantly in inorganic nitrogen, phosphorus forms, pH, and sediment organic matter. Forward selection in RDA indicated that these variables significantly explained variation in the microbial community composition of the control

treatments without triclosan exposure. We applied the same triclosan treatments across the different water–sediment combinations. In the ditch water-sediment system, which had lower nutrient availability, sediment microbial community composition changed significantly at comparatively lower (measured) sediment concentrations. In the pond water–sediment system with higher resource availability, comparable shifts were observed at comparatively higher concentrations. At a broader spatial scale, our previous work in the Maozhou River basin found significant associations between antibiotic resistance gene (ARG) abundance and water-quality parameters including DO, NH_4-N, and TOC (Wu et al., 2020), indicating that co-variation between resource and water-quality conditions and microbial indicators such as ARG abundance can also be detected in field systems.

Beyond nutrient background, sediment organic matter may further influence antimicrobial effects by reducing pollutant bioavailability. Organic matter can reduce freely dissolved concentrations of hydrophobic compounds through sorption, and, as a background carbon pool, may also influence microbial metabolic processes, thereby modifying how chemical disturbance is expressed at the community level (**Chapter 4**). Consistent with these mechanisms, reviews have emphasized that binding of hydrophobic organic contaminants to DOM and humic substances can alter mobility and bioavailability and, under certain conditions, attenuate toxicity or bioaccumulation (Kovacevic et al., 2019; Li et al., 2015c). In parallel, systems with higher resources and higher sediment organic-matter content often have more complex microbial communities and greater functional redundancy among taxa, which can buffer disturbance and reduce detectable changes in community structure (**Chapter 4**).

The outdoor microcosm experiment further showed that advanced wastewater treatment (BO_3) can simultaneously change micropollutant residues and nutrient conditions, and that the key structural equation modelling relationships among chemicals, nutrients, and basal biota differed between Day 14 and Day 42 (**Chapter 6**). At Day 14, the structural equation modelling indicated that BO_3-driven reductions in micropollutants and changes in nutrients were associated with phytoplankton biomass (chlorophyll-a), with phosphorus showing a positive association with chlorophyll-a and nitrate & nitrite a negative association. Ozone and nitrate & nitrite also showed marginal associations with the water-column microbial community composition ($P = 0.06$ and $P = 0.051$, respectively). By Day 42, the model network became notably simpler, and variation in chlorophyll-a was explained mainly by nutrient status, with higher phosphorus associated with higher chlorophyll-a. This time-dependent change in the dominant pathways (Day 14 vs Day 42) supports the view that shifts in nutrient conditions can reshape when and through which pathways effects of the different BO_3 configurations become detectable at the base of the food web (**Chapter 6**).

7.4 Trophic transfer without consistent biomagnification: implications for ecological risk assessment (RQ3)

In this thesis, **Chapter 5** showed that antimicrobials can build up substantial internal concentrations at the base of a freshwater food chain (algae), yet transfer to higher trophic levels like *Daphnia* and *Chaoborus* does not necessarily translate into increased internal concentrations. This pattern is also supported by controlled food-chain experiments. In an experimental *Scenedesmus obliquus–Daphnia magna–Carassius auratus* food chain exposed to roxithromycin, substantial internal burdens were observed in algae and *Daphnia*, but no biomagnification occurred at the *Daphnia* level or in fish tissues (BMF < 1) (Ding et al., 2015). In contrast, measurements of internal concentrations in food-webs in the field highlighted compound-specific differences in biomagnification, with Tang et al. (2022a) reporting significant trophic magnification for ciprofloxacin but not for most other antibiotics in the Pearl River food web. These results further indicate that, even in the absence of biomagnification, dietary exposure can lead to disturbances in energy acquisition processes (e.g., feeding and assimilation), resulting in a decrease in fitness-related endpoints such as growth or reproduction.

In ecological risk assessment, bioaccumulation and biomagnification do not necessarily lead to effects on structural endpoints; rather, they inform where chemicals may concentrate within the food web, helping to prioritize endpoints based on bioavailable internal exposure and relevance to the mode of action, rather than on peak concentrations alone. When bioaccumulation or biomagnification are not observed but internal concentrations persist at the base of the food web, dietary exposure is more likely to affect energy acquisition and allocation via impacts on feeding, digestion, and assimilation, ultimately translating into fitness-related outcomes. Supporting evidence is available from comparable studies: Li et al. (2020b) showed that azithromycin can alter feeding behaviour and nutrient accumulation in *Daphnia*, potentially through effects on digestive enzyme activities and oxidative stress responses; Yin et al. (2023) further reported gut enrichment and responses linked to gut microbiota/ARGs in fish under dietary exposure to sulfamethazine, indicating that no biomagnification should not be interpreted as no effect. Therefore, bioconcentration factors (BCFs) and biomagnification or trophic magnification factors (BMFs/TMFs) remain informative descriptors of internal exposure and trophic transfer, but their interpretation should be embedded in an explicit evidence chain that links measured body or tissue concentrations and trophic transfer (e.g., estimated BCFs and BMFs/TMFs) with energy acquisition and allocation endpoints and fitness-related endpoints, rather than relying on a single ratio metric as a proxy for ecological impact. Finally, although this thesis did not measure tissue/compartment-specific concentrations in the organisms at higher trophic levels, existing studies show that some macrolides can exhibit pronounced tissue-specific

accumulation in fish (e.g., liver/bile higher than muscle). Tissue-specific measurements would therefore improve the interpretation of trophic transfer by distinguishing concentrations in effect-relevant organs from residues in edible tissues, if the food chain were extended to higher trophic levels (Liu et al., 2014).

7.5 Advanced treatment as exposure reduction: residual risks and effect validation (RQ4)

Removal efficiencies for different antimicrobials differ substantially in conventional activated sludge treatment, and some compounds are therefore not sufficiently removed. As a result, wastewater treatment plant effluents remain an important input pathway to aquatic environments (Senta et al., 2013). **Chapter 6** showed that the BAC–O_3 combination markedly reduced the concentrations of micropollutants in the effluent and lowered the corresponding ecological risk derived from PNEC-based risk quotients and from a mixture risk estimate (msPAF). Mechanistically, BAC pretreatment reduces matrix interferences through sorption and by removing part of the biodegradable fraction, thereby lowering the load of a subset of target compounds. Subsequent ozonation further degrades ozone-sensitive chemicals through oxidative reactions, resulting in an overall reduction of antimicrobials and other micropollutants. Accordingly, the primary contribution of advanced treatment is to decrease the concentrations of antimicrobials and related micropollutants and, in turn, to reduce their input into receiving waters. Given the evidence provided in **Chapter 2** showing that related pressures can propagate along a continuum linking surface water, sediment and groundwater, reducing effluent inputs has clear practical ecological relevance for receiving ecosystems and their connected multi-media environments.

At the same time, a decline in overall exposure concentrations does not necessarily imply a complete risk removal. Residual risk is often driven by a small number of compounds that are removed less efficiently and persist longer in the system. In addition, ozonation can generate transformation products whose ecological effects are uncertain. As a consequence, decreases in parent compounds do not always translate into a proportional decline in overall risks. Risk metrics based on target lists and available toxicity thresholds also have their inherent limitations: unmonitored substances, compounds lacking robust PNECs, and reaction byproducts that are difficult to characterise in complex matrices may still contribute to residual effect signals even when risk metrics are lower. Under these uncertainties, the reduction in ecological risk achieved by advanced treatment should be evaluated using results that directly reflect biological effects (e.g., bioassays or ecologically relevant response endpoints), rather than inferred solely from chemical removal or a single predictive

metric. Beyond documenting reductions in chemical pressure, it is therefore important to test whether treated effluents show concurrent decreases in overall mixture toxicity or in key structural and functional ecological endpoints, and, where relevant, to distinguish immediate from delayed effects and consider recovery trajectories across different time scales. This reduces the risk of extrapolating ecological conclusions directly from removal efficiencies or from one model-based indicator (Brack et al., 2019; Völker et al., 2019).

Finally, antimicrobial resistance (AMR) was explicitly assessed only in **Chapter 2**, whereas antibiotic-resistant bacteria (ARB) and ARG endpoints were not measured in the other chapters. However, antimicrobials act not only as pollutants but also as selection pressure for AMR, and ecological risk may therefore involve not only community structure and functional endpoints but also the enrichment and environmental persistence of resistance-related traits. End-of-pipe measures may indirectly weaken selection pressure by reducing antimicrobial pressure, yet reductions in micropollutants and reductions in AMR signals are not inherently synchronous. Available evidence suggests that ozone doses applied for micropollutant control can be effective for inactivating ARBs, whereas reductions in intracellular resistance genes are less consistent and may be influenced by floc or particle shielding and by post-treatment regrowth processes (Czekalski et al., 2016). Ozonation combined with activated-carbon filtration also shows potential for ARB/ARG control, but outcomes are highly sensitive to operating conditions, matrix characteristics, and indicator selection, and responses can vary strongly among ARGs (Iakovides et al., 2021; Zhang et al., 2025). In addition, biofilms and filter media within activated-carbon units may serve as carriers or enrichment niches for AMR signals, which can lead to non-uniform directions of change across AMR indicators along the treatment train (Slipko et al., 2022). Given these uncertainties, any potential co-benefit of BAC–O_3 for AMR is best presented as a hypothesis requiring verification. Future work that incorporates AMR endpoints into comparable experimental frameworks should evaluate AMR indicators in parallel with chemical reductions and ecological endpoints to test more directly whether mitigation occurs concurrently across pollution, ecological responses, and resistance-related risks.

References

Achar, J.C., Kwon, J.-H. and Jung, J. 2020. Toxicokinetic modeling of octylphenol bioconcentration in Chlorella vulgaris and its trophic transfer to Daphnia magna. Ecotoxicology and Environmental Safety 194, 110379.

Acosta, A., Tirkaso, W., Nicolli, F., Van Boeckel, T.P., Cinardi, G. and Song, J. 2025. The future of antibiotic use in livestock. Nature communications 16(1), 2469.

Adhikari, S., Kumar, R., Driver, E.M., Perleberg, T.D., Yanez, A., Johnston, B. and Halden, R.U. 2022. Mass trends of parabens, triclocarban and triclosan in Arizona wastewater collected after the 2017 FDA ban on antimicrobials and during the COVID-19 pandemic. Water Research 222, 118894.

Aemig, Q., Hélias, A. and Patureau, D. 2021. Impact assessment of a large panel of organic and inorganic micropollutants released by wastewater treatment plants at the scale of France. Water Research 188, 116524.

Aguilar-Romero, I., Romero, E., Wittich, R.-M. and Van Dillewijn, P. 2020. Bacterial ecotoxicity and shifts in bacterial communities associated with the removal of ibuprofen, diclofenac and triclosan in biopurification systems. Science of The Total Environment 741, 140461.

Akbar, S., Gu, L., Sun, Y., Zhou, Q., Zhang, L., Lyu, K., Huang, Y. and Yang, Z. 2020. Changes in the life history traits of Daphnia magna are associated with the gut microbiota composition shaped by diet and antibiotics. Science of the Total Environment 705, 135827.

Al-Khazrajy, O.S. and Boxall, A.B. 2016. Impacts of compound properties and sediment characteristics on the sorption behaviour of pharmaceuticals in aquatic systems. Journal of hazardous materials 317, 198-209.

Amangelsin, Y., Semenova, Y., Dadar, M., Aljofan, M. and Bjørklund, G. 2023. The impact of tetracycline pollution on the aquatic environment and removal strategies. Antibiotics 12(3), 440.

Anderson, M. and Sobsey, M. 2006. Detection and occurrence of antimicrobially resistant E. coli in groundwater on or near swine farms in eastern North Carolina. Water Science and Technology 54(3), 211-218.

Ankley, G.T., Bennett, R.S., Erickson, R.J., Hoff, D.J., Hornung, M.W., Johnson, R.D., Mount, D.R., Nichols, J.W., Russom, C.L. and Schmieder, P.K. 2010. Adverse outcome pathways: a conceptual framework to support ecotoxicology research and risk assessment. Environmental toxicology and chemistry 29(3), 730-741.

Anneser, B., Pilloni, G., Bayer, A., Lueders, T., Griebler, C., Einsiedl, F. and Richters, L. 2010. High resolution analysis of contaminated aquifer sediments and groundwater—what can be learned in terms of natural attenuation? Geomicrobiology Journal 27(2), 130-142.

Ardakani, Z., Aragrande, M. and Canali, M. 2024. Global antimicrobial use in livestock farming: an estimate for cattle, chickens, and pigs. Animal 18(2), 101060.

Armitage, J.M., Erickson, R.J., Luckenbach, T., Ng, C.A., Prosser, R.S., Arnot, J.A., Schirmer, K. and Nichols, J.W. 2017. Assessing the bioaccumulation potential of ionizable organic compounds: Current knowledge and research priorities. Environmental toxicology and chemistry 36(4), 882-897.

Arnot, J.A. and Gobas, F.A. 2006. A review of bioconcentration factor (BCF) and bioaccumulation factor (BAF) assessments for organic chemicals in aquatic organisms. Environmental Reviews 14(4), 257-297.

Arreguin-Rebolledo, U., Morales-Romero, L.A., Arzate-Cárdenas, M.A., Páez-Osuna, F., Betancourt-Lozano, M. and Rico-Martínez, R. 2024. Contrasting toxicity response to a mixture of azithromycin and ivermectin between a freshwater and a euryhaline rotifer. Environmental Science and Pollution Research 31(37), 49905-49915.

Asaf, S., Numan, M., Khan, A.L. and Al-Harrasi, A. 2020. Sphingomonas: from diversity and genomics to functional role in environmental remediation and plant growth. Critical Reviews in Biotechnology 40(2), 138-152.

Asif, M.B., Li, C., Ren, B., Maqbool, T., Zhang, X. and Zhang, Z. 2021. Elucidating the impacts of intermittent in-situ ozonation in a ceramic membrane bioreactor: Micropollutant removal, microbial community evolution and fouling mechanisms. Journal of hazardous materials 402, 123730.

Aus der Beek, T., Weber, F.A., Bergmann, A., Hickmann, S., Ebert, I., Hein, A. and Küster, A. 2016. Pharmaceuticals in the environment—Global occurrences and perspectives. Environmental toxicology and chemistry 35(4), 823-835.

Backhaus, T. and Faust, M. 2012. Predictive environmental risk assessment of chemical mixtures: a conceptual framework. Environmental science & technology 46(5), 2564-2573.

Bai, H., He, L.-Y., Gao, F.-Z., Wu, D.-L., Yao, K.-S., Zhang, M., Jia, W.-L., He, L.-X., Zou, H.-Y. and Yao, M.-S. 2023. Airborne antibiotic resistome and human health risk in railway stations during COVID-19 pandemic. Environment International 172, 107784.

Bai, H., He, L.Y., Wu, D.L., Gao, F.Z., Zhang, M., Zou, H.Y., Yao, M.S. and Ying, G.G. 2022. Spread of airborne antibiotic resistance from animal farms to the environment: Dispersal pattern and exposure risk. Environ Int 158, 106927.

Balzer, F., Zühlke, S. and Hannappel, S. 2016. Antibiotics in groundwater under locations with high livestock density in Germany. Water Science and Technology: Water Supply 16(5), 1361-1369.

Barrett, H., Sun, J., Gong, Y., Yang, P., Hao, C., Verreault, J., Zhang, Y. and Peng, H. 2022. Triclosan is the predominant antibacterial compound in Ontario sewage sludge. Environmental Science & Technology 56(21), 14923-14936.

Batchu, S.R., Panditi, V.R., O'Shea, K.E. and Gardinali, P.R. 2014. Photodegradation of antibiotics under simulated solar radiation: implications for their environmental fate. Science of the total environment 470, 299-310.

Batista, A.P.S., Pires, F.C.C. and Teixeira, A.C.S. 2014. Photochemical degradation of sulfadiazine, sulfamerazine and sulfamethazine: Relevance of concentration and heterocyclic aromatic groups to degradation kinetics. Journal of Photochemistry and Photobiology A: Chemistry 286, 40-46.

Bengtsson-Palme, J. and Larsson, D.G. 2016. Concentrations of antibiotics predicted to select for resistant bacteria: Proposed limits for environmental regulation. Environ Int 86, 140-149.

Benitez, F.J., Acero, J.L., Garcia-Reyes, J.F., Real, F.J., Roldan, G., Rodriguez, E. and Molina-Díaz, A. 2013. Determination of the reaction rate constants and decomposition mechanisms of ozone with two model emerging contaminants: DEET and nortriptyline. Industrial & Engineering Chemistry Research 52(48), 17064-17073.

Benitez, F.J., Acero, J.L., Real, F.J., Roldán, G. and Rodríguez, E. 2015. Ozonation of benzotriazole and methylindole: kinetic modeling, identification of intermediates and reaction mechanisms. Journal of Hazardous Materials 282, 224-232.

Białk-Bielińska, A., Stolte, S., Arning, J., Uebers, U., Böschen, A., Stepnowski, P. and Matzke, M. 2011. Ecotoxicity evaluation of selected sulfonamides. Chemosphere 85(6), 928-933.

Bollenbach, T., Quan, S., Chait, R. and Kishony, R. 2009. Nonoptimal microbial response to antibiotics underlies suppressive drug interactions. Cell 139(4), 707-718.

Bovio-Winkler, P., Guerrero, L.D., Erijman, L., Oyarzúa, P., Suárez-Ojeda, M.E., Cabezas, A. and Etchebehere, C. 2023. Genome-centric metagenomic insights into the role of Chloroflexi in anammox, activated sludge and methanogenic reactors. BMC microbiology 23(1), 45.

Bownik, A., Ślaska, B., Bochra, J., Gumieniak, K. and Gałek, K. 2019. Procaine penicillin alters swimming behaviour and physiological parameters of Daphnia magna. Environmental Science and Pollution Research 26(18), 18662-18673.

Brack, W., Aissa, S.A., Backhaus, T., Dulio, V., Escher, B.I., Faust, M., Hilscherova, K., Hollender, J., Hollert, H. and Müller, C. 2019. Effect-based methods are key. The European Collaborative Project SOLUTIONS recommends integrating effect-based methods for diagnosis and monitoring of water quality. Environmental Sciences Europe 31(1), 1-6.

Brain, R.A., Ramirez, A.J., Fulton, B.A., Chambliss, C.K. and Brooks, B.W. 2008. Herbicidal effects of sulfamethoxazole in Lemna gibba: using p-aminobenzoic acid as a biomarker of effect. Environmental Science & Technology 42(23), 8965-8970.

Bräuner, E.V., Uldbjerg, C.S., Lim, Y.-H., Gregersen, L.S., Krause, M., Frederiksen, H. and Andersson, A.-M. 2022. Presence of parabens, phenols and phthalates in paired maternal serum, urine and amniotic fluid. Environment international 158, 106987.

Brochado, A.R., Telzerow, A., Bobonis, J., Banzhaf, M., Mateus, A., Selkrig, J., Huth, E., Bassler, S., Zamarreño Beas, J. and Zietek, M. 2018. Species-specific activity of antibacterial drug combinations. Nature 559(7713), 259-263.

Browne, A.J., Chipeta, M.G., Haines-Woodhouse, G., Kumaran, E.P., Hamadani, B.H.K., Zaraa, S., Henry, N.J., Deshpande, A., Reiner, R.C. and Day, N.P. 2021. Global antibiotic consumption and usage in humans, 2000–18: a spatial modelling study. The Lancet Planetary Health 5(12), e893-e904.

Brüssow, H. 2024. The antibiotic resistance crisis and the development of new antibiotics. Microbial Biotechnology 17(7), e14510.

Bureau, S.E.E. 2022. https://meeb.sz.gov.cn/xxgk/qt/hbxw/content/post_9958531.html.

Calero-Cáceres, W., Méndez, J., Martín-Díaz, J. and Muniesa, M. 2017. The occurrence of antibiotic resistance genes in a Mediterranean river and their persistence in the riverbed sediment. Environmental Pollution 223, 384-394.

Camel, V. and Bermond, A. 1998. The use of ozone and associated oxidation processes in drinking water treatment. Water research 32(11), 3208-3222.

Caracciolo, A.B., Topp, E. and Grenni, P. 2015. Pharmaceuticals in the environment: biodegradation and effects on natural microbial communities. A review. Journal of pharmaceutical and biomedical analysis 106, 25-36.

Carlet, J. 2012. The gut is the epicentre of antibiotic resistance. Antimicrobial resistance and infection control 1, 1-7.

Carstens, K.L., Gross, A.D., Moorman, T.B. and Coats, J.R. 2013. Sorption and photodegradation processes govern distribution and fate of sulfamethazine in freshwater–sediment microcosms. Environmental science & technology 47(19), 10877-10883.
Carvalho, I.T. and Santos, L. 2016. Antibiotics in the aquatic environments: a review of the European scenario. Environment international 94, 736-757.
Cedergreen, N. 2014. Quantifying synergy: a systematic review of mixture toxicity studies within environmental toxicology. PloS one 9(5), e96580.
Cha, X., Lin, Y., Brennan, C., Cao, J. and Shang, Y. 2023. Antibiotic Resistance of Bacillus cereus in Plant Foods and Edible Wild Mushrooms in a Province. Microorganisms 11(12), 2948.
Chabilan, A., Ledesma, D.G.B., Horn, H. and Borowska, E. 2023. Mesocosm experiment to determine the contribution of adsorption, biodegradation, hydrolysis and photodegradation in the attenuation of antibiotics at the water sediment interface. Science of The Total Environment 866, 161385.
Chalew, T.E. and Halden, R.U. 2009. Environmental exposure of aquatic and terrestrial biota to triclosan and triclocarban 1. JAWRA Journal of the American Water Resources Association 45(1), 4-13.
Chang, F., Yi, M., Li, H., Wang, J., Zhao, X., Hu, X. and Qi, Q. 2022. Antibiotic toxicity isolated and as binary mixture to freshwater algae Raphidocelis subcapitata: growth inhibition, prediction model, and environmental risk assessment. Toxics 10(12), 739.
Chen, J., Taniguchi, M., Liu, G., Miyaoka, K., Onodera, S.-i., Tokunaga, T. and Fukushima, Y. 2007. Nitrate pollution of groundwater in the Yellow River delta, China. Hydrogeology Journal 15, 1605-1614.
Chen, J., Zhang, B., Wang, C., Wang, P., Cui, G., Gao, H., Feng, B. and Zhang, J. 2024. Insight into the enhancement effect of humic acid on microbial degradation of triclosan in anaerobic sediments. Journal of Hazardous Materials 461, 132549.
Chen, S., Wang, L., Feng, W., Yuan, M., Li, J., Xu, H., Zheng, X. and Zhang, W. 2020. Sulfonamides-induced oxidative stress in freshwater microalga Chlorella vulgaris: Evaluation of growth, photosynthesis, antioxidants, ultrastructure, and nucleic acids. Scientific Reports 10(1), 8243.
Chen, Y., Huang, Y., Chen, Y., Li, Y., Sidikjan, N., Lin, N., Li, Y., Guo, X., Shen, G. and Liu, M. 2025. A systematic review of sources, occurrence, behavior and risks of global marine antibiotics. npj Emerging Contaminants 1(1), 15.
China, M.o.A.o.t.P.s.R.o. 2015. Administration regulations of veterinary (2015). Drugs 2292.
China, M.o.A.o.t.P.s.R.o. 2021. 2020 Annual report on the use of veterinary antibiotics in China. Official Veterinary Bulletin 23, 33-36.
Cichocki, J.A., Furuya, S., Venkatratnam, A., McDonald, T.J., Knap, A.H., Wade, T., Sweet, S., Chiu, W.A., Threadgill, D.W. and Rusyn, I. 2017. Characterization of Variability in Toxicokinetics and Toxicodynamics of Tetrachloroethylene Using the Collaborative Cross Mouse Population. 125(5), 057006.
Clarke, A., Azulai, D., Dueker, M.E., Vos, M. and Perron, G.G. 2019. Triclosan alters microbial communities in freshwater microcosms. Water 11(5), 961.
Conde-Cid, M., Fernández-Calviño, D., Nóvoa-Muñoz, J.C., Arias-Estévez, M., Díaz-Raviña, M., Núñez-Delgado, A., Fernández-Sanjurjo, M. and Álvarez-Rodríguez, E. 2018. Degradation of sulfadiazine, sulfachloropyridazine and sulfamethazine in aqueous media. Journal of environmental management 228, 239-248.
Conde-Cid, M., Núñez-Delgado, A., Fernández-Sanjurjo, M.J., Álvarez-Rodríguez, E., Fernández-Calviño, D. and Arias-Estévez, M. 2020. Tetracycline and sulfonamide antibiotics in soils: presence, fate and environmental risks. Processes 8(11), 1479.
Contardo-Jara, V., Meinecke, S., Feibicke, M., Berghahn, R., Schmidt, R. and Mohr, S. 2021. Fate, bioaccumulation and toxic effects of triclosan on a freshwater community–A mesocosm study. Environmental Advances 5, 100100.
Crane, M., Watts, C. and Boucard, T. 2006. Chronic aquatic environmental risks from exposure to human pharmaceuticals. Science of The Total Environment 367(1), 23-41.
Czekalski, N., Imminger, S., Salhi, E., Veljkovic, M., Kleffel, K., Drissner, D., Hammes, F., Burgmann, H. and von Gunten, U. 2016. Inactivation of antibiotic resistant bacteria and resistance genes by ozone: from laboratory experiments to full-scale wastewater treatment. Environmental science & technology 50(21), 11862-11871.
Daghrir, R. and Drogui, P. 2013. Tetracycline antibiotics in the environment: a review. Environmental chemistry letters 11, 209-227.
Dai, H., Gao, J., Li, D., Wang, Z., Cui, Y. and Zhao, Y. 2022. Family Sphingomonadaceae as the key executor of triclosan degradation in both nitrification and denitrification systems. Chemical Engineering Journal 442, 136202.
Dai, W., Zhang, J., Tu, Q., Deng, Y., Qiu, Q. and Xiong, J. 2017. Bacterioplankton assembly and interspecies interaction indicating increasing coastal eutrophication. Chemosphere 177, 317-325.
Dalla Bona, M., Zounková, R., Merlanti, R., Blaha, L. and De Liguoro, M. 2015. Effects of enrofloxacin, ciprofloxacin, and trimethoprim on two generations of Daphnia magna. Ecotoxicology and Environmental Safety 113, 152-158.

Danner, M.-C., Robertson, A., Behrends, V. and Reiss, J. 2019. Antibiotic pollution in surface fresh waters: Occurrence and effects. Science of the total environment 664, 793-804.
De Liguoro, M., Fioretto, B., Poltronieri, C. and Gallina, G. 2009. The toxicity of sulfamethazine to Daphnia magna and its additivity to other veterinary sulfonamides and trimethoprim. Chemosphere 75(11), 1519-1524.
de Wilt, A., van Gijn, K., Verhoek, T., Vergnes, A., Hoek, M., Rijnaarts, H. and Langenhoff, A. 2018. Enhanced pharmaceutical removal from water in a three step bio-ozone-bio process. Water research 138, 97-105.
DeLorenzo, M., Keller, J., Arthur, C., Finnegan, M., Harper, H., Winder, V. and Zdankiewicz, D. 2008. Toxicity of the antimicrobial compound triclosan and formation of the metabolite methyl-triclosan in estuarine systems. Environmental Toxicology: An International Journal 23(2), 224-232.
Deshpande, V. and Eriksson, K.-E. (1988) Methods in enzymology, pp. 415-424, Elsevier.
Diamond, J.S., Bernal, S., Boukra, A., Cohen, M.J., Lewis, D., Masson, M., Moatar, F. and Pinay, G. 2021. Stream network variation in dissolved oxygen: Metabolism proxies and biogeochemical controls. Ecological Indicators 131, 108233.
Ding, J., Lu, G., Liu, J. and Zhang, Z. 2015. Evaluation of the potential for trophic transfer of roxithromycin along an experimental food chain. Environmental Science and Pollution Research 22(14), 10592-10600.
Do, S.D., Haque, M.N., Kim, J., Im, D.-H. and Rhee, J.-S. 2024. Acute and chronic effects of triclosan on the behavior, physiology, and multigenerational characteristics of the water flea Moina macrocopa. Comparative Biochemistry and Physiology Part C: Toxicology & Pharmacology 276, 109810.
Dobor, J., Varga, M. and Záray, G. 2012. Biofilm controlled sorption of selected acidic drugs on river sediments characterized by different organic carbon content. Chemosphere 87(2), 105-110.
Drury, B., Rosi-Marshall, E. and Kelly, J.J. 2013a. Wastewater treatment effluent reduces the abundance and diversity of benthic bacterial communities in urban and suburban rivers. Applied and environmental microbiology 79(6), 1897-1905.
Drury, B., Scott, J., Rosi-Marshall, E.J. and Kelly, J.J. 2013b. Triclosan exposure increases triclosan resistance and influences taxonomic composition of benthic bacterial communities. Environmental science & technology 47(15), 8923-8930.
Du, B., Haddad, S.P., Luek, A., Scott, W.C., Saari, G.N., Kristofco, L.A., Connors, K.A., Rash, C., Rasmussen, J.B. and Chambliss, C.K. 2014. Bioaccumulation and trophic dilution of human pharmaceuticals across trophic positions of an effluent-dependent wadeable stream. Philosophical Transactions of the Royal Society B: Biological Sciences 369(1656), 20140058.
Dun, Y., Tang, C. and Shen, Y. 2014. Identifying interactions between river water and groundwater in the North China Plain using multiple tracers. Environmental earth sciences 72, 99-110.
Ebert, I., Bachmann, J., Kühnen, U., Küster, A., Kussatz, C., Maletzki, D. and Schlüter, C. 2011. Toxicity of the fluoroquinolone antibiotics enrofloxacin and ciprofloxacin to photoautotrophic aquatic organisms. Environmental toxicology and chemistry 30(12), 2786-2792.
Economides, C., Liapi, M. and Makris, K.C. 2012. Antibiotic resistance patterns of Salmonella and Escherichia coli in the groundwater of Cyprus. Environmental geochemistry and health 34, 391-397.
EFSA 2007. Report of the Task Force on Zoonoses Data Collection including a proposal for a harmonized monitoring scheme of antimicrobial resistance in Salmonella in fowl (Gallus gallus), turkeys and pigs and Campylobacter jejuni and C. coli in broilers. EFSA Journal 5(2), 96r.
EMA 2006. Guideline on the environmental risk assessment of medicinal products for human use. European Medicines Agency. EMEA/CHMP/SWP/4447/00 corr 2, 4-12.
EMA 2024. Guideline on the environmental risk assessment of medicinal products for human use European Medicines Agency Revision 1.
EU, E. 2016. Commission implementing decision (EU) 2016/110 of 27 January 2016 not approving triclosan as an existing active substance for use in biocidal products for product-type 1. Official J European Union L 21 87.
Falås, P., Wick, A., Castronovo, S., Habermacher, J., Ternes, T.A. and Joss, A. 2016. Tracing the limits of organic micropollutant removal in biological wastewater treatment. Water research 95, 240-249.
Fan, Y., Chen, J., Shirkey, G., John, R., Wu, S.R., Park, H. and Shao, C. 2016. Applications of structural equation modeling (SEM) in ecological studies: an updated review. Ecological processes 5(1), 19.
Fang, W., Lin, M., Shi, J., Liang, Z., Tu, X., He, Z., Qiu, R. and Wang, S. 2022. Organic carbon and eukaryotic predation synergistically change resistance and resilience of aquatic microbial communities. Science of the Total Environment 830, 154386.
Fick, J., Lindberg, R.H., Parkkonen, J., Arvidsson, B., Tysklind, M. and Larsson, D.J. 2010. Therapeutic levels of levonorgestrel detected in blood plasma of fish: results from screening rainbow trout exposed to treated sewage effluents. Environmental science & technology 44(7), 2661-2666.

Flaherty, C.M. and Dodson, S.I. 2005. Effects of pharmaceuticals on Daphnia survival, growth, and reproduction. Chemosphere 61(2), 200-207.
Food and Drug Administration, H. 2017. Safety and effectiveness of health care antiseptics; topical antimicrobial drug products for over-the-counter human use. Final rule. Federal register 82(242), 60474-60503.
Frade, P.R., Glasl, B., Matthews, S.A., Mellin, C., Serrão, E.A., Wolfe, K., Mumby, P.J., Webster, N.S. and Bourne, D.G. 2020. Spatial patterns of microbial communities across surface waters of the Great Barrier Reef. Communications biology 3(1), 442.
Fryer, J.L. and Lannan, C.N. 1994. Rickettsial and chlamydial infections of freshwater and marine fishes, bivalves, and crustaceans. Zoological studies 33(2), 95-107.
Fulaz, S., Vitale, S., Quinn, L. and Casey, E. 2019. Nanoparticle–biofilm interactions: the role of the EPS matrix. Trends in microbiology 27(11), 915-926.
Galir, A., Špoljarić Maronić, D., Stević, F., Žuna Pfeiffer, T., Prašnikar, F., Bek, N., Penava, E. and Križevac, P. 2025. Effects of Azithromycin on the Functioning of the Food Web in Freshwater Plankton. Journal of xenobiotics 15(5), 145.
García-Galán, M.J., Díaz-Cruz, M.S. and Barceló, D. 2012. Kinetic studies and characterization of photolytic products of sulfamethazine, sulfapyridine and their acetylated metabolites in water under simulated solar irradiation. Water research 46(3), 711-722.
Gillings, M.R. 2013. Evolutionary consequences of antibiotic use for the resistome, mobilome and microbial pangenome. Frontiers in microbiology 4, 4.
Gobas, F.A. and Lee, Y.S. 2019. Growth-correcting the bioconcentration factor and biomagnification factor in bioaccumulation assessments. Environmental Toxicology and Chemistry 38(9), 2065-2072.
Gobas, F.A., Lee, Y.S., Lo, J.C., Parkerton, T.F. and Letinski, D.J. 2020. A toxicokinetic framework and analysis tool for interpreting Organisation for Economic Co-Operation and Development guideline 305 dietary bioaccumulation tests. Environmental Toxicology and Chemistry 39(1), 171-188.
González-Pleiter, M., Gonzalo, S., Rodea-Palomares, I., Leganés, F., Rosal, R., Boltes, K., Marco, E. and Fernández-Piñas, F. 2013. Toxicity of five antibiotics and their mixtures towards photosynthetic aquatic organisms: implications for environmental risk assessment. Water research 47(6), 2050-2064.
Gorokhova, E., Rivetti, C., Furuhagen, S., Edlund, A., Ek, K. and Breitholtz, M. 2015. Bacteria-mediated effects of antibiotics on Daphnia nutrition. Environmental science & technology 49(9), 5779-5787.
Gothwal, R. and Shashidhar, T. 2015. Antibiotic pollution in the environment: a review. Clean–Soil, Air, Water 43(4), 479-489.
Goutte, A., Alliot, F., Budzinski, H., Simonnet-Laprade, C., Santos, R., Lachaux, V., Maciejewski, K., Le Menach, K. and Labadie, P. 2020. Trophic transfer of micropollutants and their metabolites in an urban riverine food web. Environmental science & technology 54(13), 8043-8050.
Gray, A.D. and Bernhardt, E. 2022. Are nitrogen and carbon cycle processes impacted by common stream antibiotics? A comparative assessment of single vs. mixture exposures. Plos one 17(1), e0261714.
Gray, H.K., Arora-Williams, K.K., Young, C., Bouwer, E., Davis, M.F. and Preheim, S.P. 2020. Contribution of time, taxonomy, and selective antimicrobials to antibiotic and multidrug resistance in wastewater bacteria. Environmental science & technology 54(24), 15946-15957.
Grenni, P., Ancona, V. and Caracciolo, A.B. 2018. Ecological effects of antibiotics on natural ecosystems: A review. Microchemical Journal 136, 25-39.
Griebler, C., Mindl, B., Slezak, D. and Geiger-Kaiser, M. 2002. Distribution patterns of attached and suspended bacteria in pristine and contaminated shallow aquifers studied with an in situ sediment exposure microcosm. Aquatic microbial ecology 28(2), 117-129.
Gulde, R., Rutsch, M., Clerc, B., Schollée, J.E., von Gunten, U. and McArdell, C.S. 2021. Formation of transformation products during ozonation of secondary wastewater effluent and their fate in post-treatment: From laboratory-to full-scale. Water Research 200, 117200.
Gunathilaka, M.L., Bao, S., Liu, X., Li, Y. and Pan, Y. 2023. Antibiotic pollution of planktonic ecosystems: a review focused on community analysis and the causal chain linking individual-and community-level responses. Environmental Science & Technology 57(3), 1199-1213.
Guo, J., Zhang, Y., Mo, J., Sun, H. and Li, Q. 2021. Sulfamethoxazole-altered transcriptomein green alga Raphidocelis subcapitata suggests inhibition of translation and DNA damage repair. Frontiers in microbiology 12, 541451.
Hahn, T. and Schulz, R. 2007. Indirect effects of antibiotics in the aquatic environment: a laboratory study on detritivore food selection behavior. Human and Ecological Risk Assessment 13(3), 535-542.
Halling-Sørensen, B. 2000. Algal toxicity of antibacterial agents used in intensive farming. Chemosphere 40(7), 731-739.

Hamdhani, H., Eppehimer, D.E. and Bogan, M.T. 2020. Release of treated effluent into streams: A global review of ecological impacts with a consideration of its potential use for environmental flows. Freshwater Biology 65(9), 1657-1670.

Hanna, N., Tamhankar, A.J. and Lundborg, C.S. 2023. Antibiotic concentrations and antibiotic resistance in aquatic environments of the WHO Western Pacific and South-East Asia regions: a systematic review and probabilistic environmental hazard assessment. The Lancet Planetary Health 7(1), e45-e54.

Harriage, S.J., Schultz, N.L., Barton, P.S., Saaristo, M. and Long, B.M. 2025. The trophic transfer of pharmaceuticals and personal care products: A global systematic review and meta-analysis. Journal of Hazardous Materials, 139806.

He, L.-X., He, L.-Y., Gao, F.-Z., Wu, D.-L., Ye, P., Cheng, Y.-X., Chen, Z.-Y., Hu, L.-X., Liu, Y.-S. and Chen, J. 2022. Antibiotics, antibiotic resistance genes and microbial community in grouper mariculture. Science of the Total Environment 808, 152042.

He, L.-X., He, L.-Y., Gao, F.-Z., Zhang, M., Chen, J., Jia, W.-L., Ye, P., Jia, Y.-W., Hong, B. and Liu, S.-S. 2023. Mariculture affects antibiotic resistome and microbiome in the coastal environment. Journal of Hazardous Materials 452, 131208.

Heijnen, L., de Vries, H.J., van Pelt, G., Stroobach, E., Atsma, A., Vranken, J., De Maeyer, K., Vissers, L. and Medema, G. 2024. Qualitative detection of E. coli in distributed drinking water using real-time reverse transcription PCR targeting 16S rRNA: validation and practical experiences. Water Research, 121843.

Henneberger, L. and Goss, K.-U. 2019. Environmental sorption behavior of ionic and ionizable organic chemicals. Reviews of Environmental Contamination and Toxicology Volume 253, 43-64.

Henry, R., Schang, C., Coutts, S., Kolotelo, P., Prosser, T., Crosbie, N., Grant, T., Cottam, D., O'Brien, P. and Deletic, A. 2016. Into the deep: evaluation of SourceTracker for assessment of faecal contamination of coastal waters. Water research 93, 242-253.

Hermann, M., Polazzo, F., Cherta, L., Crettaz-Minaglia, M., García-Astillero, A., Peeters, E.T., Rico, A. and Van den Brink, P.J. 2024. Combined stress of an insecticide and heatwaves or elevated temperature induce community and food web effects in a Mediterranean freshwater ecosystem. Water Research 260, 121903.

Hernando, M.D., Mezcua, M., Fernández-Alba, A.R. and Barceló, D. 2006. Environmental risk assessment of pharmaceutical residues in wastewater effluents, surface waters and sediments. Talanta 69(2), 334-342.

Heß, S., Berendonk, T. and Kneis, D. 2018. Antibiotic resistant bacteria and resistance genes in the bottom sediment of a small stream and the potential impact of remobilization. FEMS microbiology ecology 94(9), fiy128.

Heys, K.A., Shore, R.F., Pereira, M.G., Jones, K.C. and Martin, F.L. 2016. Risk assessment of environmental mixture effects. RSC advances 6(53), 47844-47857.

Hillis, D.G., Lissemore, L., Sibley, P.K. and Solomon, K.R. 2007. Effects of monensin on zooplankton communities in aquatic microcosms. Environmental science & technology 41(18), 6620-6626.

Ho, C.S., Wong, C.T., Aung, T.T., Lakshminarayanan, R., Mehta, J.S., Rauz, S., McNally, A., Kintses, B., Peacock, S.J. and de la Fuente-Nunez, C. 2025. Antimicrobial resistance: a concise update. The Lancet Microbe 6(1).

Hollender, J., Zimmermann, S.G., Koepke, S., Krauss, M., McArdell, C.S., Ort, C., Singer, H., Von Gunten, U. and Siegrist, H. 2009. Elimination of organic micropollutants in a municipal wastewater treatment plant upgraded with a full-scale post-ozonation followed by sand filtration. Environmental science & technology 43(20), 7862-7869.

Hong, Y., Boiti, A., Vallone, D. and Foulkes, N.S. 2024. Reactive oxygen species signaling and oxidative stress: transcriptional regulation and evolution. Antioxidants 13(3), 312.

Hu, A., Ju, F., Hou, L., Li, J., Yang, X., Wang, H., Mulla, S.I., Sun, Q., Bürgmann, H. and Yu, C.P. 2017. Strong impact of anthropogenic contamination on the co-occurrence patterns of a riverine microbial community. Environmental microbiology 19(12), 4993-5009.

Hu, Y., Matsui, Y. and W. Riley, L. 2020. Risk factors for fecal carriage of drug-resistant Escherichia coli: a systematic review and meta-analysis. Antimicrobial Resistance & Infection Control 9(1), 31.

Huang, A., Mangold-Döring, A., Focks, A., Zhang, C. and Van den Brink, P.J. 2022. Comparing the acute and chronic toxicity of flupyradifurone and imidacloprid to non-target aquatic arthropod species. Ecotoxicology and Environmental Safety 243, 113977.

Huang, A., van den Brink, N.W., Buijse, L., Roessink, I. and van den Brink, P.J. 2021. The toxicity and toxicokinetics of imidacloprid and a bioactive metabolite to two aquatic arthropod species. Aquatic Toxicology 235, 105837.

Huang, C.-L., Ma, H.-W. and Yu, C.-P. 2014. Substance flow analysis and assessment of environmental exposure potential for triclosan in mainland China. Science of the total environment 499, 265-275.

Huang, G., Zhang, M., Liu, C., Li, L. and Chen, Z. 2018. Heavy metal (loid) s and organic contaminants in groundwater in the Pearl River Delta that has undergone three decades of urbanization and industrialization: Distributions, sources, and driving forces. Science of the Total Environment 635, 913-925.

Huang, X., Wu, C., Hu, H., Yu, Y. and Liu, J. 2015. Sorption and degradation of triclosan in sediments and its effect on microbes. Ecotoxicology and environmental safety 116, 76-83.
Hubas, C., Jesus, B., Ruivo, M., Meziane, T., Thiney, N., Davoult, D., Spilmont, N., Paterson, D.M. and Jeanthon, C. 2013. Proliferation of purple sulphur bacteria at the sediment surface affects intertidal mat diversity and functionality. PLoS One 8(12), e82329.
Hübner, U., von Gunten, U. and Jekel, M. 2015. Evaluation of the persistence of transformation products from ozonation of trace organic compounds–A critical review. Water Research 68, 150-170.
Humphries, R., Bobenchik, A.M., Hindler, J.A. and Schuetz, A.N. 2021. Overview of changes to the clinical and laboratory standards institute performance standards for antimicrobial susceptibility testing, M100. Journal of clinical microbiology 59(12), 10.1128/jcm. 00213-00221.
Iakovides, I., Manoli, K., Karaolia, P., Michael-Kordatou, I., Manaia, C. and Fatta-Kassinos, D. 2021. Reduction of antibiotic resistance determinants in urban wastewater by ozone: Emphasis on the impact of wastewater matrix towards the inactivation kinetics, toxicity and bacterial regrowth. Journal of Hazardous Materials 420, 126527.
Illés, E., Szabó, E., Takács, E., Wojnárovits, L., Dombi, A. and Gajda-Schrantz, K. 2014. Ketoprofen removal by O3 and O3/UV processes: Kinetics, transformation products and ecotoxicity. Science of the Total Environment 472, 178-184.
Inostroza, P.A., Jessen, G.L., Li, F., Zhang, X., Brack, W. and Backhaus, T. 2025. Multi-compartment impact of micropollutants and particularly antibiotics on bacterial communities using environmental DNA at river basin-level. Environmental Pollution 366, 125487.
Jabłońska-Trypuć, A. 2023. A review on triclosan in wastewater: Mechanism of action, resistance phenomenon, environmental risks, and sustainable removal techniques. Water Environment Research 95(9), e10920.
Jiang, Y., Liu, Y. and Zhang, J. 2020. Antibiotics induced alterations in cell density, photosynthesis, microcystin synthesis and proteomic expression of Microcystis aeruginosa during CuSO4 treatment. Aquatic Toxicology 222, 105473.
Jiao, J.J., Wang, Y., Cherry, J.A., Wang, X., Zhi, B., Du, H. and Wen, D. 2010. Abnormally high ammonium of natural origin in a coastal aquifer-aquitard system in the Pearl River Delta, China. Environmental science & technology 44(19), 7470-7475.
Kang, L., Mucci, M., Fang, J. and Lürling, M. 2022. New is not always better: Toxicity of novel copper based algaecides to Daphnia magna. Ecotoxicology and Environmental Safety 241, 113817.
Kar, S. and Roy, K. 2012. Risk assessment for ecotoxicity of pharmaceuticals–an emerging issue. Expert opinion on drug safety 11(2), 235-274.
Kergoat, L., Besse-Hoggan, P., Leremboure, M., Beguet, J., Devers, M., Martin-Laurent, F., Masson, M., Morin, S., Roinat, A. and Pesce, S. 2021. Environmental concentrations of sulfonamides can alter bacterial structure and induce diatom deformities in freshwater biofilm communities. Frontiers in microbiology 12, 643719.
Kidd, K.A., Backhaus, T., Brodin, T., Inostroza, P.A. and McCallum, E.S. 2024. Environmental risks of pharmaceutical mixtures in aquatic ecosystems: Reflections on a decade of research. Environmental Toxicology and Chemistry 43(3), 549-558.
Kienle, C., Vermeirssen, E.L., Schifferli, A., Singer, H., Stamm, C. and Werner, I. 2019. Effects of treated wastewater on the ecotoxicity of small streams–Unravelling the contribution of chemicals causing effects. PloS one 14(12), e0226278.
Kim, H.Y., Jeon, J., Hollender, J., Yu, S. and Kim, S.D. 2014. Aqueous and dietary bioaccumulation of antibiotic tetracycline in D. magna and its multigenerational transfer. Journal of hazardous materials 279, 428-435.
Kim, H.Y., Lee, M.J., Yu, S.H. and Kim, S.D. 2012. The individual and population effects of tetracycline on Daphnia magna in multigenerational exposure. Ecotoxicology 21, 993-1002.
Kim, S.-C. and Carlson, K. 2007. Temporal and spatial trends in the occurrence of human and veterinary antibiotics in aqueous and river sediment matrices. Environmental science & technology 41(1), 50-57.
Klimek, D., Herold, M. and Calusinska, M. 2024. Comparative genomic analysis of Planctomycetota potential for polysaccharide degradation identifies biotechnologically relevant microbes. BMC genomics 25(1), 523.
Klump, J.V., Fitzgerald, S.A. and Waplesa, J.T. 2009. Benthic biogeochemical cycling, nutrient stoichiometry, and carbon and nitrogen mass balances in a eutrophic freshwater bay. Limnology and Oceanography 54(3), 692-712.
Klüpfel, L., Piepenbrock, A., Kappler, A. and Sander, M. 2014. Humic substances as fully regenerable electron acceptors in recurrently anoxic environments. Nature Geoscience 7(3), 195-200.
Knights, D., Kuczynski, J., Charlson, E.S., Zaneveld, J., Mozer, M.C., Collman, R.G., Bushman, F.D., Knight, R. and Kelley, S.T. 2011. Bayesian community-wide culture-independent microbial source tracking. Nature methods 8(9), 761-763.
Kobayashi, N., Tsuchiya, Y., Kosugi, Y. and Suzuki, T. 2025. Occurrence and fate of pharmaceuticals and personal care products in river water, lake water, sewage effluent, tap water, and groundwater in Japan. Environmental Toxicology and Chemistry, vgaf261.

Kock, A., Glanville, H., Law, A., Stanton, T., Carter, L. and Taylor, J. 2023. Emerging challenges of the impacts of pharmaceuticals on aquatic ecosystems: A diatom perspective. Science of the Total Environment 878, 162939.

Kovacevic, V., Simpson, A.J. and Simpson, M.J. 2019. The concentration of dissolved organic matter impacts the metabolic response in Daphnia magna exposed to 17α-ethynylestradiol and perfluorooctane sulfonate. Ecotoxicology and Environmental Safety 170, 468-478.

Kovalakova, P., Cizmas, L., McDonald, T.J., Marsalek, B., Feng, M. and Sharma, V.K. 2020. Occurrence and toxicity of antibiotics in the aquatic environment: A review. Chemosphere 251, 126351.

Kowalewska, A.A., Krebs, N., Tollrian, R. and Weiss, L.C. 2020. Elevated pCO2 affects behavioural patterns and mechano-sensation in predatory phantom midge larvae Chaoborus obscuripes. Sci Rep 10(1), 1800.

Kråkström, M., Saeid, S., Tolvanen, P., Kumar, N., Salmi, T., Kronberg, L. and Eklund, P. 2020. Ozonation of carbamazepine and its main transformation products: product determination and reaction mechanisms. Environmental Science and Pollution Research 27(18), 23258-23269.

Kristensen, E., Ahmed, S.I. and Devol, A.H. 1995. Aerobic and anaerobic decomposition of organic matter in marine sediment: which is fastest? Limnology and oceanography 40(8), 1430-1437.

Kronimus, A., Schwarzbauer, J., Dsikowitzky, L., Heim, S. and Littke, R. 2004. Anthropogenic organic contaminants in sediments of the Lippe river, Germany. Water research 38(16), 3473-3484.

Krumperman, P.H. 1983. Multiple antibiotic resistance indexing of Escherichia coli to identify high-risk sources of fecal contamination of foods. Applied and environmental microbiology 46(1), 165-170.

Kumar, S., Paul, T., Shukla, S., Kumar, K., Karmakar, S. and Bera, K.K. 2021. Biomarkers-based assessment of triclosan toxicity in aquatic environment: a mechanistic review. Environmental Pollution 286, 117569.

Lagesson, A., Fahlman, J., Brodin, T., Fick, J., Jonsson, M., Byström, P. and Klaminder, J. 2016. Bioaccumulation of five pharmaceuticals at multiple trophic levels in an aquatic food web-Insights from a field experiment. Science of the Total Environment 568, 208-215.

Lai, R., Liu, X., Hu, S., Xiao, H., Xia, F., Feng, L. and Li, H. 2022. Raindrop size distribution characteristic differences during the dry and wet seasons in South China. Atmospheric Research 266, 105947.

Lapworth, D., Gooddy, D., Allen, D. and Old, G. 2009. Understanding groundwater, surface water, and hyporheic zone biogeochemical processes in a Chalk catchment using fluorescence properties of dissolved and colloidal organic matter. Journal of Geophysical Research: Biogeosciences 114(G3).

Larsson, D.J. and Flach, C.-F. 2022. Antibiotic resistance in the environment. Nature Reviews Microbiology 20(5), 257-269.

Lawrence, J., Topp, E., Waiser, M., Tumber, V., Roy, J., Swerhone, G., Leavitt, P., Paule, A. and Korber, D. 2015. Resilience and recovery: the effect of triclosan exposure timing during development, on the structure and function of river biofilm communities. Aquatic Toxicology 161, 253-266.

Laxminarayan, R., Matsoso, P., Pant, S., Brower, C., Røttingen, J.-A., Klugman, K. and Davies, S. 2016. Access to effective antimicrobials: a worldwide challenge. The Lancet 387(10014), 168-175.

Li, D., Gao, J., Dai, H., Wang, Z. and Duan, W. 2020a. Long-term responses of antibiotic resistance genes under high concentration of enrofloxacin, sulfadiazine and triclosan in aerobic granular sludge system. Bioresource technology 312, 123567.

Li, J., Haffner, G.D., Paterson, G., Walters, D.M., Burtnyk, M.D. and Drouillard, K.G. 2018. Importance of growth rate on mercury and polychlorinated biphenyl bioaccumulation in fish. Environmental Toxicology and Chemistry 37(6), 1655-1667.

Li, L.-L., Huang, L.-D., Chung, R.-S., Ka-Hang, F. and Zhang, Y.-S. 2010. Sorption and dissipation of tetracyclines in soils and compost. Pedosphere 20(6), 807-816.

Li, M., Liu, Q., Teng, Y., Ou, L., Xi, Y., Chen, S. and Duan, G. 2019. The resistance mechanism of Escherichia coli induced by ampicillin in laboratory. Infection and Drug Resistance 12(null), 2853-2863.

Li, W., Gao, L., Shi, Y., Liu, J. and Cai, Y. 2015a. Occurrence, distribution and risks of antibiotics in urban surface water in Beijing, China. Environ Sci Process Impacts 17(9), 1611-1619.

Li, X., Atwill, E.R., Antaki, E., Applegate, O., Bergamaschi, B., Bond, R.F., Chase, J., Ransom, K.M., Samuels, W. and Watanabe, N. 2015b. Fecal indicator and pathogenic bacteria and their antibiotic resistance in alluvial groundwater of an irrigated agricultural region with dairies. Journal of environmental quality 44(5), 1435-1447.

Li, Y.-L., He, W., Liu, W.-X., Kong, X.-Z., Yang, B., Yang, C. and Xu, F.-L. 2015c. Influences of binding to dissolved organic matter on hydrophobic organic compounds in a multi-contaminant system: Coefficients, mechanisms and ecological risks. Environmental pollution 206, 461-468.

Li, Y., Ma, Y., Yang, L., Duan, S., Zhou, F., Chen, J., Liu, Y. and Zhang, B. 2020b. Effects of azithromycin on feeding behavior and nutrition accumulation of Daphnia magna under the different exposure pathways. Ecotoxicology and environmental safety 197, 110573.

Li, Z., Li, M., Zhang, Z., Li, P., Zang, Y. and Liu, X. 2020c. Antibiotics in aquatic environments of China: A review and meta-analysis. Ecotoxicol Environ Saf 199, 110668.

Li, Z., Lu, T., Li, M., Mortimer, M. and Guo, L.-H. 2023. Direct and gut microbiota-mediated toxicities of environmental antibiotics to fish and aquatic invertebrates. Chemosphere 329, 138692.
Li, Z., Xiang, X., Li, M., Ma, Y., Wang, J. and Liu, X. 2015d. Occurrence and risk assessment of pharmaceuticals and personal care products and endocrine disrupting chemicals in reclaimed water and receiving groundwater in China. Ecotoxicology and environmental safety 119, 74-80.
Liao, W., Tong, D., Li, Z., Nie, X., Liu, Y., Ran, F. and Liao, S. 2021. Characteristics of microbial community composition and its relationship with carbon, nitrogen and sulfur in sediments. Science of the Total Environment 795, 148848.
Lim, S., Shi, J.L., von Gunten, U. and McCurry, D.L. 2022. Ozonation of organic compounds in water and wastewater: A critical review. Water Research 213, 118053.
Liu, J., Lu, G., Wang, Y., Yan, Z., Yang, X., Ding, J. and Jiang, Z. 2014. Bioconcentration, metabolism, and biomarker responses in freshwater fish Carassius auratus exposed to roxithromycin. Chemosphere 99, 102-108.
Liu, S., Zhao, H., Lehmler, H.-J., Cai, X. and Chen, J. 2017a. Antibiotic pollution in marine food webs in Laizhou Bay, North China: trophodynamics and human exposure implication. Environmental science & technology 51(4), 2392-2400.
Liu, X., Lu, S., Guo, W., Xi, B. and Wang, W. 2018. Antibiotics in the aquatic environments: A review of lakes, China. Science of The Total Environment 627, 1195-1208.
Liu, Y., Chen, S., Zhang, J., Li, X. and Gao, B. 2017b. Stimulation effects of ciprofloxacin and sulphamethoxazole in Microcystis aeruginosa and isobaric tag for relative and absolute quantitation-based screening of antibiotic targets. Molecular Ecology 26(2), 689-701.
Loftin, K.A., Henny, C., Adams, C.D., Surampali, R. and Mormile, M.R. 2005. Inhibition of microbial metabolism in anaerobic lagoons by selected sulfonamides, tetracyclines, lincomycin, and tylosin tartrate. Environmental Toxicology and Chemistry 24(4), 782-788.
Lolas, I.B., Chen, X., Bester, K. and Nielsen, J.L. 2012. Identification of triclosan-degrading bacteria using stable isotope probing, fluorescence in situ hybridization and microautoradiography. Microbiology 158(11), 2796-2804.
Lonappan, L., Brar, S.K., Das, R.K., Verma, M. and Surampalli, R.Y. 2016. Diclofenac and its transformation products: environmental occurrence and toxicity-a review. Environment international 96, 127-138.
Long, S., Hamilton, P.B., Wang, C., Li, C., Xue, X., Zhao, Z., Wu, P., Gu, E., Uddin, M.M. and Li, B. 2024. Bioadsorption, bioaccumulation and biodegradation of antibiotics by algae and their association with algal physiological state and antibiotic physicochemical properties. Journal of Hazardous Materials 468, 133787.
Lu, S., Wang, N., Ma, S., Hu, X., Kang, L. and Yu, Y. 2019. Parabens and triclosan in shellfish from Shenzhen coastal waters: bioindication of pollution and human health risks. Environmental pollution 246, 257-263.
Luo, Y., Guo, W., Ngo, H.H., Nghiem, L.D., Hai, F.I., Zhang, J., Liang, S. and Wang, X.C. 2014. A review on the occurrence of micropollutants in the aquatic environment and their fate and removal during wastewater treatment. Science of the total environment 473, 619-641.
Lyu, T., Zhu, J., Yang, X., Yang, W. and Zheng, Z. 2022. Responses of gut microbial community composition and function of the freshwater gastropod Bellamya aeruginosa to cyanobacterial bloom. Frontiers in Microbiology 13, 906278.
Ma, Y., Wang, J., Liu, Y., Wang, X., Zhang, B., Zhang, W., Chen, T., Liu, G., Xue, L. and Cui, X. 2023. Nocardioides:"specialists" for hard-to-degrade pollutants in the environment. Molecules 28(21), 7433.
Mackay, D., Arnot, J.A., Gobas, F.A. and Powell, D.E. 2013. Mathematical relationships between metrics of chemical bioaccumulation in fish. Environmental toxicology and chemistry 32(7), 1459-1466.
Mackay, D. and Fraser, A. 2000. Bioaccumulation of persistent organic chemicals: mechanisms and models. Environmental pollution 110(3), 375-391.
Maes, H.M., Maletz, S.X., Ratte, H.T., Hollender, J. and Schaeffer, A. 2014. Uptake, elimination, and biotransformation of 17α-ethinylestradiol by the freshwater alga Desmodesmus subspicatus. Environmental science & technology 48(20), 12354-12361.
Magdeburg, A., Stalter, D., Schlüsener, M., Ternes, T. and Oehlmann, J. 2014. Evaluating the efficiency of advanced wastewater treatment: target analysis of organic contaminants and (geno-) toxicity assessment tell a different story. Water Research 50, 35-47.
Magiorakos, A.-P., Srinivasan, A., Carey, R.B., Carmeli, Y., Falagas, M., Giske, C., Harbarth, S., Hindler, J., Kahlmeter, G. and Olsson-Liljequist, B. 2012. Multidrug-resistant, extensively drug-resistant and pandrug-resistant bacteria: an international expert proposal for interim standard definitions for acquired resistance. Clinical microbiology and infection 18(3), 268-281.
Margot, J., Kienle, C., Magnet, A., Weil, M., Rossi, L., de Alencastro, L.F., Abegglen, C., Thonney, D., Chèvre, N. and Schärer, M. 2013. Treatment of micropollutants in municipal wastewater: ozone or powdered activated carbon? Science of the total environment 461, 480-498.
Margot, J., Rossi, L., Barry, D.A. and Holliger, C. 2015. A review of the fate of micropollutants in wastewater treatment plants. Wiley Interdisciplinary Reviews: Water 2(5), 457-487.

Martin, E.K., Kemal, S., Henrik, N.R., Alexander, E., Natalia, C., Henrik, J.C., Thomas, B., Hans, B. and Erik, K. 2020. Triclosan changes community composition and selects for specific bacterial taxa in marine periphyton biofilms in low nanomolar concentrations. Ecotoxicology 29(7), 1083-1094.

Martinez, J.L. 2009. Environmental pollution by antibiotics and by antibiotic resistance determinants. Environmental pollution 157(11), 2893-2902.

Matesun, J., Petrik, L., Musvoto, E., Ayinde, W. and Ikumi, D. 2024. Limitations of wastewater treatment plants in removing trace anthropogenic biomarkers and future directions: A review. Ecotoxicology and Environmental Safety 281, 116610.

Mayer, P., Parkerton, T.F., Adams, R.G., Cargill, J.G., Gan, J., Gouin, T., Gschwend, P.M., Hawthorne, S.B., Helm, P. and Witt, G. 2014. Passive sampling methods for contaminated sediments: Scientific rationale supporting use of freely dissolved concentrations. Integrated environmental assessment and management 10(2), 197-209.

McClellan, K. and Halden, R.U. 2010. Pharmaceuticals and personal care products in archived US biosolids from the 2001 EPA national sewage sludge survey. Water research 44(2), 658-668.

McFadden, G.I. and Roos, D.S. 1999. Apicomplexan plastids as drug targets. Trends in Microbiology 7(8), 328-333.

McMurdie, P.J. and Holmes, S. 2013. phyloseq: an R package for reproducible interactive analysis and graphics of microbiome census data. PloS one 8(4), e61217.

McNamara, P.J., LaPara, T.M. and Novak, P.J. 2014. The impacts of triclosan on anaerobic community structures, function, and antimicrobial resistance. Environmental science & technology 48(13), 7393-7400.

Medici, A., Siciliano, A., Libralato, G., Saviano, L., Guida, M., Pedatella, S., Luongo, G., Di Fabio, G. and Zarrelli, A. 2024. Percarbonate mediated advanced oxidation of irbesartan: A suitable alternative to chlorination? Science of The Total Environment 947, 174730.

Meena, R.S., Vijayakumar, V., Yadav, G.S. and Mitran, T. 2018. Response and interaction of Bradyrhizobium japonicum and arbuscular mycorrhizal fungi in the soybean rhizosphere. Plant Growth Regulation 84, 207-223.

Mejia, F.H., Fremier, A.K., Benjamin, J.R., Bellmore, J.R., Grimm, A.Z., Watson, G.A. and Newsom, M. 2019. Stream metabolism increases with drainage area and peaks asynchronously across a stream network. Aquatic Sciences 81(1), 9.

Melchiorri, D., Rocke, T., Alm, R.A., Cameron, A.M. and Gigante, V. 2025. Addressing urgent priorities in antibiotic development: insights from WHO 2023 antibacterial clinical pipeline analyses. The Lancet Microbe 6(3).

Metcalf and Eddy, A. (2014) Wastewater engineering treatment and resource recovery, McGraw-Hill Education.

Michael, I., Rizzo, L., McArdell, C., Manaia, C., Merlin, C., Schwartz, T., Dagot, C. and Fatta-Kassinos, D. 2013. Urban wastewater treatment plants as hotspots for the release of antibiotics in the environment: a review. Water research 47(3), 957-995.

Milanović, M., Đurić, L., Milošević, N. and Milić, N. 2023. Comprehensive insight into triclosan—from widespread occurrence to health outcomes. Environmental Science and Pollution Research 30(10), 25119-25140.

Miller, T.H., Bury, N.R., Owen, S.F., MacRae, J.I. and Barron, L.P. 2018. A review of the pharmaceutical exposome in aquatic fauna. Environmental pollution 239, 129-146.

Miller, T.H., McEneff, G.L., Stott, L.C., Owen, S.F., Bury, N.R. and Barron, L.P. 2016. Assessing the reliability of uptake and elimination kinetics modelling approaches for estimating bioconcentration factors in the freshwater invertebrate, Gammarus pulex. Science of The Total Environment 547, 396-404.

Mo, L., Yang, Q., Hou, Y., Jiang, F., Dai, J., Li, X. and Qin, L. 2025. Oxidative stress mechanisms underlying temporal hormesis effects induced by binary antibiotic mixtures on Scenedesmus obliquus. Ecotoxicology and Environmental Safety 291, 117889.

Monteiro, S.C. and Boxall, A.B. 2010. Occurrence and fate of human pharmaceuticals in the environment. Reviews of environmental contamination and toxicology, 53-154.

Montoya, J.M., Pimm, S.L. and Solé, R.V. 2006. Ecological networks and their fragility. Nature 442(7100), 259-264.

Motiei, A., Brindefalk, B., Ogonowski, M., El-Shehawy, R., Pastuszek, P., Ek, K., Liewenborg, B., Udekwu, K. and Gorokhova, E. 2020. Disparate effects of antibiotic-induced microbiome change and enhanced fitness in Daphnia magna. PloS one 15(1), e0214833.

Mulchandani, R., Wang, Y., Gilbert, M. and Van Boeckel, T.P. 2023. Global trends in antimicrobial use in food-producing animals: 2020 to 2030. PLOS Global Public Health 3(2), e0001305.

Mulla, S.I., Bagewadi, Z.K., Faniband, B., Bilal, M., Chae, J.-C., Bankole, P.O., Saratale, G.D., Bhargava, R.N. and Gurumurthy, D.M. 2023. Various strategies applied for the removal of emerging micropollutant sulfamethazine: a systematic review. Environmental Science and Pollution Research 30(28), 71599-71613.

Müller, A., Weiss, S.C., Beißwenger, J., Leukhardt, H.G., Schulz, W., Seitz, W., Ruck, W.K. and Weber, W.H. 2012. Identification of ozonation by-products of 4-and 5-methyl-1H-benzotriazole during the treatment of surface water to drinking water. Water research 46(3), 679-690.
Murray, C.J., Ikuta, K.S., Sharara, F., Swetschinski, L., Aguilar, G.R., Gray, A., Han, C., Bisignano, C., Rao, P. and Wool, E. 2022. Global burden of bacterial antimicrobial resistance in 2019: a systematic analysis. The lancet 399(10325), 629-655.
Nam, S.-W., Choi, D.-J., Kim, S.-K., Her, N. and Zoh, K.-D. 2014. Adsorption characteristics of selected hydrophilic and hydrophobic micropollutants in water using activated carbon. Journal of hazardous materials 270, 144-152.
Nesme, J., Cécillon, S., Delmont, T.O., Monier, J.-M., Vogel, T.M. and Simonet, P. 2014. Large-scale metagenomic-based study of antibiotic resistance in the environment. Current biology 24(10), 1096-1100.
Newton, R.J., Jones, S.E., Eiler, A., McMahon, K.D. and Bertilsson, S. 2011. A guide to the natural history of freshwater lake bacteria. Microbiology and molecular biology reviews 75(1), 14-49.
Nguyen, L.N., Commault, A.S., Kahlke, T., Ralph, P.J., Semblante, G.U., Johir, M.A.H. and Nghiem, L.D. 2020. Genome sequencing as a new window into the microbial community of membrane bioreactors–A critical review. Science of the Total Environment 704, 135279.
Nguyen, T.-D., Itayama, T., Ramaraj, R., Iwami, N., Shimizu, K., Dao, T.-S., Pham, T.-L. and Maseda, H. 2021. Chronic ecotoxicology and statistical investigation of ciprofloxacin and ofloxacin to Daphnia magna under extendedly long-term exposure. Environmental Pollution 291, 118095.
Nietch, C.T., Quinlan, E.L., Lazorchak, J.M., Impellitteri, C.A., Raikow, D. and Walters, D. 2013. Effects of a chronic lower range of triclosan exposure on a stream mesocosm community. Environmental Toxicology and Chemistry 32(12), 2874-2887.
Nilsson, F., Ekblad, M., la Cour Jansen, J. and Jönsson, K. 2017. Removal of pharmaceuticals with ozone at 10 Swedish wastewater treatment plants. Water Practice & Technology 12(4), 871-881.
Nógrády, N., Pászti, J., Pikó, H. and Nagy, B. 2006. Class 1 integrons and their conjugal transfer with and without virulence-associated genes in extra-intestinal and intestinal Escherichia coli of poultry. Avian pathology 35(4), 349-356.
Nwakoby, I., Iheukwumere, I., Iheukwumere, C., Nwakoby, N., Idigo, M. and Ike, V. 2025. Antimicrobial Resistance: A Legal and Public Health Perspective. IPS Journal of Applied Microbiology and Biotechnology 4(4), 230-236.
OECD 2011. Test No. 201: Freshwater Alga and Cyanobacteria, Growth Inhibition Test. OECD Guidelines for the Testing of Chemicals Section 2(Paris).
OECD 2019. Pharmaceutical Residues in Freshwater: Hazards and Policy Responses. OECD Studies on Water (OECD Publishing, Paris).
OECD (2021) Guidance Document on Aquatic and Sediment Toxicological Testing of Nanomaterials.
OECD 2023. Test No. 218: Sediment-Water Chironomid Toxicity Using Spiked Sediment, OECD Guidelines for the Testing of Chemicals, Section 2. OECD Publishing, Paris.
Oluwole, A.O., Omotola, E.O. and Olatunji, O.S. 2020. Pharmaceuticals and personal care products in water and wastewater: a review of treatment processes and use of photocatalyst immobilized on functionalized carbon in AOP degradation. BMC chemistry 14(1), 62.
Onesios, K.M., Yu, J.T. and Bouwer, E.J. 2009. Biodegradation and removal of pharmaceuticals and personal care products in treatment systems: a review. Biodegradation 20(4), 441-466.
Park, K.-Y., Choi, S.-Y., Lee, S.-H., Kweon, J.-H. and Song, J.-H. 2016. Comparison of formation of disinfection by-products by chlorination and ozonation of wastewater effluents and their toxicity to Daphnia magna. Environmental Pollution 215, 314-321.
Pashaei, R., Zahedipour-Sheshglani, P., Dzingelevičienė, R., Abbasi, S. and Rees, R.M. 2022. Effects of pharmaceuticals on the nitrogen cycle in water and soil: a review. Environmental Monitoring and Assessment 194(2), 105.
Paumelle, M., Donnadieu, F., Joly, M., Besse-Hoggan, P. and Artigas, J. 2021. Effects of sulfonamide antibiotics on aquatic microbial community composition and functions. Environment international 146, 106198.
Pavlaki, M.D., Ferreira, A.L., Soares, A.M. and Loureiro, S. 2014. Changes of chemical chronic toxicity to Daphnia magna under different food regimes. Ecotoxicology and Environmental Safety 109, 48-55.
Peng, F.-J., Diepens, N.J., Pan, C.-G., Ying, G.-G., Salvito, D., Selck, H. and Van den Brink, P.J. 2019. Response of sediment bacterial community to triclosan in subtropical freshwater benthic microcosms. Environmental Pollution 248, 676-683.
Periša, M., Babić, S., Škorić, I., Frömel, T. and Knepper, T.P. 2013. Photodegradation of sulfonamides and their N 4-acetylated metabolites in water by simulated sunlight irradiation: kinetics and identification of photoproducts. Environmental Science and Pollution Research 20, 8934-8946.
Pesce, S., Kergoat, L., Paris, L., Billet, L., Besse-Hoggan, P. and Bonnineau, C. 2021. Contrasting effects of environmental concentrations of sulfonamides on microbial heterotrophic activities in freshwater sediments. Frontiers in Microbiology 12, 753647.

Petrie, B., Barden, R. and Kasprzyk-Hordern, B. 2015. A review on emerging contaminants in wastewaters and the environment: current knowledge, understudied areas and recommendations for future monitoring. Water research 72, 3-27.

Picinini-Zambelli, J., Garcia, A.L.H. and Da Silva, J. 2025. Emerging pollutants in the aquatic environments: A review of genotoxic impacts. Mutation Research-Reviews in Mutation Research 795, 108519.

Pikkemaat, M., Yassin, H., Fels-Klerx, H. and Berendsen, B. 2016 Antibiotic residues and resistance in the environment, RIKILT.

Pino-Otín, M.R., Lorca, G., Langa, E., Roig, F., Terrado, E.M. and Ballestero, D. 2023. Assessing the ecotoxicity of eight widely used antibiotics on river microbial communities. International Journal of Molecular Sciences 24(23), 16960.

Pistocchi, A., Andersen, H., Bertanza, G., Brander, A., Choubert, J.-M., Cimbritz, M., Drewes, J.E., Koehler, C., Krampe, J. and Launay, M. 2022. Treatment of micropollutants in wastewater: Balancing effectiveness, costs and implications. Science of the Total Environment 850, 157593.

Poncheewin, W., Hermes, G.D., Van Dam, J.C., Koehorst, J.J., Smidt, H. and Schaap, P.J. 2020. NG-Tax 2.0: a semantic framework for high-throughput amplicon analysis. Frontiers in Genetics 10, 1366.

Posthuma, L. and de Zwart, D. 2012. Predicted mixture toxic pressure relates to observed fraction of benthic macrofauna species impacted by contaminant mixtures. Environmental Toxicology and Chemistry 31(9), 2175-2188.

Pruden, A., Pei, R., Storteboom, H. and Carlson, K.H. 2006. Antibiotic resistance genes as emerging contaminants: studies in northern Colorado. Environmental science & technology 40(23), 7445-7450.

Puri, B., Vaishya, R. and Vaish, A. 2025. Antimicrobial resistance: Current challenges and future directions. Medical Journal Armed Forces India 81(3), 247-258.

Qiu, W., Sun, J., Fang, M., Luo, S., Tian, Y., Dong, P., Xu, B. and Zheng, C. 2019. Occurrence of antibiotics in the main rivers of Shenzhen, China: Association with antibiotic resistance genes and microbial community. Sci Total Environ 653, 334-341.

Quinlan, E.L., Nietch, C.T., Blocksom, K., Lazorchak, J.M., Batt, A.L., Griffiths, R. and Klemm, D.J. 2011. Temporal dynamics of periphyton exposed to tetracycline in stream mesocosms. Environmental science & technology 45(24), 10684-10690.

R Core Team 2024. R: A language and environment for statistical computing. R Foundation for Statistical Computing, Vienna, Austria.

Ratier, A., Lopes, C., Multari, G., Mazerolles, V., Carpentier, P. and Charles, S. 2021. New perspectives on the calculation of bioaccumulation metrics for active substances in living organisms. Integrated Environmental Assessment and Management 18(1), 10-18.

Ren, B., Li, C., Zhang, X. and Zhang, Z. 2019. Fe (II)-dosed ceramic membrane bioreactor for wastewater treatment: Nutrient removal, microbial community and membrane fouling analysis. Science of the Total Environment 664, 116-126.

Ricart, M., Guasch, H., Alberch, M., Barceló, D., Bonnineau, C., Geiszinger, A., Ferrer, J., Ricciardi, F., Romaní, A.M. and Morin, S. 2010. Triclosan persistence through wastewater treatment plants and its potential toxic effects on river biofilms. Aquatic Toxicology 100(4), 346-353.

Rico, A., Dimitrov, M.R., Van Wijngaarden, R.P., Satapornvanit, K., Smidt, H. and Van den Brink, P.J. 2014. Effects of the antibiotic enrofloxacin on the ecology of tropical eutrophic freshwater microcosms. Aquatic Toxicology 147, 92-104.

Robinson, A.A., Belden, J.B. and Lydy, M.J. 2005. Toxicity of fluoroquinolone antibiotics to aquatic organisms. Environmental toxicology and Chemistry 24(2), 423-430.

Ruprecht, J., Birrer, S., Dafforn, K., Mitrovic, S., Crane, S., Johnston, E., Wemheuer, F., Navarro, A., Harrison, A. and Turner, I. 2021. Wastewater effluents cause microbial community shifts and change trophic status. Water research 200, 117206.

Sanganyado, E., Bi, R., Teta, C., Buruaem Moreira, L., Yu, X., Yajing, S., Dalu, T., Rajput, I.R. and Liu, W. 2021. Toward an integrated framework for assessing micropollutants in marine mammals: Challenges, progress, and opportunities. Critical Reviews in Environmental Science and Technology 51(23), 2824-2871.

Sansupa, C., Wahdan, S.F.M., Hossen, S., Disayathanoowat, T., Wubet, T. and Purahong, W. 2021. Can we use functional annotation of prokaryotic taxa (FAPROTAX) to assign the ecological functions of soil bacteria? Applied Sciences 11(2), 688.

Santos, L.H., Araújo, A.N., Fachini, A., Pena, A., Delerue-Matos, C. and Montenegro, M. 2010. Ecotoxicological aspects related to the presence of pharmaceuticals in the aquatic environment. Journal of hazardous materials 175(1-3), 45-95.

Sanusi, I.O., Olutona, G.O., Wawata, I.G. and Onohuean, H. 2023. Occurrence, environmental impact and fate of pharmaceuticals in groundwater and surface water: a critical review. Environmental Science and Pollution Research 30(39), 90595-90614.

Saunders, L.J. and Nichols, J.W. 2023. Models used to predict chemical bioaccumulation in fish from in vitro biotransformation rates require accurate estimates of blood–water partitioning and chemical volume of distribution. Environmental toxicology and chemistry 42(1), 33-45.

Schindler, D.W., Carpenter, S.R., Chapra, S.C., Hecky, R.E. and Orihel, D.M. 2016. Reducing phosphorus to curb lake eutrophication is a success. Environmental science & technology 50(17), 8923-8929.
Schuijt, L.M., Peng, F.-J., van den Berg, S.J., Dingemans, M.M. and Van den Brink, P.J. 2021. (Eco) toxicological tests for assessing impacts of chemical stress to aquatic ecosystems: facts, challenges, and future. Science of the total environment 795, 148776.
Schuijt, L.M., van Drimmelen, C.K., Buijse, L.L., van Smeden, J., Wu, D., Boerwinkel, M.-C., Belgers, D.J., Matser, A.M., Roessink, I. and Beentjes, K.K. 2024a. Assessing ecological responses to exposure to the antibiotic sulfamethoxazole in freshwater mesocosms. Environmental Pollution 343, 123199.
Schuijt, L.M., van Drimmelen, C.K.E., Buijse, L.L., van Smeden, J., Wu, D., Boerwinkel, M.-C., Belgers, D.J.M., Matser, A.M., Roessink, I., Beentjes, K.K., Trimbos, K.B., Smidt, H. and Van den Brink, P.J. 2024b. Assessing ecological responses to exposure to the antibiotic sulfamethoxazole in freshwater mesocosms. Environmental Pollution 343, 123199.
Schunck, F. and Liess, M. 2023. Ultra-low Esfenvalerate concentrations increase biomass and may reduce competitiveness of Daphnia magna populations. Science of The Total Environment 886, 163916.
Schüürmann, G., Ebert, R.-U., Nendza, M., Dearden, J., Paschke, A. and Kühne, R. (2007) Risk assessment of chemicals: an introduction, pp. 375-426, Springer.
Schwarz, S., Gildemeister, D., Hein, A., Schröder, P. and Bachmann, J. 2021. Environmental fate and effects assessment of human pharmaceuticals: lessons learnt from regulatory data. Environmental Sciences Europe 33(1), 68.
Senta, I., Terzic, S. and Ahel, M. 2013. Occurrence and fate of dissolved and particulate antimicrobials in municipal wastewater treatment. Water research 47(2), 705-714.
Sidjabat, H.E. and Paterson, D.L. 2015. Multidrug-resistant Escherichia coli in Asia: epidemiology and management. Expert review of anti-infective therapy 13(5), 575-591.
Sijm, D.T., Broersen, K.W., de Roode, D.F. and Mayer, P. 1998. Bioconcentration kinetics of hydrophobic chemicals in different densities of Chlorella pyrenoidosa. Environmental Toxicology and Chemistry 17(9), 1695-1704.
Simčič, T. and Brancelj, A. 1997. Electron transport system (ETS) activity and respiration rate in five Daphnia species at different temperatures. Hydrobiologia 360(1), 117-125.
Slipko, K., Reif, D., Schaar, H., Saracevic, E., Klinger, A., Wallmann, L., Krampe, J., Woegerbauer, M., Hufnagl, P. and Kreuzinger, N. 2022. Advanced wastewater treatment with ozonation and granular activated carbon filtration: inactivation of antibiotic resistance targets in a long-term pilot study. Journal of Hazardous Materials 438, 129396.
Sokołowski, A., Mordec, M., Caban, M., Øverjordet, I.B., Wielogórska, E., Włodarska-Kowalczuk, M., Balazy, P., Chełchowski, M. and Lepoint, G. 2024. Bioaccumulation of pharmaceuticals and stimulants in macrobenthic food web in the European Arctic as determined using stable isotope approach. Science of the Total Environment 909, 168557.
Song, C., Zhang, K.-X., Wang, X.-J., Zhao, S. and Wang, S.-G. 2021. Effects of natural organic matter on the photolysis of tetracycline in aquatic environment: kinetics and mechanism. Chemosphere 263, 128338.
Stanley, J.K., Perkins, E.J., Habib, T., Sims, J.G., Chappell, P., Escalon, B.L., Wilbanks, M. and Garcia-Reyero, N. 2013. The good, the bad, and the toxic: approaching hormesis in Daphnia magna exposed to an energetic compound. Environmental science & technology 47(16), 9424-9433.
Sui, Q., Cao, X., Lu, S., Zhao, W., Qiu, Z. and Yu, G. 2015. Occurrence, sources and fate of pharmaceuticals and personal care products in the groundwater: a review. Emerging Contaminants 1(1), 14-24.
Sun, M., Li, J., Zhai, Q., Ge, Q., Li, J., Zhao, F., Chang, Z. and He, Y. 2016. Environmental fate and pharmacokinetics of sulphamethazine in Fenneropenaeus chinensis shrimp production systems after oral administration. Aquaculture Research 47(11), 3526-3537.
Szmolka, A. and Nagy, B. 2013. Multidrug resistant commensal Escherichia coli in animals and its impact for public health. Frontiers in microbiology 4, 258.
Tan, W. and Xi, B. 2025. Silent crisis in water: Navigating the labyrinth of antibiotic pollution and resistome spread for smart mitigation. Environmental Chemistry and Ecotoxicology.
Tang, J., Wang, S., Tai, Y., Tam, N.F., Su, L., Shi, Y., Luo, B., Tao, R., Yang, Y. and Zhang, X. 2020. Evaluation of factors influencing annual occurrence, bioaccumulation, and biomagnification of antibiotics in planktonic food webs of a large subtropical river in South China. Water Research 170, 115302.
Tang, J., Zhang, J., Su, L., Jia, Y. and Yang, Y. 2022a. Bioavailability and trophic magnification of antibiotics in aquatic food webs of Pearl River, China: Influence of physicochemical characteristics and biotransformation. Science of The Total Environment 820, 153285.
Tang, M., Zhou, S., Huang, J., Sun, L. and Lu, H. 2022b. Stress responses of sulfate-reducing bacteria sludge upon exposure to polyethylene microplastics. Water Research 220, 118646.
ter Braak, C.J. and Šmilauer, P. 2012. Canoco reference manual and user's guide: software for ordination, version 5.0.

Thaden, J.T., Fowler, V.G., Sexton, D.J. and Anderson, D.J. 2016. Increasing incidence of extended-spectrum β-lactamase-producing Escherichia coli in community hospitals throughout the southeastern United States. infection control & hospital epidemiology 37(1), 49-54.
Thakur, A., Dhammi, P., Saini, H. and Kaur, S. 2016. Effect of antibiotic on survival and development of Spodoptera litura (Lepidoptera: Noctuidae) and its gut microbial diversity. Bulletin of Entomological Research 106(3), 387-394.
Ushiki, N., Jinno, M., Fujitani, H., Suenaga, T., Terada, A. and Tsuneda, S. 2017. Nitrite oxidation kinetics of two Nitrospira strains: the quest for competition and ecological niche differentiation. Journal of bioscience and bioengineering 123(5), 581-589.
Van den Brink, P.J. and Braak, C.J.T. 1999. Principal response curves: Analysis of time-dependent multivariate responses of biological community to stress. Environmental Toxicology and Chemistry 18(2), 138-148.
Van den Brink, P.J., Hattink, J., Bransen, F., Van Donk, E. and Brock, T.C. 2000. Impact of the fungicide carbendazim in freshwater microcosms. II. Zooplankton, primary producers and final conclusions. Aquatic Toxicology 48(2-3), 251-264.
Van den Brink, P.J., Tarazona, J.V., Solomon, K.R., Knacker, T., Van den Brink, N.W., Brock, T.C. and Hoogland, J. 2005. The use of terrestrial and aquatic microcosms and mesocosms for the ecological risk assessment of veterinary medicinal products. Environmental Toxicology and Chemistry 24(4), 820-829.
Van den Brink, P.J., Van Wijngaarden, R.P., Lucassen, W.G., Brock, T.C. and Leeuwangh, P. 1996. Effects of the insecticide Dursban® 4E (active ingredient chlorpyrifos) in outdoor experimental ditches: II. Invertebrate community responses and recovery. Environmental Toxicology and Chemistry: An International Journal 15(7), 1143-1153.
Van Gijn, K., Chen, Y., Van Oudheusden, B., Gong, S., De Wilt, H., Rijnaarts, H. and Langenhoff, A. 2021a. Optimizing biological effluent organic matter removal for subsequent micropollutant removal. Journal of Environmental Chemical Engineering 9(5), 106247.
Van Gijn, K., Sohier, J., Maasdam, R., De Wilt, H., Rijnaarts, H. and Langenhoff, A. 2021b. Optimizing micropollutant removal by ozonation; Interference of effluent organic matter fractions. Ozone: Science & Engineering 43(6), 579-591.
Van Gijn, K., Van Dam, M., De Wilt, H., de Wilde, V., Rijnaarts, H. and Langenhoff, A. 2023. Removal of micropollutants and ecotoxicity during combined biological activated carbon and ozone (BO3) treatment. Water Research 242, 120179.
Versteegen, E., Häkkinen, M., Wu, D., Heikamp-de Jong, I., Roessink, I., Peeters, E.T. and van den Brink, P.J. 2025. Effects of the drug carbamazepine on the structure and functioning of a freshwater aquatic ecosystem. Ecotoxicology and Environmental Safety 294, 118009.
Völker, J., Stapf, M., Miehe, U. and Wagner, M. 2019. Systematic review of toxicity removal by advanced wastewater treatment technologies via ozonation and activated carbon. Environmental Science & Technology 53(13), 7215-7233.
Von Gunten, U. 2003. Ozonation of drinking water: Part I. Oxidation kinetics and product formation. Water research 37(7), 1443-1467.
Wahome, C.N., Okemo, P.O. and Nyamache, A.K. 2014. Microbial quality and antibiotic resistant bacterial pathogens isolated from groundwater used by residents of Ongata Rongai, Kajiado North County, Kenya. International Journal of Biological and Chemical Sciences 8(1), 134-143.
Wang, C., Yang, H., Liu, H., Zhang, X.-X. and Ma, L. 2023. Anthropogenic contributions to antibiotic resistance gene pollution in household drinking water revealed by machine-learning-based source-tracking. Water Research 246, 120682.
Wang, H., Wu, X., Xu, J., Lu, Z., Hu, B., Zhu, L. and Lu, H. 2025. Proline Mitigates Antibiotic Resistance Evolution Induced by Ciprofloxacin at Environmental Concentrations. Journal of Hazardous Materials, 137561.
Wang, J., Chu, L., Wojnárovits, L. and Takács, E. 2020. Occurrence and fate of antibiotics, antibiotic resistant genes (ARGs) and antibiotic resistant bacteria (ARB) in municipal wastewater treatment plant: An overview. Science of the Total Environment 744, 140997.
Wang, J., Nolte, T.M., Owen, S.F., Beaudouin, R., Hendriks, A.J. and Ragas, A.M. 2022. A generalized physiologically based kinetic model for fish for environmental risk assessment of pharmaceuticals. Environmental Science & Technology 56(10), 6500-6510.
Wang, Q., Mitchell, R.-L., Hofman, R., Yu, J., Yang, M., Rietveld, L.C. and Zietzschmann, F. 2021. How properties of low molecular weight model competitors impact organic micropollutant adsorption onto activated carbon at realistically asymmetric concentrations. Water Research 202, 117443.
Wang, S. and Wang, H. 2015. Adsorption behavior of antibiotic in soil environment: a critical review. Frontiers of Environmental Science & Engineering 9, 565-574.
Wang, Y., Wen, Y., Li, J.J., He, J., Qin, W.C., Su, L.M. and Zhao, Y.H. 2014. Investigation on the relationship between bioconcentration factor and distribution coefficient based on class-based compounds: The factors that affect bioconcentration. Environmental toxicology and pharmacology 38(2), 388-396.

Warshan, D., Bay, G., Nahar, N., Wardle, D.A., Nilsson, M.-C. and Rasmussen, U. 2016. Seasonal variation in nifH abundance and expression of cyanobacterial communities associated with boreal feather mosses. The ISME journal 10(9), 2198-2208.

Wellard Kelly, H.A., Rosi-Marshall, E.J., Kennedy, T.A., Hall Jr, R.O., Cross, W.F. and Baxter, C.V. 2013. Macroinvertebrate diets reflect tributary inputs and turbidity-driven changes in food availability in the Colorado River downstream of Glen Canyon Dam. Freshwater Science 32(2), 397-410.

Wen, Y., He, J., Liu, X., Li, J. and Zhao, Y. 2012. Linear and non-linear relationships between bioconcentration and hydrophobicity: Theoretical consideration. Environmental Toxicology and Pharmacology 34(2), 200-208.

WHO (2014) Antimicrobial resistance: global report on surveillance, World Health Organization.

WHO 2023. Antimicrobial resistance report.

Wilkinson, J.L., Boxall, A.B., Kolpin, D.W., Leung, K.M., Lai, R.W., Galbán-Malagón, C., Adell, A.D., Mondon, J., Metian, M. and Marchant, R.A. 2022. Pharmaceutical pollution of the world's rivers. Proceedings of the National Academy of Sciences 119(8), e2113947119.

Wilson, B.A., Smith, V.H., deNoyelles, F. and Larive, C.K. 2003. Effects of three pharmaceutical and personal care products on natural freshwater algal assemblages. Environmental science & technology 37(9), 1713-1719.

Wu, D.-L., Zhang, M., He, L.-X., Zou, H.-Y., Liu, Y.-S., Li, B.-B., Yang, Y.-Y., Liu, C., He, L.-Y. and Ying, G.-G. 2020. Contamination profile of antibiotic resistance genes in ground water in comparison with surface water. Science of the Total Environment 715, 136975.

Wu, D., Bai, H., He, L.-Y., He, L.-X., Gao, F.-Z., Liu, C.-X., Van den Brink, P.J., Smidt, H. and Ying, G.-G. 2025. From river to groundwater: Antibiotics pollution, resistance prevalence, and source tracking. Environment International, 109305.

Wu, Q., Pan, C.-G., Wang, Y.-H., Xiao, S.-K. and Yu, K.-F. 2021. Antibiotics in a subtropical food web from the Beibu Gulf, South China: occurrence, bioaccumulation and trophic transfer. Science of the Total Environment 751, 141718.

Xie, G., Zhang, Y., Gong, Y., Luo, W. and Tang, X. 2024. Extreme trophic tales: deciphering bacterial diversity and potential functions in oligotrophic and hypereutrophic lakes. BMC microbiology 24(1), 348.

Xie, Z., Lu, G., Yan, Z., Liu, J., Wang, P. and Wang, Y. 2017. Bioaccumulation and trophic transfer of pharmaceuticals in food webs from a large freshwater lake. Environmental Pollution 222, 356-366.

Xiong, J.-Q., Kim, S.-J., Kurade, M.B., Govindwar, S., Abou-Shanab, R.A.I., Kim, J.-R., Roh, H.-S., Khan, M.A. and Jeon, B.-H. 2019. Combined effects of sulfamethazine and sulfamethoxazole on a freshwater microalga, Scenedesmus obliquus: toxicity, biodegradation, and metabolic fate. Journal of Hazardous Materials 370, 138-146.

Xiong, J.-Q., Kurade, M.B. and Jeon, B.-H. 2018. Can microalgae remove pharmaceutical contaminants from water? Trends in biotechnology 36(1), 30-44.

Xiong, Q., Hu, L.-X., Liu, Y.-S., Zhao, J.-L., He, L.-Y. and Ying, G.-G. 2021. Microalgae-based technology for antibiotics removal: From mechanisms to application of innovational hybrid systems. Environment international 155, 106594.

Xu, H. and Sun, X. 2021. The interactive modeling and joint prevention of water pollution between surface water and groundwater in maozhou river basin. Environ Eng 6, 21-26.

Yadav, P., Quattrone, A., Yang, Y., Owens, J., Kiat, R., Kuppusamy, T., Russo, S.E. and Weber, K.A. 2023. Zea mays genotype influences microbial and viral rhizobiome community structure. ISME communications 3(1), 129.

Yamamoto, H., Nakamura, Y., Moriguchi, S., Nakamura, Y., Honda, Y., Tamura, I., Hirata, Y., Hayashi, A. and Sekizawa, J. 2009. Persistence and partitioning of eight selected pharmaceuticals in the aquatic environment: laboratory photolysis, biodegradation, and sorption experiments. Water research 43(2), 351-362.

Yan, Z., Yang, Q., Wang, X., Torres, O.L., Tang, S., Zhang, S., Guo, R. and Chen, J. 2019. Correlation between antibiotic-induced feeding depression and body size reduction in zooplankton (rotifer, Brachionus calyciflorus): neural response and digestive enzyme inhibition. Chemosphere 218, 376-383.

Yang, W., Li, J., Yao, Z. and Li, M. 2024. A review on the alternatives to antibiotics and the treatment of antibiotic pollution: Current development and future prospects. Science of The Total Environment, 171757.

Yang, Y., Ok, Y.S., Kim, K.-H., Kwon, E.E. and Tsang, Y.F. 2017. Occurrences and removal of pharmaceuticals and personal care products (PPCPs) in drinking water and water/sewage treatment plants: A review. Science of the Total Environment 596, 303-320.

Yao, K.-S., Zhou, P.-L., Yang, H.-Q., Tan, L.-J., Qiao, L.-K., Zhao, Q.-H., Peng, F.-J., Ying, G.-G. and Van den Brink, P.J. 2025. Assessing triclosan-induced direct and multi-trophic cascading effects in a sub-tropical freshwater ecosystem. Environment International, 109702.

Yergeau, E., Lawrence, J.R., Waiser, M.J., Korber, D.R. and Greer, C.W. 2010. Metatranscriptomic analysis of the response of river biofilms to pharmaceutical products, using anonymous DNA microarrays. Applied and environmental microbiology 76(16), 5432-5439.

Yi, Z., Wang, J., Tang, Q. and Jiang, T. 2018. Photolysis of sulfamethazine using UV irradiation in an aqueous medium. RSC advances 8(3), 1427-1435.
Yin, X., Li, Y., Liu, Y., Zheng, J., Yu, X., Li, Y., Achterberg, E.P. and Wang, X. 2023. Dietary exposure to sulfamethazine alters fish intestinal homeostasis and promotes resistance gene transfer. Aquatic Toxicology 264, 106733.
Ying, G.-G., Yu, X.-Y. and Kookana, R.S. 2007. Biological degradation of triclocarban and triclosan in a soil under aerobic and anaerobic conditions and comparison with environmental fate modelling. Environmental Pollution 150(3), 300-305.
Ying, Z., Ji-chao, S., Guan-xing, H., Ji-hong, J., Xi, C., Jing-tao, L. and Yu-xi, Z. 2011. A preliminary study of natural background levels of groundwater in the Zhujiang River Delta. Geology in China 38(1), 190-196.
Yu, K., Duan, Y., Liao, P., Xie, L., Li, Q., Ning, Z. and Liu, C. 2020. Watershed-scale distributions of heavy metals in the hyporheic zones of a heavily polluted Maozhou River watershed, southern China. Chemosphere 239, 124773.
Yuan, M.M., Guo, X., Wu, L., Zhang, Y., Xiao, N., Ning, D., Shi, Z., Zhou, X., Wu, L. and Yang, Y. 2021. Climate warming enhances microbial network complexity and stability. Nature Climate Change 11(4), 343-348.
Yuen, P. and Sokoloski, T. 1977. Kinetics of concomitant degradation of tetracycline to epitetracycline, anhydrotetracycline, and epianhydrotetracycline in acid phosphate solution. Journal of pharmaceutical sciences 66(11), 1648-1650.
Zeng, J., Bian, Y., Xing, P. and Wu, Q.L. 2012. Macrophyte species drive the variation of bacterioplankton community composition in a shallow freshwater lake. Applied and Environmental Microbiology 78(1), 177-184.
Zeng, W., Zhang, J., Wang, A. and Peng, Y. 2016. Denitrifying phosphorus removal from municipal wastewater and dynamics of "Candidatus Accumulibacter" and denitrifying bacteria based on genes of ppk1, narG, nirS and nirK. Bioresource Technology 207, 322-331.
Zenker, A., Cicero, M.R., Prestinaci, F., Bottoni, P. and Carere, M. 2014. Bioaccumulation and biomagnification potential of pharmaceuticals with a focus to the aquatic environment. Journal of Environmental Management 133, 378-387.
Zhai, Y., Han, Y., Xia, X., Li, X., Lu, H., Teng, Y. and Wang, J. 2021. Anthropogenic organic pollutants in groundwater increase releases of Fe and Mn from aquifer sediments: Impacts of pollution degree, mineral content, and pH. Water 13(14), 1920.
Zhang, B., Wang, P., Duan, G., Liang, W., Hong, L., Wang, L., Guo, X., Yang, H. and Xi, Y. 2016. Information on the drug resistance of plasmids that are homologous to spacers in a CRISPR/Cas system and its relationship to information on the drug resistance of Shigella.
Zhang, J. and Xu, X. 2019. Practices of improvement of black-odorous water bodies in Guangdong Province. China Water Resources 5, 6-9.
Zhang, L. and Wang, W.X. 2007. Size-dependence of the potential for metal biomagnification in early life stages of marine fish. Environmental Toxicology and Chemistry 26(4), 787-794.
Zhang, L., Zhang, C., Lian, K., Ke, D., Xie, T. and Liu, C. 2021. River restoration changes distributions of antibiotics, antibiotic resistance genes, and microbial community. Science of The Total Environment 788, 147873.
Zhang, T., Zhang, X.-X. and Ye, L. 2011. Plasmid metagenome reveals high levels of antibiotic resistance genes and mobile genetic elements in activated sludge. PloS one 6(10), e26041.
Zhang, W., Huang, M.-h., Qi, F.-f., Sun, P.-z. and Van Ginkel, S.W. 2013. Effect of trace tetracycline concentrations on the structure of a microbial community and the development of tetracycline resistance genes in sequencing batch reactors. Bioresource technology 150, 9-14.
Zhang, X., Xue, X. and Hu, J. 2025. Combined ozonation-biological activated carbon process for antibiotic resistance control in treated effluent from wastewater treatment plant. Water Research 268, 122610.
Zhao, D., Huang, R., Zeng, J., Yan, W., Wang, J., Ma, T., Wang, M. and Wu, Q.L. 2012. Diversity analysis of bacterial community compositions in sediments of urban lakes by terminal restriction fragment length polymorphism (T-RFLP). World Journal of Microbiology and Biotechnology 28, 3159-3170.
Zhao, J.-L., Ying, G.-G., Liu, Y.-S., Chen, F., Yang, J.-F. and Wang, L. 2010. Occurrence and risks of triclosan and triclocarban in the Pearl River system, South China: from source to the receiving environment. Journal of Hazardous Materials 179(1-3), 215-222.
Zhao, J., Xu, Y., Peng, L., Liu, G., Wan, X., Hua, Y., Zhu, D. and Hamilton, D.P. 2019. Diversity of anammox bacteria and abundance of functional genes for nitrogen cycling in the rhizosphere of submerged macrophytes in a freshwater lake in summer. Journal of Soils and Sediments 19, 3648-3656.
Zhao, Q., De Laender, F. and Van den Brink, P.J. 2020. Community composition modifies direct and indirect effects of pesticides in freshwater food webs. Science of The Total Environment 739, 139531.

Zhao, Y., Huang, Y., Hu, S., Xu, T., Fang, Y., Liu, H., Xi, Y. and Qu, R. 2023. Combined effects of fluoroquinolone antibiotics and organophosphate flame retardants on Microcystis aeruginosa. Environmental Science and Pollution Research 30(18), 53050-53062.
Zheng, D., Yin, G., Liu, M., Chen, C., Jiang, Y., Hou, L. and Zheng, Y. 2021. A systematic review of antibiotics and antibiotic resistance genes in estuarine and coastal environments. Science of the Total Environment 777, 146009.
Zheng, Z.-Y., Zhou, J.-X., Peng, Z.-X. and Ni, H.-G. 2025. Computational simulation of bioaccumulation and trophic transfer of antibiotics mechanisms in aquatic food chain. Water Research 272, 122951.
Zhong, X., Cui, C. and Yu, S. 2017. Exploring the pathways of aromatic carboxylic acids in ozone solutions. RSC Advances 7(55), 34339-34347.
Zhou, G., Xu, X., Qiu, X. and Zhang, J. 2019. Biochar influences the succession of microbial communities and the metabolic functions during rice straw composting with pig manure. Bioresource technology 272, 10-18.
Zhou, J. and Broodbank, N. 2014. Sediment-water interactions of pharmaceutical residues in the river environment. Water research 48, 61-70.
Zhou, L.J., Wu, Q.L., Zhang, B.B., Zhao, Y.G. and Zhao, B.Y. 2016. Occurrence, spatiotemporal distribution, mass balance and ecological risks of antibiotics in subtropical shallow Lake Taihu, China. Environ Sci Process Impacts 18(4), 500-513.
Zhou, L.J., Ying, G.G., Liu, S., Zhao, J.L., Chen, F., Zhang, R.Q., Peng, F.Q. and Zhang, Q.Q. 2012. Simultaneous determination of human and veterinary antibiotics in various environmental matrices by rapid resolution liquid chromatography-electrospray ionization tandem mass spectrometry. J Chromatogr A 1244, 123-138.
Zhu, M., Chen, J., Peijnenburg, W.J., Xie, H., Wang, Z. and Zhang, S. 2023. Controlling factors and toxicokinetic modeling of antibiotics bioaccumulation in aquatic organisms: A review. Critical Reviews in Environmental Science and Technology 53(15), 1431-1451.
Zhu, M., Chen, J., Peijnenburg, W.J.G.M., Xie, H., Wang, Z. and Zhang, S. 2022. Controlling factors and toxicokinetic modeling of antibiotics bioaccumulation in aquatic organisms: A review. Critical Reviews in Environmental Science and Technology, 1-21.
Zhu, M., Wang, Z., Chen, J., Xie, H., Zhao, H. and Yuan, X. 2020. Bioaccumulation, biotransformation, and multicompartmental toxicokinetic model of antibiotics in sea cucumber (Apostichopus japonicus). Environmental Science & Technology 54(20), 13175-13185.
Zhu, Y., Zhang, Y., Ren, H.-q., Geng, J.-j., Xu, K., Huang, H. and Ding, L.-l. 2015. Physicochemical characteristics and microbial community evolution of biofilms during the start-up period in a moving bed biofilm reactor. Bioresource technology 180, 345-351.
Zilberman, A., Gozlan, I. and Avisar, D. 2023. Pharmaceutical transformation products formed by ozonation—does degradation occur? Molecules 28(3), 1227.

Summary

Antimicrobials are consistently detected in freshwater environments, with inputs associated with human medical use, discharges from livestock farming, and releases from urban wastewater systems. Freshwater ecosystems are rarely exposed to a single compound in isolation; instead, they experience multiple chemical stressors, with effects mediated through microbial processes, food-web structure, and ecosystem functioning. Therefore, under multi-stressor exposure and ecosystem interaction, empirical studies are needed to establish clear links between external exposure patterns and ecological responses. On this basis, research described in this thesis investigated freshwater ecosystems along four interconnected research lines: environmental occurrence of antimicrobials, ecological responses, internal exposure and food-web transfer, and the ecological outcomes of advanced wastewater treatment technologies. The overall aim was to provide ecologically relevant support and an analytical framework for exposure assessment, ecological interpretation, and risk management of antimicrobials.

To achieve these aims, this thesis combines river-basin field investigations with multiple types of controlled experiments. Responses were evaluated across trophic levels from microbial communities to macroinvertebrates, and effects were assessed using both structural endpoints (community composition, abundance, and diversity) and functional endpoints (e.g., feeding, decomposition, and ecosystem metabolic processes). Methods included multi-residue chemical analysis, molecular microbial approaches including community composition profiling through 16S ribosomal RNA gene amplicon sequencing, bacterial isolation and antimicrobial resistance profiling, indoor and outdoor microcosm exposure experiments, and quantitative modelling (including toxicokinetic modelling and structural equation modelling) to examine how exposure to antimicrobials induces direct and indirect effects at different scales and how they propagate through the food-web.

Chapter 2 examined antibiotic contamination in a highly urbanized river basin and its linkage across the river–sediment–groundwater continuum. River water, sediments, and groundwater were sampled in wet and dry seasons to characterize antibiotic residues and microbial community patterns. In groundwater, *Escherichia coli* was isolated to evaluate antimicrobial resistance and potential health risk, and source-tracking analyses were conducted to identify major inputs of resistance-related contamination. The results indicated that antibiotics detected in river water and sediments were associated with comparatively higher predicted risks for algal growth and bacterial resistance selection than those in groundwater, whereas predicted risks in groundwater were generally lower but not negligible. Several dominant bacterial groups in river water and groundwater were positively correlated

with measured antibiotics, indicating that local residues co-varied with community composition patterns. A high proportion of groundwater *E. coli* isolates showed resistant phenotypes, supported by gene-targeted evidence. Source-tracking further suggested that resistance-related contamination in shallow groundwater was mainly linked to river sediments, while deeper groundwater was more strongly linked to river water. Overall, this chapter showed that river pollution can influence groundwater quality through multiple pathways, and that groundwater risk assessment should account for connectivity and source inputs across the river–sediment–groundwater system.

Chapter 3 investigated the ecological effects of antibiotic mixture exposure using a simple aquatic ecosystem. Two commonly co-occurring antibiotics, sulfamethazine (SMT) and tetracycline (TC), were tested in single and combined exposures at multiple concentrations (SMT: 0.1, 1, 10 µg/L; TC: 1.5, 15, 150 µg/L) over 28 days. Responses were evaluated across different trophic levels including primary producers, zooplankton, benthic macroinvertebrates and microbial communities, and key ecosystem process endpoints. The results showed that mixture responses did not follow a consistent additive extension of single-compound patterns. Single-compound exposures reduced algal biomass at some concentrations, whereas combined exposures did not result in a stable change in the same direction across concentration combinations. Zooplankton community structure changed under both single and combined exposures, and patterns differed across dose levels, including both stimulatory and adverse responses. Microbial responses were compartment-dependent: trajectories differed between the water column and sediment, and compared with single-compound exposures, combined exposures did not yield a detectable structural shift in water-column microbial communities, while changes were still observed in the sediment. Functionally, leaf-litter decomposition accelerated across multiple treatments, consistent with strengthened microbially driven processing. Overall, this chapter demonstrates that responses to single versus combined antibiotic exposure differed across trophic levels and endpoints, supporting caution when extrapolating single-compound effects to mixture scenarios.

Chapter 4 used triclosan as a model antimicrobial to assess how differences in environmental conditions modifies microbial community responses in sediments. Microcosms were established with natural pond and ditch sediments as well as a standardized artificial sediment, and these sediments were then exposed under the same laboratory conditions following field pre-incubation. Microbial community composition was assessed after exposure, and relationships between response patterns and environmental factors (including overlying-water nutrient conditions and sediment organic matter content) were evaluated. Sediment origin and type strongly influenced baseline community composition. Following triclosan exposure, clear community shifts occurred in some

sediment systems at higher exposure levels, together with increases in bacterial groups associated with triclosan degradation or tolerance. The magnitude of responses was related to environmental conditions: overlying-water nutrient status and sediment organic matter co-varied with community shifts, and higher organic matter likely reduced bioavailability through sorption, weakening observed effects. This chapter showed that pollutant effects can differ across sediment types and water conditions, and that both sediment properties and overlying-water characteristics should be considered when extrapolating effects to different field settings.

Chapter 5 addressed internal exposure and trophic transfer of an antibiotic within a simplified freshwater food chain. Using *Scenedesmus obliquus–Daphnia magna–Chaoborus obscuripes*, toxicokinetic analyses and trophic transfer experiments were combined to evaluate azithromycin accumulation, transfer efficiency, and indirect effects at higher trophic levels. Strong internal accumulation was observed in *Scenedesmus obliquus* and *Daphnia magna*, whereas transfer to higher trophic levels was relatively minor. Despite the low transfer efficiency, predators (*C. obscuripes*) feeding on contaminated prey (*D. magna*) showed sublethal fitness-related effects in the predators, such as reduced growth. Overall, this chapter indicated that the absence of biomagnification does not exclude ecologically relevant impacts, and it supports the inclusion of dietary internal exposure and sensitive fitness endpoints in food-web risk evaluation.

Chapter 6 evaluated the ecological gain achieved by different advanced wastewater treatment methods from a risk-management perspective by assessing whether reductions in micropollutant pressure are accompanied by concurrent decreases in mixture toxicity and adverse ecological responses. Outdoor freshwater microcosms were used to compare treatment scenarios including bioactivated carbon filtration, two ozonation intensities, and their combinations over 42 days. Micropollutant residues and mixture toxicity pressure were tracked alongside multi-trophic ecological responses, and structural equation modelling was applied to relate chemical changes and resource/nutrient conditions to biological patterns. Untreated effluents maintained higher and more persistent mixture toxicity pressure, while combined bioactivated carbon and ozonation resulted in lowest residue concentrations, which continued to decline over time. Ecological responses differed across trophic levels. Primary producers responded more strongly to the treatment scenarios, while higher-consumer community structure remained comparatively robust. Water-column microbial communities showed pronounced, treatment-dependent restructuring, and high-intensity ozonation coincided with a functional impairment, reflected by reduced representation of key functional groups. Structural equation modelling indicated that, at the early time point (Day 14), micropollutant levels and nutrient conditions primarily influenced primary producers, with weaker propagation to higher consumers. Overall, this chapter highlighted

the need to balance chemical removal performance with ecological effects when selecting advanced treatment strategies, and to consider treatment-driven shifts in resource conditions alongside reductions in chemical pressure.

Chapter 7 synthesized cross-chapter findings and discussed implications for ecological risk assessment and freshwater management. Ecological effects of antimicrobials were strongly context-dependent, with response direction and magnitude jointly shaped by exposure composition (single compounds versus mixtures), environmental background conditions (including nutrient status and compartment characteristics), and trophic level. Comparison of results across chapters also showed that structural community metrics alone were insufficient to infer ecological consequences, whereas process-based endpoints and fitness-related responses provide more direct information on ecological outcomes. The food-chain study illustrated that a lack of biomagnification does not imply a lack of ecological risk, because dietary internal exposure can still translate into sublethal effects at higher trophic levels. Finally, the assessment of advanced treatment showed that ecological benefits cannot be inferred from removal performance alone; they require evaluation of both reduced chemical pressure and treatment-driven shifts in resource conditions and microbial functional restructuring.

Together, the thesis supports integrated consideration of external exposure, internal exposure, mixture pressure, and functional ecological responses to inform more ecologically relevant freshwater management.

Acknowledgements

Time has passed so quickly. Five years have gone by, yet I still feel as if I were the person who had just arrived in the Netherlands and just begun my PhD, still full of wonder at the beauty of spring in Wageningen. The daffodils have come up again through the grass, lowering their heads and opening gently in the wind. Tulips and hyacinths are blooming one after another. Greylag geese graze on the lawns, and waterbirds stand quietly in the ditch beside Lumen, as if daydreaming. It is spring again. It feels as though nothing has changed, and yet, very truly, I have finished my PhD. Over these years, I seem to have changed a great deal, and at the same time, perhaps not at all. If I had to sum up these years in two words, they would be luck and growth.

I feel deeply fortunate to have come here for my PhD, to have begun a completely new chapter of life in Wageningen, in the Netherlands, and to have met so many wonderful people along the way. They are people I will remember for a long time, and be grateful to for the rest of my life.

My greatest good fortune in academic life has been to have such a wonderful supervisory team: **Paul**, **Hauke**, and **Ying**. First of all, thank you, **Paul**, for welcoming me and giving me the opportunity to join the AEW group. I am deeply grateful for the freedom you gave me to explore, and I always enjoyed talking with you about research and data. You are rigorous in your work, yet humorous and easygoing in daily life. Beyond academia, you often joked with us, chatted with us, and brought people together through drinks, dinners, potlucks, and group outings. I feel genuinely lucky to have done my PhD under your guidance and to have experienced such a free, equal, and welcoming atmosphere. You always gave people space and treated everyone with respect and understanding. In my heart, you have always been the scientific father of the group. I think this will stay with me and shape the way I work, as well as the way I hope to treat others in the future. **Hauke**, I also feel incredibly lucky to have had you as my supervisor. You are wise, kind, generous, and hardworking, and you have so many qualities I deeply admire. In academic work, you are always thoughtful and patient, and your knowledge spans a wide range of disciplines. You never hesitate to discuss ideas from different fields. I was often amazed to see you replying to my emails late at night and already reviewing my manuscripts again early the next morning. You are also deeply considerate. You always speak with care and always encouraging. I always came away from our meetings feeling calmer. I am also very grateful for the research platform and the learning opportunities you gave me. I have grown so much because of them, and because of you. **Ying**, you were not only my MSc supervisor, but also my co-promotor during my PhD. Perhaps you do not know this, but my earliest interest in scientific research began when I listened to you present a project idea during a group meeting and describe the vision behind it. Since my MSc, your support, guidance, and encouragement have gradually led me toward the world of science. You always have new ideas, and you are always closely connected to what is happening at the front edge of research. That has always inspired me and filled me with motivation. I am also very grateful that you encouraged me to come to the Netherlands for my PhD and gave me the chance to move closer to science.

I also feel very lucky to have joined both AEW and MIB. Across these two groups, I met some of the best and kindest colleagues I could have hoped for.

At AEW, I would first like to thank **Nancy** and **Koos** for all their help with administrative and financial matters. I am also grateful to **Annie**, **Marlies**, **Wendy**, **Dorine**, and **Frits** for their help and guidance in the lab. Without your help, my experiments would never have gone so smoothly.

I am very grateful to my colleagues and friends in the Chemical Stress Ecology group: **Ayesha**, **Banchi**, **Dana**, **Giulia**, **Iim**, **Judith**, **Kaisheng**, **Pierina**, **Shuwen**, **Tatiana**, **Vera**, **Yujun**, and **Zeyuan**. Thank you for the biweekly group meetings, the group outing, the Christmas potlucks, and all the food, laughter, and good moments we shared together. **Ayesha**, we shared an office for a long time and spent many lovely moments together. Thank you for inviting me to your home for dinner. Your cooking is truly wonderful. **Banchi**, you are always so kind and humble. **Iim**, my sister, I have treasured the many conversations we shared. **Judith**, I really admire your brightness and energy. **Pierina**, one day I will go and see Angel Falls, which you once told me about. **Shuwen**, thank you for sharing your story with me. You are a very strong person. **Kaisheng**, we have known each other since 2019. Thank you for all the experiments you helped me with over the years, the data we discussed, the meals we shared, the many conversations we had about life, and the many wonderful trips and moments along the way. **Zeyuan**, we shared many meals together, and I really appreciate your honesty and openness toward life.

I would also like to thank former members of the Chemical Stress Ecology group who had already graduated: **Anna**, **Annika**, **Elien**, **Markus**, and **Lara**. During my PhD, you helped me in so many ways, not only in work and experiments, but also in life more broadly. **Lara**, thank you for doing experiments together at Sinderhoeve, and for your suggestions on my papers. **Anna**, thank you for helping me with experiments and data analysis, and for your advice on my papers. **Annika**, thank you for all the coffees, walks around campus, and the Doraemon conversations we had. **Elien**, I have always admired your positive and optimistic spirit. I really enjoyed discussing data with you, and I learned a lot from the many useful suggestions you gave me, both in work and in life. **Markus**, thank you for your help with my experiments. I still remember the coffees and lunches you invited me to, and the time you invited us to Walibi to ride roller coasters. You are such a thoughtful and interesting person, and every conversation with you felt warm and easy. I learned a lot from you.

I would also like to thank my other colleagues in AEW. **Agustin**, I have always really enjoyed talking with you. You are wise and thoughtful, and we often find ourselves thinking along the same lines in unexpected ways. I hope your coral reef conservation foundation, and the foundation I hope to build one day to support children's education, will both grow well. **Yuxin**, every time I see you, it feels as though we could keep talking without end. I wish you all the very best in the future, and I hope you and your dog will soon be able to live together. **Li Kang**, I really admire your energy, and I am always impressed by your love for both work and life. **Qinyi**, although you only joined our group this year, I already feel that I should have met you much earlier. I really admire your quick mind, your sense of order, and your ability to get things done. **Taylor**, your warmth and energy always make people want to talk to you. **Yanning**, thank you for your advice and encouragement on many

occasions. **Yutong** and **Siting**, thank you for the meals and conversations we shared. **Ira**, thank you for inviting me to your home for food. **Britt**, thank you for sharing hiking routes with me, and also for being Kaisheng's paranymph together with me. **Margherita**, thank you for the PhD afterwork gatherings we went to together. **Karin** and **Ana**, thank you for the conversations we shared. **Sven**, I really enjoyed our conversations about coffee, tea, and milk tea. **Edwin**, every time I met you in the hallway, you greeted me with a smile and a wave. I really admire your spirit. Thank you all for making my PhD life so rich and enjoyable.

I am equally grateful to have become part of the MIB family and to have met so many interesting and supportive colleagues there. My thanks go to **Anja**, **Sarash**, **Erna**, and **Christine** for their administrative support; to **Philippe** for giving me a lab tour when I first joined the lab; to **Ineke** and **Merlijn** for their help with lab work; to **Felix** and **Victor** for their help with bioinformatics and data analysis; to **Martha** for her support with sequencing; and to **Valentina A**, **Nancy**, and **Anna M** for their help with bioinformatics analyses.

I am especially grateful for the MolEco morning meetings every Thursday, hosted by **Hauke**, **Erwin**, **Detmer**, and **Clara**. They gave me the chance to share my work and also to learn what everyone else was doing. Even though I was always nervous before my turn to present, I have to admit that from my first year to my last, I grew a great deal.

I would also like to thank my wonderful office mates, **Sofia**, **Pavlo**, **Baris**, **Nancy**, and **Gwen**. Going to laser tag with you was such a happy memory. I also want to thank **Yan Lin**, who joined our office later. You were like an older sister to me, often helping me think through things I was facing in both work and life. I am also grateful to **Zhuang** and **Chen** for often inviting me to meals and looking after me so kindly.

Thank you as well to all the friends who joined the PhD trip to Japan: **Sofia**, **Pavlo**, **Mike**, **Kelly**, **Valentina**, **Federica**, **Gwen**, **Carl**, **Caglar**, **Gerben**, **Yassin**, **Panos**, **Thomas**, and many others. You made that trip unforgettable. I still remember walking back to the hotel with **Kelly** in the rain, and how your singing stayed with me afterward. Thank you to **Mike** and **Pavlo** for taking me to a maid café. Thank you to **Thomas** for walking with me and sharing stories. Thank you to all of you for the conversations, the meals, the songs, and the stories we shared.

I would also like to thank everyone from the MolEco group retreat, the Thursday cakes, and the yearly Sinterklaas dinners, all of which brought me so much joy and so many memories. **Valentina,** thank you for always speaking to me with such warmth. I truly enjoyed every conversation with you. **Federica**, you are also such a kind and warm person. I really enjoyed the Chinese meals I shared with both of you. Thank you to **Veronika** for the badminton gift during Sinterklaas. Thank you to **Evy** for always being so kind and caring. Thank you to **Gnanesh**, **Samuel**, **Merlijn**, and **Maryse** for the Mafia games, which were always so much fun. **Merlijn**, next time you are a wolf, please try not to answer "yes" when someone calls "wolf" — haha. Thank you to **Francesco** for your suggestions for my trip to South Africa. Thank you to **Tamara**, **Alejandra**, **Nial**, and **Subhash** for the fun moments during retreat, to **Colombe** and **Felix** for teaching me French, and to **Takumi** for sharing snacks. It is hard to describe how much I smiled while writing this part.

I would also like to thank **Koen** for the experiments we carried out together, and for your contributions to the writing and discussion of the data. I also treasure the conversations we had and the meals we shared. I still remember very clearly that during my first field experiment, you shared your bread and cheese with me. Thank you to **Myrthe**, with whom I also worked closely in experiments. You were the first friend I made in the Netherlands. I still remember cycling back from Sinderhoeve after an experiment when we got caught in heavy rain and were soaked through. We looked at each other and burst out laughing, and you said, "Welcome to the Netherlands." Thank you to **Ivo** and **Marie-Claire** for your help with my experiments. **Ivo**, you are always humorous and helpful, and I truly appreciated your support. **Claire**, thank you for teaching me zooplankton identification. I am very grateful for your patience and kindness.

I would also like to thank the students I supervised: **Mirjam**, **Siemon**, **Jet**, and **Harley**. Thank you for your contributions to my experiments. **Mirjam**, you always struck me as someone gentle at heart, yet full of strength. I still remember very clearly the way you said, "I am not from sugar." **Siemon**, during the time we worked together, we had many deep conversations. You are curious and humble, and it was a real pleasure to share part of the journey with you.

I would like to give my special thanks to my paranymphs, **Maryse** and **Anna**. I truly feel very lucky to have had both of you by my side as my paranymphs. During the preparation for my defense, you gave me so much support and help, and in the midst of all my nervousness, I often felt how fortunate I was to have you with me. **Maryse**, you are such a thoughtful and warm person, and being with you always feels easy and comfortable. I am very grateful for the conversations we shared and the meals we had together. I also still remember the way you said "shark" in Chinese. **Anna**, having you as my paranymph feels very complete and meaningful to me. In work, from experiments to data analysis to writing, you always gave me very helpful advice. In life, we also shared many beautiful memories. And here, I would also like to thank you and **Xixi** together: for the road trip in Ireland, for driving from the Netherlands to Paris, for weekends of bouldering, for meals, and for badminton.

Beyond work, I would also like to give my heartfelt thanks to my friends in life. To my close friends **Xiaojue**, **Yan Li**, **Jiaoyi**, **Quanxing**, **Shuhao**, and **Kecen**, and also to friends who have already left Wageningen, **Gang**, **Chenyu**, and **Bochi**: thank you for all the countless meals we shared in each other's homes, the weekly badminton games, the concerts, the films, the trips to the shore, the tulip fields, and the travels we took together. Thank you for the many beautiful moments, the stories we shared, and the countless times we laughed. Your presence was one of the brightest parts of my PhD years. A very special thank you goes to **Xiaojue**, who put so much time and energy into designing the cover and chapter illustrations for this thesis.

Thank you to **Dengxiao**, **Shuo**, **Jingwei**, **Ke**, and **Liang** for the late-night mahjong games we played together, and for all the moments of life we shared. **Dengxiao**, thank you for so often cooking delicious meals for us. **Shuo**, I have always admired how beautifully you write poetry. I wish **Dengxiao** and **Shuo** a joyful marriage and a happy life together. **Jingwei**, thank you for the many meals we shared and the moments of life we shared together. I

wish you and **Zixuan** a very happy marriage. **Ke**, thank you for all the meals we shared during the early years of my PhD, and for the road trip we took together through Austria and Hungary. I wish you, **Xuenan**, and your daughter all the very best. Thank you to **Wenxuan** and **Lubin** for the meals we shared and the conversations we had. Thank you to **Man Pu** and **Xin Wei** for the Mediterranean cruise trip we took together. Thank you to **Yaoyu** and **Wenxin** for inviting us for hotpot. I also want to thank **Yaoyu**, **Jianchen** (**Sam**), and **Yan Zhang** for the many meals we shared, the many games of Guandan we played, and the hiking trip in the Dolomites. Thank you to **Xiaomeng** and **Zhongchen** for your help when I first arrived in Wageningen, and for being such kind neighbours. Thank you to **Jinsong** for your help when I had just arrived in Wageningen. Thank you to **Bangding** for sharing your visions of artificial intelligence with me. Thank you to **Wanhen** and **Bo** for the many meals and bike rides we shared. Thank you to **Yinan**, **Ruoling**, **Liangyu**, **Qiong** and **Yun** for the badminton games, the interesting conversations, and the discussions about our research. I wish all my friends beautiful lives ahead.

There are also a few especially precious friends in my life, some near, some far away. **Bai**, you have been my best friend since my MSc. During your visiting year in Wageningen, we studied and discussed data together, took walks after meals, cycled around, and imagined the future. That kind of life felt so beautiful. Whenever I ran into difficulties, you always tried to see things completely from my point of view, and shared the best of yourself with me without holding anything back. **Lucy**, although we have not seen each other often in recent years, every time we meet, it still feels as though there is nothing we cannot talk about. You trust me just as I trust you. I hope our friendship will last for a very long time, until we are both grey-haired. **Yujun**, although you were only in Wageningen for one year, we became lasting friends. Thank you for the trips we took together, for the ease with which we could talk about anything, for your support in life and in spirit, and for the meals we shared in Guangzhou. **Rui**, I am grateful for your trust, and for how openly you shared everything with me. I deeply admire your passion for and dedication to sports education for deaf and hard-of-hearing people. Life seems to place unexpected challenges in your path, yet you have always met them with strength and perseverance. I hope your health recovers soon, and that you become once again the lively, energetic Big Rui.

I would also like to give my deepest thanks to my partner, **Nuo**. Since the day we met, you have always been by my side. You have been endlessly patient and caring, and you helped me through difficult times. We have witnessed each other grow, and together we have slowly become better versions of ourselves. We have also come to understand more clearly the kind of future we want to build together. We have travelled through so many places together: we met in the elevator at Bornsesteeg, we decided to be together under the northern lights in Tromsø, and you proposed to me on the summit of Kilimanjaro. And now, you are my husband. You once told me that we would write our future together. I truly feel so lucky to have met you, on that day and in that place.

Finally, I would like to thank my parents and my family. **Mom**, thank you for always supporting me in so many ways. Your strength and kindness have shaped me deeply. We are like friends, and also each other's strongest support. **Uncle Luo**, you were not my biological father, but you loved and supported me like one. You brought joy and warmth to our family, and you supported every decision I made. From university to my master's, and

then to my PhD, I was always studying far from home. You always said, "Let Dailing fly as far as she wants. Do not break her wings." You were kind and gentle. You remembered the birthdays of my mother and me, as well as every holiday, and you gave so much to our family quietly and generously. Yet just before you could see me finish my PhD, you left my mother and me forever. I will always remember you and your smile. I would also like to thank my uncle **Renjun** for his support over the years. He has always believed in me, and that faith has given me great strength.

At the very end, I would like to repeat the words I wrote at the end of my master's thesis: "Every stage of life teaches us something different. I treasure the time I have now more than anything. I only hope that, when I look back on this moment in the future, I will feel at peace with my heart."

最后，我想感谢我的父母和家人。妈妈总是给我很多支持，你的坚韧与善良一直深深影响着我。我们像朋友一样，也是彼此最坚定的依靠。罗伯，你不是我的亲生父亲，却胜似亲父。你让我们这个家庭充满幸福与欢乐，也支持我做出的每一个决定。从大学到硕士，再到博士，我一直在离家很远的地方求学。你总说："黛灵想飞多远，就让她飞多远，不要折了她的翅膀。"你善良而温和，会记得我和妈妈的生日和每一个节日，默默为我们付出，却在即将看到我博士毕业的时候，永远地离开了我和妈妈。我会永远记得你微笑的样子。我也想感谢我的舅舅一直以来对我的支持。舅舅总是欣赏我，而这种欣赏无疑给了我很大的力量。

最后的最后，我想重提我写在硕士毕业论文最后的话："人生每一个阶段能让我们学到的都不一样，我无比珍惜现在的时光。但求将来回看现在时，无愧于心。"

Dailing Wu (吴黛灵)

Wageningen, March, 2025

Scientific publications (2021-2026)

Wu, D., Van Gijn, K., Schuijt, L., Van Venetië, M., Ying, G.G., Smidt, H. and Van den Brink, P.J., 2026. The ecological gain of using bioactivated carbon and ozone sewage treatments assessed using freshwater microcosms. *Water Research*, https://doi.org/10.1016/j.watres.2026.125811.

Wu, D., Yao, K., Hermann, M., Chen, N., Huang, A., Ying, G.G., Smidt, H. and Van den Brink, P.J., 2026. Individual and mixture effects of the antibiotics sulfamethazine and tetracycline on freshwater ecosystems. *Journal of Hazardous Materials*, p.141237.

Wu, D., van den Brink, P.J., Smidt, H., Bai, H., Ying, G.G. and Schuijt, L.M., 2025. The effects of triclosan on microbial communities in different sources of water and sediments. *Ecotoxicology and Environmental Safety*, *303*, p.118778.

Wu, D., Bai, H., He, L.Y., He, L.X., Gao, F.Z., Liu, C.X., Van den Brink, P.J., Smidt, H. and Ying, G.G., 2025. From river to groundwater: antibiotics pollution, resistance prevalence, and source tracking. *Environment international*, *196*, p.109305. (**Highly Cited Paper**)

Wu, D., Huang, A., Ying, G.G., Smidt, H. and Van den Brink, P.J. Trophic transfer and biological effects of azithromycin across a freshwater food chain. Under review.

Wang, Y.C., He, L.Y., **Wu, D.L.**, Gao, F.Z., Liu, Y.S. and Ying, G.G., 2025. Long-term manure applications promote persistent antibiotic resistance in soil. *Journal of Hazardous Materials*, p.140476.

Versteegen, E., Häkkinen, M., **Wu, D.**, Heikamp-de Jong, I., Roessink, I., Peeters, E.T. and van den Brink, P.J., 2025. Effects of the drug carbamazepine on the structure and functioning of a freshwater aquatic ecosystem. *Ecotoxicology and Environmental Safety*, *294*, p.118009.

Versteegen, E., Mou, T., **Wu, D.**, Heikamp-de Jong, I., Roessink, I., Peeters, E.T. and van den Brink, P.J., 2025. Effects of environmentally relevant concentrations of citalopram in freshwater mesocosms. *Environmental Pollution*, *367*, p.125570.

Schuijt, L.M., van Drimmelen, C.K., Buijse, L.L., van Smeden, J., **Wu, D.**, Boerwinkel, M.C., Belgers, D.J., Matser, A.M., Roessink, I., Beentjes, K.K. and Trimbos, K.B., 2024. Assessing ecological responses to exposure to the antibiotic sulfamethoxazole in freshwater mesocosms. *Environmental Pollution*, *343*, p.123199.

Schuijt, L.M., van Smeden, J., van Drimmelen, C.K., Buijse, L.L., **Wu, D.**, Boerwinkel, M.C., Belgers, D.J., Matser, A.M., Roessink, I., Heikamp-de Jong, I. and Beentjes, K.K., 2024. Effects of antidepressant exposure on aquatic communities assessed by a combination of morphological identification, functional measurements, environmental DNA metabarcoding and bioassays. *Chemosphere*, *349*, p.140706.

Bai, H., He, L.Y., Gao, F.Z., **Wu, D.L.**, Yao, K.S., Zhang, M., Jia, W.L., He, L.X., Zou, H.Y., Yao, M.S. and Ying, G.G., 2023. Airborne antibiotic resistome and human health risk in railway stations during COVID-19 pandemic. *Environment International*, *172*, p.107784.

He, L.X., He, L.Y., Gao, F.Z., **Wu, D.L.**, Ye, P., Cheng, Y.X., Chen, Z.Y., Hu, L.X., Liu, Y.S., Chen, J. and Ying, G.G., 2022. Antibiotics, antibiotic resistance genes and microbial community in grouper mariculture. *Science of the Total Environment*, *808*, p.152042.

Bai, H., He, L.Y., **Wu, D.L.**, Gao, F.Z., Zhang, M., Zou, H.Y., Yao, M.S. and Ying, G.G., 2022. Spread of airborne antibiotic resistance from animal farms to the environment: dispersal pattern and exposure risk. *Environment international*, *158*, p.106927.

He, L.Y., He, L.K., Gao, F.Z., **Wu, D.L.**, Zou, H.Y., Bai, H., Zhang, M. and Ying, G.G., 2021. Dissipation of antibiotic resistance genes in manure-amended agricultural soil. *Science of the total environment*, *787*, p.147582.

Zou, H.Y., He, L.Y., Gao, F.Z., Zhang, M., Chen, S., **Wu, D.L.**, Liu, Y.S., He, L.X., Bai, H. and Ying, G.G., 2021. Antibiotic resistance genes in surface water and groundwater from mining affected environments. *Science of The Total Environment*, *772*, p.145516.

About the author



Dailing Wu was born in Yueyang, Hunan, China, on October 23, 1993, and grew up in Changsha. From an early age, she developed a strong interest in nature and the environment. In 2012, she began her undergraduate studies in Environmental Science at Qilu University of Technology (Shandong Academy of Sciences). During her undergraduate years, she also pursued a second degree in English Literature. She was actively involved in the university environmental protection association and participated in student innovation projects. As team leader of one such project, she investigated the removal of Cr(VI) using activated carbon prepared from corn husk residues and published one peer-reviewed paper. For her bachelor's thesis, she studied the effects of pesticides on the weed seed bank in maize farmland, for which she was awarded an Excellent grade. She graduated ranked first in her major, received multiple university-, provincial-, and national-level scholarships during her undergraduate studies, and was recognized as an Outstanding Graduate of Shandong Province in 2016.

Driven by her enthusiasm for scientific research, Dailing joined the research group of Professor Guang-guo Ying at South China Normal University in 2017 to pursue her master's degree. Her research focused on the occurrence of antibiotics and antibiotic resistance genes in groundwater. During this period, she also contributed to several environmental projects in southern China, extending this work to rivers, drinking water sources, livestock farming areas, and mining-affected environments. She completed her master's degree with an Excellent thesis. During her master's studies, she published two first-author papers as well as several additional papers as a co-author.

In 2021, Dailing started her PhD at Wageningen University & Research under the supervision of Professors Paul J. van den Brink, Hauke Smidt, and Guang-guo Ying. Her PhD research, entitled *The Effects of Antimicrobials on Aquatic Ecosystems*, focused on understanding how antimicrobial compounds influence the structure and functioning of freshwater ecosystems. During her PhD, her passion for research continued to grow, and she became increasingly certain that she wished to pursue research as her future career. As first author, she completed five manuscripts, four of which have been published, including one recognized as a Highly Cited Paper. She also actively contributed to the scientific community as a reviewer for several international journals, including *Water Research*, *Environment International*, and *Journal of Hazardous Materials*. As of March 2026, her publications had received more than 1,000 citations on Google Scholar, with an *h*-index of 12.

Netherlands Research School for the
Socio-Economic and Natural Sciences of the Environment

D I P L O M A

for specialised PhD training

The Netherlands research school for the
Socio-Economic and Natural Sciences of the Environment
(SENSE) declares that

Dailing Wu

born on 23-10-1993 in Hunan, China

has successfully fulfilled all requirements of the
educational PhD programme of SENSE.

Wageningen, 8 May 2026

SENSE coordinator PhD education

Dr Ir Peter Vermeulen

The SENSE Director

Dr Jampel Dell'Angelo

The SENSE Research School declares that **Dailing Wu** has successfully fulfilled all requirements of the educational PhD programme of SENSE with a workload of 43.0 EC, including the following activities:

SENSE PhD Courses

- A1: Environmental Research in Context (2021)
- A2 Research in context activity: 'Organizing a workshop to bring together Environmental Technology (ETE), Microbiology (MIB) and UNLOCK (2023)

Other PhD and Advanced MSc Courses

- Speaking Skills, Wageningen into language (2021)
- Introduction to R, PE&RC (2022)
- Reviewing a Scientific Manuscript, Wageningen Graduate School (2023)
- Mixed linear models, PE&RC (2024)
- Chemometrics (Multivariate Statistics), VLAG (2024)
- Genome Assembly, PE&RC (2024)
- Career Orientation, Wageningen Graduate School (2025)

External training at a foreign research institute

- PhD trip Tokyo-Kyoto, Japan (2024)

Management and Organisational activities

- Session chair of "Innovations in Aquatic Ecotoxicology: From Tradition to Future Thinking", SETAC 9th World Congress, Johannesburg, South Africa (2025)

Teaching and supervision

- Supervising a BSc student with thesis entitled 'The Effect of Citalopram on the Foraging Behaviour of *Gammarus pulex*' (2023)
- Supervising MSc student with thesis entitled 'Transferability and Toxicity of Azithromycin across an Aquatic Food Chain' (2023)
- Chairing a Thesis Ring for MSc students (2024)

Oral Presentations

- *The Effects of Different Bio-ozone Treated Effluents on the Structure and Functioning of Freshwater Ecosystems*. SETAC 9th World Congress/SETAC Africa 12th Biennial Meeting, 29.09-03-10 2025, Johannesburg, South Africa
- *Individual and Mixture Effects of Antibiotics on Freshwater Ecosystems.* SETAC 9th World Congress/SETAC Africa 12th Biennial Meeting, 01-10 2025, Johannesburg, South Africa
- *The long-term ecological effects of single antibiotics and their mixtures on freshwater ecosystems*. Netherlands Annual Ecology Meeting 2024, 13.02-14.02 2024, Lunteren, The Netherlands

The research described in this thesis was financially supported by China Scholarship Council.

The research was carried out at the Aquatic Ecology and Water Quality Management Group and the Laboratory of Microbiology, Wageningen University, the Netherlands.

Financial support from Wageningen University for printing this thesis is gratefully acknowledged.

Cover design by Dailing Wu and Xiaojue Wang
Layout design by Dailing Wu, Xiaojue Wang and ProefschriftMaken
Printed by ProefschriftMaken

